Fractionation of tyre derived oil (TDO)

by

Mphai Marvin Ngwetjana

Thesis presented in partial fulfilment
of the requirements for the Degree

of

MASTER OF ENGINEERING
(CHEMICAL ENGINEERING)

in the Faculty of Engineering
at Stellenbosch University

Supervisor
Prof CE Schwarz

Co-Supervisor
Dr P Van der Gryp

March 2017

Declaration

By submitting this thesis electronically, I declare that the entirety of the work contained therein is my own, original work, that I am the sole author thereof (save to the extent explicitly otherwise stated), that reproduction and publication thereof by Stellenbosch University will not infringe any third party rights and that I have not previously in its entirety or in part submitted it for obtaining any qualification.

Date: March 2017

Abstract

Tyre derived oil (TDO) has shown to be a source of *dl*-limonene, a valuable chemical compound with a diverse industrial application. There has been an ever increasing interest in the recovery of *dl*-limonene from TDO. Separation of *dl*-limonene from TDO by ordinary distillation poses a challenge due to the presence of other chemical compounds with similar properties to *dl*-limonene. These compounds are impurities and need to be removed. Before *dl*-limonene can be sold as commercial product it needs to be purified in excess of 90wt%. The main objective of this work is to develop process models using Aspen Plus ® V8.2 to separate *dl*-limonene from TDO at a sufficient purity, validate the model with experimental data and analyse the economic viability of the developed processes.

As distillation cannot achieve the desired separation, enhanced distillation was adopted in this study as it has the ability to separate compounds with similar properties. This thesis investigates the production of high purity (> 90 wt%) *dl*-limonene from TDO using extractive and azeotropic distillation.

A selection of candidate entrainers was identified. The entrainers investigated include diethylene glycol, triethylene glycol, n,n-dimethylformamide, n-methyl-2-pyrrolidone, quinoline, 4-formylmorpholine and tetratethylene glycol dimethyl ether.

The thermodynamic models used in the simulation include the non-random two-liquid (NRTL) and the universal quasichemical activity coefficient (UNIQUAC) model. The missing thermodynamic properties are predicted by the universal functional activity coefficient (UNIFAC) model. The process models developed in Aspen Plus® V8.2 using various entrainers in extractive and azeotropic distillation showed that it is possible to obtain *dl*-limonene recoveries in excess of 95% and at purities as high as 99wt%.

Experimental verification of the modelling results was conducted in a batch distillation setup at a pressure of 60 kPa and entrainer to feed ratio of 2, 4 and 6. Aspen Plus ® V8.2 results were compared with experimental data. The ability of the thermodynamic models to predict all sets of experimental data was determined by calculating percentage error. It was found that none of the models could predict experimental data with acceptable accuracy. This shows there is a need for experimental determination of detailed vapour-liquid equilibrium

(VLE) and vapour-liquid-liquid equilibrium (VLLE) data for binary and ternary systems (chemical compounds in TDO and entrainers).

A techno economic analysis was conducted to investigate the economic viability of different process models developed. From an economic point of view, four out of seven process options developed using different entrainers proved to be profitable. The best process in terms of economic performance was found to be extractive distillation using tetraethylene glycol dimethyl ether with a payback period of 1.23 years and a discounted cash flow rate on return (DCFROR) of 83.21%. The worst process option was found to be azeotropic distillation using n-methyl-2-pyrrolidone with a payback period of greater than 15 years and a DCFROR of 7.72%.

As the thermodynamic models do not accurately predict the phase equilibrium data, the economic analysis conducted is not of the desired level of accuracy. Nevertheless, the separation of *dl*-limonene from TDO using azeotropic/extractive distillation process has shown to be a potential method.

Opsomming

Dis bevind dat die olie wat vanaf motor bande (MBO) verkry kan word, as ’n bron dien vir *dl*-limonene wat ’n waardevolle chemiese verbinding is met verskeie industriële toepassings. Daar is ‘n toenemende belangstelling om *dl*-limonene van MBO te herwin. Skeiding van *dl*-limonene van MBO deur standaarde distillasie is ‘n uitdaging omdat die ander chemiese verbindings wat teenwoordig is soortgelyke eienskappe as *dl*-limonene het. Hierdie verbindings is onsuiwerhede en die verwydering daarvan is van kardinale belang. *dl*-Limonene het slegs kommersiële waarde tensy dit ’n suiwerheid van 90%(m/m) of meer het. Die hoofdoel van hierdie studie is om proses modelle te ontwikkel wat *dl*-limonene van MBO skei tot ’n voldoende suiwerheid, bevestiging van die modelle deur van eksperimentele data gebruik te maak asook om die ekonomiese vatbaarheid van die ontwikkelde proses te analiseer.

Standaarde distillasie skeidingstegnieke kan nie alle vloeistof mengsels skei nie. Daarom was gevorderde distillasie gekies omdat dit nie net die kapasiteit het om verbindings te skei met soortgelyke eienskappe, maar ook omdat dit ’n breë operasionele band het. Hierdie verslag bespreek die skeidings prosedure van hierdie komponente deur ekstraktiewe en azeotropiese distillasie om sodoende die suiwerheid van *dl*-limonene te verbeter. Ekstraktiewe en azeotropiese distillasie behels die gebruik van ’n massa skeidingsagent om die skeiding van die vloeistof mengsel te fasiliteer wat nie haalbaar is deur standaard distillasie.

‘n Lys van moontlike skeidingsagente was ondersoek. Hierdie sluit in diëtileen glikol, triëtileen glikol, n,n-dimetielformamiede, n-metiel-2-pyrrolidon, kinolien, 4-formylmorfoline.

Aspen Plus® V8.2 was gebruik om die skeidings proses te modelleer. Die termodinamiese modelle wat in die simulasie gebruik was, is die *Non-Random Two Liquid* (NRTL) model en die *Universal quasi chemical activity coefficient* (UNIQUAC) model. Die onbekende termodinamiese eienskappe was bepaal deur gebruik te maak van die *Universal functional activity coeffiecient* (UNIFAC) model. Die proses modelle wat in Aspen Plus® V8.2 ontwikkel was, wys dat dit moontlik is om minstens 95% van die *dl*-limonene te herwin met ’n suiwerheid van so hoog as 99% (m/m).

Eksperimentele werk was uitgevoer in ‘n enkellade distillasie opstelling wat by ‘n druk van 60 kPa bedryf was met ’n skeidingsagent tot toevoer verhouding van 2, 4 en 6 onderskeidelik. Aspen Plus® V8.2 resultate was vergelyk met die eksperimentele data. ‘n Persentasie fout was bereken om die akkuraatheid van die gebruik van termodinamiese modelle om eksperimentele data te voorspel, te bepaal. Dit was gevind dat nie een van die modelle gebruik kan word nie om eksperimentele data te voorspel met aanvaarbare akkuraatheid. Hierdie dryf dus die nood vir eksperimentele data vir damp-vloeistof ewewigsdata (DVE) en damp-vloeistof-vloeistof ewewigsdata (DVVE) van binêre en drieledige sisteme (chemiese verbindings in MBO en skeidingsagent).

’n Tegno-ekonomiese analise was uitgevoer om die ekonomiese vatbaarheid van verskillende proses modelle te ondersoek. Vanuit ’n ekonomiese standpunt, vier uit sewe proses keuses wat verskillende skeidingsagente gebruik blyk om meer winsgewend te wees. Die beste proses opsie in terme van ekonomiese prestasie was ekstraktiewe distillasie met ’n terugbetaalde periode van 1.23 jaar en ’n VKOK van 83.21 %. Die minder gunstige proses opsie was die azeotropiese distillasie wat die skeidingsagent n-metiel-2-pyrrolidon gebruik met ’n terugbetaal periode van 15 jaar en ’n VKOK van 7.72%.

Dit is bevind dat weens die onakkuraatheid van die termodinamiese modelle vir die voorspelling van fase-ewewig, die verlangde vlak van akkuraatheid vir die ekonomiese ontledings nie geskik is nie. Gevorderde distillasie wat azeotropiese/ekstraktiewe distillasie proses gebruik, het dus die potensiaal om die ekonomiese uitdagings rondom die afval van motorbande deur pirolise tegnologie te verbeter of aan te spreek.

Acknowledgements

I would like to effusively thank the following people for their full assistance and support through the year.

- ✓ I thank the Lord Jesus Christ for the strength, wisdom and guidance throughout
- ✓ My supervisor Prof CE Schwarz and co supervisor Dr Percy Van der Gryp for superior guidance, motivation and intellectual stimulation
- ✓ Lab Technician Mr Alvin Peterson and the workshop crew for assisting with the equipment for the experiment
- ✓ Mrs Hanlie Botha and Levine Simmer for assisting with the analytical techniques
- ✓ My parents for their countless support
- ✓ My siblings for the constant encouragement
- ✓ Separation technology research group for providing a great environment for learning
- ✓ Redisa group for financial support
- ✓ Aspen Technology
- ✓ Vital Alexandre, Leanne Brits, Waylin Peddie and Siphesihle Khoza for being very marvellous

Dedication....

Mmapula Ledile Ngwetsana

Table of Contents

Declaration i
Abstract ii
Opsomming iv
Acknowledgements vi
Abbreviations xii
Nomenclature xiii
Chapter 1 Introduction 1
1.1 Background and motivation 1
1.2 Aims and objectives 3
1.3 Thesis outline 3
1.4 References 6
Chapter 2 Literature and background information 8
2.1. Introduction 8
2.2. Tyre pyrolysis 8
2.2.1. Tyre pyrolysis condition 8
2.2.2. Characterisation of TDO 9
2.2.3. Economic of tyre pyrolysis processing 10
2.3. Limonene production 11
2.4. TDO fractionation state of the art and outlook 12
2.4.1. Separation of TDO 12
2.4.2. Purification of TDO products 15
2.4.3. Separation technologies for evaluation 15
2.5. Enhanced distillation 21
2.5.1. Extractive distillation 21
2.5.2. Homogeneous azeotropic distillation 23
2.5.3. Heterogeneous azeotropic distillation 24
2.5.4. Example of application of enhanced distillations 25
2.5.5. Process modelling of enhanced distillation process 30
2.5.6. Residue curve map (RCM) technology 33
2.6. Phase behaviour and thermodynamics 35
2.6.1. Thermodynamic models 35
2.6.2. Selection of thermodynamic models 36

2.6.3. Binary VLE data 37
2.7. Conclusion 39
2.8. References 42
Chapter 3 Process modelling for recovery of *dl*-limonene from TDO 48
3.1. Introduction 48
3.2. Fractionation of TDO 49
3.2.1. Problem definition and approach 49
3.2.2. Selection of thermodynamic model 53
3.2.3. Process model for feed 1 53
3.2.4. Process model for feed 2 64
3.2.5. Comparison of results 67
3.3. Enhanced distillation: Upgrading of light naphtha cut to *dl*-limonene rich stream 68
3.3.1. Problem definition and approach 68
3.3.2. Entrainer selection 70
3.3.3. Selection of thermodynamic model 83
3.3.4. Process model for diethylene glycol 83
3.3.5. Process model for triethylene glycol 97
3.3.6. Process model for 4-formylmorpholine 99
3.3.7. Process model for quinoline 102
3.3.8. Process model for tetraethylene glycol dimethyl ether 105
3.3.9. Process model for n,n-dimethylformamide 108
3.3.10. Process model for n-methyl-2-pyrrolidone 112
3.4. Comparison 117
3.5. Sensitivity of *dl*-limonene concentration 119
3.6. Conclusion 121
3.7. References 123
Chapter 4 Experimental validation of process modelling 125
4.1. Introduction 125
4.2. Set-up and methodology 125
4.2.1. Experimental set-up 125
4.2.2. Experimental design 129
4.2.3. Analytical method 131
4.2.4. Material used 131

4.3. Results and discussion....132
4.3.1. Vapour pressure verification....132
4.3.2. Fractionation of TDO....136
4.3.3. Purification of light naphtha cut....137
4.4. Conclusion....145
4.5. References....148
Chapter 5 Economic Analysis....150
5.1. Introduction....150
5.2. Assumptions and framework....150
5.2.1. Estimate of capital cost....153
5.2.2. Operating cost estimation....153
5.2.3. Estimation of revenue....154
5.2.4. Economic modelling assumptions....154
5.3. Results: Cost estimations....156
5.3.1. Capital cost investment....156
5.3.2. Operating costs estimation....157
5.3.3. Estimation of revenue....158
5.4. Results: Profitability analysis....158
5.5. Results: Sensitivity analysis....159
5.5.1. Effect of raw material price....160
5.5.2. Effect of *dl*-limonene price....161
5.5.3. Effect of interest rate....163
5.5.4. Effect of feed rate....164
5.6. Concluding remarks....165
5.7. References....168
Chapter 6 Conclusions and recommendations....170
6.1. Conclusions....170
Identifying candidate entrainers....170
Conducting process modelling....170
Testing process models experimentally....171
Conducting economic analysis....171
Providing outcome as to possible separation....172
6.2. Recommendations....172

Appendix A GC Calibration curves 174
Appendix B Vapour pressure data 176
Appendix C Purification of light naphtha 178
C.1.1. Feed 178
C.1.2. Azeotropic distillation using n,n-dimethylformamide 178
C.1.3. Azeotropic distillation using n-methyl-2-pyrrolidone 179
C.1.1. Extractive distillation using quinoline 180
C.1.2. Azeotropic distillation using triethylene glycol 180
C.1.1. Sythetic solution azeotropic distillation 181
Appendix D Property model selection 182
Appendix E Sensitivity analysis 191
E.1. Process model for feed 2 (Fractionation) 191
E.1.1. Distillation column (T101) 191
E.1.2. Distillation column (T102) 195
E.2. Triethylene glycol 199
E.2.1. Azeotropic distillation column 199
E.2.2. Entrainer recovery column 201
E.3. 4-Formylmorpholine 202
E.3.1. Azeotropic distillation column 202
E.3.2. Entrainer recovery column 205
E.4. Quinoline 206
E.4.1. Extractive distillation 206
E.4.2. Entrainer recovery column 208
E.5. Triethylene glycol dimethyl ether 209
E.5.1. Extractive distillation 209
E.5.2. Entrainer recovery column 212
E.6. n-Methyl-2-pyrrolidone 213
E.6.1. Azeotropic distillation 213
E.6.2. Water addition 215
E.6.3. Entrainer recovery 218
E.7. n,n-Dimethylformamide 219
E.7.1. Azeotropic distillation 219
E.7.2. Water addition 222

Appendix F Equipment sizing 225
Appendix G Cash flow analysis 228

Abbreviations

Abbreviation	Description
Abs	Absolute
B_i	Bottoms product of column i
C_i	Carbon with number of atoms i
CAPEX	Capital expenditure
CEPCI	Chemical engineering plant cost index
D_i	Distillate of column i
DCFROR	Discounted cash flow rate of return
EOS	Equations of state
GC	Gas chromatography
GC-MS	Gas chromatographic mass spectroscopy
LLE	Liquid-liquid equilibrium
NPV	Net present value
NRTL	Non-random Two Liquid
OPEX	Operational expenditure
PBP	Pay back period
PAH	Polycyclic aromatic hydrocarbons
RCM	Residue curve maps
E/F	Entrainer to feed ratio
TDO	Tyre derived oil
UNIFAC	Universal Functional Activity Coefficient
UNIQUAC	Universal Quasichemical Theory
VLE	Vapor-liquid equilibrium
VLLE	Vapour-liquid-liquid equilibrium

Nomenclature

Symbol	Description	Units
a	Activity	
$\hat{f}_i$	Fugacity of component *i*	Pa
M_w	Molecular mass	$g.mol^{-1}$
n	Number of moles	Mol
P	Total system pressure	Pa
P_i^{sat}	Vapour pressure of component *i*	Pa
T	Temperature	K
x_i	Mole fraction of component *i* in the liquid phase	
y_i	Mole fraction of component *i* in the vapour phase	
α_{ij}	Relative volatility	
γ_i	Activity coefficient	

Chapter 1 Introduction

1.1 Background and motivation

There are approximately 1.5 billion tyres produced worldwide per annum and they eventually end up as waste tyres (Williams, 2013). Disposal of waste tyres is challenging. The complex nature of tyres makes them resistant to biological degradation (Pilusa *et al*., 2014). At the same time, tyres take up plenty of space at the landfill and pose environmental and health threats (Wotjowicz and Serio, 1996).

Alternative waste tyre management methods for tyre recycling include: retreading, crumbing and incineration. However, these alternative waste management methods are not enough to eliminate the stockpile of tyres at the landfill site as the products derived from these processes have limited application and low market (Muzenda and Popa, 2015). Additionally, incineration of waste tyres pose environmental and health threats (Jang *et al.,* 1998).

Pyrolysis of waste tyres is gaining popularity as a method of waste tyre recycling (Pilusa *et al.,* 2014). During pyrolysis, the tyre is thermally decomposed in the absence of oxygen into low molecular weight products that can be used as chemical feedstock, or as alternative fuel (Williams and Cunliffe, 1998). The inorganic matter of tyres and non-volatile carbon black remain as solid residue/char and may be used either as fuel or pyrolysis char (Williams and Cunliffe, 1998). The liquid product of tyre pyrolysis, known as tyre pyrolysis oil or tyre derived oil (TDO), is a mixture of hundreds of organic and inorganic compounds. These compounds have a wide range of chemical functionality (Williams and Cunliffe, 1998). There have been several proposed uses for TDO. The primary uses being substitution for conventional fuel and as chemical feedstock (Pilusa and Muzenda, 2013).

Waste tyre pyrolysis projects have not been commercially successful due to unfeasible process economics (Wotjowicz and Serio, 1996). The selling price of the pyrolysis products yields low returns because of the low market value of fuels. However, TDO has shown to be a source of light hydrocarbons, which command a higher market value than the raw oil (Wotjowicz and Serio, 1996). It would thus be desirable to develop a process based on the recovery of high market value products, at a sufficient quality, to improve the waste tyre pyrolysis economics. These value added chemicals include: benzene, toluene, xylene,

ethylbenzene, styrene and *dl*-limonene (Wotjowicz and Serio, 1996). In this study, interest lies in the extraction of *dl*-limonene.

dl-Limonene (dipentene) is a major component of TDO (Pakdel *et al*., 1991). The yield of *dl*-Limonene varies between 0.01 and 27.97 wt%, based on initial tyre fed to the pyrolysis reactor (Danon *et al*., 2015). Limonene is a monocyclic monoterpene that exists in two forms: *d*-limonene, the most naturally abundant, and *l*-limonene (Pakdel *et al*., 2001). *dl*-Limonene, which exist in TDO, is a mixture of limonene isomers. *dl*-Limonene has a widespread application. It is used in the manufacturing of food, cosmetic products, and medicines and in industries as a green solvent (Williams and Cunliffe, 1998).

Limonene is produced commercially from citrus oils (Florida Chemicals Co., 1991a, b, c). Due to its wide range of applications, combined with its low production volume, the demand might soon outweigh its supply. Limonene is available commercially as a food grade, in an untreated technical grade, and as a lemon-lime grade at a purity of 97, 95 and 70% respectively. (Florida Chemicals Co., 1991a, b, c). The sale price of limonene from citrus oil depends on purity and range between 8 and 25 US $/kg (Florida Chemicals Co., 1991a, b, c).

This project focuses on the recovery of the major component *dl*-limonene from TDO. Several studies conducted by Pakdel *et al*. (1991) and Stanciulescu and Ikura (2006,2007) have shown that it is not easy to obtain a highly concentrated *dl*-limonene fraction of sufficient quality from TDO. This is because during the pyrolysis process, thermal decomposition of *dl*-limonene occurs, forming benzene and cyclohexadiene derivatives. These derivatives have boiling points close/similar to that of *dl*-limonene, making it difficult to achieve separation by distillation without extensive additional operating costs.

In this study, the separation process for recovery of valuable *dl*-limonene will be developed using Aspen Plus ® V8.2 simulation tool. Various process options will be developed and evaluated on a techno-economic analysis before making a decision on the final design best suited to defined project objectives. Extraction of valuable *dl*-limonene on an industrial scale is believed to improve process economics of waste tyre pyrolysis and minimise the problem of waste tyre littering.

1.2 Aims and objectives

TDO has shown to be a source of valuable *dl*-limonene. Due to the presence of close boiling compounds, a separation process for recovery of a high concentrated *dl*-limonene fraction of sufficient quality, applicable on an industrial scale, has not been extensively discussed in literature (Pakdel *et al*., 1991; Pakdel *et al*., 2001). The main objective of this work is to develop process models to separate *dl*-limonene from TDO, resulting in sufficient purity (in excess of 90 wt%), to meet current market demands.

As separation of TDO using simple distillation cannot achieve high purity *dl*-limonene, there is a need for employment of other separation technologies. Separation technologies employed in industries for separation of close boiling compounds, or as alternatives to simple distillation techniques include: extractive distillation, salt distillation, pressure-swing distillation, homogenous and heterogeneous azeotropic distillation, and reactive distillation (Henley *et al*., 2011). The aim of this thesis is to investigate the use of alternative distillation technologies for production of high purity *dl*-limonene. In particular, extractive and azeotropic distillation will be considered. In order to achieve this aim, the following objectives need to be achieved:

1. Identify entrainers
2. Conduct process modelling
3. Test process models experimentally
4. Conduct economic analysis
5. Provide outcome as to possible separation

1.3 Thesis outline

Figure 1.1 gives a flow diagram of the thesis layout. The thesis is divided into six chapters.

Chapter 1 gives a background and objectives of this study.

Chapter 2 gives literature study of the proposed investigation. The chapter presents a general overview of waste tyre pyrolysis, TDO fractionation methods and state of the art of this project. This chapter also gives an overview of basic terminologies and concepts associated with the separation of hydrocarbons. Thereafter the focus is placed on the separation method and thermodynamic principles best suited for *dl*-limonene recovery.

Chapter 3 discusses the design and approach used for the process modelling of separation of TDO. This provides information on the separation objective, the selection of thermodynamic models, the discussion of important process parameters and assumptions and details of the final process models and comparison.

Chapter 4 gives details of experimental work carried to validate the developed Aspen Plus® V8.2 model for separation of TDO. This includes: experimental setup and methodology as well as a comparison of model and experimental data.

Chapter 5 gives the economic analysis of the separation process models. This entails cost estimation, profitability analysis and sensitivity analysis of the selected process option to economic conditions such as changes in prices, feed rate and interest rate.

Chapter 6 summarises the main findings from this study and recommendation for further work.

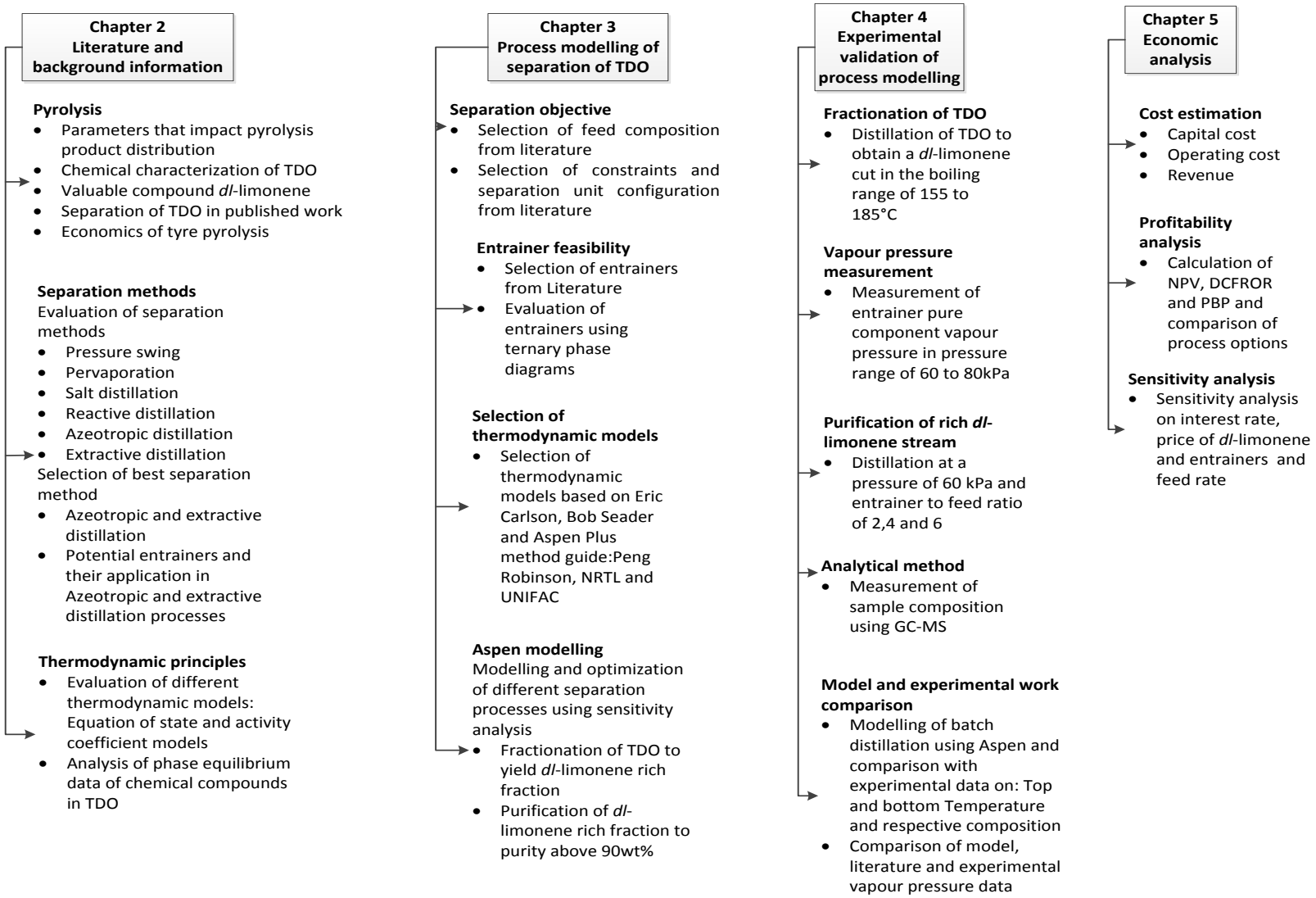

Figure 1.1 Flow diagram of thesis layout

1.4 References

Aydin, H. and Ilkilic, C. 2012. Optimisation of fuel production from waste vehicle tyres by pyrolysis and resembling to diesel fuel by various desulfurization methods. *Fuel,* 102: 605–612.

Choi, G.G., Jung, S.H., Oh, S.J. and Kim, J.S. 2014. Total utilization of waste tire rubber through pyrolysis to obtain oils and CO2 activation of pyrolysis char. *Fuel Processing Technology*, 123: 57–64.

Cunliffe, A.M. and Williams, P.T. 1998a. Composition of oils derived from the batch pyrolysis of tyres. *Journal of Analytical and Applied Pyrolysis*, 44: 131-152.

Danon, B., Van der Gryp, P., Schwarz, C.E. and Görgens, J.F. 2015. A review of dipentene (*dl*-limonene) production from waste tire pyrolysis. *Journal of Analytical and Applied Pyrolysis, 112*: 1–13.

Florida Chemical Co., 1991a. Marketing Data Sheet: d-limonene. Lake Alfred, FL.

Florida Chemical Co., 1991b. Product Data Sheet: d-limonene. Lake Alfred, FL.

Florida Chemical Co., 1991c. Material Safety Data Sheet: d-limonene. Lake Alfred, FL.

Henley, E.J., Seader, J.D. and Roper, D.K. 2011. *Separation Process Principles*. Wiley.

Jang, J.W., Yoo, T.S., Oh, J.H. and Iwasaki, I. 1998. Discarded tire recycling practices in the United States, Japan and Korea. *Resources, Conservation and Recycling*, 22: 1–14.

Muzenda, E. and Popa, C. 2015. Waste Tyre Management in Gauteng, South Africa: Government, Industry and Community Perceptions. *International Journal of Environmental Science and Development* 6: 311–315.

Pakdel, H., Pantea, D.M. & Roy, C. 2001. Production of *dl*-limonene by vacuum pyrolysis of used tires. *J. Anal. Appl. Pyrolysis*, 57: 91–107.

Pakdel, H., Roy, C., Aubin, H. and Jean, G., Coulombe, S. 1991. Formation of *dl*-limonene in used tire vacuum pyrolysis oils. *Environmental Science & Technology,* 25: 1646–1649.

Pilusa, J., Shukla, M. and Muzenda, E. 2014. Economic assessment of waste tyres pyrolysis technology: a case study for Gauteng Province, South Africa.

Pilusa, J. and Muzenda, E. 2013. Qualitative analysis of waste rubber-derived oil as an alternative diesel additive. *International Conference on Chemical and Environmental Engineering*.

Stanciulescu, M. and Ikura, M. 2006. Limonene ethers from tire pyrolysis oil. *J. Anal. Appl. Pyrolysis,* 75: 217–225.

Stanciulescu, M. and Ikura, M. 2007. Limonene ethers from tire pyrolysis oil. *J. Anal. Appl. Pyrolysis,* 78: 76–84.

Turton, R., Baile, R.C., Whiting, W.B. and Shaeiwitz, J.A.2009. *Analysis, synthesis, and design of chemical processes* .Prentice Hall international series in the physical and chemical engineering sciences. Prentice Hall, Upper Sad*dl*e River, NJ.

Williams, P.T. 2013. Pyrolysis of waste tyres: A review. *Waste Management,* 33: 1714–1728.

Wojtowicz, M.A. and Serio, M.A. 1996. Pyrolysis of Scrap tires: Can it be profitable?. *ChemTech.*

Qu, W., Zhou, Q., Wang, Y.Z., Zhang, J., Lan, W.W., Wu, Y.H., Yang, J.W. and Wang, D.Z. 2006. Pyrolysis of waste tire on ZSM-5 zeolite with enhanced catalytic activities. *Polymer Degradation and Stability,* 91: 2389–239.

Chapter 2 Literature and background information

2.1. Introduction

The aim of this chapter is to introduce tyre pyrolysis technology, by giving an overview of the basic terminology and concepts associated with waste tyre pyrolysis, and the separation techniques used for recovery of the valuable compound, *dl*-limonene, based on current research related to this investigation.

The design of separation units requires understanding of thermodynamic principles, as it assists in evaluating the viability and efficiency of separation systems (Smith *et al*., 2005). Therefore, the chapter will provide an overview of the thermodynamic principles related to the separation of TDO components.

This chapter is divided into seven sections, excluding Section 2.1; Section 2.2 introduces tyre pyrolysis technology by briefly discussing chemical characterisation of TDO, the effect of pyrolysis process parameters on the chemical composition of TDO and the economics of tyre pyrolysis. Section 2.3 discusses the end use of TDO, with a specialised focus on *dl*-limonene. Section 2.4 discusses different separation technologies currently used for separation of TDO and state of the art, and outlook. Section 2.5 gives a brief discussion of alternative separation technology for recovery of value added product, *dl*-limonene, from TDO and the selection of the most suitable separation technology. Section 2.6 gives an overview of thermodynamic models and the selection of the correct thermodynamic model. Section 2.7 summarises the main findings of this chapter.

2.2. Tyre pyrolysis

2.2.1. Tyre pyrolysis condition

Tyre pyrolysis is the process of decomposition of a tyre into liquid (TDO), char and gas, by subjecting the tyre to heat in a reduced or oxygen-free environment. Tyre pyrolysis products can be used as chemical sources or fuels (Williams, 2013).

The rubber content of tyres is mainly made from styrene-butadiene-rubber (SBR), natural rubber (polyisoprene) and/or polybutadiene rubber (PBR) (Seidelt *et al*., 2006). The main degradation product from natural rubber is xylene and isoprene dimer, and the main degradation product from SBR is styrene, ethylbenzene and cumene (Seidelt *et al*., 2006).

The rubber crum used for pyrolysis may be a mixture of different brands and types. The different tyres have different ratios of natural rubber to synthetic rubber. Kyari *et al*. (2005) investigated the effect of different tyre brands and types on pyrolysis and noticed that the yield of TDO, gas and char were not influenced significantly. However, there was a significant difference in the composition of TDO and gases.

The product distribution of tyre pyrolysis products also depend on the process conditions of the pyrolysis reactor. The formation of TDO is favoured by high heating rates, with short residence time and rapid quenching of the products (Cunliffe and Williams, 1998). This is because the pyrolysis gases and vapours are condensed before they are decomposed into other gaseous products. Primary vapours, which are produced in the pyrolysis process, degrade to secondary tars and gases with an increase in temperature and residence time (Cunliffe and Williams, 1998). This decomposition is a secondary reaction and increases the yield of char at the expense of TDO yield.

2.2.2. Characterisation of TDO

TDO contains more than 100 identified compounds (Williams, 2013). One-dimensional gas chromatography (GC) has been used and confirmed in excess of 130 compounds. Further analysis by two dimensional GC confirmed several hundred compounds (Laresgoiti *et al.,* 2004). Quantification of chemical compounds from TDO is challenging due to the presence of a large number of chemical compounds. Additionally, many compounds have similar physical properties and elute at similar retention times.

The quality and characteristics of TDO mainly depend on the compounds in the mixture, which are influenced by pyrolysis operating conditions, process temperature and nature of the tyre rubber (Kyari *et al.,* 2005). Knowledge of the composition of TDO is important for design of chemicals recovery processes.

TDO contains aliphatic, aromatic, heteroatom and polar fractions (Williams, 2013). Dai *et al.* (2001) reported a TDO composition of 26.77 wt% alkanes, 42.09 wt% aromatics and 26.64 wt% non-hydrocarbons, and 4.05 wt% asphalt from a fluidised bed pyrolysis reactor. Conesa *et al.* (1996) reported a TDO composition of 39.5 wt% aliphatics, 19.1 wt% aromatics, 21.3 wt% hereto-atoms and 20.1 wt% polar fractions from pyrolysis in a fluidised bed reactor at laboratory scale at 700°C. Laresgoti *et al.* (2004) reported that the aromatic fraction increased

(from 53.4 to 74.8wt% obtained in their study) with increasing pyrolysis temperature (300 to 700°C).

TDO can be separated into fractions that can be used as fuels or intermediate feedstock to petrochemical industries (Pilusa and Muzenda, 2013). Impurities in TDO include moisture, sediments, salt, metals, sulphur compounds and nitrogen compounds. The removal of these impurities is a vital step in processing TDO (Pilusa and Muzenda, 2013).

Distillation of TDO has been conducted by various authors but increasing attention has been on recovery of *dl*-limonene as it is the main constituent of TDO and command a high market value. The yield of *dl*-limonene can go as high as 27.97wt% based on initial tyre fed to the pyrolysis reactor (Danon *et al*., 2015).

2.2.3. Economic of tyre pyrolysis processing

Wotjowicz and Serio (1996) report that, more than 30 commercial pyrolysis projects conducted have been unsuccessful due to the low market value of TDO and low quality carbon black. A preliminary economic feasibility estimate was conducted by Wotjowicz and Serio (1996) on pyrolysis of waste tyres based on a 5 year project life. Waste tyre pyrolysis project was found to be economical when considering tyre processing of 100 ton/day, which is equivalent to 4 million tyres per year processed, assuming one tyre weighs approximately 9 kg. TDO yield of 45% was assumed. Due to low market value of raw TDO, Wotjowicz and Serio (1996) investigated the possibility of converting it to high quality pyrolysis char, which was found to have a higher market value than TDO. The process was found to be economical when considering selling all pyrolysis products, including steel. Wotjowicz and Serio (1996) further recommended the recovery of valuable chemicals from TDO to improve the economics of tyre pyrolysis.

A preliminary economic feasibility estimate was also conducted by Muzenda and Popa (2015) on pyrolysis of waste tyres based on a 5 year project life. The waste tyre pyrolysis project was found to be economical when considering a pyrolysis process capacity of 10 ton tyres/day. However, there is no information on the type of tyres processed. The process yields a positive return when considering selling TDO, steel and pyrolysis char. TDO produced from tyre processing of 10 ton/day is approximately 104 000.00 litres per month assuming 40% yield. The economic analysis was conducted assuming continuous supply of waste tyres and product market availability.

This study will consider recovery of *dl*-limonene, as it is the most abundant chemical in TDO and has a wide industrial application. Thereafter, an economic analysis is done to ascertain whether the process will yield positive returns.

2.3. Limonene production

The annual production of d-limonene from citrus oils was approximated as 45000 tonnes per annum around 1991 (Schulz, 1972). Citrus planting was expected to increase the production to 73000 tonnes per annum within a decade (Florida Chemical Co., 1991a,b,c). Due to its diverse application, the production is rising fast. It is predicted that the demand for limonene will soon outweigh its supply as the citrus supply tightens when the citrus season ends. *dl*-Limonene content in TDO is quite significant. The recovery of *dl*-limonene from TDO is therefore important to increase the *dl*-limonene production volume.

Limonene price and application depends on the purity. The major impurities in *dl*-limonene obtained from TDO are different from that obtained from citrus oil. The major impurities in limonene from citrus oil include cymene, octanal, nonanal, pinene, myrcene and careen (Florida Chemical Co, 1991a, b, c). Impurities in *dl*-limonene distilled from TDO include toxic sulfur compounds and light aromatic compounds. Sulfur containing compounds such as thiophene and benzothiazole as well as their derivatives, were detected. Detailed sulfur analysis of *dl*-limonene enriched naphtha has revealed that even traces of sulfur compounds result in an unpleasant odor (Pakdel *et al.,* 2001). The impurities in TDO limit its application in the food industry.

Desulfurisation is an important step and many petrochemical products are reduced to be almost sulfur-free as the price of the products is influenced by the sulfur content. Additionally, the operation cost and environmental risks increases as fractions rich in sulfur are being processed (Javadli and de Klerk, 2012).

There is limited information on the price of *dl*-limonene for different grades, either produced from TDO or citrus oil. The price of *dl*-limonene for this project is obtained from Green Terpene ™ (GreenTerpene, 2014). Figure 2.1 shows the price of d-limonene from citrus oil as a function of purity. The data shows the price for technical grade (90 wt% purity), food grade (95 wt% purity) and high purity grade (98.5 wt% purity) d-limonene. The mid-season food grade purity range between 80 and 90 wt% and is sold at a price between 8 and 15 $/kg

(GreenTerpene, 2014). The high selling price of limonene encourages its recovery from TDO and is believed to improve the process economics of tyre pyrolysis.

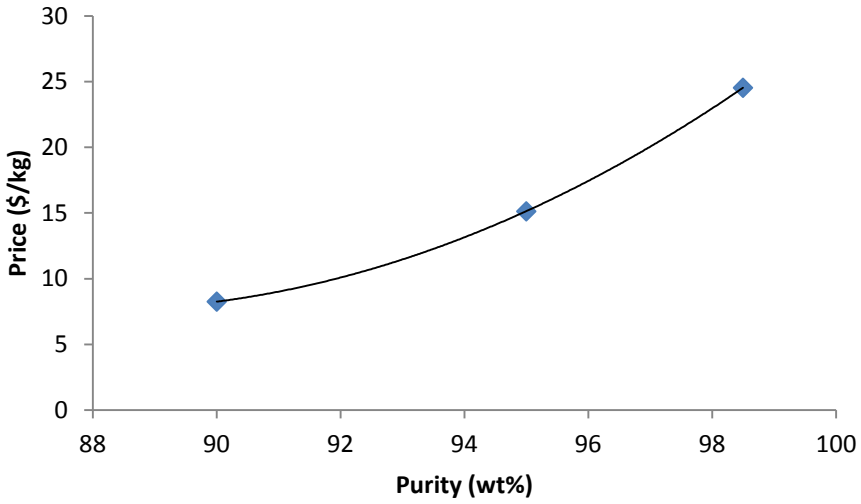

Figure 2.1 d-Limonene price at different grades (Green Terpene ™, 2015)

2.4. TDO fractionation state of the art and outlook

Extensive research has been made into increasing the value and quantity of TDO production through techniques such as the use of catalyst, the use of selective temperature and post pyrolysis selective condensation during tyre pyrolysis to influence product distribution (Williams, 2013). However these techniques are rendered unworthy if the derived products are not upgraded. Distillation of TDO has been conducted by various authors to obtain a concentrated *dl*-limonene fraction. The following section focus on previous work done in the distillation of TDO to produce *dl*-limonene.

2.4.1. Separation of TDO

It is reported that 30 wt% of TDO boils between 70 and 210°C, and 75 wt% boils below 310°C (Pilusa and Muzenda, 2013). The fraction between 70 and 210°C contains mostly single aromatics and the major product, *dl*-limonene, which is an aliphatic. The normal boiling point of *dl*-limonene is around 175.5-176.5 °C (Pakdel *et al.,* 1991).

Stanciulescu and Ikura (2006) studied the production of *dl*-limonene enriched naphtha cut from TDO using distillation. The distillation process was conducted under atmospheric pressure and as well as vacuum conditions (0.07 – 0.13 kPa). A feed of 2-4 kg was considered and two consecutive distillations were performed.

The first distillation was used for separation of naphtha, with a normal boiling point of less than 190° at atmospheric pressure, and from this, *dl*-limonene enriched naphtha was separated. The fraction with a normal boiling point of less than 190°C was analysed and found to contain 23.8 wt% m-xylene, which was the highest component concentration. Benzene, toluene and styrene were detected at average concentrations of 3, 11 and 8 wt% respectively. Terpenes were obtained at 26.6 wt%, in which *dl*-limonene was approximately 63 wt% of terpenes. The balance concentration was hydrocarbons with acyclic or cyclic structure, and heteroatoms sulfur and nitrogen compounds. The sulfur content in naphtha was 0.43%, which was less than the original 1 wt%, indicating that the naphtha contained less sulfur compounds than heavy oil fraction. The *dl*-limonene rich cut from the first distillation was fed to the second distillation process operated under vacuum. The second distillation increased the *dl*-limonene concentration to approximately 32-37 wt% when considering a narrow cut of 10-15°C above and below *dl*-limonene boiling point.

Stanciulescu and Ikura (2006) studied distillation at different temperatures to determine suitable conditions to improve yield and concentration of *dl*-limonene. Due to the complexity of naphtha composition, i.e. the presence of several compounds that have a similar, or very close boiling point to *dl*-limonene, its collection was difficult.

Stanciulescu and Ikura (2006) also employed another technique to separate *dl*-limonene from *dl*-limonene enriched naphtha, as the use ordinary distillation was limiting. Stanciulescu and Ikura (2006) studied the esterification of *dl*-limonene, using methanol and isopropanol as alkoxylation reactants to convert *dl*-limonene, in the *dl*-limonene enriched fraction, into a more polar and slightly hydrophilic compound. Limonene ether (methyl ether) is the product of esterification and has a boiling point of 198°C, which is higher than pure *dl*-limonene's normal boiling point. The conversion of esterification went as high as 100% and selectivity as high as 71.6% at reaction times of up to 20 hours. The resulting products were separated through the use of ordinary distillation techniques. Due to the fact that the selectivity was not high enough, aromatic hydrocarbons were still present in the distillation products.

Stanciulescu and Ikura (2007) also studied the esterification of *dl*-limonene using different reactor configurations and operating conditions. A feed of 9-13 kg was considered. *dl*-Limonene obtained was distilled from TDO using the same technique of two consecutive

distillations at a pressure of 3 kPa. The distillation cuts were collected between the initial boiling point and 250°C. This cut represented 20 wt% of the original TDO and contained 6% *dl*-limonene. The highest concentration of *dl*-limonene obtained was approximately 75wt% in the temperature range of 170-190°C, but the cut represented only 6.6% of TDO. Analysis of *dl*-limonene enriched naphtha revealed that 19 other compounds, isomers and styrene derivatives were present. The highest conversion of *dl*-limonene enriched naphtha to ether was 70%. The selectivity for limonene ether production was poor.

Pakdel *et al.* (2001) studied the production of *dl*-limonene from three different tyres and pyrolysis conditions. TDOs derived from different tyres had different chemical product distributions. TDOs from different feedstocks were distilled separately to obtain concentrated *dl*-limonene fractions. The distillation was carried in a pilot packed batch distillation column to recover naphtha fractions. A column with 25 theoretical plates at an operating 1:30 reflux ratio was used. Two consecutive distillations columns were used.

The capacity of the first distillation column was 300L and the second distillation column was 5L. The naphtha fractions from the first distillation were enriched in the second distillation to obtain *dl*-limonene enriched naphtha. The distilled TDO fractions were analysed and shown to contain different *dl*-limonene concentrations due to variable *dl*-limonene yields obtained from different pyrolysis reactors. The three *dl*-limonene enriched fractions contained compounds which have similar or close boiling points to *dl*-limonene, and could not be enriched further using distillation. The compounds obtained in significant amounts together with *dl*-limonene included: 1,2,3-trimethylbenzene, m-cymene and indane. Other compounds were benzene and cyclohexadiene derivatives, which were from the ultimate degradation of *dl*-limonene or isoprene. The maximum *dl*-limonene concentrations achieved were 50, 62 and 92 wt% from distillation of the three TDO fractions from pyrolysis of different tyre brands. Sulfur containing compounds were detected. These compounds were removed during the distillation process, but detailed sulfur analysis revealed that traces of sulfur compounds remain (around 228ppm of dimethylthiophene, diethylthiophene and tert-butylthiophene) resulting in an unpleasant odor. Membrane purification method was utilised and resulted in a *dl*-limonene fraction nearly sulfure free, with less odor.

2.4.2. Purification of TDO products

Pakdel *et al.* (1991) studied the separation and purification of *dl*-limonene from TDO on a laboratory scale. TDO was distilled at atmospheric pressure and temperatures of up to 204°C to separate the naphtha fraction. A 1 g portion of naphtha was fractionated over 20 g of impregnated silica gel. The fraction was analysed and found to contain 80 wt% *dl*-limonene. The purity was further increased to 95 wt% by thin-layer chromatography.

Purification of *dl*-limonene enriched fraction remains a challenge that needs to be addressed. A suitable separation process for purification needs to be designed on an industrial scale. For large scale peoduction, Pakdel *et al.* (1991) anticipated that separation of TDO for recovery of high purity *dl*-limonene will require two consecutive distillations, followed by a purification step. The design of new separation units requires evaluation of potential separation technologies, after which the best separation technology that suit the desired product specification is selected.

2.4.3. Separation technologies for evaluation

Maximising TDO yield, as well as *dl*-limonene yield in TDO, has been successfully executed in previous work on optimum pyrolysis conditions. Obtaining a *dl*-limonene enriched naphtha fraction from TDO, using batch distillation techniques, has been investigated by various authors and proved possible. Obtaining high purity *dl*-limonene from TDO remains a relatively untouched field in current research. Therefore, there is a need for the design of the fractionation process of TDO on an industrial scale.

The difficulty in obtaining a pure *dl*-limonene fraction is due to the presence of compound, with a similar boiling point to that of *dl*-limonene. Close boiling mixtures have a relative volatility close to one another and their separation can be achieved using technologies applied to azeotropic mixtures.

TDO is a multicomponent liquid mixture and the concentration differs for different types of tyres processed and pyrolysis conditions. A potential separation method should be able to handle a high throughput and variable feed concentration.

The chemical properties of significant compounds (derived from Aspen Plus ® V8.2) and their concentration range found by Pakdel *et al. (*2001) in the *dl*-limonene enriched fraction are given in Table 2.1.

Table 2.1 Physical properties of chemicals in *dl*-limonene enriched fraction

Component	Structure	Molar mass (g/mol)	Specific gravity	Dipole Moment (D)	Boiling point (°C)
Limonene (50-92 wt%)	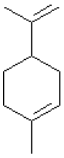	136.23	0.84	0.64	177.45
Indane (0-8 wt%)	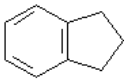	118.75	0.86	0.67	176.50
1,2,3-Trimethylbenzene (0-19 wt%)	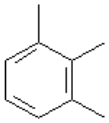	120.20	0.90	0.56	176.12
Cymene (0-22 wt%)	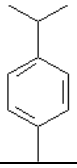	134.20	0.87	0.36	175.10

It can be seen from Table 2.1 that the compounds have similar physical properties and thus explains the challenge in their separation. *dl*-Limonene is the only aliphatic in the *dl*-limonene-rich fraction, and other compounds are aromatics. A technique that separates them based on their molecular structure can be used.

Enhanced distillation is the oldest and most used technique for separating mixtures that are close boiling or form azetropes. This happens either by pressure variation or addition of a mass separating agent that alters the phase behaviour of the mixture, allowing the compounds to be recovered separately as overhead and bottoms product (Henley *et al.,* 2011).

Membrane separation is an alternative technique that is commonly combined with distillation for the separation of azeotropes. When a combination of distillation and other separation techniques are used, it is referred to as hybrid distillation (Henley *et al.,* 2011). This section outlines three promising methods for separation of TDO: membrane distillation hybrids, pressure swing and mass separating agent addition distillation methods.

Membrane distillation hybrids

Pervaporation is a membrane distillation hybrid process. Pervaporation utilises composite membrane with a low pressure on the permeate side of the membrane to evaporate the

permeate (Seader and Henley, 1998). The advantage of using membranes as a method of separation is that the selectivity is independent of the vapour-liquid equilibria. Pervaporation has relatively low permeate fluxes and the condensation temperature is very low, resulting in increased operational costs (Rautenbach and Vier, 1995). As industrial applications involve large throughput, pervaporation is not favoured as it can handle limited volumes (Rautenbach and Vier, 1995).

Pressure swing

By increasing or decreasing the pressure in a column, the azeotrope and/or the distillation boundaries can be moved. When pressure change results in an appreciable change in azeotrope composition, pressure-swing distillation can be used as an alternative separation technique. A change in azeotropic composition of at least 5% is required to render the technique feasible. Pressure swing entails the use of two columns; a low pressure column and high pressure column operated in series to recover the compounds separately in the two columns (Henley *et al.,* 2011).

However, the chemical compounds to be separated in TDO have high boiling temperatures at atmospheric pressure and increased pressure operation may lead to product degradation and also high energy requirements in the column. Therefore pressure swing distillation cannot be considered as an alternative to recovery of *dl*-limonene.

Mass separating agent addition methods

Homogenous azeotropic distillation: The entrainer facilitates the separation by forming a homogenous azeotrope with the original mixture components. This can be carried out in a single or double feed distillation column. The entrainer is added either at the upper or lower trays depending on whether the azeotrope is removed as overhead or bottoms (Henley *et al.,* 2011).

Heterogeneous azeotropic distillation: The entrainer facilitates the separation by forming a heterogeneous azeotrope with the original mixture components. This is usually carried out in a distillation column combined with a decanter system. The two liquid phases formed are separated with a decanter at the overhead, where one liquid is refluxed and the other removed as product (Henley *et al.,* 2011).

Extractive distillation: The entrainer facilitates the separation by being selective to one of the components of the original mixture. This is usually carried out in a double feed column, where the entrainer is introduced in upper trays above the original feed mixture (Henley *et al.*, 2011).

The main disadvantages with azeotropic/extractive distillation are the high energy consumption and large volumes of entrainer required.

Reactive distillation: The mass separating agent facilitates the separation by reacting preferentially and reversibly with one of the original components. The reaction products are separated from the unreacted components by distillation and the reaction is reversed to recover the targeted initial component as well as the mass separating agent. This is carried out in one column (Henley *et al.,* 2011).

Reactive distillation has advantages in that it supresses side product formation, can result in high selectivity and utilises the heat released from exothermic reactions, avoiding exhaustion of the reboiler. But the problems with reactive distillation include expensive packing/catalyst and complex design (Henley *et al.,* 2011).

Salt distillation: An ionic entrainer facilitates separation by dissociating in the original mixture and changing the relative volatilities sufficiently. The salt reduces the vapour pressure of the component it is more soluble in, allowing it to be recovered in the bottoms. This is carried in one column (Henley *et al.,* 2011).

The problems accompanied with salt distillation is corrosion, feeding and dissolving the salt in the reflux may cause clogging if the solubility of the salt is low and salt crystallization may occur within the column (Henley *et al.,* 2011).

The design of separation units requires understanding of thermodynamic principles to evaluate the viability of separation systems. Therefore, a study of properties of components in *dl*-limonene rich fraction is important.

Azeotropic systems

An azeotropic state is defined as a state in which the composition of a vapour (y_i) and liquid (x_i) phase remains the same (Perry and Green, 2003). At low to moderate pressure, the vapour-liquid equilibrium (VLE) compositional relationship can be expressed, as shown in Equation 2.1 (Smith *et al.*, 2005)

$$y_i P = x_i \gamma_i P_i^{sat} \quad (2.1)$$

At the azeotropic state, x_i=y_i for all i.

An ideal liquid has an activity coefficient (γ_i) of 1 and Equation 2.1 simplifies to Raoult's law. If (γ_i) > 1, the liquid is non-ideal and is said to show positive deviation from Raoult's law, and conversely negative deviation from Raoult's law if (γ_i) < 1. The deviation may be so large that temperature-composition phase diagram reach extrema. At such maxima and minima, the vapour and liquid composition remain constant and the azeotrope is formed (Perry and Green, 2003).

The azeotropic mixture has a constant boiling point. The azeotropic mixture's boiling temperature may be higher or lower than that of pure components in a mixture, i.e azeotropic-forming mixtures exhibit either maximum or minimum boiling points. Minimum boiling azeotrope occurs when deviations from Raoult's law are positive, and maximum boiling azeotrope is formed when deviation from Raoult's law are negative. Mixtures with small deviation from Raoult's law generally do not form an azeotrope. An azeotrope may be formed if the components are close boiling. Mixtures which boiling points difference is more than 30°C generally do not form azeotrope, even if large deviations from Raoult's law are present (Perry and Green, 2003).

Additionally, the azeotrope can be homogenous or heterogeneous. A homogenous azeotrope is when only one liquid exists; if more than one liquid phase is present, the azeotrope is heterogeneous. Heterogeneous azeotropes are minimum-boiling because activity coefficient must be greater than one to form two liquid phases (Perry and Green, 2003). However, immiscibility does not guarantee that the azeotrope will be heterogeneous. The system temperature and/or composition may fall outside the temperature and/or composition range at which the azeotrope forms (Perry and Green, 2003).

Phase equilibrium curves for binary systems are shown in Figure 2.2. The binary phase equilibria are expressed on a T-x-y (at constant pressure, P). Where x and y are the mole fraction in the liquid and vapour phase respectively measured at different temperatures, T. These diagrams can be expressed alternatively on an x-y or P-x-y diagram. The different phase equilibrium curves behaviour belongs to the following types (Raal and Mülbauer, 1998):

(a) Miscible systems with no azeotrope formation and have an intermediate boiling point

(b) Maximum boiling homogenous azeotrope systems

(c) Minimum boiling homogenous azeotrope systems

(d) Partially miscible liquid phases with a single heterogeneous azeotrope with a minimum or intermediate azeotropic temperature

(e) Systems with both homogenous and heterogeneous azeotrope and partial miscibility

(f) Partially miscible phases at intermediate pure component condensation temperature

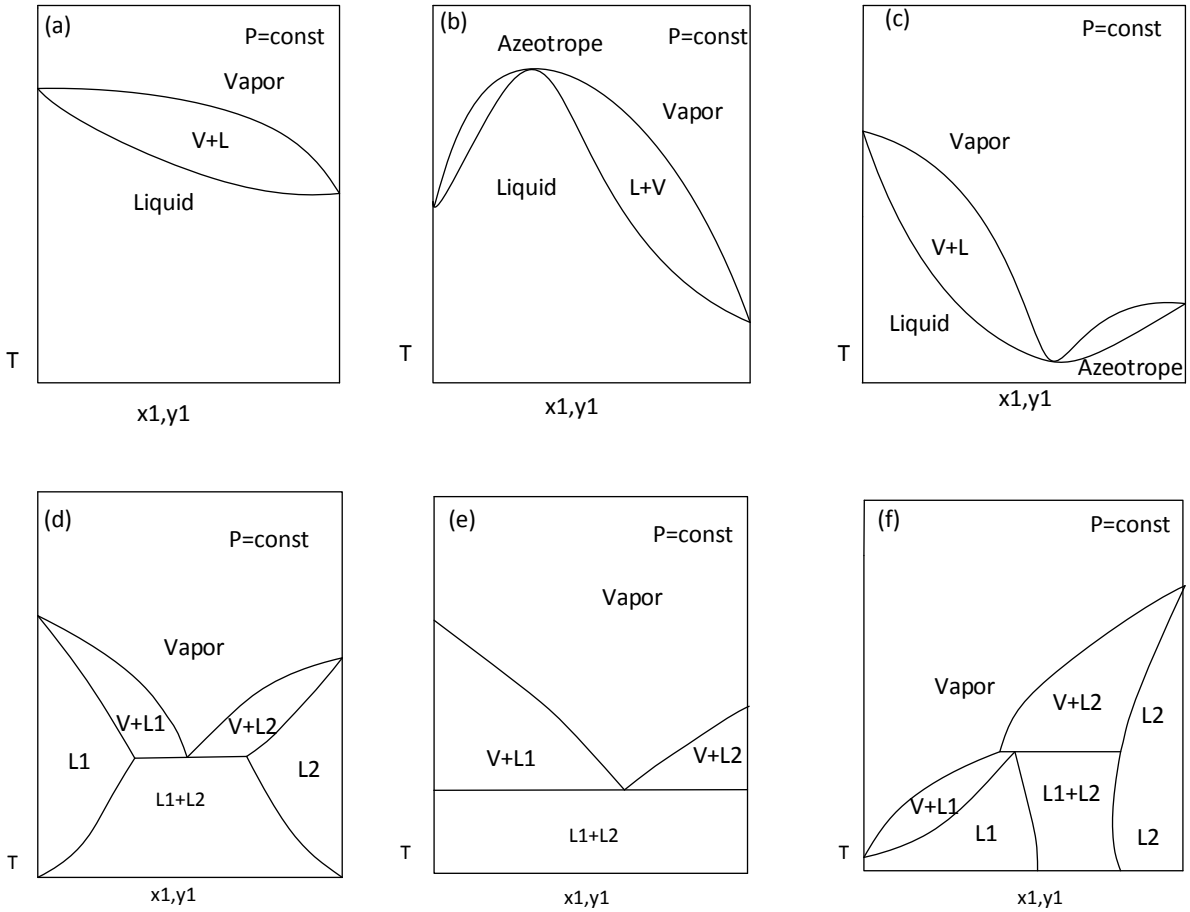

Figure 2.2 Phase diagrams with (a) intermediate boiling with no azeotrope; (b) maximum boiling azeotrope; (c) minimum boiling azeotrope; (d) immiscible liquid phases; (e) partially miscible liquid phases; (f) partially miscible phases at intermediate pure component condensation temperature (Redrawn from Raal and Mülbauer, 1998).

Proposed separation technology

In the petroleum and petrochemical industries, extractive/azeotropic distillation has been found effective in separating mixtures of aromatics/nonaromatics and naphthenes/ parafins. Extractive/azeotropic distillation uses both entrainer selectivity and volatility, therefore, it has one extra dimension to facilitate separation, resulting in high purity products. Azeotropic and extractive distillation technology has been fully developed in detail and a range of capable entrainers have been investigated (Lee, 2000).

Additionally, extractive/azeotropic distillation has the advantage of demanding less equipment i.e an extractive/azeotropic distillation column and entrainer recovery column. The number of units may increase, depending on the type of process feed and product specifications.

An example of a system similar to this study is the purification of 1,2,3-trimethylbenzene. Extractive distillation has been used successfully to purify 1,2,3-trimethylbenzene from solvent oil that contains mostly 1,2,3-trimethylbenzene and indane. A purity of over 99 wt% and recovery of 94% was achieved (Yu, 2008). This technique proved to be feasible, and therefore can be applied for *dl*-limonene enriched fraction, as it contains compounds with similar properties.

Although extractive/azeotropic distillation is used widely, information is required on the influence of operating conditions on the performance of the processes. The methods to be considered in these studies include extractive distillation and azeotropic distillation. These are discussed in detail in Section 2.5.

2.5. Enhanced distillation

2.5.1. Extractive distillation

Extractive distillation facilitates separation of close boiling or azeotropic mixtures by the addition of a suitable entrainer, which alters the mixture's relative volatility. The flow diagram of extractive distillation process is shown in Figure 2.3. This consists of an extractive distillation with a double feed and an entrainer recovery column.

Feed mixture is charged to the extractive distillation and the entrainer is fed at the upper section of the column, so it can remain largely in the liquid phase in the column. The entrainer facilitates separation by allowing one compound to be recovered as distillate, D1, and the other compound and entrainer to be recovered as bottoms, B1. The bottom products are fed to the entrainer recovery column. The recovery column is an ordinary distillation column which serves to separate the entrainer from the impurities, allowing them to be recovered as distillate, D2 and the entrainer as bottoms product, B2. The entrainer is recycled back to the extractive column.

To facilitate separation by extractive distillation, the entrainer must portray the following features (Perry and Green, 2003):

1. The entrainer must affect the phase behaviour of components of interest differently.
2. The entrainer must have a lower vapour pressure than key components in the extractive distillation column in order to remain mainly in the liquid phase.
3. The entrainer should not form additional azeotropes with feed components.

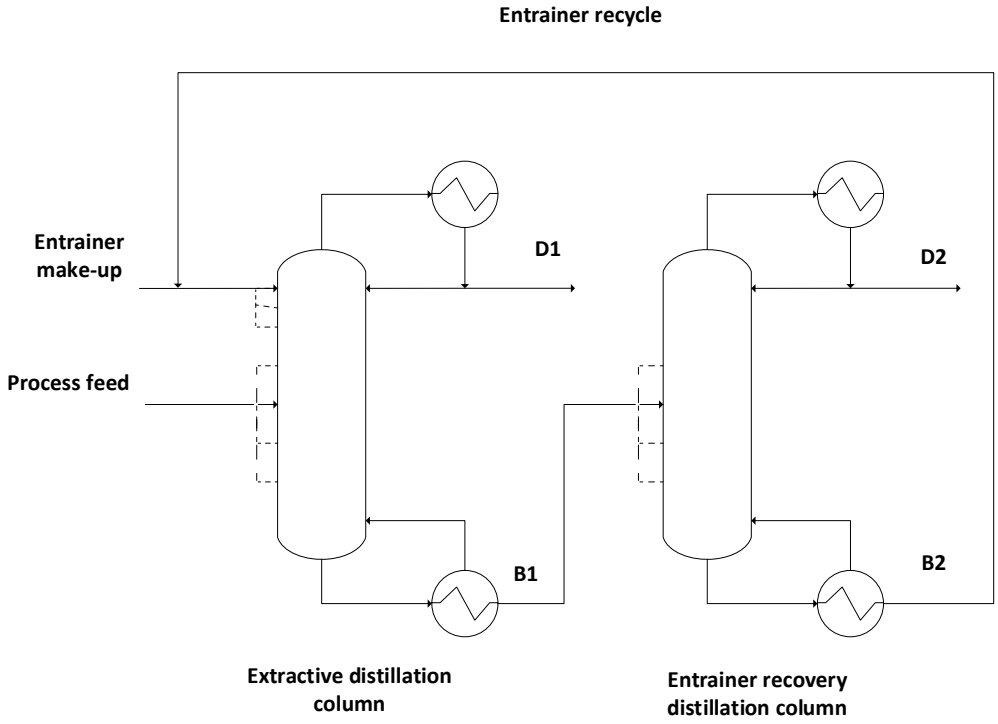

Figure 2.3 Flow diagram of extractive distillation process

The proper choice of an entrainer is necessary as it determines the viability of separation. Generally high entrainer to feed ratios are required. Not only does the entrainer need to adhere to the above mentioned characteristics, it must also be thermally stable, cheap, non-toxic, and easy to recover (Düssel & Warter 1998). If the entrainer is not easily recovered, additional recycling processes would need to be incorporated, which means additional investment and operation costs resulting from the added unit operations.

The activity coefficient has a greater influence on the relative volatility, as it is strongly dependent on composition and temperature. The entrainer reduces the non-ideality of the key component, with liquid phase behaviour similar to the entrainer, while enhancing the non-ideal behaviour of the different key component, resulting in positive deviation from Raoult's law. The activity coefficient of a component approaches unity, or may show negative deviation from Rault's law, if solvation or complexation interactions result (Perry and Green, 2003).

2.5.2. Homogeneous azeotropic distillation

Homogenous azeotropic distillation provides a flexible approach to separation. Unlike extractive distillation, homogenous azeotropic distillation is not limited by the formation of a new azeotrope or its boiling point (Henley *et al.,* 2011). Azeotropic distillation exploits azeotrope formation to change the boiling characteristics of the mixture. The entrainer may, therefore form a homogenous azeotrope with one or more components in the original mixture. The azeotropes formed may be minimum or maximum boiling, depending on whether the entrainer is low, intermediate or high boiling (Perry and Green, 2003). The boiling point and azeotropic formation of the entrainer assists efficiently in the screening of entrainers. Entrainers that do not show acceptable boiling point characteristics in the system can be discarded.

The flow diagram of homogenous distillation is shown in Figure 2.4. This consists of a single feed azeotropic distillation column and an entrainer recovery column. Azeotropic distillation columns can have a double feed like extractive distillation columns, depending on the optimisation of the process design. Feed mixture and entrainer are charged to the azeotropic distillation column. The entrainer allows one compound to be recovered as distillate, D1, and the other compound and entrainer to be recovered as bottoms, B1. The bottom products are fed to the entrainer recovery column. The recovery column can be ordinary distillation, liquid-liquid extraction or another enhanced distillation technique, which serves to separate the entrainer from the impurities, allowing them to be recovered as distillate, D2, and the entrainer as bottoms product, B2. The entrainer is recycled back to the extractive column. The type of the entrainer recovery column depends on the azeotropic composition and the azeotrope boiling temperature (Henley *et al.,* 2011). The entrainer may form a minimum boiling azeotrope with the distillate and result in entrainer loss with distillate (Lee, 2000). Henley *et al.* (2011) reported that it is not easy to find an entrainer for homogeneous

azeotropic distillation that involves a sequence of azeotropic distillation and ordinary distillation.

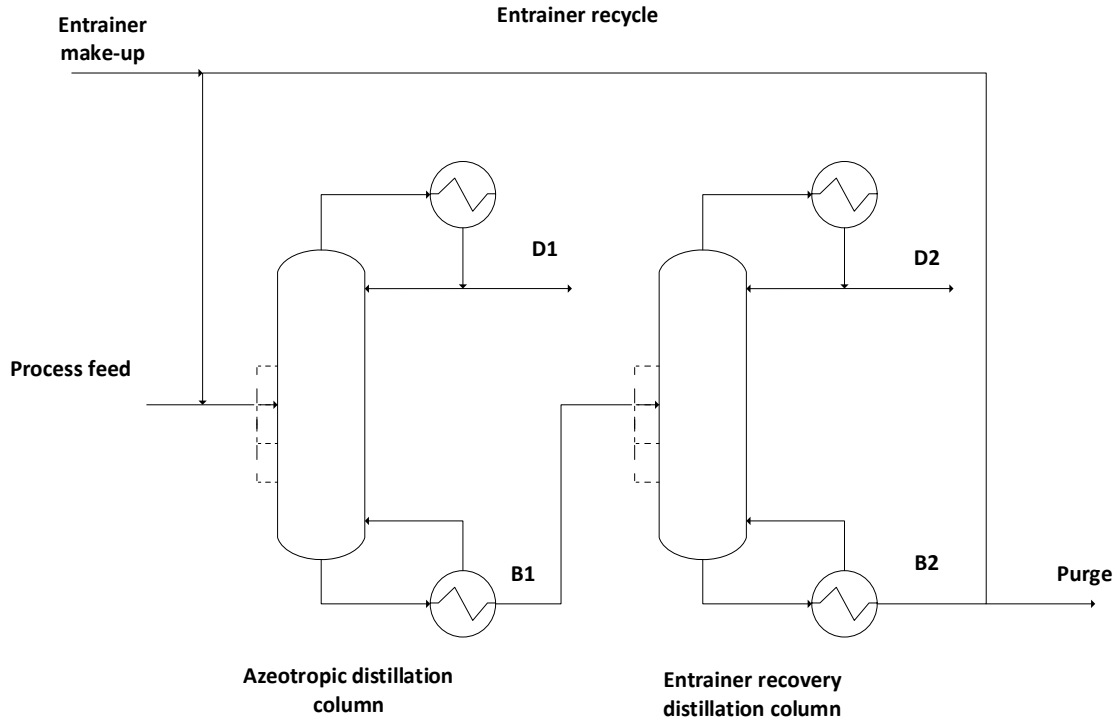

Figure 2.4 Flow diagram of homogenous azeotropic distillation process

2.5.3. Heterogeneous azeotropic distillation

Heterogeneous azeotropic distillation is an alternative to homogenous azeotropic distillation, since separation is achieved by utilising an entrainer that forms a binary or ternary heterogeneous azeotrope. Heterogenous azeotrope has two (or more) liquid phases (the organic phase and aqueous phase). The overall liquid phase composition is equal to that of the vapour phase. Therefore, if two liquid phases and a vapour phase are formed, all three phases will ultimately have different compositions (Henley *et al.,* 2011). Two liquid phase formation simplifies entrainer recovery and the recycling process and as a result, two liquid phases can simply be separated by the use of a decanter. Because two liquid phases are formed and can be easily separated, the restrictions that limit homogenous azeotropic distillation are overcome (Henley *et al.,* 2011).

The flow diagram of heterogeneous distillation is shown in Figure 2.5. This consists of a single feed azeotropic distillation column and an entrainer recovery column. Azeotropic distillation columns can have a double feed like extractive distillation columns, depending on

optimisation of the process design. Feed mixture and entrainer are charged to the azeotropic distillation column. The entrainer allows one compound to be recovered as distillate, D1, and the other compound and entrainer to be recovered as bottoms, B1. The bottom products are fed to the entrainer recovery column. The recovery column is ordinary distillation, which serves to separate the entrainer from the impurities, allowing them to be recovered as distillate, D2, and the entrainer as bottoms product, B2. The entrainer is recycled back to the extractive column (Henley *et al.,* 2011).

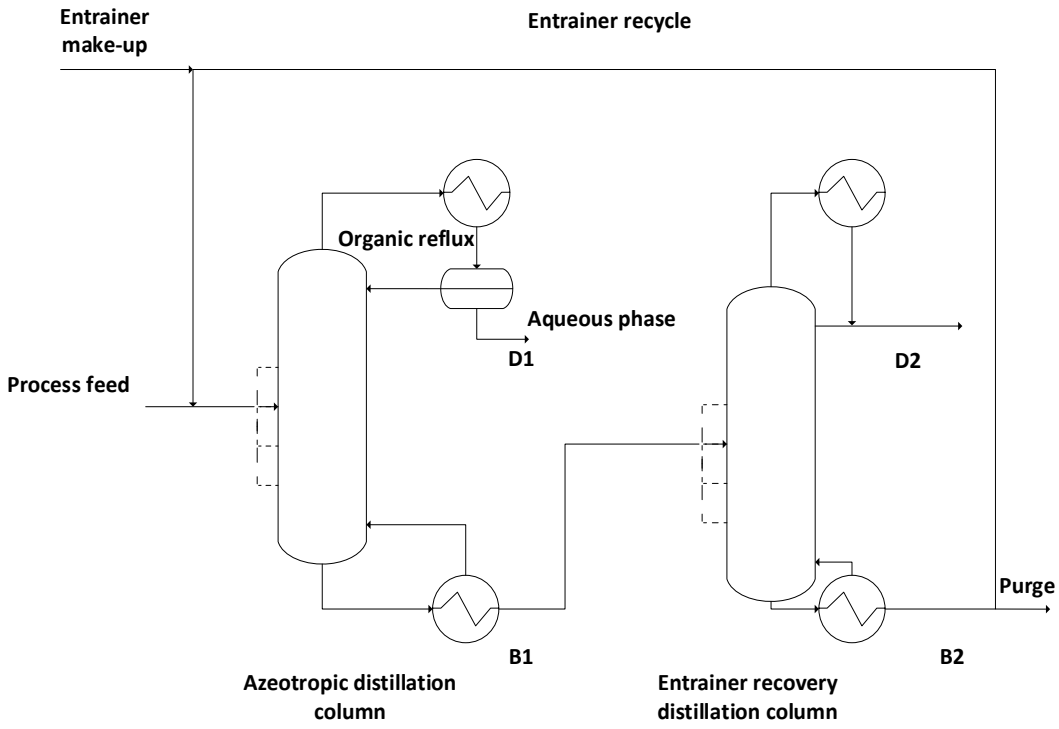

Figure 2.5 Flow diagram of heterogeneous azeotropic distillation process for a low boiling point azeotrope

2.5.4. Example of application of enhanced distillations

Separation of aromatic compounds from naphtha reforming is a common task in petrochemical plants. The feed consisting of a mixture of hydrocarbons is separated by ordinary distillation into fractions, after which a purification process is carried out. Fractionation columns of hydrocarbon feed mixture in petrochemical industries typically involve 47 to 75 number of theoretical stages (Yeo *et al.,* 2001; Zivdar *et al.,* 2014). This process entails utilisation of a series of distillation columns to concentrate the fractions. The

most common process is the separation of benzene, toluene and xylene (BTX) from naphtha (Kim *et al.,* 2003).

The capital cost of distillation columns is determined largely by the number of trays and the diameter. The operating cost is determined largely by the cost of utilities, i.e condenser cooling water and steam for the reboiler. As a large number of stages is required for most distillation processes, various works have been published on finding better control strategies.

Motahari and Arjmand (2002) investigated pre-fractionation and re-streaming of the feed to the distillation columns to conserve energy in the column for a BTX fraction. This was done by introducing a flash drum for pre-fractionation prior to feeding to the distillation column. The top and bottom product of the flash drum are fed in upper and lower trays of the distillation column respectively. This arrangement was found to minimise column diameter and reboiler duty (Motahari and Arjmand, 2002)

Zivdar *et al.* (2014) investigated the effect of revamping tray columns with structured packing. Mellapak structured packing was used for the investigation. The replacement of trays with packing was found to reduce pressure and therefore energy consumption of the column. Mellapak structured packing was found to reduce height of the tower and improve product quality for the separation of benzene and toluene from heavy aromatics.

The systematic design approach for recovery of *dl*-limonene, using continuous distillation columns is an important industrial process, but cannot be found in published work. In the petrochemical industries, extractive distillations have been found to be effective in separating mixtures of aromatics and non-aromatics. This section summarises the development of extractive and azeotropic distillation technologies for applications in the areas of aromatics and aliphatic purification from a mixture of hydrocarbons, which is believed to serve as guide in separating *dl*-limonene from a mixture of compounds in TDO.

Potential entrainers available in literature for extractive and azeotropic distillation of hydrocarbons are evaluated. These might not be the only entrainers available for such practise. The aim is to compare the degree of separation that can be achieved with different entrainers. This also entails eliminating certain inefficient entrainers upfront. The number of entrainers studied will be reduced, and only feasible entrainers will be used for the simulation

of the separation process. Examples of entrainers used by various authors are given in Table 2.2.

Table 2.2 Summary of previous work done for separation of aromatics and non-aromatics using extractive and azeotropic distillation

Citation	Process	Entrainer	Feed	Enhanced distillation Parameters	Entrainer recovery distillation Parameters	Result
Abushwireb *et al. (*2007)	Extractive distillation	n-Methyl pyrrolidone	C_5 to C_9 cut	E/F: 2 Number of stage: 72	Number of stages: 60	99 wt% purity of aromatics, non-aromatics and entrainer
Lee (2000)	Extractive distillation	Ethylene glycol	Cyclohexane and 2.3-dimethylpentane	E/F: 16 Reflux ratio: 0.48 Number of stages: 25 Entrainer feed stage: 12 Process feed stage: 24		85 wt% purity of cyclohexane
		Triethylene glycol	Cyclohexane and 2.3-dimethylpentane	E/F: 16 Reflux ratio: 0.48 Number of stages: 25 Entrainer feed stage: 12 Process feed stage: 24		92.4 wt% purity of cyclohexane
		n-Methyl pyrrolidone	Cyclohexane and 2.3-dimethylpentane	E/F: 16 Reflux ratio: 0.48, Number of stages: 25 Entrainer feed stage: 12 Process feed stage: 24		91wt% purity of cyclohexane
Ko *et al. (2002)*	Extractive distillation	Formyl-morpholine	C_5 to C_9 cut	E/F: 3.5 Number of stages: 77		99% extraction of aromatics

Table 2.2 (cont.) Summary of previous work done using various entrainers

Citation	Process	Entrainer	Feed	Enhanced distillation Parameters	Entrainer recovery distillation Parameters	Result
Vega *et al.* (1997)	Homogenous azeotropic distillation	Dimethyl formamide	C_5 to C_9 cut	E/F: 3 Reflux ratio: 3 Number of stages: 15		99% extraction of aromatics
Suppino and Cobo (2014)	Extractive distillation	Ethylene glycol and water	Benzene, cyclohexene and cyclohexane	Number of stages: 50 Reflux ratio: 3 Entrainer feed stage: 2 Process feed stage :10	Number of stages: 10 Reflux ratio: 3	99 wt% purity of benzene cyclohexene and cyclohexane
		Methyl pyrrolidone and water	Benzene, cyclohexene and cyclohexane	Number of stages: 30 Reflux ratio: 1.3 Entrainer feed stage: 1 Process feed stage: 14	Number of stages: 30 Reflux ratio: 3	99 wt% purity of benzene, cyclohexene and cyclohexane
Mikitenko *et al.* (1975)	Heterogeneous azeotropic distillation	Dimethyl formamide and Water	Benzene cut	Number of stages: 65 E/F: 3.2 Reflux ratio: 2.4	Number of stages: 40 Reflux ratio: 0.67	99 wt% purity of benzene

2.5.5. Process modelling of enhanced distillation process

A methodology for the design and optimisation of extractive and azeotropic distillation proposed by Lek-utaiwan *et al.* (2011) is presented in this section. This is a general technique used in process modelling of extractive/azeotropic distillation systems. Lek-utaiwan *et al.* (2011) illustrated the use of this method for separation of ethylbenzene and xylene rich mixture with various entrainers from chemical group of aromatic, amine, aldehyde, ester, amide and ketone. A block flow diagram of the process modelling procedure is shown in Figure 2.6.

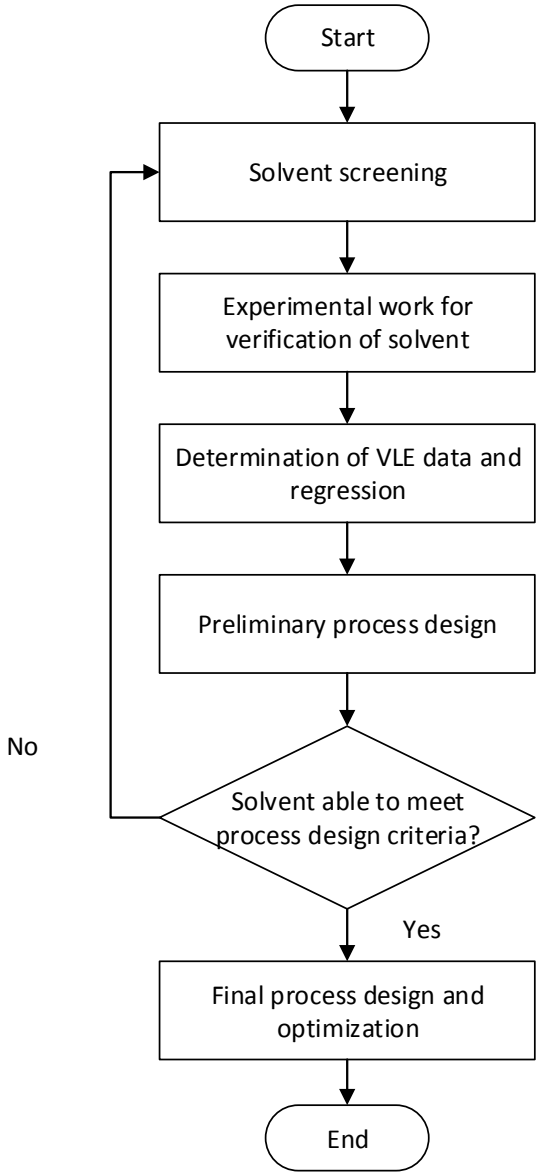

Figure 2.6 Designed methodology for extractive/azeotropic distillation (Lek-utaiwan *et al.,* 2011).

The first step entails entrainer screening and ranking of candidate entrainers. This entails analysis of ternary systems, which includes the entrainer and the binary mixtures to be separated using a computer simulator such as Aspen Plus® with various property models. Activity coefficient models are recommended as they have better accuracy in predicting the behaviour of systems containing non-ideal components with different molecular structures. Residue curve maps (RCM) are used for analysis of entrainer feasibility. The selection of the best entrainer is based on the degree at which the entrainer can alter the driving force. This driving force is defined as the difference in composition between the light key component vapour and liquid composition. The ranking of the entrainers using this approach may be inconclusive without a good property prediction model, owing to missing or inaccurate interaction parameters. Experimental verification is required to validate the selected entrainer (Lek-utaiwan *et al.,* 2011).

The second step entails verification of three to five promising entrainers from the first step using experimental work. The effect of entrainer to feed ratio (E/F) on the driving force is determined. The driving force from experimental work and prediction by simulation models for extractive distillation were compared by Lek-utaiwan *et al.* (2011) for a system consisting of xylene and ethylbenzene, using various entrainers. Lek-utaiwan *et al.* (2011) found large deviations between model and experimental data, with percentage errors as high as 300%. Experimental and model data also led to different entrainer rankings and entrainer effectiveness, showing the relevance of experimental verification and the need for VLE data.

The third step entails the determination of VLE data and regression of the data to obtain improved accuracy of the process simulation. This step can also be done using readily available VLE data in literature.

The fourth step entails preliminary process design of the azeotropic/extractive distillation column, and the entrainer recovery column. A computer simulator such as Aspen Plus ® is used with the regressed VLE data. A basic economic evaluation is conducted and the entrainer that results in low energy consumption and capital costs, is chosen for the final detailed design and optimisation.

The final step entails optimisation of the process design using the best entrainer and separation process configuration. Optimisation is attained by setting an appropriate objective

function, such as the payback period or annual cost objective. The manipulated variables in the extractive/azeotropic distillation are entrainer to feed ratio (E/F), reflux ratio (RR), distillate to feed ratio (D/F), feed locations and number of stages. The algorithm for optimisation of the process design is shown in Figure 2.7.

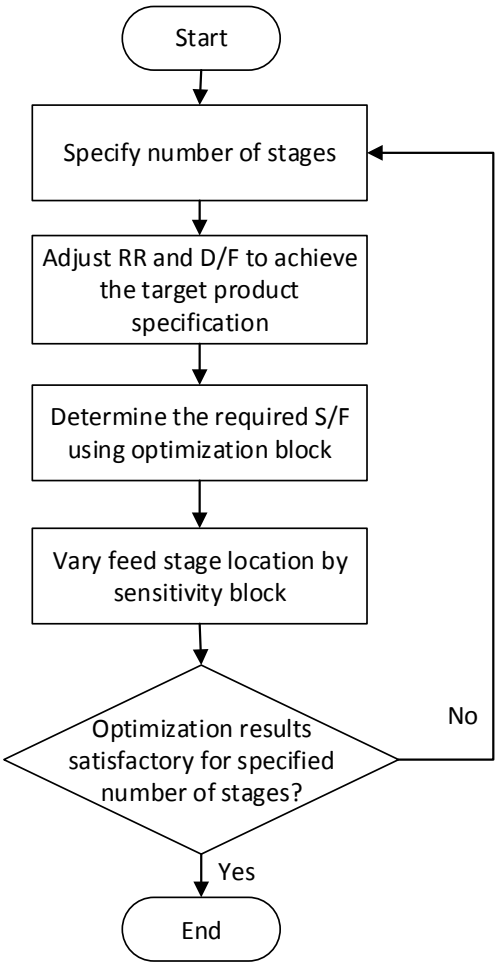

Figure 2.7 Optimization algorithm (Lek-utaiwan *et al.,* 2011).

In the first step, the number of stages is estimated. The RR and D/F are varied to achieve the targeted product specification in the second step. The E/F ratio is then varied and optimised, using the optimisation block in the third step. Lastly, the feed location is varied using a sensitivity block. The optimum conditions at the specified number of stages can be found. The number of stages can be varied manually and the cycle is repeated to find optimum design parameters.

Lek-utaiwan *et al.* (2011) demonstrated the applicability of the proposed methodology for separation of ethylbenzene and mixed xylenes. The separation of these compounds to attain a purity above 99% would require 202 stages, which is impractical.

The lack of accurate interaction parameters for the property model can result in incorrect entrainer selection and inaccurate process design. Experimental verification of candidate entrainers for extractive/azeotropic selection is very important. Moreover, VLE data is required to obtain accurate binary interaction parameters in Aspen Plus ® for accurate and detailed design.

2.5.6. Residue curve map (RCM) technology

The feasibility test of entrainers is of utmost importance. RCM technology is a popular method used for this purpose. RCM is a geometric representation of phase behaviour of multicomponent mixtures. It represents the liquid-residue composition (mass or mole fraction) in the still, with time, during continuous evaporation at a fixed pressure and condition of vapour-liquid equilibrium (Henley *et al.,* 2011). It shows the phase behaviour that directly impacts on distillation. This is represented on a triangular diagram with pure component on the vertices, connected by lines to form binary edges binding a composition area. Boiling points and azeotropes, whether binary (on the borders of the triangle) or ternary (within the triangle), are indicated on the diagram. The composition trajectories move from lightest component to the heaviest in the mixture. This is due to the increase in temperature as the liquid-residue gets richer in the heavier component. More details on residue curves can be found elsewhere (Doherty and Malone, 2001). A typical RCM diagram for a mixture containing a typical mixture of compound A and B and entrainer E, is shown in Figure 2.8 for illustration.

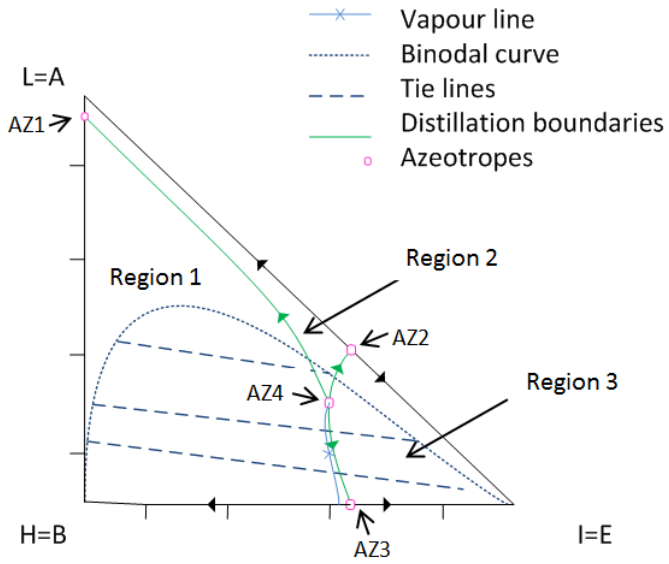

Figure 2.8 RCM (Redrawn from Seader *et al.* (2009))

where L is the Lowest boiler, I is the intermediate boiler and H is the highest boiler.

As can be seen in Figure 2.8, this multicomponent mixture forms two binary homogenous azeotropes; AZ1 and AZ2, and two heterogeneous azeotropes; AZ3 and AZ4. The residue curve starts at the lightest boiler, which is AZ4 and moves towards AZ1, AZ2 and AZ3. This creates a boundary connecting the azeotropes. The distillation boundary divides the composition space into three distillation regions. In each region the residue curves move in a different direction.

A binodal curve exists, which represent an area of liquid-liquid equilibrium. A vapour line which shows the vapour composition in equilibrium with the two liquid phases is shown on the diagram. The two liquid phase compositions for a specific vapour composition can be obtained from the two ends of the tie-lines.

A distillation boundary may be crossed if a binodal curve exits. If a region of liquid-liquid de-mixing does not exist, the distillation boundary cannot be crossed and the two components to be separated need to lie in the same distillation region in order for them to be removed separately as distillate and bottom products (Henley *et al.,* 2001).

Aspen Plus® is available for generating RCM from thermodynamic physical-property model for the system under investigation. A method for screening entrainers suggested by Julka *et al.* (2009) is explained below.

1. Compile a list of entrainers; these may be components that are already present in the mixture to be separated or entainers used for similar systems. A good starting point is choosing water as it forms heterogeneous azeotropes with many components.

2. Construct an RCM using a detailed thermodynamic physical property model. If there is no phase equilibrium data, UNIFAC activity coefficient model can be used to estimate missing properties. However, this needs to be verified experimentally.

3. Analyse the RCM to see if distillation boundaries, azeotropes and liquid-liquid regions exist. An entrainer is considered feasible if, either the entrainer does not divide the components to be separated into separate distillation regions, or the entrainer forms a region of liquid-liquid equilibrium allowing crossing of the distillation boundaries.

When the type of entrainer is known, the number of distillation columns and decanters and their interconnections can be determined and the separation processes can be designed. The entrainers are lastly evaluated on the overall process economics (Julka *et al.,* 2009).

2.6. Phase behaviour and thermodynamics

2.6.1. Thermodynamic models

Phase equilibrium describes the distribution of species among two or more phases in equilibrium, which determines the extent to which separation can be achieved (Smith *et al.,* 2005). Phase equilibrium is calculated based on the fugacity, which is the measure of the tendency of a component to exit a phase. Equilibrium is reached when the fugacity of the component are equal in all phases (Smith *et al.,* 2005). In this study, the two types of property models are briefly discussed.

1. **Equations of state models:** An equation of state (EOS) is a pressure-molar volume-temperature (PVT) relation used to determine thermodynamic properties. This includes the cubic and the virial EOS's. There are several EOS used for different systems. Examples of cubic EOS include: Peng-Robinson and the Soave-Redlich-Kwong EOS and their variations (Smith *et al,* 2005).
2. **Activity coefficient models:** For systems where the liquid phase deviate from ideality, the fugacities of the components in the solution deviate from that of the pure component. The ratio of the fugacity in solution to that of pure component is defined as the activity (Smith *et al.,* 2005). There are several activity coefficient models. The models include: NRTL, Wilson, Van Laar, UNIFAC and UNIQUAC. In these models, the activity coefficient approach is used to calculate the liquid properties, while the vapour phase properties are calculated using EOS (Smith *et al,* 2005).

When the activity coefficient is greater than 1, it means that the fugacity of a component in mixture is higher than that of pure component. Thus, the same component will have higher tendency to vaporise when in a mixture than in its pure state. This is a result of increased repulsion between molecules with mixtures. When the activity coefficient is less than unity, it indicates that there is increased attraction between molecules. In this case the liquid will have a low tendency to vaporize (Smith *et al,* 2005).

EOS models are recommended for non-polar systems and in supercritical regions where activity coefficient models are limiting. Activity coefficient models are recommended for complex liquid mixtures. The use of activity coefficient models requires accurate vapour pressure data at the system temperature. Prediction of vapour pressure in Aspen Plus® V8.2 can be done using equations like Antoine or Wagner (Laar, 2006). Activity coefficient models are accurate for phase equilibrium calculations, provided that binary interaction parameters are available (Smith *et al,* 2005).

A choice of the correct thermodynamic model is essential, and it depends on the system under investigation and the error margin. Binary VLE data can be used to obtain the binary interaction parameters using regression. The resulting model prediction can be plotted with experimental data to check the fit. The model which gives a better fit at the region of operating condition of the separation process, is then used. For binary pairs with no readily available VLE data, the UNIFAC model can be used to estimate the binary interaction parameters. However, these parameters are unreliable and may increase uncertainty in the model. Additionally, activity coefficient models and binary interaction parameters generally do not predict ternary systems well. Binary interaction for EOS models can also be estimated using group contribution models (Smith *et al,* 2005).

2.6.2. Selection of thermodynamic models

Many thermodynamic models have been developed over the years and are used widely in industries for design of chemical processes. The thermodynamic model can be chosen initially based on heuristics. It is important that the thermodynamic model provide the desired level of accuracy. Eric Carlson, Bob Seader and Aspen Plus® package provide recommendations for selecting a thermodynamic model (Henley *et al.,* 2001; Seider *et al.,* 2004). If there is readily available VLE data, different thermodynamic models can be fitted to the data to see which model predicts the data best.

Table 2.3 provides commonly used methods with hydrocarbon systems such as those involved in the oil and gas industries, which contain compounds similar to TDO (Chen and Mathias, 2002).

Table 2.3 Choice property models used in process industries (Chen and Mathias, 2002)

Chemical systems	Primary choice model	Secondary choice models	Problem areas
Petroleum and refining	BK 10, Chao-Seader, Grayson-Streed, Peng-Robinson, Soave-Redlich-Kwong		Heavy crude characterization
Petrochemicals-VLE	Peng-Robinson, Soave-Redlich-Kwong, PSRK	NRTL, UNIQUAC, UNIFAC	Data, Parameters
Petrochemicals-LLE	NRTL, UNIQUAC		Data, Parameters, Models for VLLE systems
Oligomers	Polymer NRTL	UNIQUAC, UNIFAC	Pure component fugacity, Databanks

From Table 2.3 it can be seen that NRTL and UNIQUAC have found diverse applications in petrochemical industries, which is where this study falls in. Therefore, a detailed study of the viability of these models is required.

2.6.3. Binary VLE data

This section provides graphical representation of readily available VLE data in literature with different property models in Aspen Plus® V8.2. The binary interaction parameters are estimated with the UNIFAC model. The model predictions are plotted against published experimental data obtained from Zhangfa *et al.* (2009) in Figure 2.9 on a T-x-y diagram for l-limonene and p-cymene. Both activity coefficient and equation of state models are tested for verification. Pure component vapour pressures data for limonene and cymene (type of isomer unknown) obtained from Perry and Green (2003), are compared to that predicted by Aspen Plus® V8.2, as shown in Figure 2.10 and Figure 2.11.

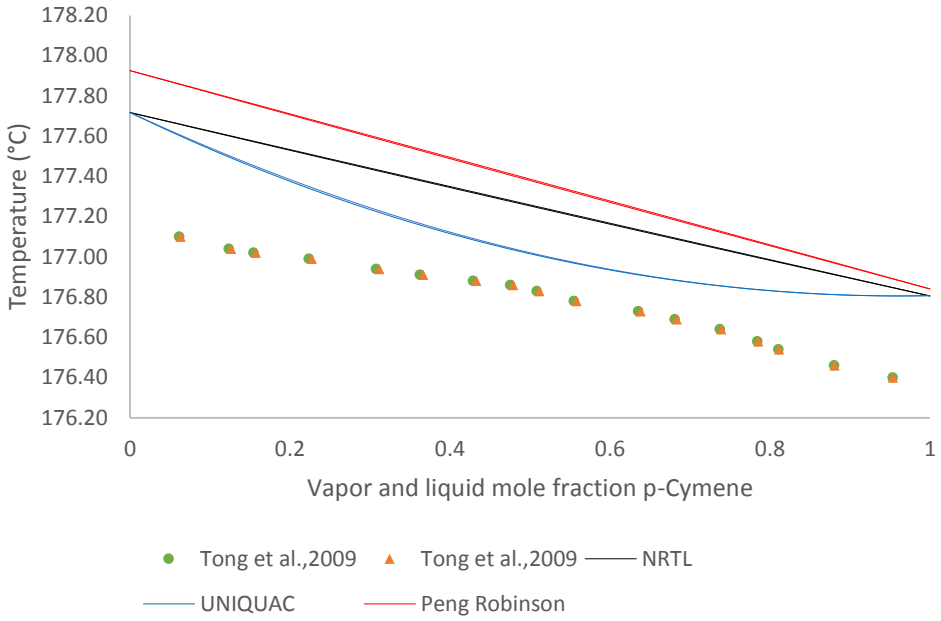

Figure 2.9 Binary Txy phase diagram of p-cymene/l-limonene VLE data at 1 bar

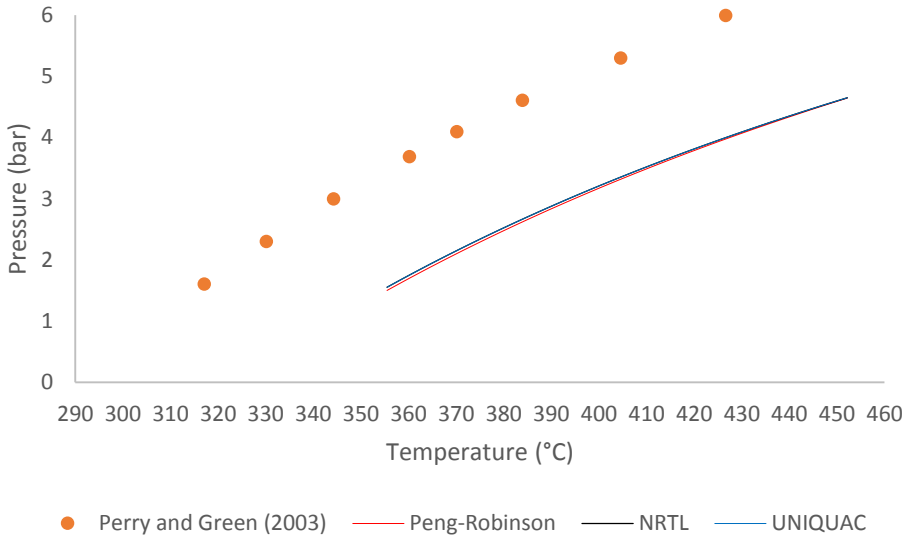

Figure 2.10 Pure component vapour pressure curve for cymene

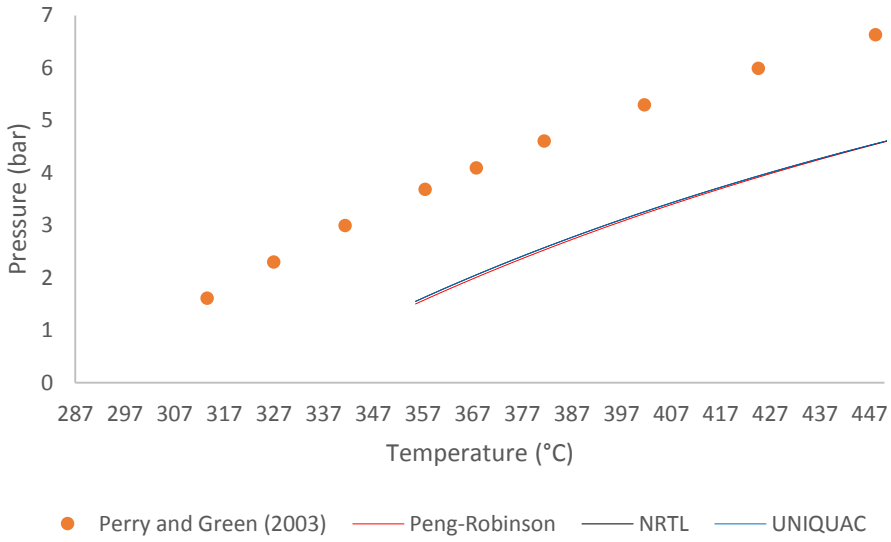

Figure 2.11 Pure component vapour pressure curve for *d*-limonene

From Figure 2.9 it can be seen that the mole fraction of p-cymene in each phase at equilibrium is constant. This indicates that the relative volatility of the components is close to one, and therefore p-cymene cannot easily be separated from l-limonene by ordinary distillation. This agrees with findings obtained by Pakdel *et al*. (2001) where *dl*-limonene could not be separated from m-cymene. From Figure 2.9 it can also be seen that there is an error in prediction of experimental data for l-limonene and p-cymene, with estimated binary interaction parameters in Aspen Plus® V8.2.

From Figure 2.10 it can be seen that the activity coefficient models and Peng-Robinson over predict the pure component pressure of cymene. A similar behaviour is observed for pure component vapour pressure curve for limonene, as seen in Figure 2.11. The thermodynamic models over predict the boiling point of d-limonene at atmospheric pressure, which explains the inability of the model to fit experimental binary VLE data of p-cymene and l-limonene accurately. Therefore, it is necessary to obtain accurate experimental pure component and VLE data prior to regression in Aspen Plus® V8.2.

2.7. Conclusion

Obtaining a *dl*-limonene enriched naphtha fraction from TDO has been investigated by various authors and proved possible. However, getting a high purity *dl*-limonene has not been executed successfully, due to the presence of close boiling compounds not separable by ordinary distillation.

Separation of chemical compounds from TDO therefore remains a relatively untouched field in current research. Literature provides information on separation and purification of aromatics and non-aromatics from petrochemical cuts, but presents no information specifically on purification of systems containing *dl*-limonene on an industrial scale. Feasibility of separation of *dl*-limonene from TDO using the same principles can be tested using simulation models. This will assist in evaluating different process configurations and understanding impact of changes in process variables on the recovery of high purity *dl*-limonene.

When considering extractive/azeotropic distillation to enhance separation, different types of entrainers from chemical groups of polyols, amides and amines have been investigated, and resulted in high recovery and purity of aromatic and non-aromatic hydrocarbons. Therefore, investigating the influence of these entrainers for removal of aromatics from *dl*-limonene enriched naphtha fraction is worth the exercise.

Thermodynamic properties data is required to design and analyse the operation of separation equipment. The NRTL, UNIQUAC and Peng-Robinso model failed to predict binary VLE data as well as pure component vapour pressure data of limonene and cymene. Phase equilibrium data of compounds available in TDO and entrainers are required to determine the degree of separation. Due to insufficient vapour-liquid and vapour-liquid-liquid equilibrium data, estimation method using UNIFAC model will be used to predict the missing parameters. However, VLE and VLLE estimated from binary data, or methods such as UNIFAC, may not be able to accurately predict the phase equilibrium, but provide for a good base case.

Azeotropic and extractive distillation has shown to be a viable technique for separation of close boiling compounds.The feasibility of candidate entrainers used in literature will be investigated in this thesis.

A methodology for the design and optimisation of extractive and azeotropic distillation proposed by Lek-utaiwan *et al.* (2011), proved to be effective in understanding the impact of different process variables in the design of extractive and azeotropic distillation column. The methodology by Lek-utaiwan *et al.* (2011) will offer guidelines in developing process models for separation of TDO using extractive and azeotropic distillation. The method illustrated that incorporating entrainer screening, experimental verification of entrainers, VLE data analysis, process design, economic evaluation and optimisation are essential in completing a

separation process design exercise for system forming azeotropes, and/or close boiling in nature.

Wotjowicz and Serio (1996) recommended the recovery of valuable chemicals from TDO to improve the economics of tyre pyrolysis. This study will consider recovery of *dl*-limonene, as it is the most abundant chemical in TDO. Thereafter, an economic analysis will be done to access the economic performance of the developed process models.

Experimental techniques used in literature resulted in low purity limonene. Fractionation of TDO to obtain a *dl*-limonene enriched naphtha fraction in a single stage batch distillation setup used in studies by Stanciulescu and Ikura (2006) will serve purpose in this study, after which purification is done using enhanced distillation.

2.8. References

Abushwireb, F., Elakrami, H. and Emtir, M. 2007. Recovery of aromatics from pyrolysis gasoline by conventional and energy integrated extractive distillation. 17th European symposium on computer aided process engineering. *Elsevier B.V*.

ASPEN TECHNOLOGY. 2009. Aspen Simulation User guide. Burlington, MA: Aspen Techchnology.

Banar, M., Akyildiz, V., Özkan, A., okaygil, Z.C and Ö. Onay. 2012. Characterization of pyrolytic oil obtained from pyrolysis of TDF (Tire Derived Fuel). *Energy Convers. Manage*, 62: 22–30.

Billal, S.F., Elamin, I.H.M., Mustafa, H.M. and Gasmalseed, G.A. n.d. Separation of Azeotropes by Shifting the Azeotropic Composition.

Boxiong, S., Chunfei, W., Binbin, G. and Rui, W., 2007. Pyrolysis of waste tyres: the influence of USY catalyst/tyre ratio on products. *Appl. Catal. B: Environ*, 78: 243-249.

Brown, W.D. 1963. Economics of Recovering Acetic Acid. *Chem. Eng. Prog,* 59: 65–68.

Chen, B., Lei, Z. and Li, J. 2003. Separation on Aromatics and Non-aromatics by Extractive Distillation with NMP. *Journal of chemical engineering of Japan,* 36: 20–24.

Chen, C.C. and Mathias, P.M. 2002. Applied thermodynamics for process modeling. *AIChE Journal,* 48: 194–200.

Choi, G.G., Jung, S.H., Oh, S.J. and Kim, J.S. 2014. Total utilization of waste tire rubber through pyrolysis to obtain oils and CO2 activation of pyrolysis char. *Fuel Processing Technology*, 123: 57–64.

Conesa, J.A., Font, R. and Marcilla, A. 1996. Gas from the pyrolysis of scrap tires in a fluidised bed reactor. *Energy and Fuels,* 10: 134–140.

Cunliffe, A.M., Williams, P.T., 1998a. Composition of oils derived from the batch pyrolysis of tyres. *Journal of Analytical and Applied Pyrolysis, 44*: 131–152.

Dai, X., Yin, X., Wu, C., Zhang, W. and Chen, Y., 2001. Pyrolysis of waste tires in a circulating fluidized-bed reactor. *Energy,* 26: 385–399.

Danon, B., van der Gryp, P., Schwarz, C.E. and Görgens, J.F., 2015. A review of dipentene (*dl*-limonene) production from waste tire pyrolysis. *Journal of Analytical and Applied Pyrolysis,* 112: 1–13.

Perry, E. S. and Weissberger, A. 1965. *Distillation*. New York: Wiley and Sons.

Doherty, M.F. and Malone, M.F. 2001. *Conceptual design of distillation systems*. New York: McGraw-Hill.

Düssel, R., Wei*dl*ich, U., Warter, M. and Stichlmair, J. 1998, Systematisierung der Azeotroprektifikation und thermodynamische Kriterien zur Entrainerauswahl. *GVC-Jahrestagung, Freiburg*.

EI-Bassuoni, A.A. and Esmael, K.K. 2004. Extraction of Aromatics from Heavy Naphtha Using Different Solvents.

Florida Chemical Co., 1991a. Marketing Data Sheet: d-limonene. Lake Alfred, FL

Florida Chemical Co., 1991b. Product Data Sheet: d-limonene. Lake Alfred, FL

Florida Chemical Co., 1991c. Material Safety Data Sheet: d-limonene. Lake Alfred, FL

Gmehling, J., J. Menke, J. Krafczyk and K. Fischer. 1994. *Azeotropic Data, Part I and Part II*. New York: VCH-Publishers, Weinheim.

Green Terpene ™.2014. [Online]. Available: www.greenterpene.com [2014, June 20]

Henley, E.J., Seader, J.D. and Roper, D.K. 2011. *Separation Process Principles*. Wiley.

Henley, E.J., Seader, J.D., Roper, D.K. 2011. *Separation Process Principles*. Wiley.

Hildebrand, J.H. and Scott, R.L. 1950. Solubility of none electrolytes. Monograph Series, New York: Reinhold

Hömmerich, U. and R. Rautenbach. 1998. Design and Optimization of Combined Pervaporation/Distillation Processes for the Production of MTBE. *J. Membrane Sci*, 146: 53–64

Javadli, R. and de Klerk, A. 2012. Desulfurization of heavy oil. *Appl Petrochem Res*, 1:3–19

Jukić, A. n.d. Petroleum Refining and Petrochemical Processes. Croatia: University of Zagreb.

Julka, V., Chiplunkar, M. and O'Young, L. 2009. Selecting entrainers for azeotropic distillation. Clearwaterbay technology.

Kaminsky, W. and Sinn, H. 1980. Pyrolysis of plastic waste and scrap tyres using a fluidised bed process. *American Chemical Society Symposium Series,* 130.

Kaminsky, W., Mennerich, C. and Zhang, Z. 2009. Feedstock recycling of synthetic and natural rubber by pyrolysis in a fluidized bed. *Journal of Analytical and Applied Pyrolysis,* 85: 334–337.

Kim, Y.H., Choi, D.W. and Hwang, K.S. 2003. Industrial application of an extended fully thermally coupled distillation column to BTX separation in a naphtha reforming plant. *Korean Journal of Chemical Engineering*, 20: 755–761.

Ko, M.S., Na, S., Cho, J. and Kim, H. 2002. Simulation of the aromatic recovery process by extractive distillation. *Korean Journal of Chemical Engineering*, 19: 996–1000.

Kyari, M., Cunliffe, A. and Williams, P.T. 2005. Characterisation of oils, gases and char in relation to the pyrolysis of different brands of scrap automotive tires. *Energy and Fuels*, 19: 1165–1173.

Laar, V. 2006. Activity Coefficient Models. Aspen Physical Property System 77.

Laresgoiti, M.F., Caballero, B.M., de Marco, I., Torres, A., Cabrero, M.A. and Chomón, M.J. 2004. Characterization of the liquid products obtained in tyre pyrolysis. *Journal of Analytical and Applied Pyrolysis*, 71: 917–934.

Lee, F.M.2000.Extractive distillation. *GTC Technology Corporation*. Houston, TX, USA.

Lek-utaiwan, P., Suphanit, B., Douglas, P.L. and Mongkolsiri, N. 2011. Design of extractive distillation for separation of close-boiling mixtures: Solvent selection and column optimization. *Computer and Chemical engineering,* 35: 1088-1100.

Luyben, W.L., Chien, I.L. 2011. Design and Control of Distillation Systems for Separating Azeotropes. John Wiley & Sons.

Mikitenko, P., Cohen, G. and Asselineau, L. 1975. Process for purifying benzene and toluene by extractive azeotropic distillation. Institut Francais du Petrole, des Carburants et Lubrifiants.

Mikitenko, P. and Asselineau, L. 1979. Process for purifying benzene and toluene by extractive azeotropic distillation. Institut du Petrole.

Motahari, K., Arjmand, M., 2010. Flash zone optimization of BTX fractionation unit. 2nd International Conference on Engineering Optimization.

Muzenda, E. and Popa, C. 2015. Waste Tyre Management in Gauteng, South Africa: Government, Industry and Community Perceptions. *International Journal of Environmental Science and Development*, 6: 311–315.

Pakdel, H., Pantea, D.M. & Roy, C. 2001. Production of *dl*-limonene by vacuum pyrolysis of used tires. *J. Anal. Appl. Pyrolysis*, 57: 91–107.

Pakdel, H., Roy, C., Aubin, H. and Jean, G., Coulombe, S. 1991. Formation of *dl*-limonene in used tire vacuum pyrolysis oils. Environmental Science & Technology 25, 1646–1649.

Perry, R.H. and Green, D.W. 2003. Perry's chemical engineers' handbook. New York: McGraw-Hill.

Pilusa, J. and Muzenda, E. 2013. Qualitative analysis of waste rubber-derived oil as an alternative diesel additive. *International Conference on Chemical and Environmental Engineering.*

Prausnitz, J.M and Anderson, R. 1961. Thermodynamics of solvent selectivity in extractive distillation of hydrocarbons. *AIChE J*.

Prayoonyong, P. and Jobson, M., 2010. Design of complex distillation columns separating ternary heterogeneous azeotropic mixtures. UK: The University of Manchester.

Qu, W., Zhou, Q., Wang, Y.Z., Zhang, J., Lan, W.W., Wu, Y.H., Yang, J.W. and Wang, D.Z. 2006. Pyrolysis of waste tire on ZSM-5 zeolite with enhanced catalytic activities. *Polymer Degradation and Stability,* 91: 2389–2395.

Raal, J.D. and Muhlbauer, A.L. 1998. Phase equilibria measurement and computation. Taylor and Francis.

Rautenbach, R. and J. Vier.1995. Design and Analysis of Combined Distillation/Pervaporation Processes. Proc. *Seventh International Conference on Pervaporation Processes in the Chemical Industry, Reno (NV)*, 70–85.

Rofiqul, I.M., Haniu, H. and Rafiqul, A.B.M. 2007. Limonene-rich liquids from pyrolysis of heavy automotive tire wastes. *J. Environ. Eng,* 2: 681–695.

Roy, C. and Unsworth, J. 1989 Pilot plant demonstration of used tires vacuum pyrolysis. *Elsevier Applied Science*.

Roy, C., Chaala, A. and Darmstadt, H., 1999. The vacuum pyrolysis of used tires: end uses for oil and carbon black products. *Journal of Analytical and Applied Pyrolysis*, 51: 201–221.

Seader, J.D. and E.J. Henley. 1998. *Separation Process Principles*. John Wiley & Sons, Inc.

Seidelt, S., Muller-Hagedorn, M., Bockhorn, H. 2006. Description of tire pyrolysis by thermal degradation behaviour of main components. *Journal of Analytical and Applied Pyrolysis*, 75: 11–18.

Sinnott, R.K., Coulson, J.M., Richardson, J.F. and Sinnott, R.K. 2006. *Chemical engineering design*. Amsterdam. Elsevier, Butterworth-Heinemann.

Smith, J.M., Ness, H.V. and Abbott, M.M. 2005. *Introduction to Chemical Engineering Thermodynamics*. McGraw-Hill Education.

Stanciulescu, M. and Ikura, M. 2006. Limonene ethers from tire pyrolysis oil. *J. Anal. Appl. Pyrolysis,* 75: 217–225.

Stanciulescu, M. and Ikura, M. 2007. Limonene ethers from tire pyrolysis oil. *J. Anal. Appl. Pyrolysis*, 78: 76–84.

Suppino, R.S. and Cobo, A.J.G. 2014. Influence of solvent nature on extractive distillation of the benzene hydrogenation products. *Ind. Eng. Chem. Res*, 53: 16397-16405.

Sweeney, W.A. and Bryan, P.F. 1996. BTX processing. *Kirk-Othmer Encyclopedia of Chemical Technology*.

Teng, H., Serio, M.A., Wojtowicz, M.A., Bassilakis, R. and Solomon, P.R. 1995. Reprocessing of used tires into activated carbon and other products. *Industrial Engineering Chemistry Research,* 34: 3102–3111.

Thomas, A.F. and Bessiere, Y. 1989. Limonene. *Natural Product Reports,* 6: 291–309.

Tong, Z. F., Yang, Z. Y., Liao, D. K., Wei, T. Y. and Chen, X. P. 2009. Measurement and correlation of VLE data for α-pinene + limonene amd p-cymene + limonene. *J. Chem. Ind. Eng. (China)*, 60: 1877–1881.

Turton, R., Baile, R.C., Whiting, W.B. and Shaeiwitz, J.A.2009. *Analysis, synthesis, and design of chemical processes 3rd* .Prentice Hall international series in the physical and chemical engineering sciences. Upper Sad*dl*e River, NJ: Prentice Hall.

Vega, A., Diez, F., Esteban, R. and Coca, J. 1997. Solvent selection for cyclohexane-cyclohexene-benzene separation by extractive distillation using non-steady-stae gas chromatography. *Ind. Eng. Chem. Res,* 36: 803-807.

Williams, P.T. and Bottrill, R.P. 1995. Sulphur-polycyclic aromatic hydrocarbons in tyre derived oil.

Williams, P.T., 2013. Pyrolysis of waste tyres: A review. *Waste Management*, 33: 1714–1728.

Williams, P.T., Besler, S. and Taylor, D.T. 1990. The pyrolysis of scrap automotive tyres: the influence of temperature and heating rate on product composition. *Fuel,* 69: 1474–1482.

Yeo, Y., Lee, J., Song, K.W., Kim, I., Kwang, H.S. 2001. Operating strategies and optimum feed tray locations of fractionation unit of BTX plants for energy conservation. *Korean J. Chem. Eng*, 18: 428-431.

Yu, C. 2008. Study on purification of 1,2,3-trimethylbenzene from solvent oil via extractive distillation. Tianjin University.

Zivdar, M., Zadeh, M.H., Samadi, A. and Abdoullahi, M. 2014. Simulation and Revamping of BTX Distillation Column of Bu-Ali Sina Petrochemical Complex.

Chapter 3 Process modelling for recovery of *dl*-limonene from TDO

3.1. Introduction

The purpose of this Chapter is to develop an Aspen Plus® V8.2 simulation model of the separation process to recover *dl*-limonene from TDO. Distillation is favoured, as it can handle a large throughput and various feed concentrations. In the first step of the separation process, ordinary distillation is used to separate TDO into fractions with narrow boiling ranges i.e. light, middle (*dl*-limonene rich fraction) and heavy fractions. Parameters that influence the desirable performance of the fractionation process are studied to establish suitable operating conditions.

In the second step, extractive/azeotropic distillation is used to improve the purity of the *dl*-limonene naphtha cut obtained in the first step, to a value in excess of 90 wt%. The design of the extractive/azeotropic distillation process involves entrainer screening and determining the number of distillation columns and their interconnection, after which optimal operating conditions can be determined.

The chapter is subdivided into 4 sections. Section 3.2 describes the procedure followed in the simulation of fractionation of TDO. This includes; the selection of thermodynamic model, a description of important process parameters, modelling and optimization of the process and the final process flow diagram with the mass and energy balance generated. Section 3.3 describes the procedure followed in the simulation of azeotropic and extractive distillation to purify *dl*-limonene obtained from the fractionation step. This includes; the selection of entrainers, the selection of thermodynamic model, a description of important process parameters, modelling and optimisation of the process using different entrainers and the final process flow diagram with the mass and energy balance generated. Section 3.4 gives a comparison of extractive/azeotropic processes models developed using different entrainers on attainable purity and recovery, distillation column process parameters and energy consumption. Section 3.5 summarises the important findings from the investigation.

3.2. Fractionation of TDO

3.2.1. Problem definition and approach

The aim of this separation process model is to fractionate TDO and obtain a *dl*-limonene enriched fraction with *dl*-limonene purity in excess of 50wt%. TDO feed composition depends on the pyrolysis conditions. The upstream process therefore imposes specification on the feed stream of the separation process to be designed. The TDO composition used in this study is obtained from published work on two different pyrolysis processes. In this work, heat integration is not investigated and waste streams are not processed any further. The information required in successfully executing the simulation task in this project for the fractionation of TDO is discussed in this section.

Feed composition

The feed composition used in the separation process is obtained from studies by Qu *et al.* (2006) and Choi *et al.* (2014). Identified and quantified compounds in TDO from studies by Qu *et al.* (2006) represents 65.56 wt% of the oil, and that done by Choi *et al.* (2014) represents 74.46 wt% of the oil. TDO from Qu *et al.* (2006) forms feed 1 of the process, and that from Choi *et al.* (2014) forms feed 2 of the process.

The *dl*-limonene rich fraction generated from the two feeds will be compared and the process with more *dl*-limonene content will form part of the purification process by enhanced distillation. A fraction with more *dl*-limonene content will require a small distillation column as well as a low entrainer to feed ratio (E/F) to achieve a high *dl*-limonene purity compared to a fration with less *dl*-limonene content. This will in turn reduce the capital cost and operation cost.

The TDO component mass fractions from two sources are normalised and used as feed stream in the separation process model, using Aspen Plus ® V8.2. This may result in overestimation of *dl*-limonene composition. The chemical compounds contain a range of hydrocarbons, including: cyclic and acyclic aliphatics, single ring aromatics, polycyclic aromatics and heteroatoms. The undetected compounds from studies by Qu *et al.* (2006) and Choi *et al.* (2014) are likely to be heavy compounds. The compounds of interest are those that have a boiling point close to *dl*-limonene, which are mostly single ring aromatics. Other compounds outside this boiling point range are represented by model chemical compounds, i.e two or

more compounds are selected to represent alkanes, cycloalkanes, alkenes, cycloalkenes and polycyclic aromatics. This minimises the number of compounds included in Aspen Plus ® simulation. The single ring aromatics are all included, as their separation is the main concern in the recovery of high purity *dl*-limonene. Table 3.1 gives a list of chemicals included in the simulation model and their respective weight percent. Aspen Plus® V8.2 has one type of limonene isomer, which is d-limonene, and will therefore be used for the rest of this study to represent *dl*-limonene, which exists in TDO.

Table 3.1 Feed stream used in this study

	Feed 1		Feed 2	
Component	**Qu *et al.* (2006) wt%**	**Qu *et al.* (2006) normalised wt%**	**Choi *et al.* (2014) wt%**	**Choi *et al.* (2014) normalised wt%**
Cyclopropane	1.14	1.74		
Aminopropane			0.11	0.15
Cyclopentene	1.69	2.58	1	1.34
Cyclopentane	0.86	1.31		
Pentene	5.32	8.11		
2-Methyl-2-butene	0.2	0.31		
Methylbutane	0.2	0.31		
Pentane	0.14	0.21		
Benzene	0.73	1.11		
Cyclohexene	10.23	15.6		
Cyclohexane	0.7	1.07	0.69	0.93
Hexene	3.62	5.52		
n-Hexane	0.51	0.78		
Toluene	2.31	3.52		
Cycloheptene	0.28	0.43		
2-Heptene	1.2	1.83		
n-Heptane	0.29	0.44		
Styrene	0.24	0.37		
m-Xylene	3.25	4.96	3.18	4.27
Ethylbenzene	1.79	2.73		
p-Phenylenediamine			0.11	0.15
n-Octene	0.46	0.7		
2-Octene	0.36	0.55		
Indene			0.92	1.24
Indane			0.2	0.27
alpha-methylstyrene	2.91	4.44	4.64	6.23
1,2,3-Trimethylbenzene			6.97	9.36
1-Methyl-2-Ethylbenzene			3.78	5.08
Isopropylbenzene	1.24	1.89		
1-Ethyl-3-methylbenzene	2.13	3.25		

Table 3.1 (cont.) Feed stream used in this study

	Feed 1		Feed 2	
Component	**Qu *et al.* (2006) wt%**	**Qu *et al.* (2006) normalised wt%**	**Choi *et al.* (2014) wt%**	**Choi *et al.* (2014) normalised wt%**
p-Cymene	5.39	8.22	3.63	4.88
1,2,3,4-Tetramethylbenzene			1.03	1.38
5-Ethyl-m-xylene			2.6	3.49
1-Methyl-2-propylbenzene				
n-Butylbenzene	0.8	1.22		
1-methyl-2-isopropylbenzene	0.72	1.1	0.5	0.67
dl-Limonene	13.58	20.71	6.65	8.93
8-Methylquinoline			4.63	6.22
2-Metcaptobenzothiazole			4.77	6.41
d-Limonene			0.65	0.87
n-Pentadecane			0.56	0.75
n-Heptadecane			0.48	0.64
Stearic acid			0.11	0.15
Naphthalene	2.13	3.25	10.85	14.57
Methylindene			10.91	14.65
2-Phenylbutene	3.27	4.99		
Dimethylstyrene			5.49	7.37
Total	65.56	100	74.46	100

Separation objective

The TDO from the two sources is fractionated to obtain *dl*-limonene rich fraction, with a *dl*-limonene content preferably in excess of 50wt%. This is the minimum purity of the *dl*-limonene enriched fraction obtained by Pakdel *et al.* (2001). The two sources of TDO used in this study have different *dl*-limonene to impurity ratios, and the maximum attainable purity cannot be the same. As such, *dl*-limonene recovery is the only fixed parameter. A recovery of 99% is targeted to ensure minimal product losses.

Input and output parameters

The following process parameters for the column must be specified in modelling of distillation processes.

1. Feed stream i.e. composition, temperature, flowrate and pressure.
2. The operating pressure.
3. The number of stages.
4. The feed location.

5. The reflux ratio.
6. Distillate rate.

Separation of TDO using continuous distillation has not been reported in the open literature. The initial values for the number of theoretical plates or stages required for the separation, reflux ratio, distillate rate, rate of vaporisation, etc. are determined from Aspen Plus® V8.2 short-cut methods. The shortcut method with the model DSTWU, uses the simplified short method of Winn-Underwood-Gilliland and only require selection of key compounds and specification of the targeted recovery (Henley *et al*., 2011). Consequently, the results of the simulation with the model DSTWU are used as initial estimate in a rigorous model RadFrac. RadFrac includes material balances, energy and equilibrium relationships calculations in all the stages inside the column (Aspen Technology, 2009).

To find the effect of variation of a particular independent variable on dependent variable in the process, a sensitivity analysis is done. Aspen Plus® V8.2 has a sensitivity analysis tool that assists in evaluating the process alternatives and can help in optimisation by eliminating non-sensitive parameters. Parameters associated with distillation column, such as the number of stages, reflux ratio, etc. can be varied.

Parameters from heuristics

Several heuristics are used to guide in the optimisation, design and cost of the separation processes, and to reduce the number of manipulated variables. These guidelines are used for the fractionation of TDO and enhanced distillation process model.

For the fractionation process and enhanced distillation process, vacuum operation is chosen due to the heat sensitive nature of hydrocarbons. Vacuum distillation is generally used when the boiling point of a compound is above 150°C in order to distil compounds without significant decomposition (Turton *et al.,* 2009; Zubrick, 1997)

Low pressure operation decreases the operating temperature of the column. This, in turn, decreases the load on the reboiler, while simultaneously increasing the load on the condenser. Reducing reboiler duty will minimise operating costs, as the price of steam is significantly more expensive than that for cooling water required for condensation (Henley *et al.,* 2001). Cooling water temperature is taken as 30°C. Considering a 10°C increase in cooling water outlet from condensers, the distillate temperature can be taken to a minimum of 40°C

without overloading the condenser. The column pressure can be lowered to a minimum ensuring that the distillate temperature is above 40°C. The reboiler preferably uses low-pressure or medium pressure steam, which is at a temperature of 160°C and 184°C respectively. The liquid bottoms should therefore not exceed this temperature (Turton *et al.,* 2009). High pressure steam is costly, as it places a heavy load on the boilers and is not easy to handle due to large insulation required, as it is likely to condense in the steam pipes (Turton *et al.,* 2009).

The feed location chosen is the one that results in a low reflux ratio. Increasing the reflux ratio will result in increased flow in the column and high energy requirements. This will in turn decrease the number of theoretical stages but increase the column diameter. A favourable design is one with a few trays and a small diameter to reduce capital cost of the column (Turton *et al.,* 2009).

The type of distillation preferred for vacuum operation is structured packed distillation column (Sinnott and Towler, 2009). Structured packings are favourable due to their low HETP (height equivalent to theoretical plate) of typically less than 0.5 m, and low pressure drop (approximately 100 Pa/m) (Sinnott and Towler, 2009).

3.2.2. Selection of thermodynamic model

Due to lack of accurate VLE data to cover all possible interactions between *dl*-limonene and the components in TDO, several heauristics are used as guide to select a suitable thermodynamic model. From Aspen method guide, Eric Carlson and Bob Seader's recommendation given in Appendix D, EOS models are required for prediction of the phase equilibrium for hydrocarbons. Peng Robinson is the recommended property model in the method guides considered and is therefore used for the design of the fractionation process. Peng-Robinson is favourable for large temperatures and pressure changes, and is able to predict the phase equilibrium with acceptable accuracy (Laar, 2006; Seider *et al.,* 2004; Aspen Technology, 2009).

3.2.3. Process model for feed 1

3.2.3.1 Define process model

The process contains two units; a flash drum (V101) and a distillation column (T101), as shown in Figure 3.1. In this process, the feed (stream 1) is raw cold TDO, which is preheated using a

heat exchanger (E101). The partially vaporised TDO is introduced to a flash drum, where the light gases are separated and recovered as vapour product (stream 3). The bottom product of the flash drum is introduced to a distillation column operated under vacuum, where the light fraction, which is rich in single ring aromatics, is recovered as the top product (stream 7), and the middle fraction, which is rich in *dl*-limonene, is recovered as bottom product (stream 8). The distillation unit uses a partial condenser to remove excess light gases (stream 6). The bottom product (stream 9) of the distillation column is sent to the downstream process, which uses enhanced distillation. The stream table for the final process is given in Table 3.2. The input parameters for major units are discussed in the following sections.

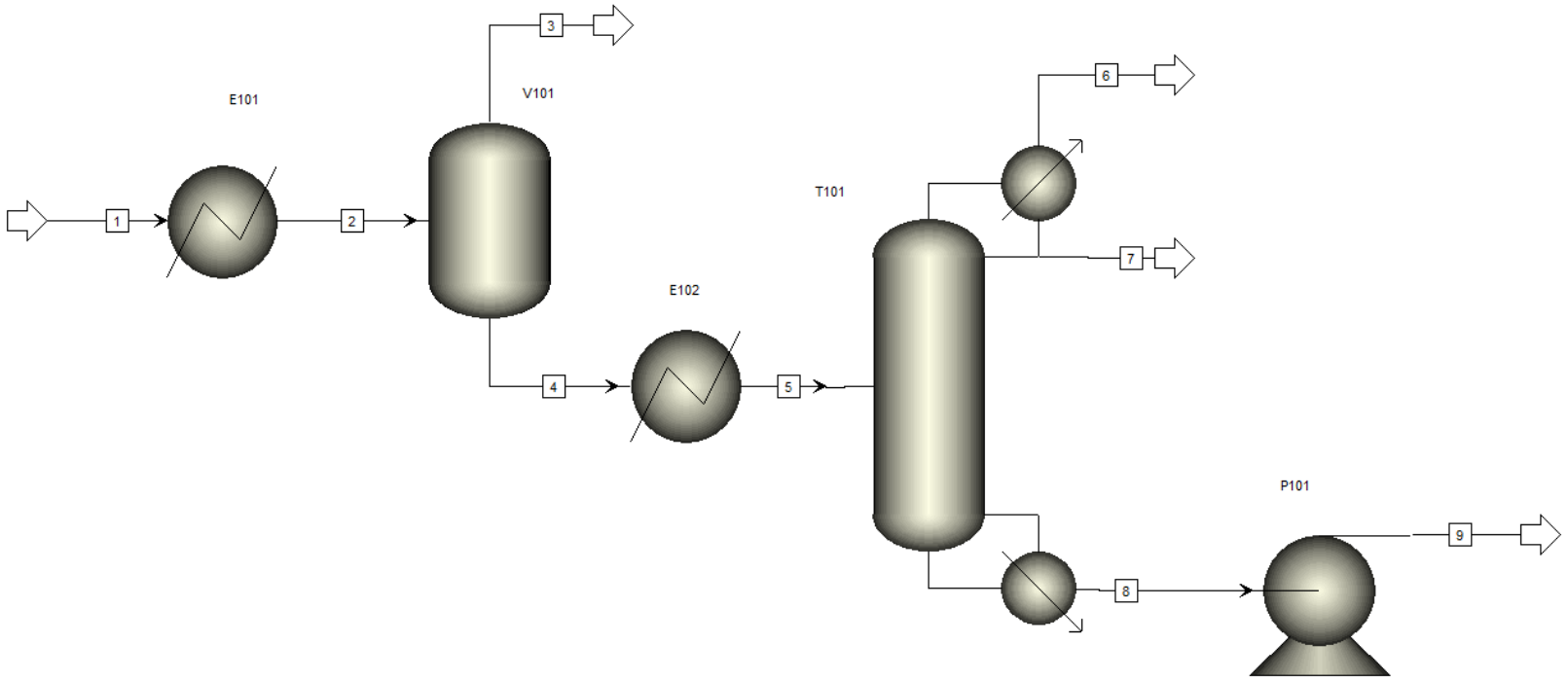

Figure 3.1 Process model for feed 1

Table 3.2 Stream table for feed 1 process model

Stream number	1	2	3	4	5	6	7	8	9
dl-Limonene (wt%)	20.71	20.71	0.63	22.17	22.17	0.02	0.44	57.13	57.13
Impurities (wt%)	79.29	79.29	99.37	77.83	77.83	99.98	99.56	42.87	42.87
Mole flow (kmol/hr)	5.09	5.09	0.51	4.58	4.58	1.14	2.11	1.33	1.33
Mass flow (kg/hr)	500.00	500.00	33.85	466.15	466.15	87.77	199.00	179.37	179.37
Temperature (°C)	25.00	25.00	52.10	52.10	100.00	63.25	63.25	159.48	159.48
Pressure (bar)	1.00	1.00	0.60	0.60	1.00	0.60	0.60	0.62	1.00
Vapour fraction	0.00	0.00	1.00	0.00	0.30	1.00	0.00	0.00	0.00

Input parameters for the flash drum (V101)

The feed to the flash drum (V101) for the process flowsheet in Figure 3.1 is partially vaporised TDO, at a constant pressure of 0.6 bar. Vacuum operation result in better separation in the flash-drum while allowing low temperature operation. A pressure of 0.6 bar is selected based on economic consideration. Vessels operated under 0.5 bar are more expensive compared to vessels operated above 0.6 bar (Turton *et al.,* 2009). The feed TDO is partially vaporised to give a vapour fraction of 0.1, after which the removal of light gases, mainly cyclopropane and butane, can be achieved in the flash drum at no *dl*-limonene expense. A temperature of 52 °C at a pressure of 0.6 bar result in the desired 10% vaporisation of the feed TDO.

Recovery of cyclopropane in the vapour product of the flash drum for different vaporization rates can be seen in Figure 3.2. From Figure 3.2, it can be seen that an increase in vaporisation of the TDO, will result in an increase in cyclopropane recovery in the vapour stream. As more TDO is vaporised, part of *dl*-limonene is lost in the vapour stream, which is not desired. As such, approximately 70% of cyclopropane can be removed with less than 1% of the feed *dl*-limonene lost in the vapour stream. As there are still light gases present in the bottom stream of the flash drum, distillation column (T101) from Figure 3.1 uses a partial condenser to remove excess light gases.

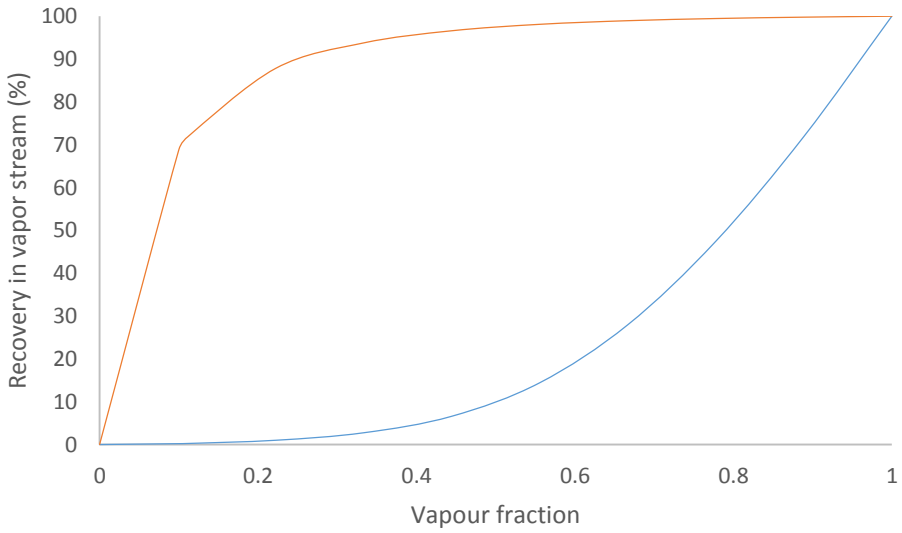

Figure 3.2 Cyclopropane – and *dl*-limonene – recovered in vapour product of the flash drum unit

Input parameters for T101

The input parameters for the DSTWU model, which calculates the required distillation column parameters, are given in Table 3.3. The DSTWU model uses Winn's method to estimate the minimum number of stages, Underwood's method to estimate the minimum reflux ratio and Gilliland's correlation to estimate the required reflux ratio for a specified number of stages or vice versa (Seader et al., 2011). The calculated parameters are used as initial estimate for the Radfrac model suitable for final process design and equipment sizing.

The selected light key compound is α-methylstyrene, which boils 12°C below *dl*-limonene. α-Methylstyrene is present in a significant concentration as can be seen from Table 3.1. It would be desirable to recover it as an overhead product to minimise its content in the *dl*-limonene enriched fraction. *dl*-Limonene is selected as the heavy key, as it is desirable to recover it completely as the bottom product. The estimated number of stages is 60. This is the approximate number of stages used to separate hydrocarbon mixtures with less than 20°C difference in boiling point (Mosayeb and Mortaza, 2014).

A pressure of 0.6 bar is used. This pressure results in column operating temperature that can be maintained by medium pressure steam in the reboiler and cooling water available at ambient temperature in the condenser. Justification of the chosen feed rate of TDO will form part of the economic analysis discussion. A feed flow rate of 12000 kg/day is used.

Table 3.3 DSTWU input parameters for T101 of feed 1

Input	Values
Light Key Recovery : α-Methylstyrene	99.00%
Heavy Key Recovery : *dl*-limonene	1.00%
Estimate number of stages	60
Pressure (bar)	0.60
Distillate vapour fraction	0.35
Feed (kg/day)	12000.00

The DSTWU model calculated the parameters that are used as input to the Radfrac model, as given in Table 3.4. These are base case parameters and are used in sensitivity analysis to establish optimal design conditions. A sensitivity analysis is performed to investigate the effect of number of stages, reflux ratio, feed location and feed temperature on the separation.

Table 3.4 Radfrac input parameters for T101 of feed 1

Parameter	Values
Actual reflux ratio	0.51
Number of actual stages	60
Feed stage	31
Distillate to feed fraction	0.71

3.2.3.3 Sensitivity analysis

The effect of process variables on purity, column reboiler duty and recovery of *dl*-limonene enriched fraction is investigated in the Radfrac model. For illustration, T101 from the process flow diagram of feed 1 is used. When the effect of one parameter is investigated, all other parameters are fixed at their base case values.

Effect of feed temperature

In Figure 3.3 the effect of feed temperature on purity of *dl*-limonene in the bottom product for different molar reflux ratio is presented. It can be observed in Figure 3.3 that above a reflux ratio of 1.6, the effect of temperature on *dl*-limonene purity is insignificant. At a low reflux ratio below 1.6, the purity decreases with increasing temperature. This is because at a high feed temperature, part of *dl*-limonene found in the stages vaporises, increasing its content in the distillate and resulting in a low purity in the bottoms.

The effect of feed temperature on the reboiler duty is given in Figure 3.4. For a reflux ratio above 2.7, the feed should be kept at temperatures between 85 and 125°C to obtain *dl*-limonene at the maximum attainable purity, at a minimum reboiler duty. Low reboiler duty corresponds to a high feed temperature and low reflux ratios. Justification on the chosen temperature is not based entirely on minimization of reboiler energy but on maximization of *dl*-limonene purity while avoiding exhaustion of the reboiler. The effect of feed temperature on the total energy i.e the duty of the pre-heater and the distillation column condenser and reboiler at the maximum attainable *dl*-limonene purity of 57 wt% is given in Figure 3.5.
Energy consumption is not the only parameter considered. An increase in temperature result in an increase in *dl*-limonene purity. To achieve the desired product specification, the chosen feed temperature for this process is 100°C. This temperature results in the highest *dl*-limonene purity at the lowest total energy consumption.

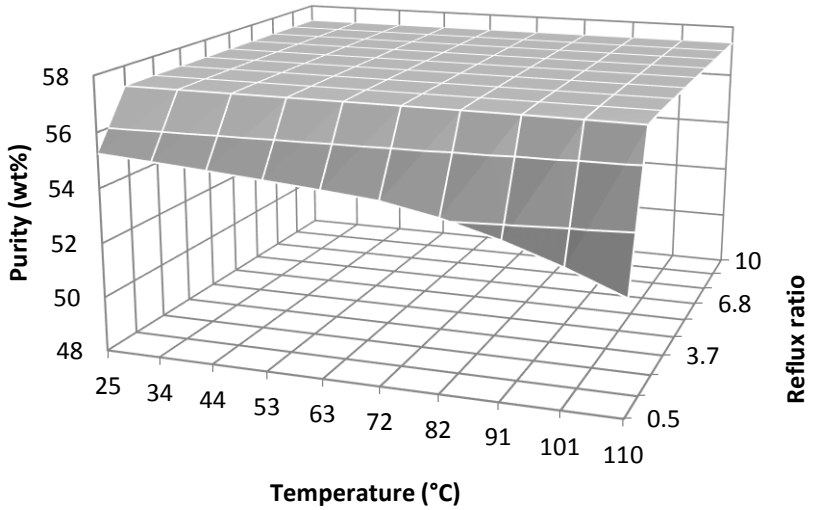

Figure 3.3 Effect of feed temperature on the distillate purity of *dl*-limonene for different molar reflux ratios.

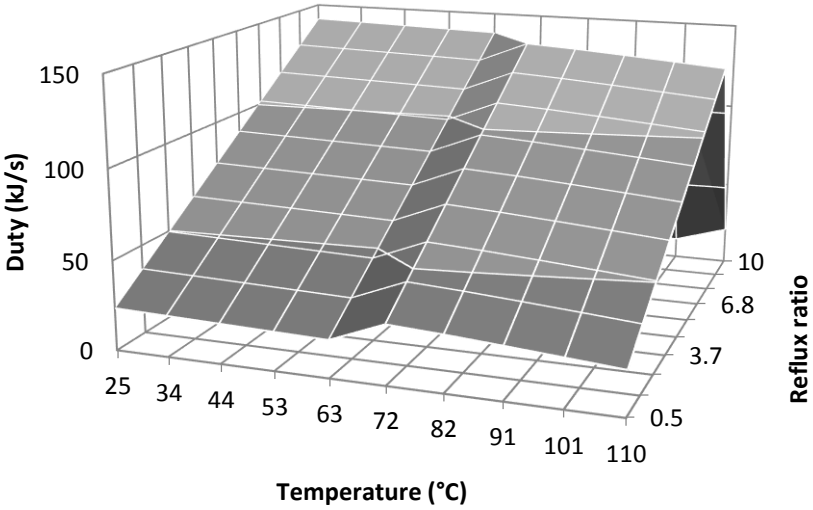

Figure 3.4 Effect of feed temperature on the distillation column reboiler duty for different molar reflux ratios

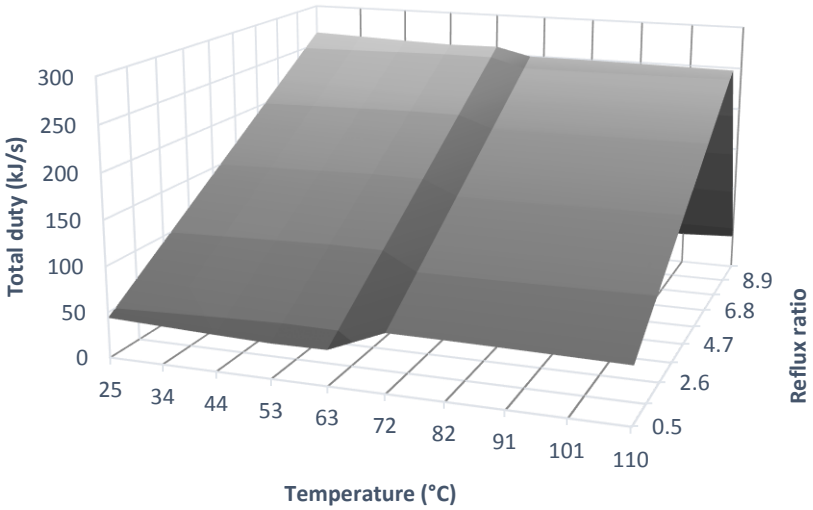

Figure 3.5 Effect of feed temperature on the total duty for different molar reflux ratios

Effect of feed location

Figure 3.6 presents the effect of feed stage on *dl*-limonene purity for various molar reflux ratios. It can be seen from Figure 3.6 that as the feed stage is increased (the feed is closer to the reboiler), *dl*-limonene purity increases. This is due to the rectification of the light hydrocarbons, which results in their content increasing up to a maximum in the distillate. As the feed stage approaches the reboiler, it is expected that vaporisation of *dl*-limonene will increase, which will become part of the vapour going up the top stages and withdrawn as distillate.

The effect of feed stage on the reboiler duty is shown in Figure 3.7. From Figure 3.7, it can be seen that the feed location has no significant effect on the reboiler duty for a fixed reflux ratio. Therefore, varying the reflux ratio has a greater effect on the consumption of reboiler energy than the feed stage. The chosen feed stage is 31, as it results in high *dl*-limonene purity. The selected feed temperature (100°C) and feed location (31) are used to determine the optimum number of stages.

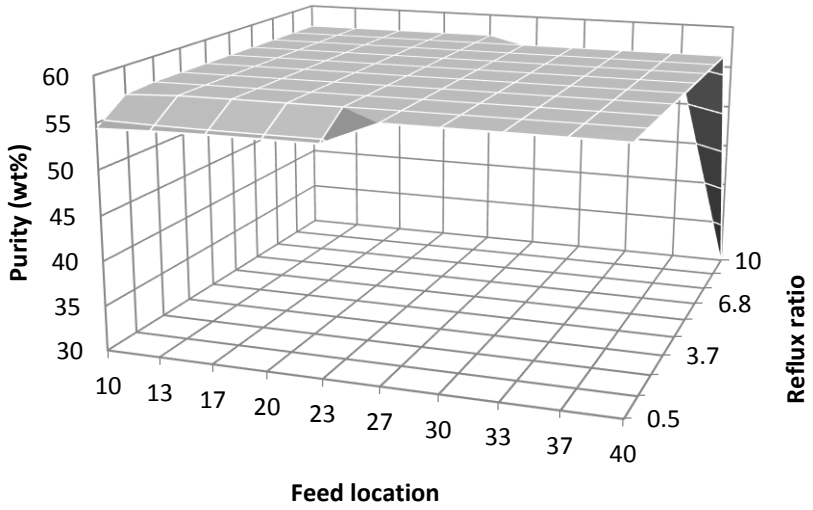

Figure 3.6 Effect of feed stage on *dl*-limonene purity for different molar reflux ratios

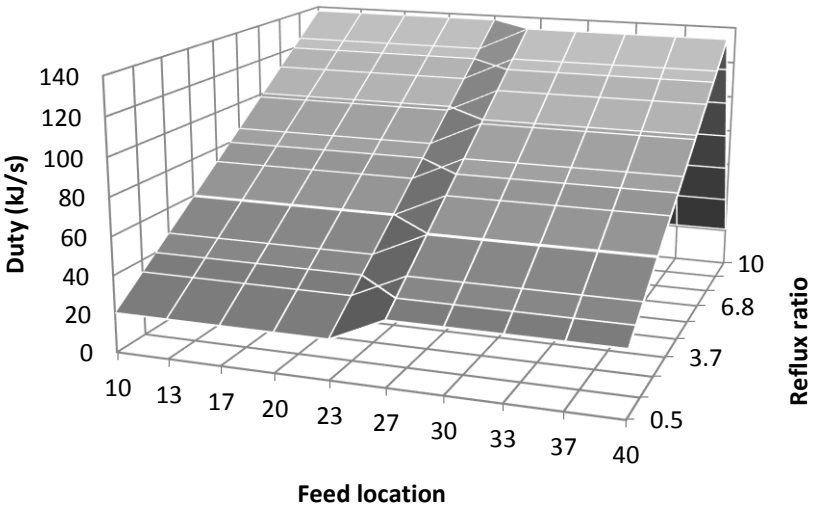

Figure 3.7 Effect of feed stage on the distillation column reboiler duty for different molar reflux ratios

Optimum number of stages

The feed temperature and feed location are changed to the new established values of 100°C and 31 respectively. Other parameters are fixed at their base case values. In Figure 3.8 to Figure 3.10, the effect of the number of theoretical stages on *dl*-limonene purity, recovery and the reboiler duty of the distillation column are presented for different molar reflux ratios. From Figure 3.8 it can be observed that for number of stages above 40, the purity of *dl*-limonene remains nearly constant for reflux ratios above 2.7. For number of stages below 35, a high reflux ratio will be required to obtain the maximum obtainable purity. A high reflux ratio result in increased energy consumption.

The effect of the number of stages on the reboiler duty for different molar reflux ratio is presented in Figure 3.9. It can be seen from Figure 3.9 that the energy consumption remains approximately constant, with increasing number of stages at a fixed reflux ratio. It would be desirable to increase the number of stages to facilitate separation, rather than to increase the reflux ratio.

The recovery of *dl*-limonene is monitored to ensure it does not drop below 99%. The effect of number of stages on the recovery of *dl*-limonene for different molar reflux ratios is presented in Figure 3.10. It can be seen from Figure 3.10 that an increase in number of stages and reflux ratio result in an increase in the recovery of *dl*-limonene in the bottoms product.

The trade-off between reflux ratio and the number of stages is evaluated. The fixed capital cost for the column for various number of trays and the operational cost of steam and cooling water are calculated to give the total cost over an assumed project life of 15 years (Turton *et al.*, 2009). The combination of the reflux ratio and number of stages to be used should be the most economical one, which result in the lowest total cost (Peter and Timmerhaus, 1991). The capital expenditure (CAPEX), operational expenditure (OPEX) and the total cost are shown in Figure 3.11.

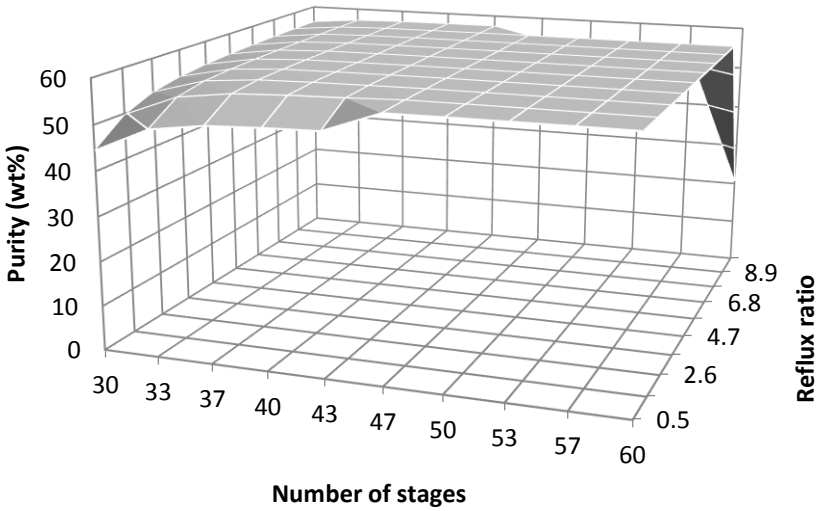

Figure 3.8 Effect of number of stages on the distillate purity of *dl*-limonene for different molar reflux ratios

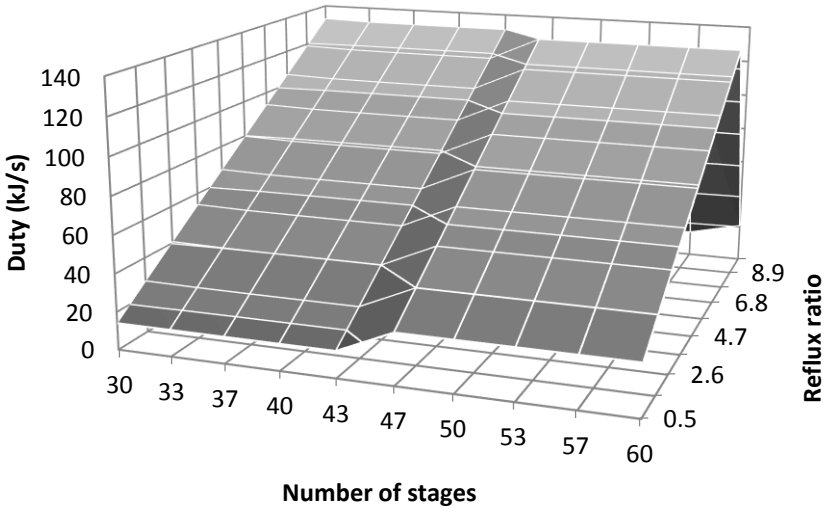

Figure 3.9 Effect of number of stages on the distillation column reboiler duty for different molar reflux ratios

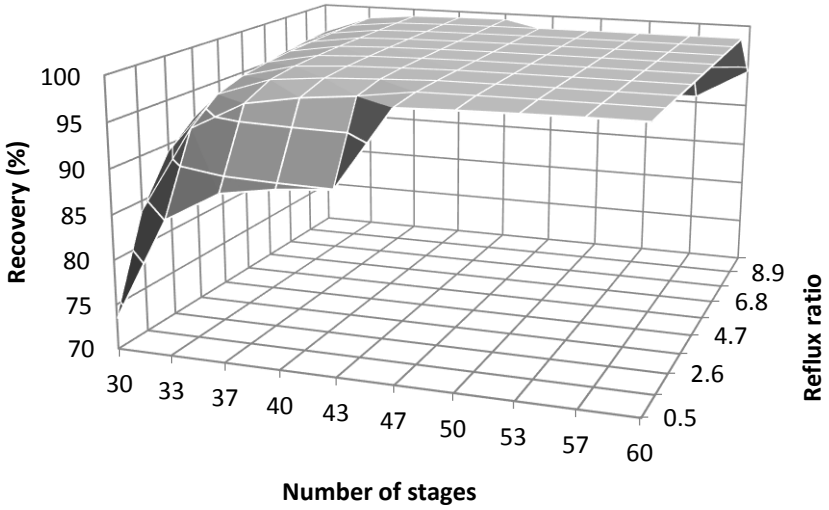

Figure 3.10 Effect of number of stages on *dl*-limonene recovery for different molar reflux ratios

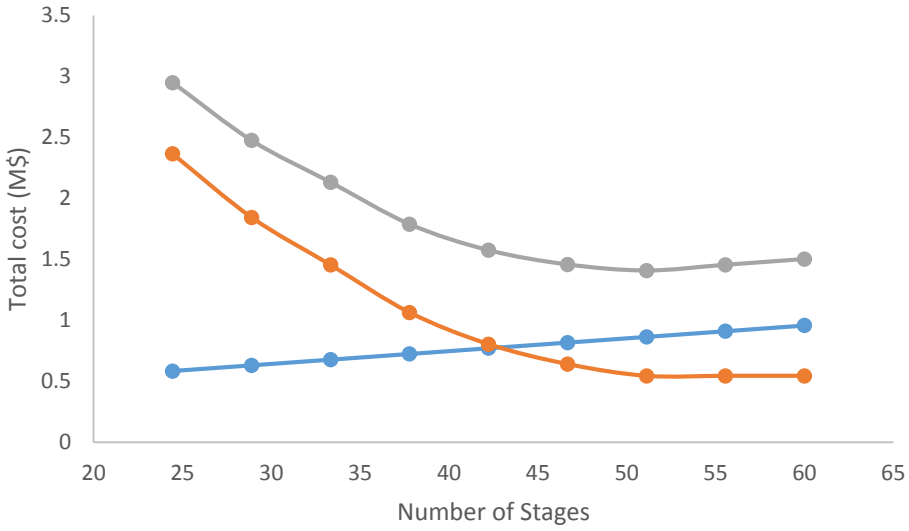

Figure 3.11 CAPEX ●, OPEX ● and total cost ● for distillation operation

From Figure 3.11 it can be seen that, in order to operate at the least total cost whilst ensuring a high *dl*-limonene purity and recovery, 50 stages is required in the fractionation column which correspond to a reflux ratio of 1.6.

It can be concluded that the combination of established process parameters, i.e feed location, feed temperature, number of stages and reflux ratio facilitate fractionation of TDO to obtain a *dl*-limonene stream, with purity in excess of 50 wt%. The derived operating conditions for the distillation column are summarised in Table 3.5.

Table 3.5 Operating conditions obtained for the distillation column of feed 1

Parameters	Fractionating column
Number of stages	50
Feed stage	31
Reflux ratio	1.6
Feed temperature (°C)	100
Operating pressure (bar)	0.6

3.2.4. Process model for feed 2

3.2.4.1 Define process model

The process contains two distillation columns (T101 and T102), connected in series as shown in Figure 3.12. Feed (stream 1) is preheated to a temperature slightly below the saturated liquid temperature at the distillation column (T101) operating pressure. Preheated TDO is introduced to the first distillation column (T101). In the first distillation column, the light fraction, which is rich in single aromatics, is recovered as the top product (stream 3) and the

bottom product (stream 4) is introduced to the second distillation column (T102). In the second distillation column the heavy aromatics are recovered as bottoms (stream 6), and separated from the middle fraction, which is rich in *dl*-limonene, and recovered at the top (stream 5). The final process flowsheet and stream table is given in Figure 3.12 and Table 3.7 respectively.

3.2.4.2 Sensitivity analysis

The effect of process variables on *dl*-limonene purity, reboiler duty and recovery of *dl*-limonene enriched fraction, as done for process feed 1, is investigated. The initial operating conditions and the final established operating conditions, after sensitivity analysis for the two distillation columns (T101 and T102), are summarised in Table 3.6. The sensitivity plots are given in Appendix E.

Table 3.6 Operating conditions obtained for two distillation columns of feed 2

Parameters	**Initial**		**Final**	
	T101	**T102**	**T101**	**T102**
Number of stages	60	30	60	30
Feed stage	31	20	31	9
Reflux ratio	3.46	1.91	4.70	3.70
Distillate to feed fraction	0.29	0.40	0.15	0.41
Feed temperature (°C)	95.00	172.85	95.00	172.85
Condenser / top stage pressure (bar)	0.60	0.60	0.60	0.60
Reboiler duty (kJ/s)	51.31	55.64	60.16	73.66
dl-Limonene bottoms purity (wt %)	10.12	-	10.13	-
dl-Limonene recovery in bottoms (%)	99.99	-	99.99	-
dl-Limonene distillate purity (wt %)	-	21.29	-	26.69
dl-Limonene recovery in distillate (%)	-	99.00	-	99.00

From Table 3.6, it can be seen that the input parameters derived from the DSTWU model, when used in the Radfrac model, result in a lower *dl*-limonene purity for the two columns compared to process model of feed 1. The outcomes after sensitivity analysis for a fixed recovery result in nearly the same *dl*-limonene purity as before sensitivity analysis thereby indicating the limitation of distillation. An increase in the number of stages does not increase the purity any further; this is due to the presence of close boiling compounds. A change in the feed location and feed temperature does not have a significant impact on separation, hence parameters before and after sensitivity analysis are almost the same.

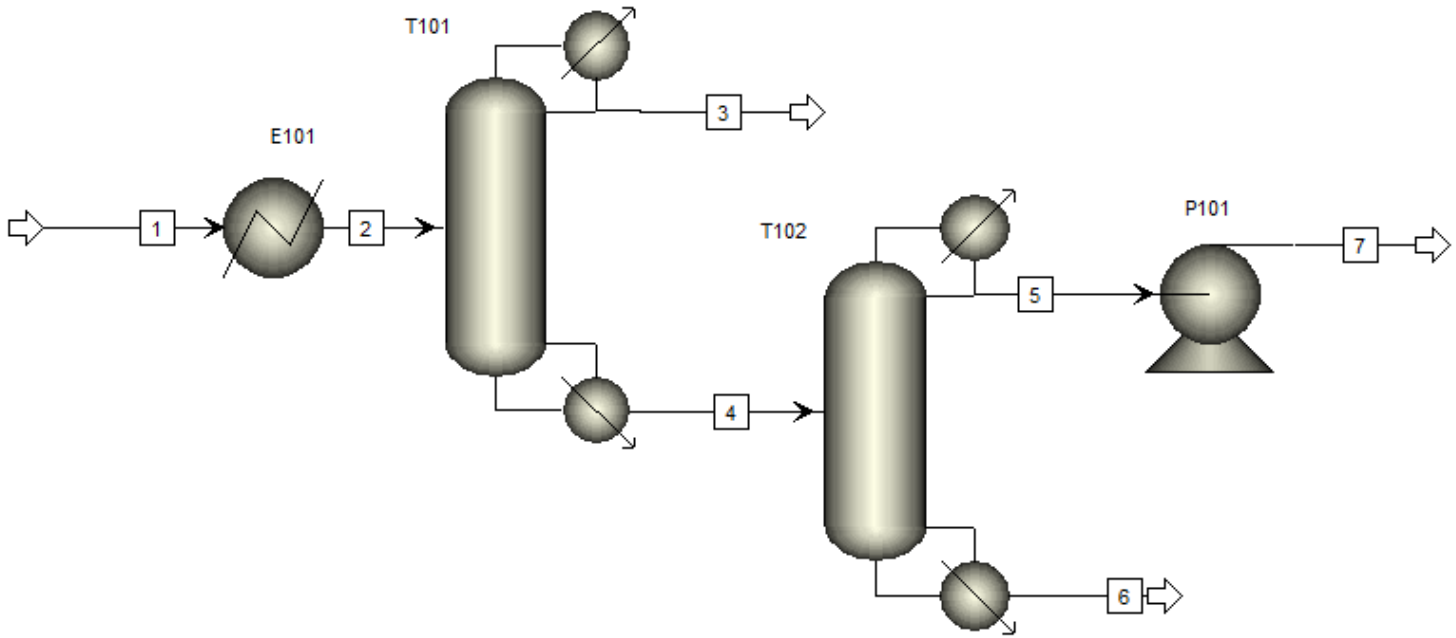

Figure 3.12 Process model for feed 2

Table 3.7 Stream table for feed 2 process model

Stream number	1	2	3	4	5	6	7
dl-Limonene (wt%)	8.93	8.93	0.02	10.13	25.68	0.11	25.68
Impurities (wt%)	91.07	91.07	99.98	89.87	74.32	99.89	74.32
Mole flow (kmol/hr)	3.90	3.90	0.58	3.31	1.36	1.95	1.36
Mass flow (kg/hr)	500.00	500.00	59.33	440.67	172.63	268.03	172.63
Temperature (°C)	25.00	95.00	73.00	172.78	155.12	189.87	155.19
Pressure (bar)	1.00	1.00	0.60	0.63	0.60	0.61	1.00
Vapor fraction	0.00	0.00	0.00	0.00	0.00	0.00	0.00

3.2.5. Comparison of results

The *dl*-limonene enriched fractions obtained from fractionation of TDO from feed 1 and 2 have shown to contain close boiling compounds, as reported in literature (Pakdel *et al.,* 2001). The two process models are compared in Table 3.8.

Table 3.8 Comparison of process models for feed 1 and 2

	Process model	
	Feed 1	Feed 2
Number of distillation columns	1	2
Total reboiler duty (kJ/s)	82.53	133.82
dl-Limonene recovery (%)	99.00	99.00
dl-Limonene purity (wt %)	57.12	25.68
CAPEX(M$)	0.86	1.85
OPEX(M$)	0.54	0.73
Total cost (M$)	1.41	2.58

From Table 3.8, it can be seen that *dl*-limonene enriched fraction from feed 1 has a higher *dl*-limonene content, require less units and consumes less energy resulting in the lowest total cost. The *dl*-limonene content in the enriched fraction is greater than 50 wt%, which fulfils the design criteria, and comparable to that, obtained by Pakdel *et al.* (2001). The downstream separation process in this work is designed based on feed 1.

3.3. Enhanced distillation: Upgrading of light naphtha cut to *dl*-limonene rich stream

3.3.1. Problem definition and approach

The purity of *dl*-limonene stream obtained from feed 1 process model is not at a sufficient quality as it is below 90 wt%. To reach this requirement of 90 wt% purity, close boiling and azeotrope forming compounds forming impurities have to be removed. Because ordinary distillation can only achieve partial separation when used for fractionation of TDO, azeotropic and extractive distillation is adopted to purify the *dl*-limonene naphtha cut. The optimization algorithm by P. Lek-utaiwan *et al.* (2012) given in Chapter 2 is used in this study.

Column parameters are initially specified based on literature values and heuristics, for similar systems. Sensitivity analysis is used to determine the effect of process variables on the *dl*-limonene purity. Process variables that have significant impact on separations are used for optimization. In the optimization block, the process variables are varied to obtain *dl*-limonene purity at recovery and purity in excess of 99% and 90 wt% respectively, with the minimum number of stages and low energy consumption.

Feed composition

Table 3.9 gives a list of components included in the simulation model and their respective weight percentage.

Table 3.9 Composition of *dl*-limonene stream obtained after fractionation process feed 1

Component	Concentration (wt %)
p-Cymene	22.27
Butylbenzene	3.40
1-Methyl-2-isopropylbenzene	3.03
2-Phenyl-butene	13.87
dl-Limonene	57.13
Others	0.30

Separation objective

The upgrading of *dl*-limonene rich fraction using extractive/azeotropic distillation is conducted at the operational constraints given in Table 3.10.

Table 3.10 Operational constraints

Parameters	Constraints	Validation/References
dl-Limonene purity (wt%)	≥90	Commercial limonene purity (GreenTerpenes TM, 2014)
dl-Limonene recovery (%)	95	To avoid large product losses (Yu, 2008)
Entrainer to feed ratio (E/F)	≤6	Commonly used in enhanced distillation processes (Mikitenko *et al.,* 1975 ; Suppino and Cobo, 2014; Yu, 2008)
Number of stages	≤60	Average number of stages used in typical enhanced distillation columns (Mikitenko *et al.,* 1975 ; Suppino and Cobo, 2014; Yu, 2008)
Recycled entrainer purity (wt%)	≥99	A high purity entrainer is required for effective separation (Düssel & Warter 1998)
Recycled entrainer recovery (%)	≥99	To minimise operational cost by recycling entrainer (Düssel & Warter 1998)
Overhead temperature (°C)	≥50	To avoid overloading the condenser, assuming ambient conditions may sometimes be above 35°C (Turton *et al.,* 2009).
Bottoms temperature (°C)	≤184	To ensure that the temperature of mild steam is not exceeded (Turton *et al.,* 2009)

The purity of *dl*-limonene is set at a value close to the commercial purity of *dl*-limonene derived citrus oils. The recovery is set at a high value to increase the production rate of *dl*-limonene. The E/F and number of stages are set at values close to what is used in a typical enhanced distillation process in literature. The entrainer purity and recovery are set at high values to ensure that the entrainer can be re-used in the process. The overhead and bottoms temperature are determined by utility limitations.

In the simulation of enhanced distillation, the initial values for operational parameters are determined from enhanced distillation processes using similar entrainers in published work. These parameters are used as initial estimates to the Radfrac model conducted in Aspen Plus ® V8.2 for azeotropic/extractive distillation and entrainer recovery. Sensitivity analysis is done to verify whether operating at these conditions is feasible for the system under investigation. Sensitivity analysis also assists in establishing new operating parameters which are not fully specified in literature for extractive/azeotropic distillation design.

3.3.2. Entrainer selection

Entrainer selection is an important step as it determines the feasibility of azeotropic/extractive distillation process. The entrainer facilitates separation by changing the relative volatility of the components in question. Entrainers are specific to the mixture in question and there are no universal entrainers, e.g. acetone is an entrainer for separating benzene and cyclohexane, but not for separating benzene and cyclohexene (Henley *et al.,* 2011). Entrainers determine the separation process configuration i.e. the number of distillation columns and decanters, and how they are interconnected (Henley *et al.,* 2011). The separation process configuration in turn determines the process economics. Therefore, entrainer selection is a critical step in the conceptual design and synthesis of extractive/azeotropic distillation processes.

Identification of entrainers

Different techniques can be used to determine suitable entrainers. Entrainers can be selected based on experience or with similar processes. However, this approach does not allow identification of novel entrainers. The method followed in choosing an entrainer involve, broad screening by functional groups or chemical families (Perry and Green, 2003).

Robbins Chart serves as a good reference and starting point for entrainer selection procedure (Robbins, 1980). A candidate entrainer should give positive or no deviation from Raoult's law for the key component preferred in the distillate, and negative or no deviation for the other key component (Perry and Green, 2003). Turning to Robbins Chart in Table 3.11, it can be noted that entrainers that may cause positive deviation and negative deviation for aromatics and aliphatics come from group 4, 7, 8 and 9, which consist of polyol, amine, amide and ether (Perry and Green, 2003). In the *dl*-limonene rich stream, major impurities are aromatic compounds and *dl*-limonene is the major aliphatic compound. If the entrainer (A) and the key component (B) give positive deviation from Raoult's law, the molecular attraction between A-B is weaker than that of A-A and B-B, then the tendency of molecules A-B to exit the solution is greater than that of pure components. If the entrainer (A) and the key component (B) give negative deviation from Raoult's law, the molecular attraction between A-B is stronger than that of A-A and B-B, then the tendency of molecules A-B to exit the solution is less than that of pure components. The molecular interactions are a result of different factors such hydrogen bonding, dipole-dipole attraction, etc. (Smith *et al.,* 2005).

Knowing the chemical group, a search for candidate entrainers can be conducted, for example; candidate entrainers used in published literature, chemical compounds in Aspen Plus ® V8.2 that meet the entrainer selection criteria and compounds that already exist in TDO. The selected entrainers and their origin are given in Table 3.12.

Table 3.11 Entrainer and solute interaction (Robbins, 1980)

		Solvent class											
Solute class	**Group**	**1**	**2**	**3**	**4**	**5**	**6**	**7**	**8**	**9**	**10**	**11**	**12**
	H-donor												
1	Phenol	0	0	-	0	-	-	-	-	-	-	-	-
2	Acid, thiol	0	0	-	0	-	-	0	0	0	0	-	-
3	Alcohol, water	-	-	0	+	+	0	-	-	-	-	-	-
4	Active-H on multihalo paraffin	0	0	+	0	-	-	-	-	-	-	0	-
	H-acceptor												
5	Ketone, amide with no H on N, sulfolane, phosphine oxide	-	-	+	-	0	+	-	-	-	+	-	-
6	Tertamine	-	-	0	-	+	0	-	-	0	+	0	0
7	Secamine	-	0	-	-	+	+	0	0	0	0	0	-
8	Pri amine, ammonia, amide with 2H on N	-	0	-	-	+	+	0	0	-	+	-	-
9	Ether, oxide, sulfoxide	-	0	+	-	+	0	0	-	0	+	0	-
10	Ester, aldehyde, carbonate, phosphate, nitrate, nitrite, nitrile, intramolecular bonding, e.g o-nitro phenol	-	0	+	-	+	+	0	-	-	0	-	-
11	Aromatic, olefin, halogen aromatic, multihalo paraffin without active H, monohalo paraffin	+	+	+	0	+	0	0	-	0	+	0	0
	Non-H-bonding												
12	Paraffin, carbon disulfide	+	+	+	+	+	0	+	+	+	+	0	0

Key

0 No deviation from Roult's Law

+ Positive deviation from Roult's Law

- Negative deviation from Roult's Law

Table 3.12 Potential entrainers for azeotropic/extractive distillation of *dl*-limonene enriched fraction

Entrainer	Chemical group	Reference
n,n-Dimethylformamide	Amine/amide	Vega et al. (1997)
n-Methylpyrrolidone	Polyfunctional (C,H,O,N)	Abushwireb et al. (2007)
Quinoline	Amine/amide	Selected from TDO
4-Formylmorpholine	Polyfunctional (C,H,O,N)	Lee (2000)
Diethylene glycol	Polyol	Suppino and Cobo (2014)
Tetraethylene glycol dimethyl ether	Ether	Selected from Aspen
Triethylene glycol	Polyol	Suppino and Cobo (2014)

Entrainer feasibility

The effect of entrainer on the relative volatility of the mixture is studied and finally the residue curve maps are constructed with the aid of Aspen Plus® V8.2. The relative volatility and RCM for d-limonene/p-cymene/entrainer is used to determine entrainer feasibility. This is because it is more difficult to separate p-cymene and d-limonene as they belong to the same chemical class, i.e. terpene. *dl*-Limonene is an aliphatic terpene, while p-cymene is an aromatic terpene. An entrainer that allows separation of d-limonene and p-cymene is likely to facilitate separation of *dl*-limonene from other aromatics or impurities in the mixture.

The evaluation of the effect of entrainer on relative volatility is done at constant pressure of 1 bar and entrainer to feed ratio (E/F) of 4. This value of E/F is commonly used in extractive/azeotropic distillation applications. Since this is only entrainer screening, variation of entrainer flowrate and pressure is not necessary. The aim is to identify the ability of the entrainer to alter the relative volatility. To calculate the relative volatility, a typical flash drum is modelled in Aspen Plus ® V8.2 using NRTL activity coefficient model. The feed is brought to its saturated vapour in the flash drum. Aspen Plus ® V8.2 gives the K-values, which are used to calculate the relative volatilities. The relative volatility using different entrainers are given in Table 3.13.

Table 3.13 The effect of different entrainers on the relative volatility of *dl*-limonene/p-cymene

Entrainer	Relative volatility
Tetraethylene glycol dimethyl ether	1.33
Triethylene glycol	1.44
Quinoline	1.54
Diethylene glycol	1.55
n-Methylpyrrolidone	1.65
n,n-Dimethylformamide	1.94
4-Formylmorpholine	2.41

From Table 3.13 it can be seen that the candidate entrainers increased the relative volatility from unity. The relative volatilities fall outside the extreme range of 0.95-1.05 where distillation is not economical (Van Winkle, 1967). This criterion cannot only be used to discard the candidate entrainers, futher analysis using residue curve map technology as well as investigation of process economics is necessary.

Residue curve map (RCM) technology

RCM technology is used to determine entrainer feasibility. Figure 3.13 to Figure 3.21 shows the RCM for ternary systems calculated via the NRTL thermodynamic model generated through Aspen Plus® V8.2.

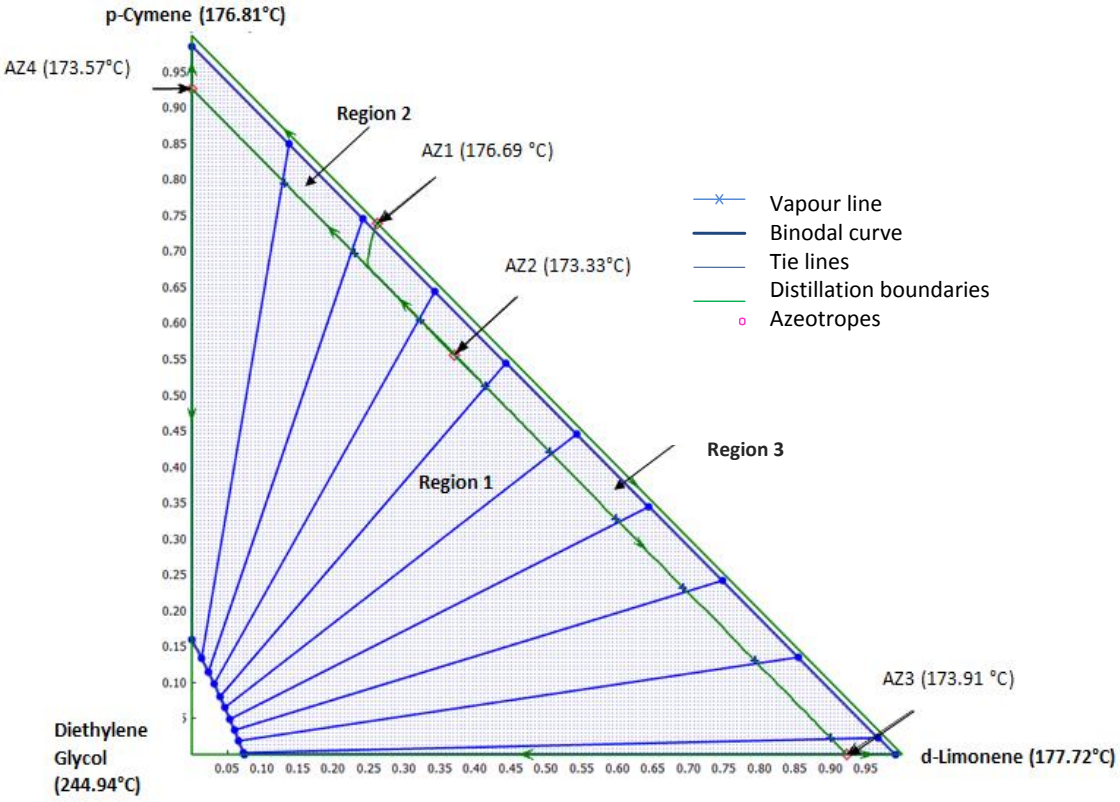

Figure 3.13 RCM for p-cymene-d-limonene-diethylene glycol system at 1 bar

In Figure 3.13, the RCM is divided into three distillation regions. Figure 3.13 shows that a distillation boundary can be crossed as it has a two-liquid phase region. A typical operation for such a system entails a feed with an overall composition, which lies in region 1. When the vapour is condensed, the two liquid phases split in the decanter, giving a *dl*-limonene rich phase, which lies in region 3 and an entrainer rich phase, which lies in region 1. Products of the column is an overhead stream with a composition approaching that of AZ3 and the bottoms of a nearly pure p-cymene. The entrainer rich phase is taken as reflux and recovered with the bottom product. The bottom product can be separated via ordinary distillation and the entrainer can be recycled. Diethylene glycol is a regarded as a feasible entrainer as it results in the formation of heterogeneous azeotropes allowing d-limonene and p-cymene to be separated.

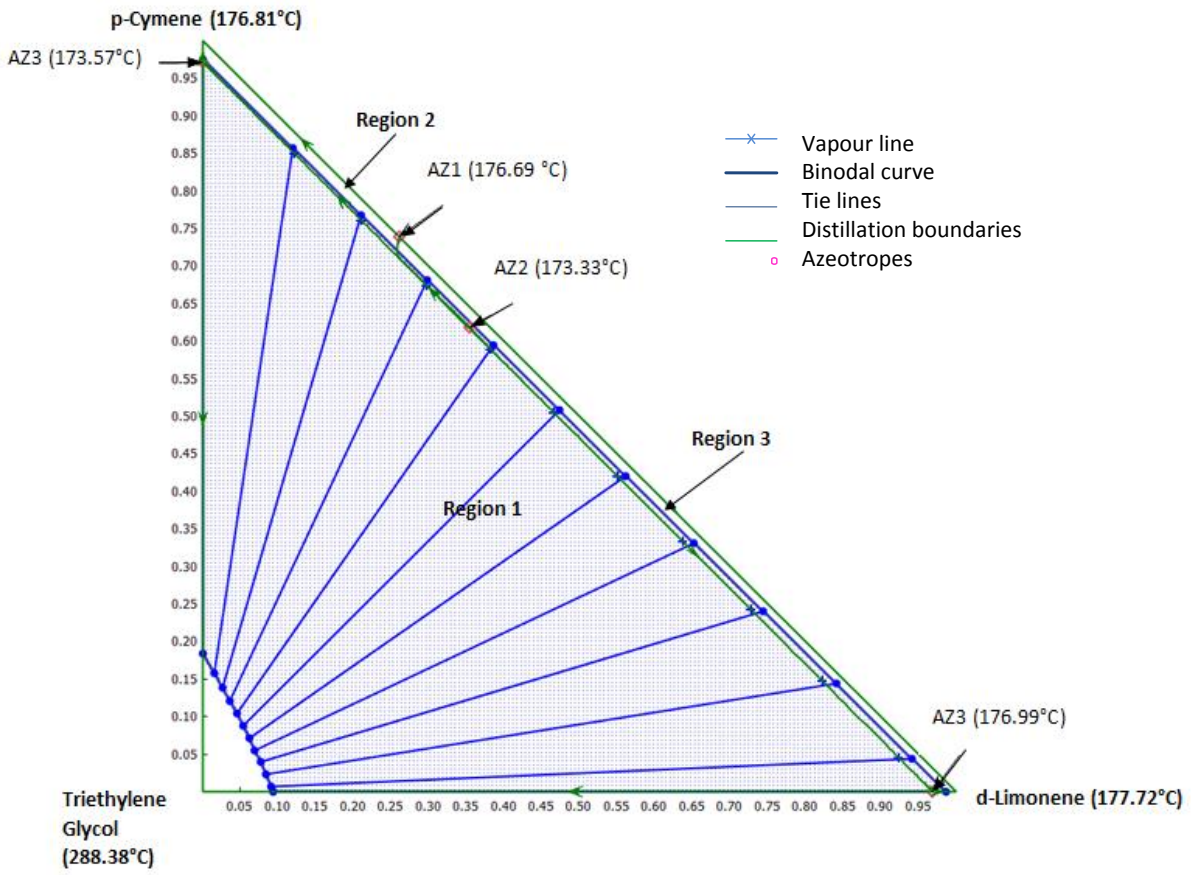

Figure 3.14 RCM for p-cymene-d-limonene-triethylene glycol system at 1 bar

From Figure 3.14, it can be seen that triethylene glycol causes the occurrence of a region of liquid-liquid de-mixing, allowing crossing of the distillation boundary. From the diagram, there are three binary azeotropes similar to the system using diethylene glycol. Therefore, triethylene glycol is a regarded as a feasible entrainer. The choice between diethylene glycol and triethylene glycol will depend on process economics.

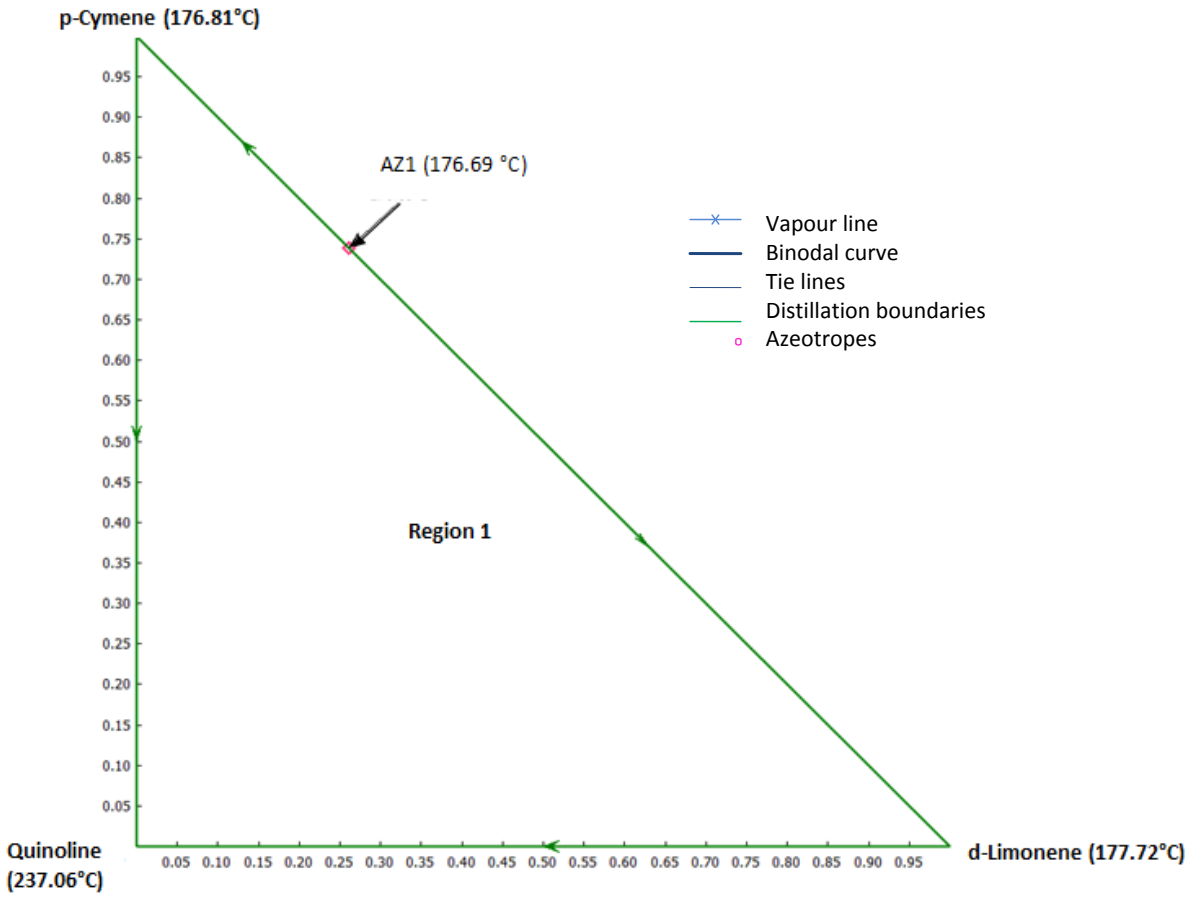

Figure 3.15 RCM for p-cymene-d-limonene-quinoline system at 1 bar

From Figure 3.15, it can be seen that no distillation boundary exists. Quinoline does not form an azeotrope with any of the component. Quinoline is a regarded as a feasible entrainer as it causes a change in relative volatility, and allows separation by extractive distillation.

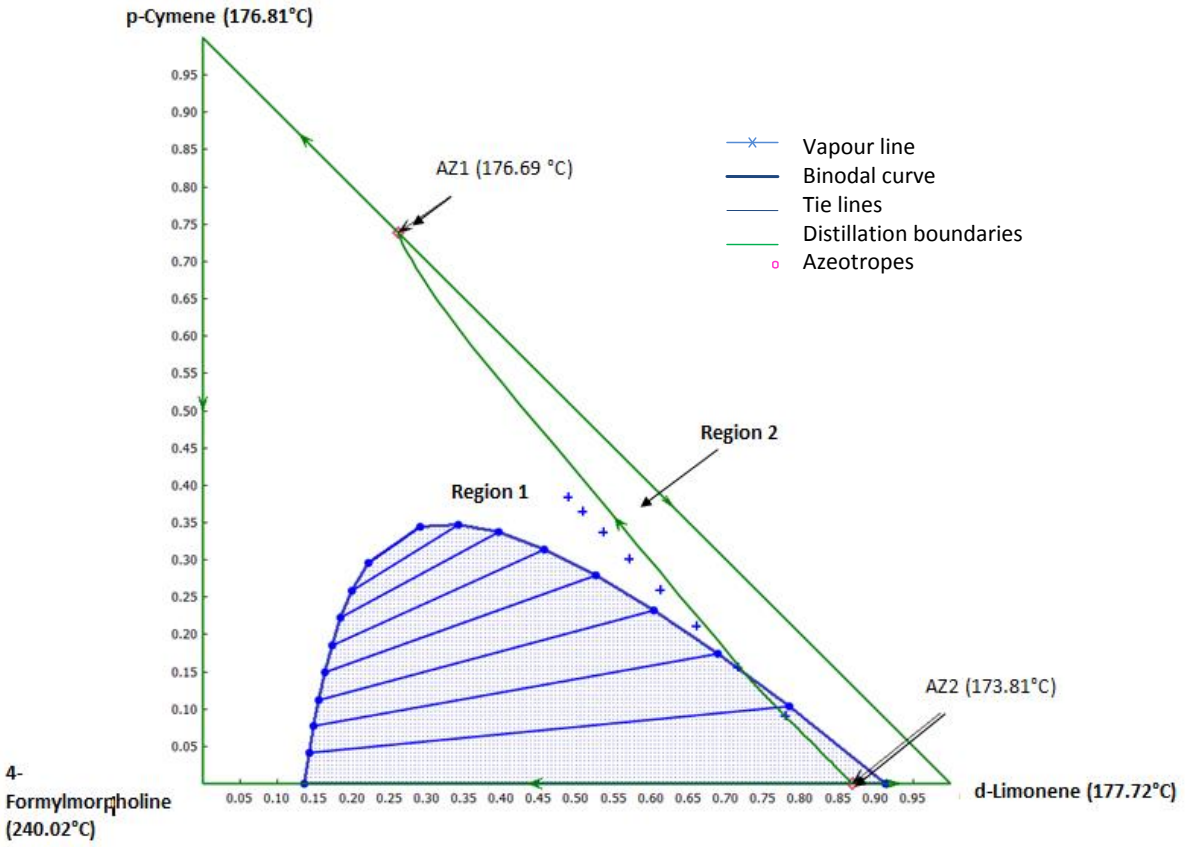

Figure 3.16 RCM for p-cymene-d-limonene-4-formylmorpholine system at 1 bar

In Figure 3.16, the RCM is divided into two distillation regions. Region 1 has a binodal curve (liquid-liquid solubility) smaller than that observed in Figure 3.13 and Figure 3.14. A vapour line which shows the vapour composition in equilibrium with the two liquid phases is in region 1. The composition of the two liquid phases can be obtained from the two ends of the tie lines that pass through the vapour line. The two liquid phase formation, however, terminates at the binodal curve. To avoid the restriction of the distillation boundary, the feed must lie in region 1 and within the binodal curve.

The overhead product can have a composition approaching that of AZ2. When the vapour is condensed, the two liquid phases split in the decanter giving a *dl*-limonene rich phase, which lies in region 2, and an entrainer rich phase, which lies in region 1. The bottoms can be a nearly pure p-cymene. The entrainer rich phase can be taken as reflux and recovered with the bottom product. The bottom product can be separated via ordinary distillation and the entrainer recycled. 4-Formylmorpholine is a regarded as a feasible entrainer as it results in the formation of heterogeneous azeotropes, allowing *d*-limonene and *p*-cymene to be separated.

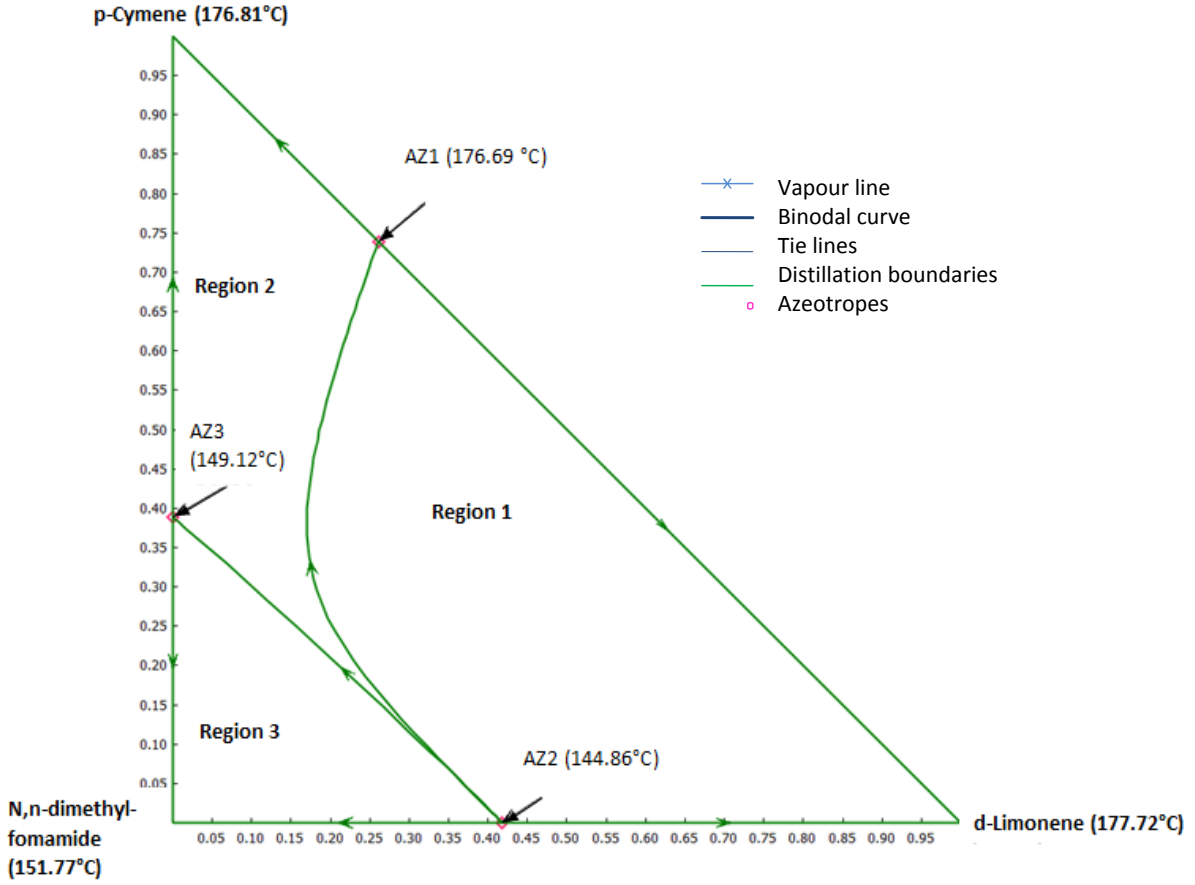

Figure 3.17 RCM for p-cymene-d-limonene-n,n-dimethylformamide system at 1 bar

From Figure 3.17, it can be seen that a distillation boundary which cause d-limonene and p-cymene to lie in different regions, exits. n,n-Dimethylformamide cause the formation of a homogenous azeotropes and is not regarded as a feasible entrainer. However, it is reported that water breaks the azeotropes between n,n-dimethylformamide and hydrocarbons (Mikitenko *et al*., 1975). Therefore, a typical operation entails a feed with a composition in region 3. An overhead product with a composition approaching AZ2, and a bottoms product with a composition approaching AZ3 is attainable.

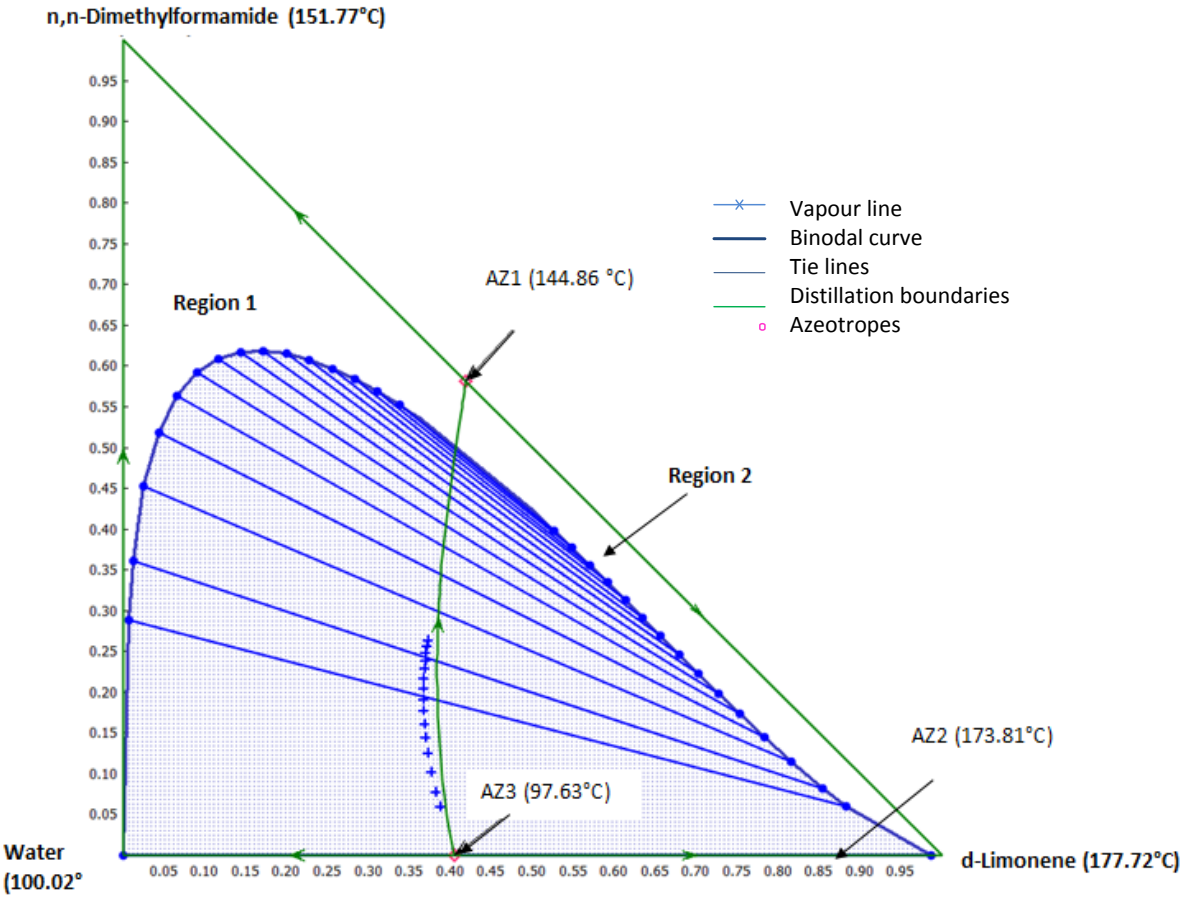

Figure 3.18 RCM for water-d-limonene-n,n-dimethylformamide system at 1 bar

From Figure 3.18, the d-limonene-n,n-dimethyformamide azeotrope obtained from the pre-concentrator column in Figure 3.18 can be broken by the addition of water. Water forms a heterogeneous azeotrope, which allows crossing of the distillation boundary. A typical operating condition would be a feed to a column with a composition that lies in region 1. This can give an overhead vapour, which when condensed, results in phase splitting to give a d-limonene rich phase and a water rich phase. A bottom product can be nearly pure entrainer.

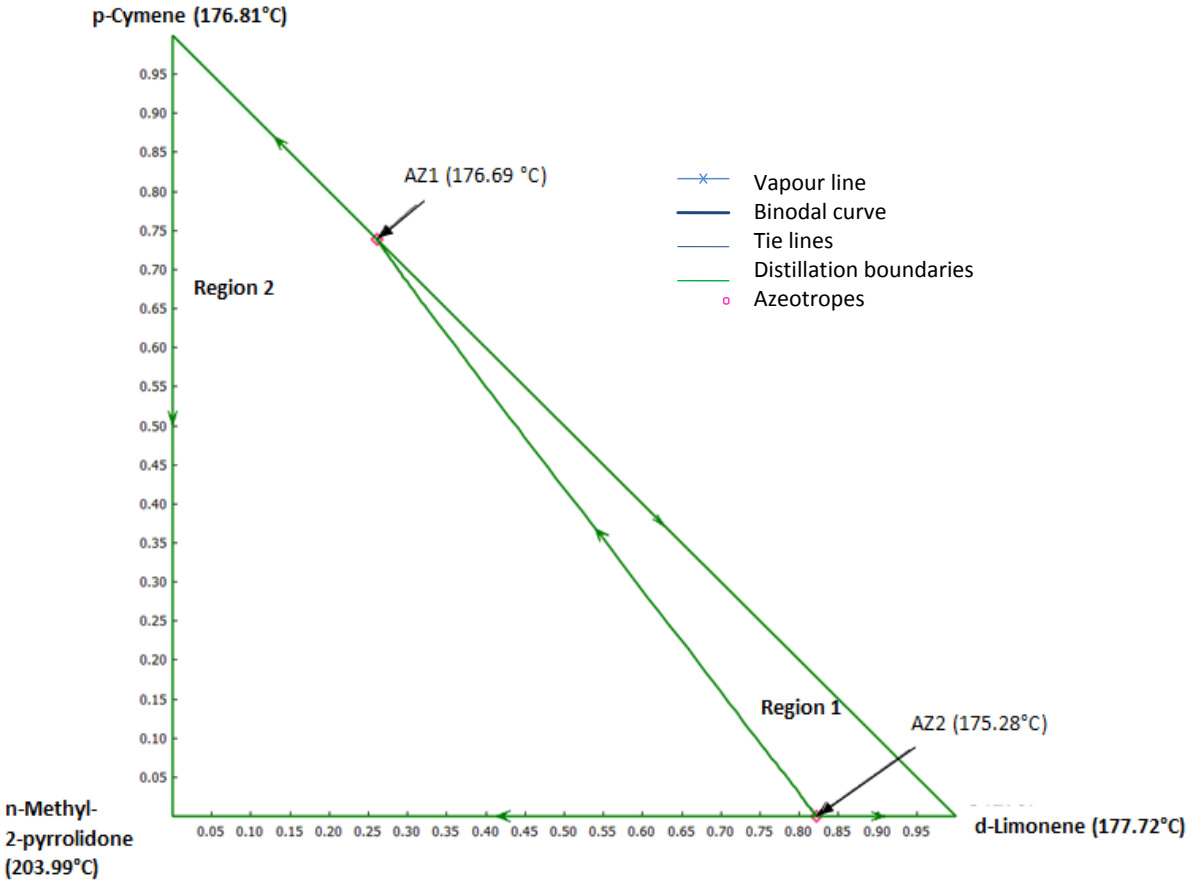

Figure 3.19 RCM for p-cymene-d-limonene-n-methyl-2-pyrrolidone system at 1 bar

From Figure 3.19, it can be seen that a distillation boundaries exist that cause d-limonene and p-cymene to lie in different regions. n-Methyl-2-pyrrolidone cause the formation of a homogenous azeotropes and is not regarded as a feasible entrainer. However, it is known from Figure 3.18 that water breaks the azeotropes between amides and hydrocarbons. Therefore, a typical operation entails a feed with a composition in region 2. An overhead product with a composition approaching AZ2, and a bottoms product with a nearly pure entrainer, is attainable.

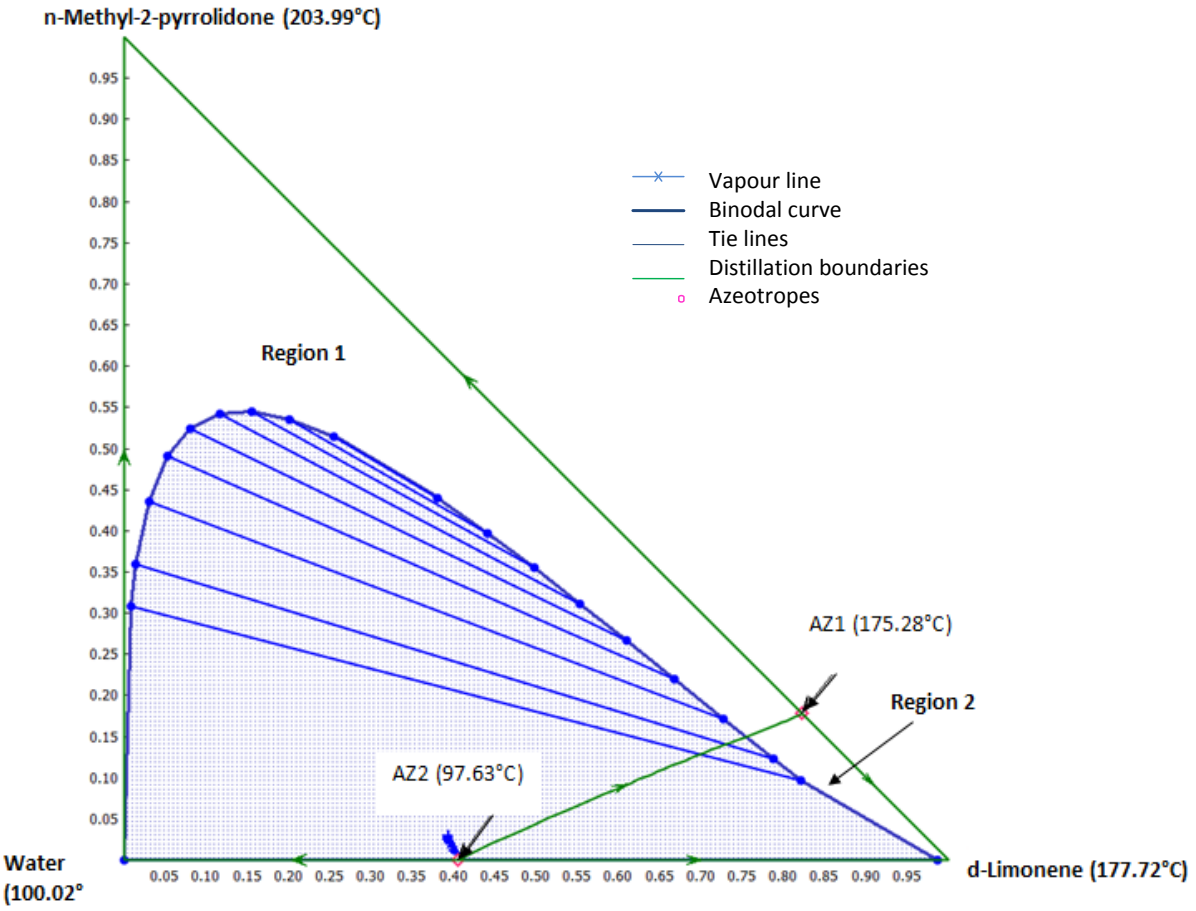

Figure 3.20 RCM for water-d-limonene-n-methyl-2-pyrrolidone system at 1 bar

From Figure 3.20, the d-limonene-n-methyl-2-pyrrolidone azeotrope obtained from the pre-concentrator column in Figure 3.19 can be crossed by the addition of water. Water forms a heterogeneous azeotrope and a region of two liquid phase formation, which allows crossing of the distillation boundary. A typical operating condition would be a feed to a column with a composition that lies in region 1. This can give an overhead vapour, which when condensed, result in phase splitting to give a *d*-limonene rich phase and a water rich phase. A bottom product can be nearly pure entrainer.

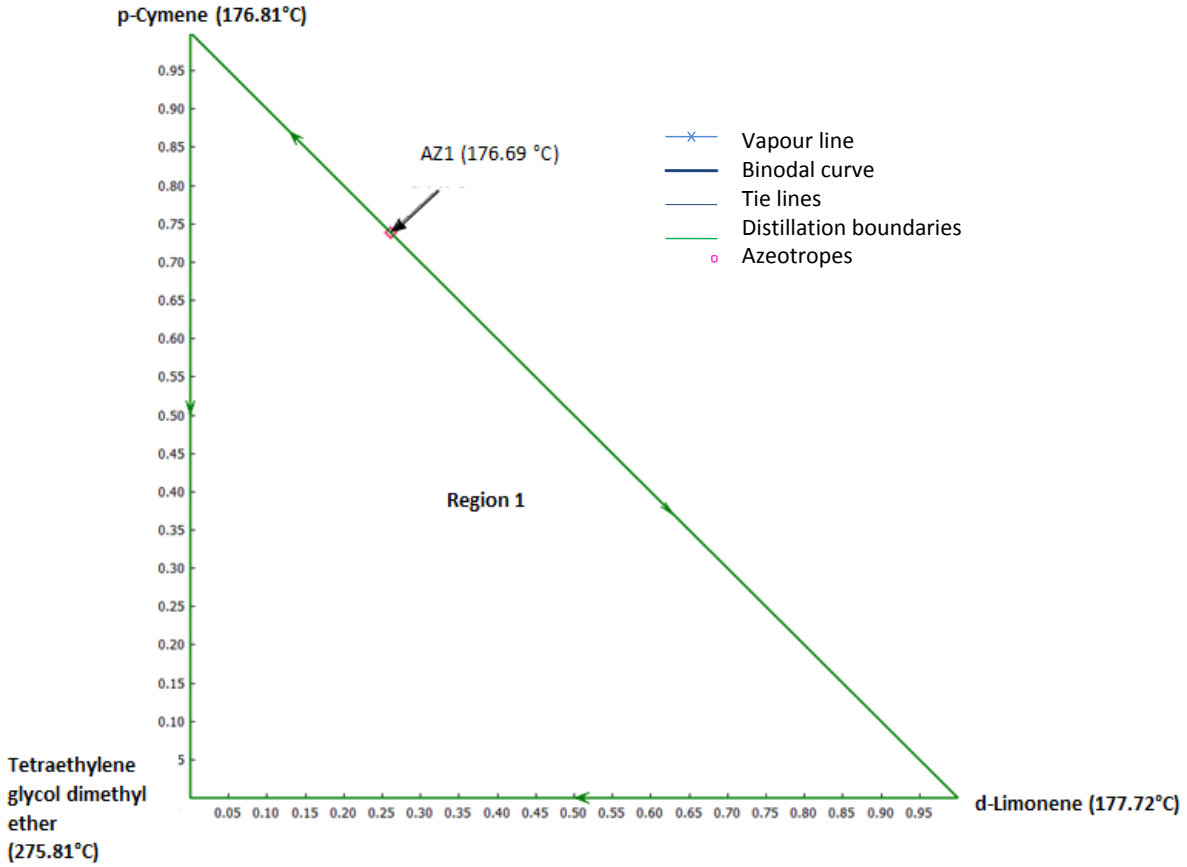

Figure 3.21 RCM for p-cymene-d-limonene-tetraethylene glycol dimethyl ether system at 1 bar

From Figure 3.21, it can be seen that no distillation boundary exist. Tetraethylene glycol dimethyl ether does not form any azeotrope with any of the components. Tetraethylene glycol dimethyl ether is a regarded as a feasible entrainer, as it causes a change in relative volatility and allows separation by extractive distillation.

The guidelines followed in selecting entrainers proved to be reliable. Entrainers to be used in the process modelling of the separation process include: diethylene glycol, triethylene glycol, n,n-dimethylformamide, n-methyl-2-pyrrolidone, quinoline, 4-formylmorpholine and tetratethylene glycol dimethyl ether. All entrainers investigated using RCM technology has shown to alter the relative volatility of *dl*-limonene and p-cymene mixture and enabling their separation.

3.3.3. Selection of thermodynamic model

Based on recommendations on the selection of thermodynamic model from Aspen Plus® method guide, Eric Carlson and Bob Seader's given in Appendix D and thermodynamic models used in industries (Table 2.3), it can be deduced that for extractive and azeotropic distillation feed, which contains a mixture of polar and apolar species, an activity coefficient model should suffice. NRTL and UNIQUAC are favoured due to their ability to predict liquid-liquid equilibrium. However, due to lack of binary interaction coefficient to cover all possible interactions between the components studied in this work, the UNIFAC property model is selected to estimate the missing binary interaction coefficient (Seider *et al*., 2004; Chen and Mathias, 2002; Smith *et al.,* 2005). NRTL is used with UNIFAC for process modelling in this study. However, UNIFAC property model used for predicting binary vapour liquid equilibrium (VLE) data should be accepted with caution, as there might be significant errors in the results.

3.3.4. Process model for diethylene glycol

Diethylene glycol is a high boiling entrainer and introduces a heterogeneous azeotrope when used as an entrainer. The flowsheet for the heterogeneous azeotropic distillation process using diethylene glycol simulated in Aspen Plus® V8.2 is shown in Figure 3.22. The stream table for the final process is given in Table 3.14. The process follows the classical configuration of heterogeneous azeotropic distillation and consists of two distillation columns. This includes: a double feed azeotropic distillation column (T102) with a decanter, and the entrainer recovery column (T102). The recycle stream and purge stream are not shown in the process models but are included in the mass balance.

In the process shown in Figure 3.22, the feed (stream 10) obtained from the upstream fractionation process model in Figure 3.1, is fed to the middle section of the azeotropic distillation column (T102). The entrainer (Stream 11) is preheated and fed to the upper section of the azeotropic distillation column. In the azeotropic distillation column, impurities and *dl*-limonene are separated. The decanter allows separation of the *dl*-limonene rich phase and entrainer rich phase. High purity *dl*-limonene is recovered as distillate (stream 13), and the refluxed entrainer and impurities are recovered as bottoms (stream 14). The *dl*-Limonene stream is cooled and taken as the final product of the process. The bottom products of the azeotropic distillation column are sent to the entrainer recovery column. The entrainer recovery column (T103) is used to separate impurities and the entrainer. The impurities are

recovered at the top (stream 16) of the recovery column and the entrainer is recovered at the bottom (stream 15). The entrainer is recycled back to the azeotropic distillation column with a 10% purge. The entrainer make-up stream is added in the mass balance but not shown on the flowsheet. The impurities streams form part of the waste stream and are not processed further in this work.

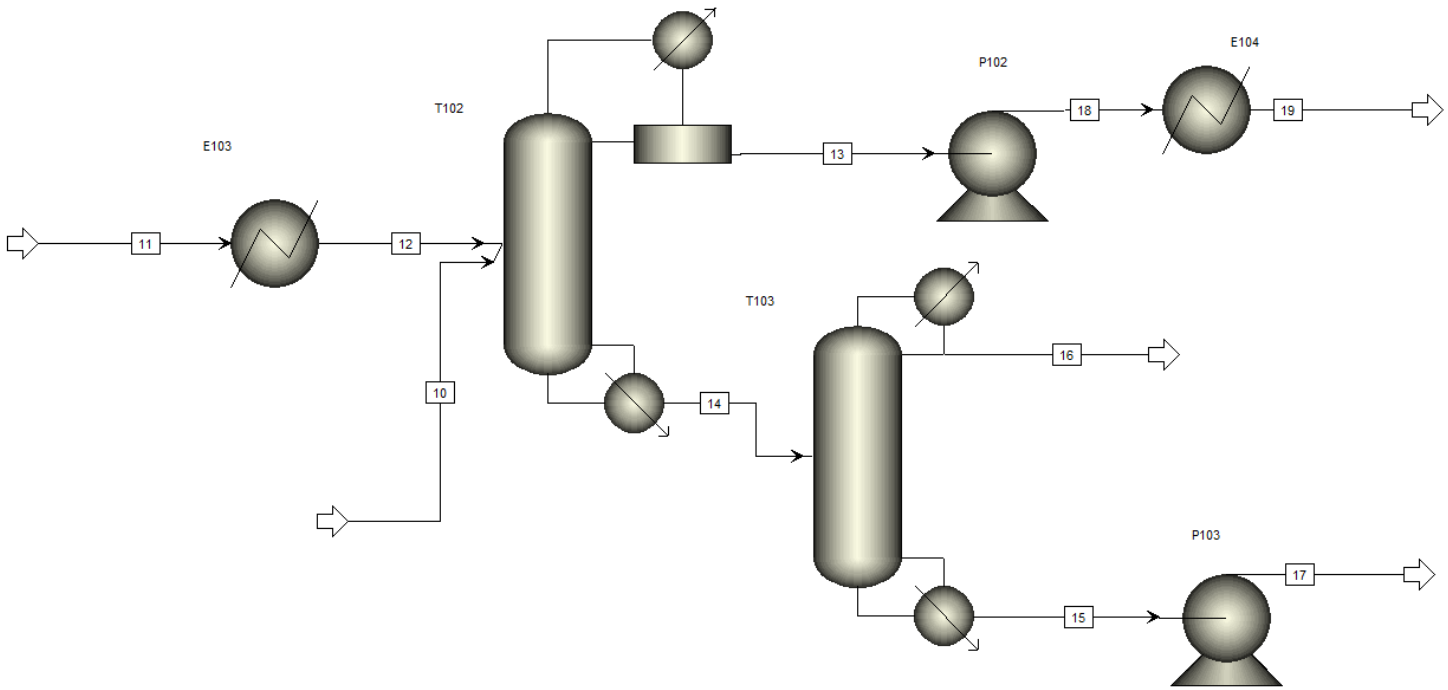

Figure 3.22 Process model for diethylene glycol

Table 3.14 Stream table for process model with diethylene glycol

Stream number	10	11	12	13	14	15	16	17	18	19
dl-Limonene (wt%)	57.02	0.00	0.00	95.16	0.51	0.00	6.74	0.00	95.16	95.16
Impurities (wt%)	42.98	0.00	0.00	1.97	7.09	0.27	90.69	0.27	1.97	1.97
Entrainer (wt%)	0.00	100.00	100.00	2.87	92.41	99.73	2.57	99.73	2.87	2.87
Mole flow (kmol/hr)	1.33	9.27	9.27	0.76	9.85	9.25	0.60	9.25	0.76	0.76
Mass flow (kg/hr)	179.71	984.00	984.00	102.01	1061.70	981.70	80.00	981.70	102.01	102.01
Temperature (°C)	159.25	25.00	100.00	154.49	170.22	172.67	107.43	172.67	157.95	25.00
Pressure (bar)	1.00	1.00	1.00	0.60	0.63	0.12	0.12	1.00	1.00	1.00
Vapor fraction	0.00	0.00	0.00	0.00	0.00	0.00	0.00	0.00	0.00	0.00

3.3.4.2 Sensitivity analysis

Input parameters for the azeotropic distillation are obtained from studies by Suppino and Cobo (2014), and are given in Table 3.15. These parameters are used as initial estimate for the Radfrac model conducted in Aspen Plus ® V8.2. Sensitivity analysis is done to investigate which parameters have a significant impact on separation (*dl*-limonene purity) and from these, the decision parameters for optimization can be determined. Sensitivity analysis is shown for entrainer 1. The same procedure is carried for other entrainers.

Table 3.15 Input parameters for azeotropic distillation and entrainer recovery

Parameter	Azeotropic distillation column	Entrainer recovery column
Number of stages	50	10
Entrainer feed stage	2	-
dl-limonene fraction feed stage	10	-
Reflux	3	3
Impurities and entrainer feed stage	-	5

Effect of entrainer feed stage

Figure 3.23 shows the effect of entrainer feed stage on purity of *dl*-limonene in the distillate at various reflux ratios. From Figure 3.23, it can be seen that when the entrainer is fed in stage 2, the purity of *dl*-limonene in the distillate is at the maximum, however, when the entrainer is fed in stages 3 through 9, the *dl*-limonene concentrations decrease for all reflux ratios. This decrease may result from vaporisation of the entrainer entering the column, which becomes part of the vapour going to the condenser and withdrawn as distillate. The entrainer should be fed closer to the condenser so it can remain largely in the liquid phase for it to be effective. Stage 2 is chosen as the entrainer feed stage.

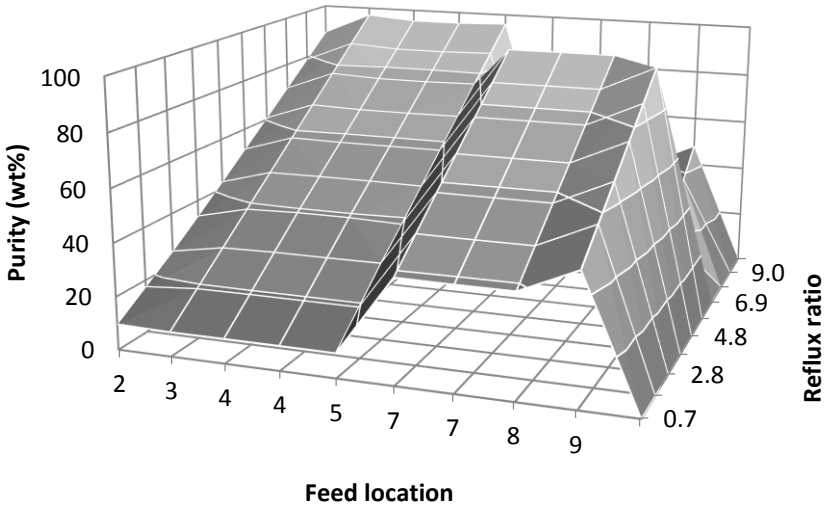

Figure 3.23 Effect of entrainer feed stage on distillate purity of *dl*-limonene for azeotropic distillation with diethylene glycol for different molar reflux ratios

Effect of entrainer feed temperature

Figure 3.24 show the effect of entrainer feed temperature on the purity of *dl*-limonene in the distillate for various reflux ratios. It can be seen from Figure 3.24 that as the entraner feed temperature increases, the concentration of *dl*-limonene in the distillate decreases. This because as the entrainer feed temperature is increased, part of the impurities from the *dl*-limonene rich stream found in the liquid in the column stages vaporises, increasing their content in the distillate and decreasing *dl*-limonene purity. It can be seen further in Figure 3.24 that increasing the reflux ratio is necessary to negate this effect. To avoid reduction in *dl*-limonene purity, it is favourable to operate at a feed temperature around 100°C at a reflux ratio of 1.6.

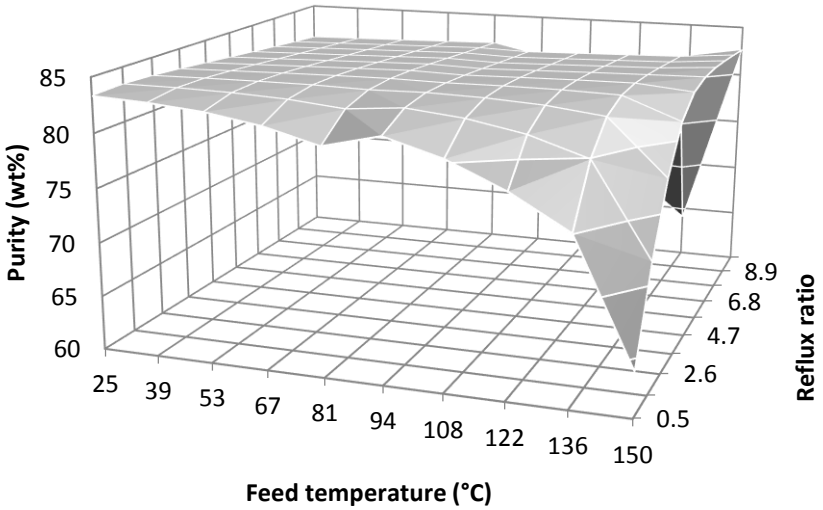

Figure 3.24 Effect of entrainer feed temperature on distillate purity of *dl*-limonene for azeotropic distillation with diethylene glycol for different molar reflux ratios,

Effect of *dl*-limonene rich naphtha cut feed stage

Figure 3.24 shows the effect of the *dl*-limonene rich naphtha cut feed stage on the composition of *dl*-limonene in the distillate for various reflux ratios. From Figure 3.24, it can be seen that as the feed stage approaches the reboiler, *dl*-limonene content increases up to a maximum, after which it remains essentially constant. Therefore, as the feed stage is at the lower part of the column, rectification of the light compounds occurs. This also allows more contact between the down flowing entrainer and the compounds. This shows that the biggest separation takes place in the rectifying section of the column. Stage 30 is chosen as the feed stage for *dl*-limonene rich naphtha cut in order to obtain high concentration of *dl*-limonene in the distillate.

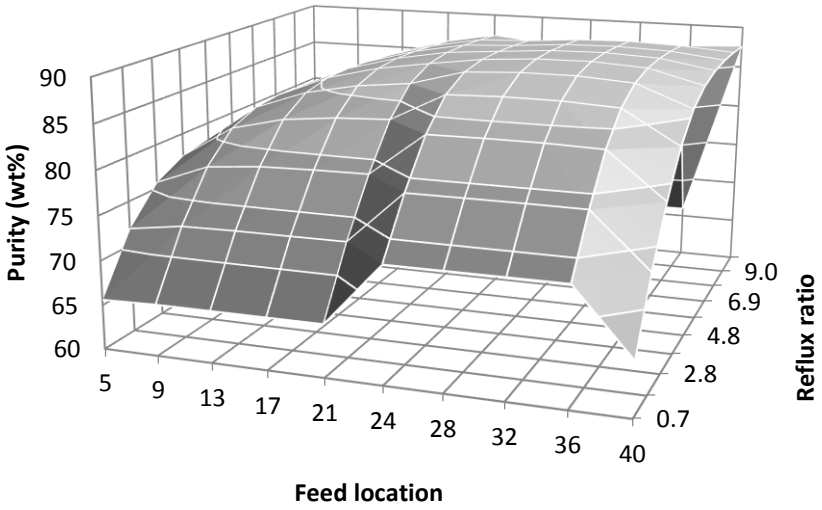

Figure 3.25 Effect of *dl*-limonene rich naphtha cut feed location on distillate purity of *dl*-limonene for azeotropic distillation column with diethylene glycol for different molar reflux ratios

Effect of entrainer to feed ratio (E/F)

In Figure 3.26, the effect of entrainer to feed ratio (E/F) on *dl*-limonene purity in the distillate is presented for different molar reflux ratios. From Figure 15, it can be seen that an increase in E/F results in an increase in *dl*-limonene concentration in the distillate. A high E/F leads to a better separation compared to the one obtained with a higher reflux ratio. Increasing the reflux ratio leads to the dilution of the entrainer, weakening its effect. High E/F is needed to make the dilution effect, caused by high refluxes, insignificant. The purity of *dl*-limonene increased above that obtained from using the E/F at base case conditions. Therefore an E/F of 6 is chosen.

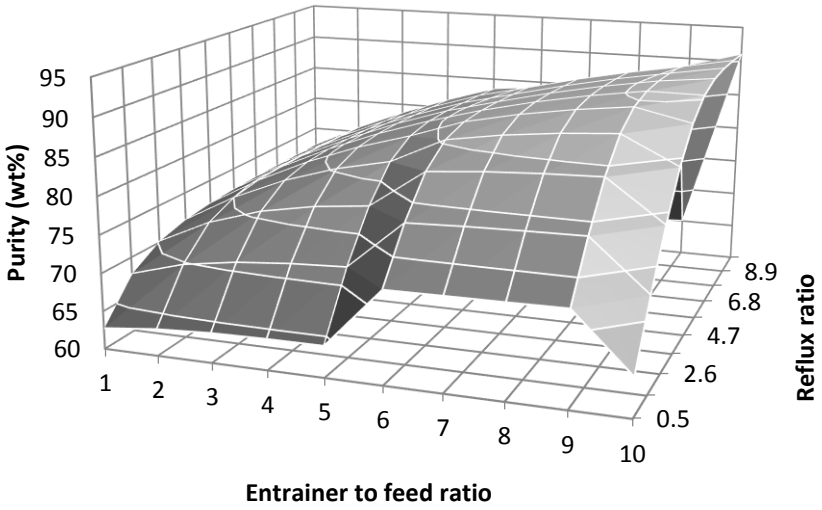

Figure 3.26 Effect of E/F ratio on azeotropic distillation with diethylene glycol on distillate purity of *dl*-limonene for molar reflux ratio,

Summary of the preffered operating conditions derived from sensitivity analysis is given in Table 3.16. From sensitivity analysis, it can be deduced that parameters that have a significant effect on the design are: the feed location, reflux ratio and E/F. These are taken as decision parameters in the optimisation step. Other parameters are fixed. When one parameter is investigated, others are fixed. Optimisation is done to determine the optimum number of stages.

Table 3.16 Operating conditions obtained for the distillation column of feed 1

Parameters	T102
Process feed stage	30
Entrainer feed stage	2
E/F	6
Reflux ratio	1.6
Entrainer feed temperature (°C)	100

Optimum operating conditions

To get an optimized design, the number of stages, reboiler duty and E/F must be kept at the lowest value possible, as they contribute largely to the operating cost and capital expenditure. The major concern with separation of close boiling compounds is the large number of stages required, which falls outside the typical industrial practise for column design (Lek-utaiwan *et al.,* 2011; Muñoz *et al.,* 2006). Therefore, the optimum design is shifted towards minimisation of number of stages. This in turn reduces the capital investment, which is important when constructing new projects (Lek-utaiwan *et al.,* 2011).

Optimum number of stages for various feed stages of light naphtha cut

Figure 3.27 and Figure 3.28 show the effect of feed stages on the purity of *dl*-limonene in the distillate and the energy consumption in the reboiler, with increasing number of stages.

From Figure 3.27, it can be seen that the maximum purity is achieved at a number of stages above 45, and as the feed of *dl*-limonene rich naphtha cut is increased. For feed stages above 30, with the number of stages above 45, an increase in purity is not significant.

From Figure 3.28, it can be seen that the reboiler duty increases with feed stages, for feed stages below 25. For the number of stages above 45 and feed stages above 25, the purity reaches its maximum and remains essentially constant. Above a feed stage of 25, a decrease in reboiler energy can be observed. Therefore, a column with a feed stage above 25 is chosen, with a minimum number of stages of 45 to ensure maximum purity of *dl*-limonene in the distillate.

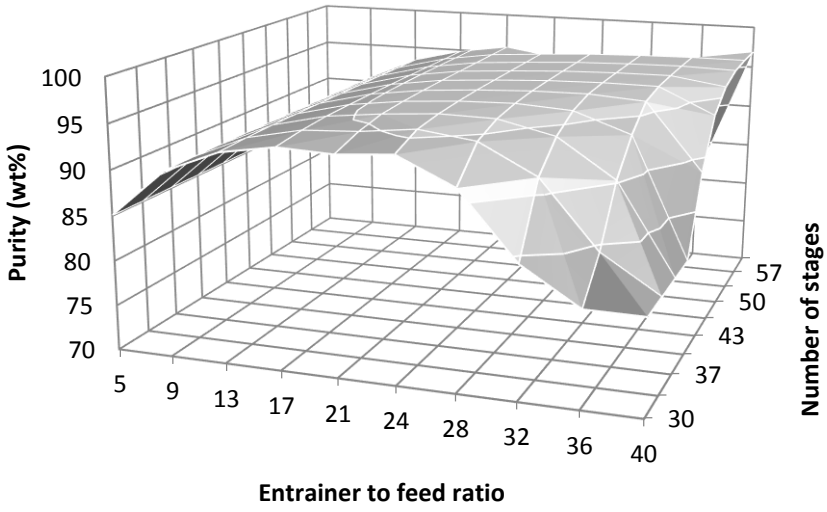

Figure 3.27 Effect of feed stage on *dl*-limonene purity for different number of stages

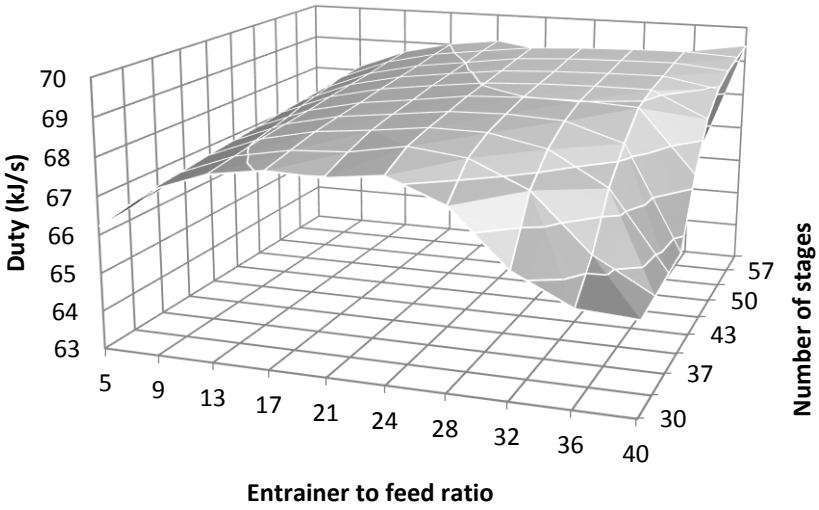

Figure 3.28 Effect of feed stage on azeotropic distillation column reboiler duty for various number of stages

Optimum number of stages for various E/F

Figure 3.29 and Figure 3.30 show the effect of E/F on the concentration of *dl*-limonene in the distillate and the energy consumption in the reboiler, with an increasing number of stages.

From Figure 3.29, it can be seen that increases in the number of stages and E/F, result in increases in purity of *dl*-limonene in the distillate. From Figure 3.29, it can also be seen that the purity continues to increase slowly, even with the number of stages above 50 and E/F above 5. Therefore, an operation with an E/F of 6 and minimum number of stages of 50 is required to ensure a high purity of *dl*-limonene in the distillate.

From Figure 3.30 it can been seen that an increase in E/F considerably affect the energy consumption for any number of stages. As both the reflux ratio and E/F increase energy consumption, the reflux ratio must be operated in the lowest possible value, so the E/F can be increased to reach the desired product composition without high energy consumption.

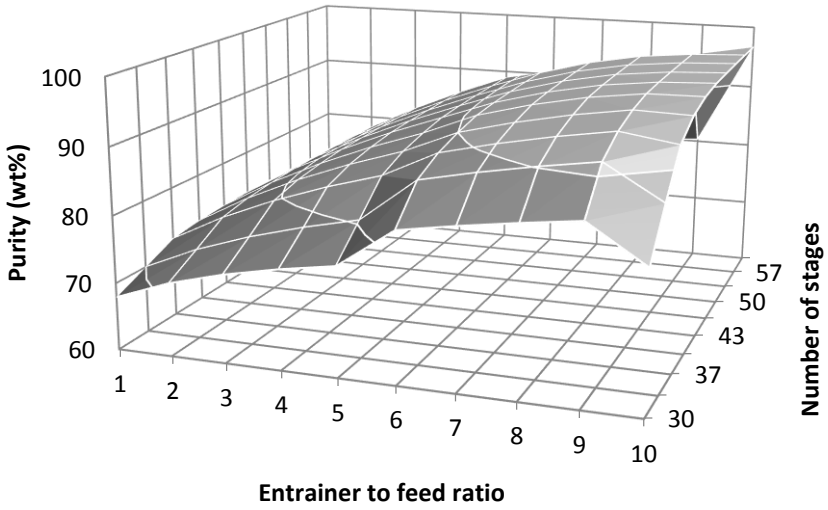

Figure 3.29 Effect of E/F on *dl*-limonene purity in the distillate for various number of stages,

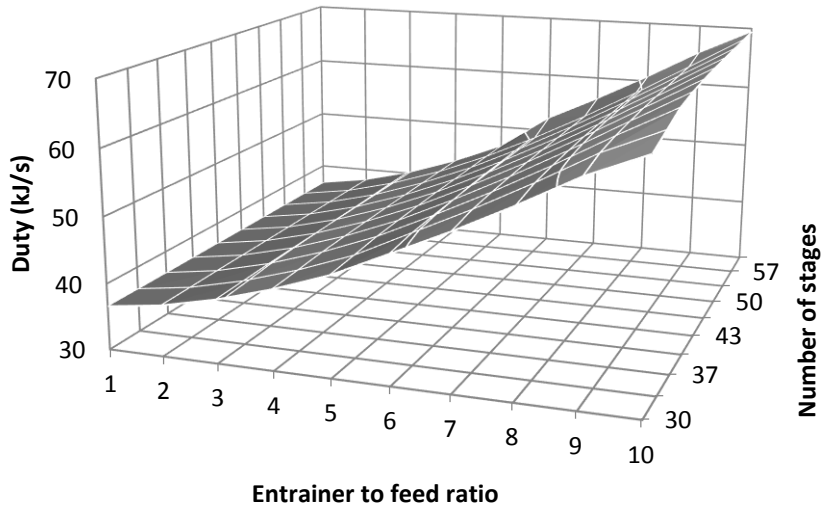

Figure 3.30 Effect of E/F on the reboiler duty of the azeotropic distillation column for various number of stages

Optimum number of stages for various reflux ratios

Using the selected E/F of 6, feed stage of 30, and knowing the required minimum number of stages, the optimum number of stages can be determined. Figure 3.31 to Figure 3.33 shows the results for the composition of *dl*-limonene in the distillate, the energy consumption in the reboiler and product recovery for different number of stages and reflux ratios.

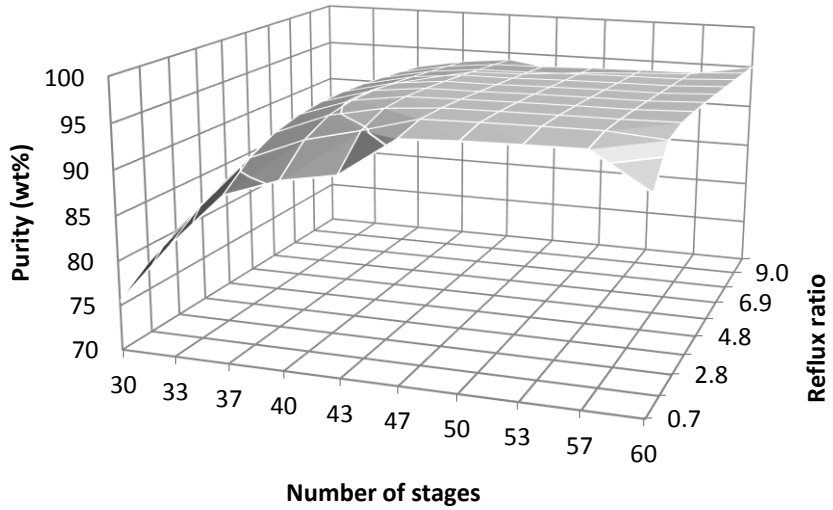

Figure 3.31 Effect of number of stages on *dl*-limonene purity in the distillate for different molar reflux ratios

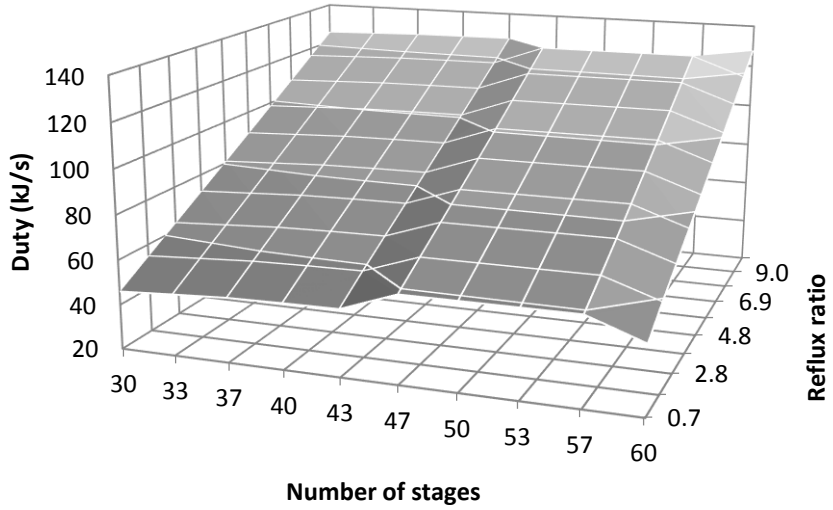

Figure 3.32 Effect of number of stages on the extractive distillation reboiler duty for different molar reflux ratios

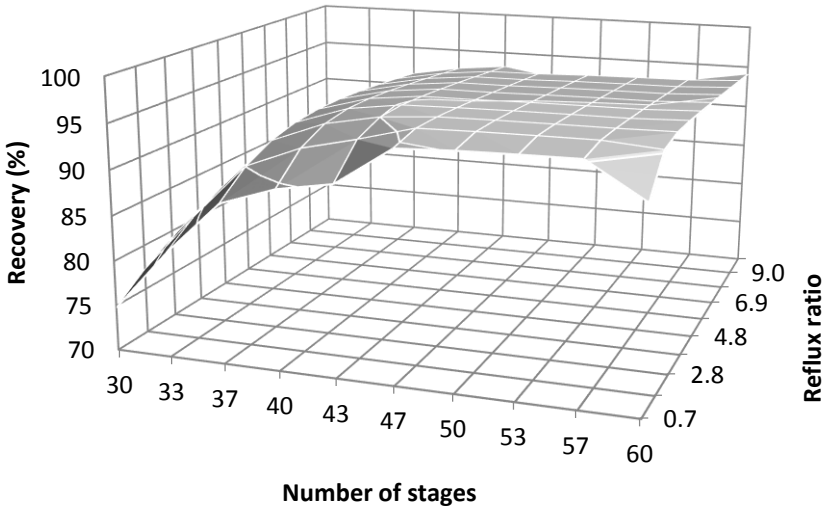

Figure 3.33 Effect of number of stages on recovery of *dl*-limonene for different molar reflux ratios

From Figure 3.31, it can be seen that an increase in the number of stages results in an increase in the purity of *dl*-limonene. For number of stages above 50, at a fixed reflux ratio, an increase in purity is not significant.

From Figure 3.32, it can be seen that the reboiler duty is not largely affected by an increase in the number of stages for a fixed reflux ratio. From Figure 3.33, it can be seen that the recovery of *dl*-limonene increases with an increase in the number of stages, after which it remains constant. Because both the reflux ratio and E/F contribute largely to energy consumption, one parameter must be operated at a low value. A high E/F leads to a better separation compared to the one obtained with a higher reflux ratio.The most economical operation and a high *dl*-limonene purity and recovery, require 55 stages in the fractionation column which correspond to at a reflux ratio of 1.6. The fixed capital cost for the column for various number of trays and the operational cost of steam and cooling water are calculated to give the total cost over an assumed project life of 15 years in Figure 3.34 (Turton *et al.*, 2009).

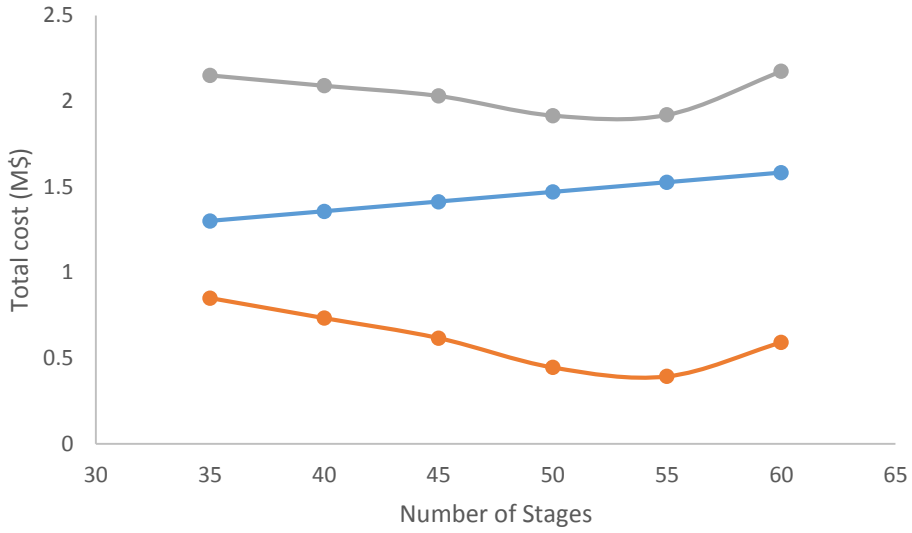

Figure 3.34 CAPEX ●, OPEX ● and total cost ● for heterogeneous azeotropic distillation operation

From Figure 3.34, it can be seen that, in order to operate at the least total cost whilst ensuring and a high *dl*-limonene purity and recovery, 55 is the number of stages chosen is required for in the fractionation column which correspond to at a reflux ratio of 1.8 to meet the targeted purity and recovery. The operating parameters for azeotropic distillation column before and after sensitivity analysis are summarised in Table 3.17.

Table 3.17 Operating conditions obtained for diethylene glycol process model before and after sensitivity analysis

Parameters	**Initial**		**Final**	
	T102	**T103**	**T102**	**T103**
Number of stages	50	10	55	10
Naphtha feed stage	10	-	24	-
Reflux ratio	3.00	3.00	1.80	1.60
Entrainer feed stage	2	-	2	-
Entrainer Feed temperature (°C)	95.00	-	95.00	-
Entrainer to feed ratio (E/F)	3.00	-	5.50	-
Feed stage of the recovery column	-	5	-	4
Condenser / top stage pressure (bar)	0.60	0.12	0.60	0.12
Reboiler duty (kJ/s)	71.14	26.33	58.39	17.54
dl-Limonene distillate purity (wt%)	90.22	-	95.18	-
Entrainer bottoms purity (wt%)	-	99.00	-	99.00
dl-Limonene recovery in distillate (%)	95.00	-	95.00	-
Entrainer bottoms recovery (%)	-	-	-	99.00

3.3.5. Process model for triethylene glycol

Triethylene allows separation by heterogeneous azeotropic distillation, and the process configuration is similar to that using diethylene glycol as an entrainer. The flowsheet for the process simulated in Aspen Plus® V8.2 is shown in Figure 3.35.

Input parameters for this process model are obtained from the process model developed using diethylene glycol. These parameters are used as initial estimate for the Radfrac model of azeotropic distillation using triethylene glycol. Sensitivity analysis is done to verify and establish final operating conditions. The operating parameters for azeotropic distillation columns before and after sensitivity analysis are summarised in Table 3.18. Sensitivity analysis plots for important parameters can be seen in Appendix E.

Table 3.18 Operating conditions obtained for triethylene glycol process model before and after sensitivity analysis.

Parameters	**Initial**		**Final**	
	T102	**T103**	**T102**	**T103**
Number of stages	55	10	55	5
Naphtha feed stage	24	-	29	-
Reflux ratio	1.80	3.00	1.80	2.70
Entrainer feed stage	2	-	2	-
Entrainer Feed temperature (°C)	95.00	-	95.00	-
Entrainer to feed ratio (E/F)	5.50	-	5.87	-
Entrainer recovery column feed stage	-	5	-	2
Condenser / top stage pressure (bar)	0.60	0.02	0.60	0.02
Reboiler duty (kJ/s)	71.18	20.25	74.73	14.94
dl-Limonene distillate purity (wt %)	95.02	-	95.98	-
Entrainer bottoms purity (wt%)	-	99.00	-	99.00
dl-Limonene recovery in distillate (%)	95.00	-	95.00	-
Entrainer bottoms recovery (%)	-	99.00	-	99.00

From Table 3.18, it can be seen that process parameters established for process model for diethylene glycol, are suitable for the process model for triethylene glycol. The recovery and purity of *dl*-limonene reach the targeted value. Triethylene glycol is a suitable entrainer as the desired product specification is achieved within the specified operational constraints. The stream table for the final process is given in Table 3.19. From sensitivity analysis it can be deduced that an increase in the number of stages and E/F result in an increase in *dl*-limonene purity. It can also be deduced that a better separation is achieved when the entrainer is fed at the upper stages and the naphtha is fed in the middle stages.

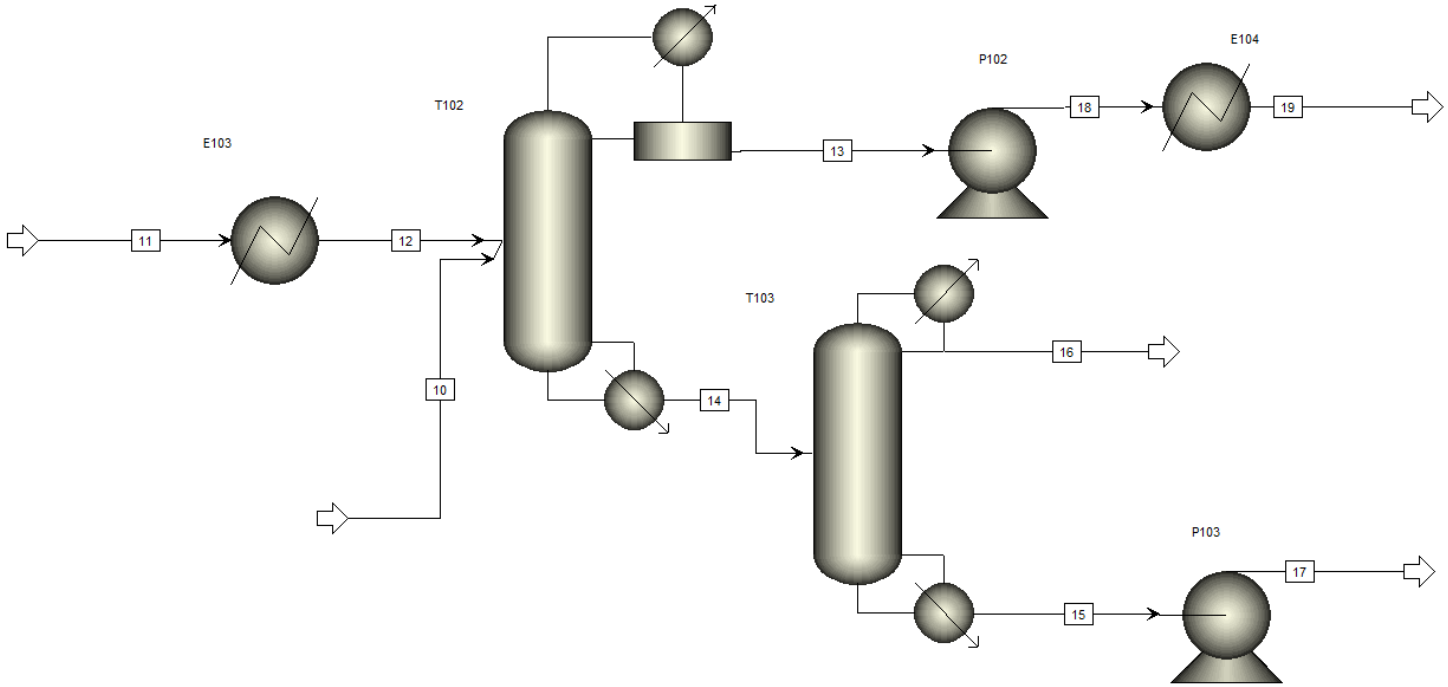

Figure 3.35 Process model for triethylene glycol

Table 3.19 Stream table for process model with triethylene glycol

Stream number	10	11	12	13	14	15	16	17	18	19
dl-Limonene (wt%)	57.02	0.00	0.00	96.26	0.36	0.00	5.09	0.00	96.26	96.26
Impurities (wt%)	42.98	0.00	0.00	2.61	6.61	0.00	94.13	0.00	2.61	2.61
Entrainer (wt%)	0.00	100.00	100.00	1.14	93.03	100.00	0.55	100.00	1.14	1.14
Mole flow (kmol/hr)	1.33	6.99	6.99	0.75	7.57	6.98	7.57	6.98	0.75	0.75
Mass flow (kg/hr)	179.70	1050.00	1050.00	102.27	1127.43	1048.43	79.00	1048.43	102.27	102.27
Temperature (°C)	159.25	25.00	100.00	156.58	179.27	169.04	66.72	169.04	156.58	25.00
Pressure (bar)	1.00	1.00	1.00	0.60	0.60	0.02	0.02	1.00	1.00	1.00
Vapor fraction	0.00	0.00	0.00	0.00	0.00	0.00	0.00	0.00	0.00	0.00

3.3.6. Process model for 4-formylmorpholine

4-Formylmorpholine allows separation by heterogeneous azeotropic distillation and the process configuration is similar to that using diethylene glycol as an entrainer. The flowsheet for the distillation process using 4-formylmorpholine simulated in Aspen Plus® V8.2 is shown in Figure 3.36.

Input parameters for azeotropic distillation using 4-formylmorpholine are obtained from studies by Kim *et al.* (2002). These parameters are used as initial estimates for the Radfrac model. Sensitivity analysis is done to establish the final operating conditions. The chosen operating parameters for azeotropic distillation columns before and after sensitivity analysis are summarised in Table 3.20. Sensitivity analysis plots can be seen in Appendix E.

Table 3.20 Operating conditions obtained for 4-formylmorpholine process model before and after sensitivity analysis.

Parameters	**Initial**		**Final**	
	T102	**T103**	**T102**	**T103**
Number of stages	60	10	30	7
Naphtha feed stage	30	-	20	-
Reflux ratio	0.50	3.00	0.50	1.70
Entrainer feed stage	2	-	2	-
Entrainer Feed temperature (°C)	114.00	-	114.00	-
Entrainer to feed ratio (E/F)	3.50	-	3.00	-
Entrainer recovery column feed stage	-	5	-	3
Condenser / top stage pressure (bar)	0.60	0.10	0.60	0.15
Reboiler duty (kJ/s)	40.42	19.33	35.21	13.02
dl-Limonene distillate purity (wt %)	91.02	-	91.02	-
Entrainer bottoms purity (wt%)	-	99.00	-	99.00
dl-Limonene recovery in distillate (%)	95.00	-	95.00	-
Entrainer bottoms recovery (%)	-	97.00	-	97.00

From Table 3.20, it can be seen that operating conditions derived from studies by Kim *et al.* (2002), are not suitable for the process model for 4-formylmorpholine. The same product specification can be achieved with fewer number of stages and energy consumption after optimization. For this system, *dl*-limonene forms an azeotrope with the entrainer. Nevertheless, the recovery and purity of *dl*-limonene meet the targeted value. 4-Formylmorpholine is a suitable entrainer as the desired product specification is achieved within the specified operational constraints. The stream table for the final process is given in Table 3.21. From sensitivity analysis it can be deduced that an increase in the number of stages and E/F result in increases in *dl*-limonene purity. It can also be deduced that a better

separation is achieved when the entrainer is fed at the upper stages and the naphtha is fed in the middle stages.

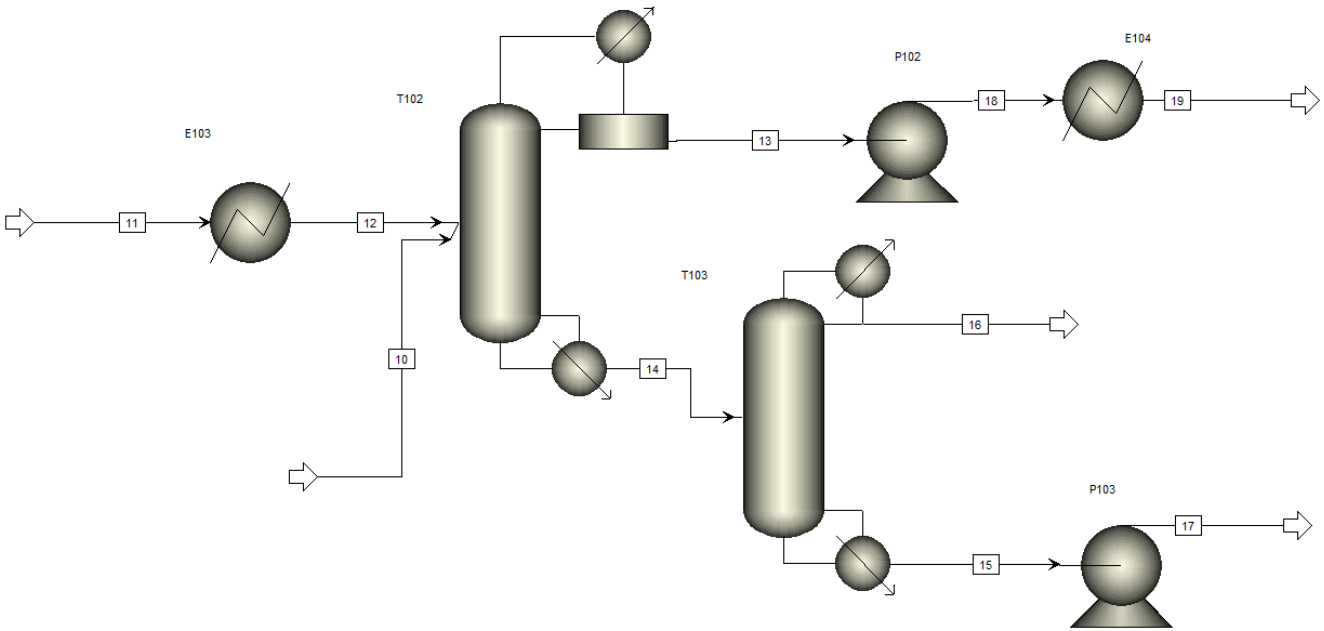

Figure 3.36 Process model for 4-formylmorpholine

Table 3.21 Stream table process model with 4-formylmorpholine

Stream number	10	11	12	13	14	15	16	17	18	19
dl-Limonene (wt%)	57.02	0.00	0.00	91.01	0.84	0.00	6.14	0.00	91.01	91.01
Impurities (wt%)	42.98	0.00	0.00	0.05	12.72	0.89	87.67	0.89	0.05	0.05
Entrainer (wt%)	0.00	100.00	100.00	8.94	86.44	99.11	6.19	99.11	8.94	8.94
Mole flow (kmol/hr)	1.33	4.64	4.64	0.80	5.17	4.55	0.63	4.55	0.80	0.80
Mass flow (kg/hr)	179.70	534.00	534.00	107.00	606.70	524.00	82.70	524.00	107.00	107.00
Temperature (°C)	159.25	25.00	114.00	154.10	177.11	165.10	115.03	166.60	158.79	25.00
Pressure (bar)	1.00	1.00	1.00	0.60	0.61	0.15	0.15	1.00	1.00	1.00
Vapor fraction	0.00	0.00	0.00	0.00	0.00	0.00	0.00	0.00	0.00	0.00

3.3.7. Process model for quinoline

Quinoline is a high boiling chemical compound and introduces no azeotropes when used as an entrainer. The flowsheet for extractive distillation process simulated in Aspen Plus® V8.2 is shown in Figure 3.37. The difference between the separation process configuration in Figure 3.22 and Figure 3.37 is that in Figure 3.37, no decanter is used with the distillation column (T101) as there is no formation of two liquid phases.

Quinoline can be considered a novel entrainer as there is a lack of information in literature on its use as an entrainer in extractive distillation processes. Input parameters for extractive distillation using quinoline are derived from azeotropic distillation, using 4-formylmorpholine, as they belong to the same chemical group, and their influence on the relative volatility is almost the same, as can be seen in Table 3.13. It is known that when considering a high boiling entrainer to facilitate separation, the entrainer is fed at upper trays and the naphtha at the middle section of the column. In addition, a low reflux ratio is required. The operating parameters for extractive distillation columns before and after sensitivity analysis are summarised in Table 3.22. Sensitivity analysis plots can be seen in Appendix E.

Table 3.22 Operating conditions obtained for quinoline process model before and after sensitivity analysis**.**

Parameters	Initial		Final	
	T102	T103	T102	T103
Number of stages	55	10	45	15
Naphtha feed stage	24	-	25	-
Reflux ratio	1.80	3.00	2.70	2.60
Entrainer feed stage	2.00	-	9.00	-
Entrainer Feed temperature (°C)	114.00	-	114.00	-
Entrainer to feed ratio (E/F)	5.50	-	5.00	-
Entrainer recovery column feed stage	-	5.00	-	6.00
Condenser / top stage pressure (bar)	0.30	0.20	0.30	0.20
Reboiler duty (kJ/s)	15.52	4.92	60.36	23.18
dl-Limonene distillate purity (wt %)	98.15	-	98.70	-
Entrainer bottoms purity (wt%)	-	95.10	-	99.00
dl-Limonene recovery in distillate (%)	95.00	-	95.00	-
Entrainer bottoms recovery (%)	-		-	99.00

From Table 3.22, it can be seen that operating conditions established for this process model with initial parameters from process model for 4-formylmorpholine, yield a high purity *dl*-limonene after optimisation. It can also noticeable that extractive distillation and hetereogeneous azeotropic distillation require a high E/F and more number of stages.

Quinoline is a suitable entrainer as the desired product specification is achieved within the specified operational constraints. The stream table for the final process is given in Table 3.23. From sensitivity analysis it can be deduced that an increase in the number of stages and E/F result in an increase in *dl*-limonene purity. It can also be deduced that a better separation is achieved when the entrainer is fed at the upper stages and the naphtha is fed in the middle stages.

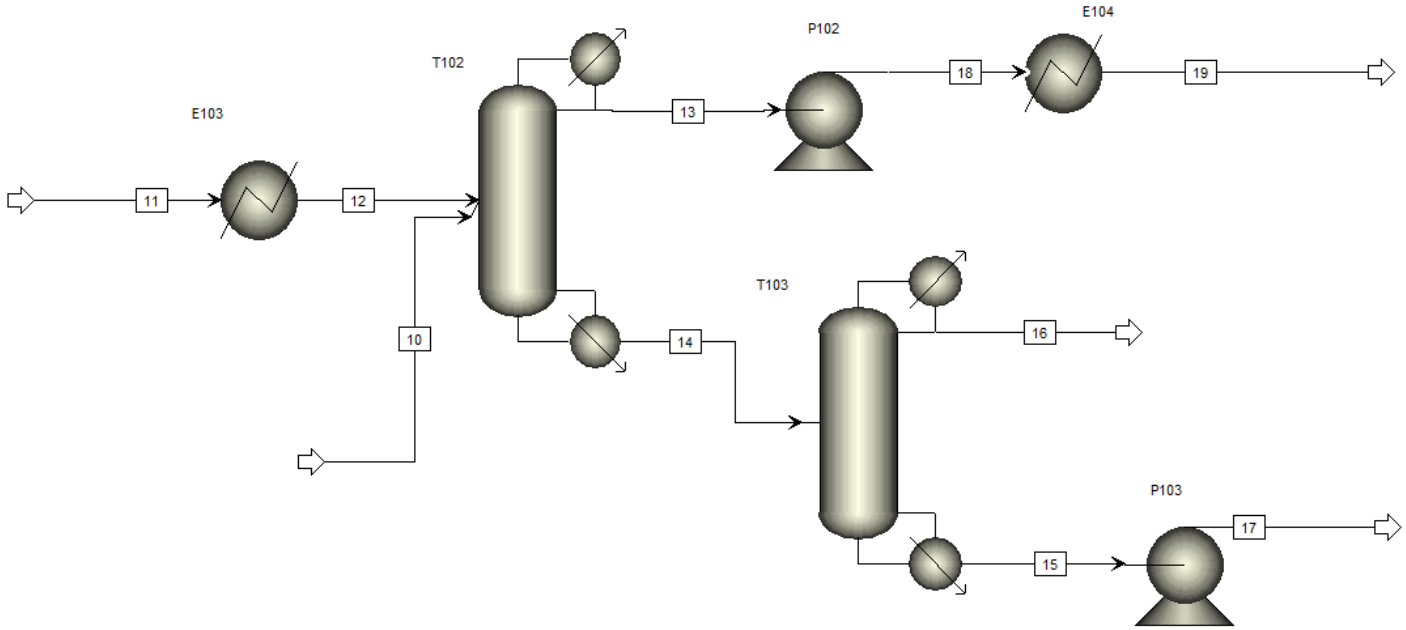

Figure 3.37 Process model for quinoline

Table 3.23 Stream table process model with quinoline

Stream number	10	11	12	13	14	15	16	17	18	19
dl-Limonene (wt%)	57.02	0.00	0.00	98.70	0.49	0.00	5.85	0.00	98.70	98.70
Impurities (wt%)	42.98	0.00	0.00	0.93	7.83	0.96	83.68	0.96	0.93	0.93
Entrainer (wt%)	0.00	100.00	100.00	0.37	91.68	99.04	10.47	99.04	0.37	0.37
Mole flow (kmol/hr)	1.33	6.92	6.92	0.73	7.53	6.92	0.61	6.92	0.73	0.73
Mass flow (kg/hr)	179.70	894.00	894.00	99.00	974.70	893.70	81.00	893.70	99.00	99.00
Temperature (°C)	159.25	25.00	114.00	132.98	178.13	174.34	125.25	176.93	136.64	25.00
Pressure (bar)	1.00	1.00	1.00	0.30	0.32	0.21	0.20	1.00	1.00	1.00
Vapor fraction	0.00	0.00	0.00	0.00	0.00	0.00	0.00	0.00	0.00	0.00

3.3.8. Process model for tetraethylene glycol dimethyl ether

Tetraethylene glycol dimethyl ether is a high boiling entrainer and introduces no azeotrope when used as an entrainer. The flowsheet for the distillation process simulated in Aspen Plus® V8.2 is that shown in Figure 3.37.

There is a lack of information in literature on extractive distillation using tetraethylene glycol dimethyl ether. Input parameters for the extractive distillation using Tetraethylene glycol dimethyl ether are derived from azeotropic distillation diethylene and triethylene glycol as they are similar in that they both have hydroxyl functional groups. The chosen operating parameters for azeotropic distillation column after sensitivity analysis and optimisation are summarised in Table 3.24. Sensitivity analysis plots can be seen in Appendix E.

Table 3.24 Operating conditions obtained for tetraethylene glycol dimethyl ether process model before and after sensitivity analysis.

Parameters	Initial		Final	
	T102	T103	T102	T103
Number of stages	55	10	55	7
Naphtha feed stage	24	-	35	-
Reflux ratio	1.80	3.00	2.70	1.70
Entrainer feed stage	2.00	-	6.00	-
Entrainer Feed temperature (°C)	95.00	-	114.00	-
Entrainer to feed ratio (E/F)	5.50	-	6.00	-
Entrainer and entrainer feed stage	-	5.00	-	3.00
Condenser / top stage pressure (bar)	0.20	0.04	0.20	0.04
Reboiler duty (kJ/s)	72.57	26.67	72.39	17.82
dl-Limonene distillate purity (wt %)	95.48	-	98.61	-
Entrainer bottoms purity (wt%)	-	99.00	-	99.00
dl-Limonene recovery in distillate (%)	95.00	-	95.00	-
Entrainer bottoms recovery (%)	-	99.00	-	99.00

From Table 3.24, it can be seen that operating conditions derived from the process model for triethylene glycol, yield a high purity *dl*-limonene in the process model for tetraethylene glycol dimethyl ether. Extractive distillation using tetraethylene glycol dimethyl ether requires a high E/F and more number of stages similar to azeotropic distillation using triethylene glycol. Quinoline is a suitable entrainer as the desired product specification is achieved within the specified operational constraints. The stream table for the final process is given in Table 3.25.

From sensitivity analysis it can be deduced that an increase in the number of stages and E/F result in an increase in *dl*-limonene purity. It can also be deduced that a better separation is

achieved when the entrainer is fed at the upper stages and the naphtha is fed in the middle stages.

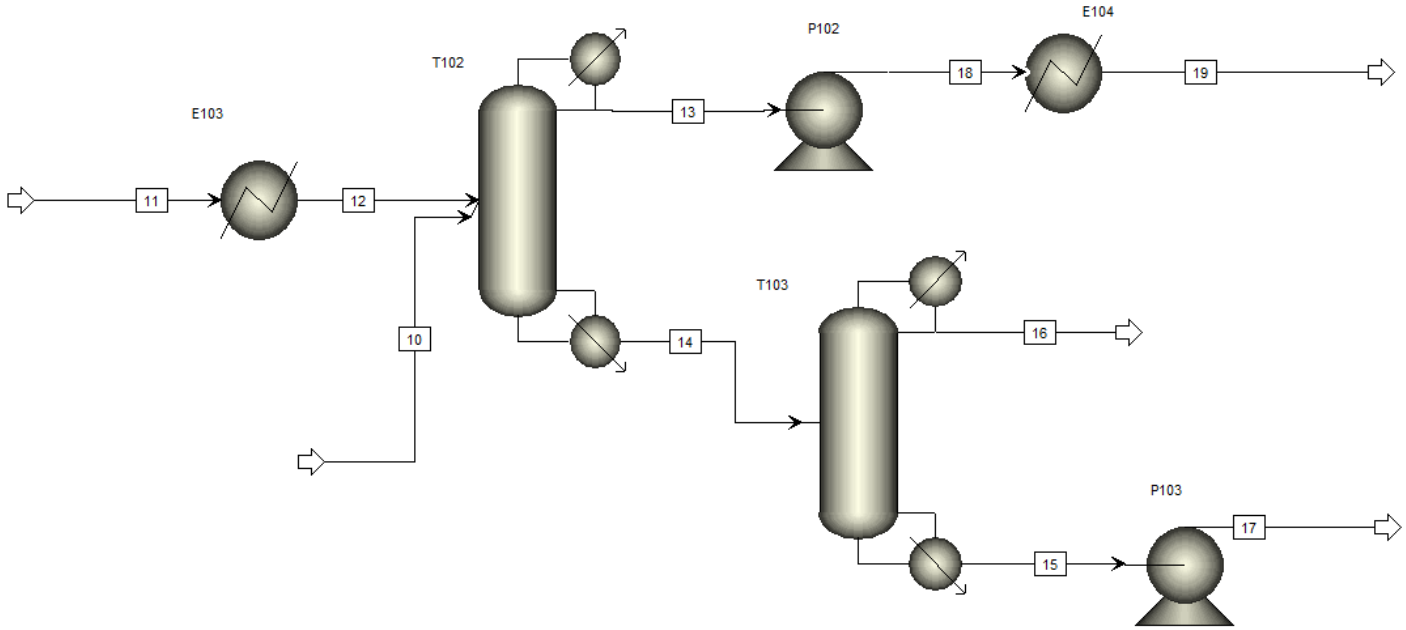

Figure 3.38 Process model for tetraethylene glycol dimethyl ether

Table 3.25 Stream table process model with tetraethylene glycol dimethyl ether

Stream number	10	11	12	13	14	15	16	17	18	19
dl-Limonene (wt%)	57.02	0.00	0.00	98.61	0.42	0.00	6.00	0.00	98.61	98.61
Impurities (wt%)	42.98	0.00	0.00	1.39	6.63	0.04	93.54	0.04	1.39	1.39
Entrainer (wt%)	0.00	100.00	100.00	0.00	92.95	99.96	0.46	99.96	0.00	0.00
Mole flow (kmol/hr)	1.33	4.79	4.79	0.73	5.39	4.79	0.60	4.79	0.73	0.73
Mass flow (kg/hr)	179.70	1064.00	1064.00	99.00	1144.70	1064.00	80.70	1064.00	99.00	99.00
Temperature (°C)	159.25	25.00	114.00	120.34	172.96	175.41	81.46	181.30	123.54	25.00
Pressure (bar)	1.00	1.00	1.00	0.20	0.23	0.04	0.04	1.00	1.00	1.00
Vapor fraction	0.00	0.00	0.00	0.00	0.00	0.00	0.00	0.00	0.00	0.00

3.3.9. Process model for n,n-dimethylformamide

n,n-Dimethylformamide is a low boiling entrainer and introduces a homogenous azeotrope when used as an entrainer. It is reported that n,n-dimethylformamide forms minimum boiling azeotropes with aliphatics with 6-8 carbon atoms (Mikitenko *et al*., 1975). This causes entrainer loss during azeotropic distillation processes, as the entrainer exit with the top and bottom products. Water has the ability to break the n,n-dimethylformamide-hydrocarbons azeotrope and is used often during homogenous azetropic distillation processes with n,n-dimethylformamide (Mikitenko *et al*., 1975).

The flowsheet for the distillation process using n,n-dimethylformamide simulated in Aspen Plus® V8.2 is shown in Figure 3.39. In this work, homogenous azeotropic distillation process with n,n-dimethylformamide features two distillation column units, i.e. the homogeneous azeotropic distillation column (T102) and the entrainer recovery column (T103).

Input parameters for the azeotropic distillation are obtained from studies by Vega *et al.* (1997). Vega *et al.* (1997) found that extractive distillation with n,n-dimethylformamide for separation of aliphatics and aromatics required 15 theoretical stages. The chosen operating parameters for azeotropic distillation column after sensitivity analysis are summarised in Table 3.26.

In the process shown in Figure 3.39, the feed (stream 10) obtained from the upstream fractionation process model in Figure 3.1, is fed to the middle section of the homogenous azeotropic distillation column (T102). The entrainer (Stream 11) is preheated and fed to the upper section of the azeotropic distillation column. Light naphtha enriched with *dl*-limonene is fed in the middle section of the column. The overhead product of the azeotropic distillation column is the entrainer and *dl*-limonene with composition close to the azeotrope (stream 15). The azeotropic mixture is sent to the entrainer recovery column. In the entrainer recovery column, water is added at the top section of the column to break the azeotrope. Water forms a heterogeneous azeotrope with the mixture and allows separation by heterogeneous azeotropic distillation. In the heterogeneous azeotropic distillation column, *dl*-limonene, water and n,n-dimethylformamide are separated. *dl*-Limonene rich phase (stream 18) and water rich phase (stream 18) are recovered separately in the overhead by the use of a decanter. n,n-Dimethylformamide is recovered as a bottom product (stream 20) of the heterogeneous azeotropic distillation column. n,n-Dimethylformamide recovered from the bottom of the heterogeneous azeotropic distillation column is recycled back to the

homogenous azeotropic distillation column. The bottom product (stream 14) of the homogeneous azeotropic distillation contains impurities and partially entrained n,n-dimethylformamide. The impurities and the entrained n,n-dimethylformamide cannot be separated further using ordinary distillation and require other techniques. In this work, they form part of the waste stream and are not processed further.

Table 3.26 Operating conditions obtained for n,n-dimethylformamide process model before and after sensitivity analysis**.**

Parameters	Initial		Final	
	T102	T103	T102	T103
Number of stages	15	40	30	20
Naphtha feed stage	9	-	9	-
Reflux ratio	3	3.5	3.5	1.5
Entrainer feed stage	3	-	9	-
Entrainer Feed temperature (°C)	100	-	100	-
Entrainer to feed ratio (E/F)	3	-	1	-
Feed stage	-	10	-	10
Condenser / top stage pressure (bar)	0.60	0.60	0.60	0.60
Reboiler duty (kJ/s)	139.69	240.53	138.99	132.52
dl-Limonene distillate purity (wt %)	37.43	96.08	40.42	95.77
Entrainer purity (wt%)	-	99.00	-	99.00
dl-Limonene recovery in distillate (%)	99.02	99.00	98.80	99.00
Entrainer recovery (%)	-	80.56	-	80.56

From Table 3.26, it can be seen that operating conditions derived from studies by Vega *et al.* (1997) are not suitable for the process model for entrainer 5. For this system, *dl*-limonene form an azeotrope with the entrainer indicating that not only does n,n-dimethylformamide form azeotropes with C_6-C_8 hydrocarbons reported by Mikitenko *et al.* (1975), but with C_{10} hydrocarbons as well. It can also be seen from Table 3.26 that entrainer recovery is difficult and would require further steps to achieve more than 99% entrainer recovery. Nevertheless, the desired *dl*-limonene and water recovery and purity is achieved. n,n-dimethylformamide cannot be used as an entrainer without the use of water.The stream table for the final process is given in Table 3.27. From sensitivity analysis it can be deduced that an increase in the number of stages has a significant impact on separation, while a change in feed location and an increase E/F has no significant impact *dl*-limonene purity. It can also be deduced that a better separation in the entrainer recovery column is achieved at low water to feed ratio with feed location in the middle section of the column.

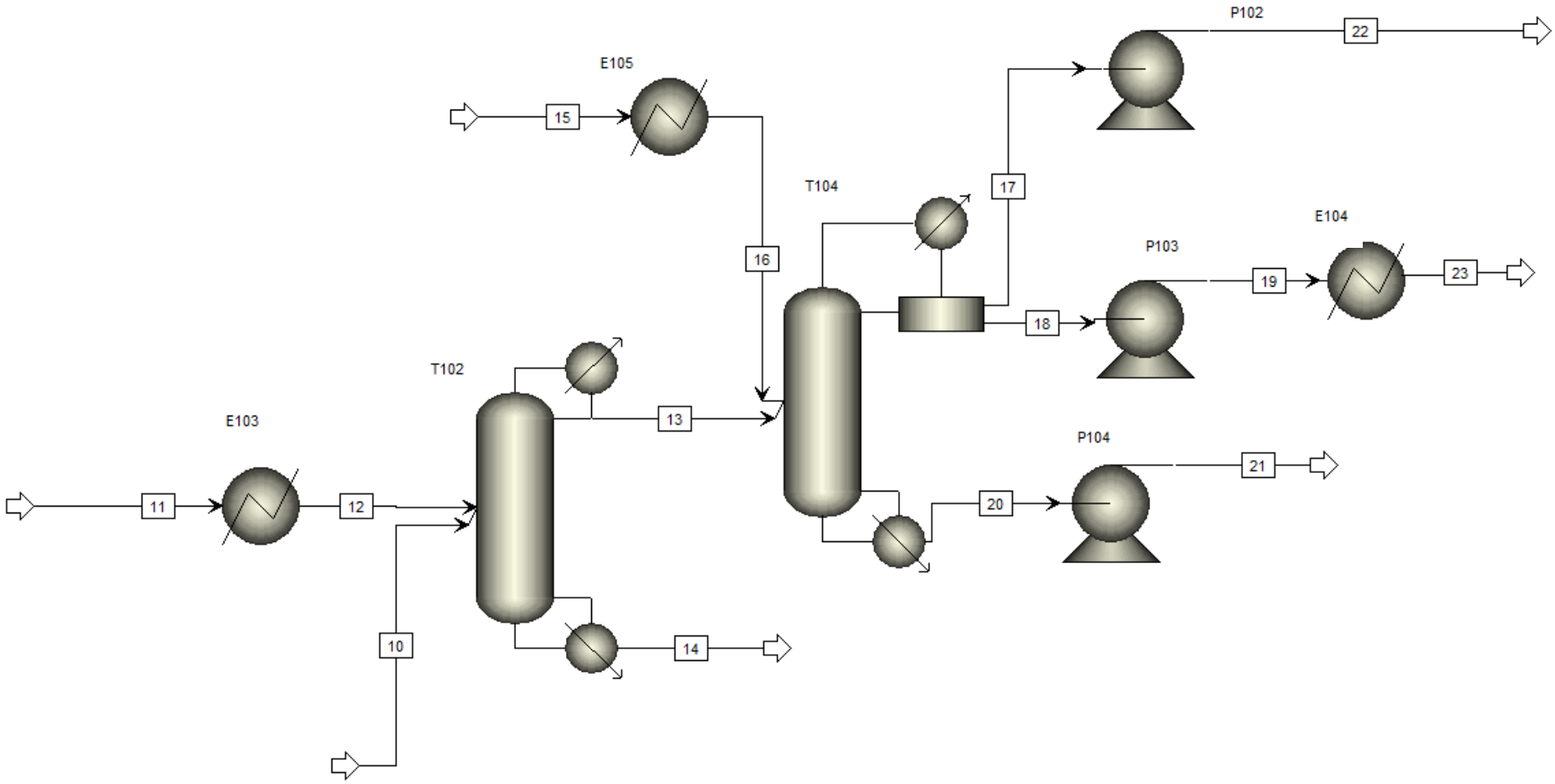

Figure 3.39 Process model for n,n-dimethylformamide

Table 3.27 Stream table for process model with n,n-dimethylformamide

Stream number	10	11	12	13	14	15	16	17	18	19
dl-Limonene (wt%)	57.02	0.00	0.00	40.42	1.53	0.00	0.00	0.02	95.77	95.77
Impurities (wt%)	42.98	0.00	0.00	1.42	66.77	0.00	0.00	0.27	3.03	3.03
Entrainer (wt%)	0.00	100.00	100.00	58.16	31.70	0.00	0.00	0.24	0.02	0.02
Water(wt%)	0.00	0.00	0.00	0.00	0.00	100.00	100.00	99.48	1.18	1.18
Mole flow (kmol/hr)	1.33	2.46	2.46	2.75	1.04	3.89	3.89	3.82	0.83	0.83
Mass flow (kg/hr)	179.71	180.00	180.00	249.33	110.38	70.00	70.00	69.12	105.21	105.21
Temperature (°C)	159.25	25.00	100.00	126.92	134.88	25.00	100.00	83.93	83.85	83.85
Pressure (bar)	1.00	1.00	1.00	0.60	0.61	1.00	1.00	0.60	0.60	1.00
Vapor fraction	0.00	0.00	0.00	0.00	0.00	0.00	0.00	0.00	0.00	0.00

Table 3.27 (cont.) Stream table for process model with n,n-dimethylformamide

Stream number	20	21	22	23
dl-Limonene (wt%)	0.01	0.01	0.02	95.77
Impurities (wt%)	0.12	0.12	0.27	3.03
Entrainer (wt%)	99.88	99.88	0.24	0.02
Water(wt%)	0.00	0.00	99.48	1.18
Mole flow (kmol/hr)	1.98	1.98	3.82	0.83
Mass flow (kg/hr)	145.00	145.00	69.12	105.21
Temperature (°C)	133.31	133.31	83.93	25.00
Pressure (bar)	0.60	1.00	1.00	1.00
Vapor fraction	0.00	0.00	0.00	0.00

3.3.10. Process model for n-methyl-2-pyrrolidone

n-Methyl-2-pyrrolidone is a high boiling entrainer and introduces a homogenous azeotrope when used as an entrainer. The flowsheet for the distillation process using n-methyl-2-pyrrolidone simulated in Aspen Plus® V8.2 is shown in Figure 3.40.

Input parameters for the azeotropic distillation are obtained from studies by Abushwireb *et al.* (2007). Abushwireb *et al.* (2007) found that extractive distillation with n-methyl-2-pyrrolidone for separation of aliphatics and aromatics required 72 theoretical stages and entrainer recovery column with 60 stages. In this work, the maximum number of theoretical stages is set at 60. Therefore, a 72 theoretical stage column is not be used. The chosen operating parameters for azeotropic distillation columns after sensitivity analysis are summarised in Table 3.28.

In this work, homogenous azeotropic distillation process with 2-methyl-2-pyrrolidone features four process units, i.e. the homogeneous azeotropic distillation column, two entrainer recovery columns and the water recovery column.

In the process shown in Figure 3.40, the feed (stream 10), obtained from the upstream fractionation process model in Figure 3.1, is fed to the middle section of the homogenous azeotropic distillation column (T102). The entrainer (Stream 11) is preheated and fed to the upper section of the azeotropic distillation column (T102). The overhead product (stream 15) of the azeotropic distillation column is the entrainer and *dl*-limonene close to the azeotropic composition. The azeotropic mixture is sent to the entrainer recovery column (T104).

Water forms a heterogeneous azeotrope with many compounds, so it is used in the recovery column, although the use of water increases the load on waste water treatment. It is essential that all the added water used is recovered with minimal impurities, so that it can be reused in the process.

In the entrainer recovery column, water (stream 18) is added to break the azeotrope. Water forms a heterogeneous azeotrope with the mixture and allows separation by heterogeneous azeotropic distillation. *dl*-Limonene rich stream (stream 20) and water rich stream (stream 21) are recovered separately in the overhead by the use of a decanter. n-Methyl-2-pyrrolidone is recovered as a bottom product (stream 28). The bottom product of the homogeneous azeotropic distillation (T102) contains impurities and partially entrained n-methyl-2-pyrrolidone, and is sent to an entrainer recovery column (T103), which utilises ordinary distillation to obtain an entrainer rich stream in the bottoms (stream 16) and

impurities in the overhead (stream 15). Because the water rich stream (stream 21) still contains impurities, it is sent to an additional distillation column (T105) to remove excess impurities. The high purity water (stream 26) is recycled back to the heterogeneous azeotropic distillation column.

Table 3.28 Operating conditions obtained for n-methyl-2-pyrrolidone process model before and after sensitivity analysis**.**

Parameters	**Initial**			**Final**			
	T102	**T103**	**T104**	**T102**	**T103**	**T104**	**T105**
Number of stages	60	60	40	50	30	35	4
Naphtha feed stage	30	-		30	-	-	-
Reflux ratio	3.5	3.5	3.5	3.7	5.5	2.5	1.5
Entrainer feed stage	3	-	-	12	-	-	-
Entrainer Feed temperature (°C)	114	-	-	114	-	-	-
Entrainer to feed ratio (E/F)	2	-	0.5	2	-	0.5	-
Entrainer and impurities mixture feed stage	-	30	9	-	20	9	2
Condenser pressure (bar)	0.60	0.50	0.50	0.60	0.50	0.50	0.40
Reboiler duty (kJ/s)	68.49	25.96	232.56	65.70	42.04	177.68	98.49
dl-Limonene distillate purity (wt %)	76.08	-	88.21	81.54	-	95.19	-
Entrainer bottoms purity (wt%)	-	95.67	-	-	99.00	-	-
dl-Limonene recovery in distillate (%)	98.04	-	95.00	99.00	-	95.00	-
Entrainer bottoms recovery (%)	-	85.53	-	-	93.89	-	-

From Table 3.28, it can be seen that operating conditions derived from studies by Abushwireb *et al.* (2007) are not suitable for the process model for n-methyl-2-pyrrolidone. For this system *dl*-limonene form an azeotrope with the entrainer indicating that n-methylpyrrolidone like n,n-dimethylformamide form azeotropes with C_{10} hydrocarbons. It can also be seen from Table 3.26 that entrainer recovery is difficult and require further distillation steps to achieve more than 99% entrainer recovery. n-Methylpyrrolidone can be used as an entrainer with an additional step of water addtion. The stream table for the final process is given in Table 3.29. From sensitivity analysis it can be deduced that an increase in the number of stages has a significant impact on separation and a low E/F is required.

It can also be deduced that a better separation is achieved when the entrainer is fed at the upper stages and the naphtha is fed in the middle stages. In the recovery column, it can be

deduced that better separation is achieved at low water to feed ratio with feed location in the middle section of the column.

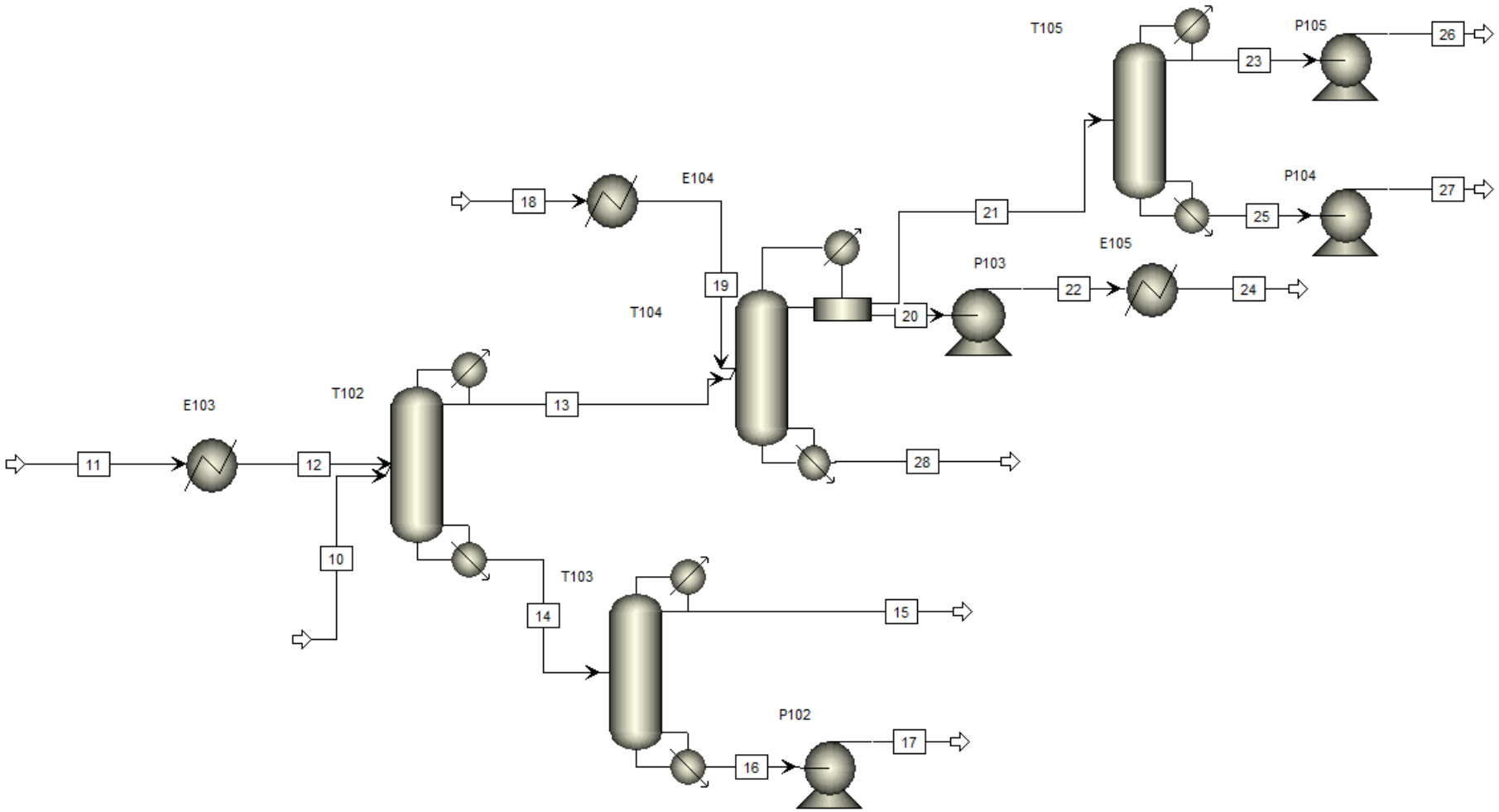

Figure 3.40 Process model for n-methyl-2-pyrrolidone

Table 3.29 Stream table process model with n-methyl-2-pyrrolidone

Stream number	10	11	12	13	14	15	16	17
dl-Limonene (wt%)	57.02	0.00	0.00	81.53	0.13	0.73	0.00	0.00
Impurities (wt%)	42.98	0.00	0.00	2.95	17.74	95.83	0.58	0.58
Entrainer (wt%)	0.00	100.00	100.00	15.52	82.13	3.44	99.42	99.42
Mole flow (kmol/hr)	1.33	3.63	3.63	0.97	3.99	0.57	3.42	3.42
Mass flow (kg/hr)	179.70	360.00	360.00	125.00	414.70	74.70	340.00	340.00
Temperature (°C)	159.25	25.00	114.00	155.32	175.44	152.94	177.66	179.48
Pressure (bar)	1.00	1.00	1.00	0.60	0.62	0.50	0.51	1.00
Vapor fraction	0.00	0.00	0.00	0.00	0.00	0.00	0.00	0.00

Table 3.29 (cont.) Stream table process model with n-methyl-2-pyrrolidone

Stream number	18	19	20	21	22	23	24	25	26	27	28
dl-Limonene (wt%)	0.00	0.00	95.32	0.11	95.32	0.13	95.32	0.01	0.13	0.01	31.90
Impurities (wt%)	0.00	0.00	1.69	0.16	1.69	0.18	1.69	0.02	0.18	0.02	11.64
Water (wt%)	100.00	100.00	1.74	86.65	1.74	99.56	1.74	5.20	99.56	5.20	0.00
Entrainer (wt%)	0.00	0.00	1.25	13.09	1.25	0.13	1.25	94.78	0.13	94.78	56.45
Mole flow (kmol/hr)	3.44	3.44	0.83	3.44	0.83	3.32	0.83	0.12	3.32	0.12	0.14
Mass flow (kg/hr)	62.00	62.00	101.49	69.51	101.49	60.00	101.49	9.51	60.00	9.51	16.00
Temperature (°C)	25.00	100.00	79.92	79.92	74.15	57.96	25.00	109.57	58.00	90.07	154.35
Pressure (bar)	1.00	1.00	0.50	0.50	1.00	0.40	1.00	0.40	1.00	1.00	0.52
Vapour fraction	0.00	0.00	0.00	0.00	0.00	0.00	0.00	0.00	0.00	0.00	0.00

3.4. Comparison

The process models developed using different entrainers are compared in Table 3.30.

Table 3.30 Comparison of process models for different entrainers

Parameter	**Entrainer**			
	Diethylene glycol	Triethylene glycol	4-formyl morpholine	Tetraethylene glycol dimethyl ether
Number of distillation columns	2	2	2	2
Total reboiler duty (kJ/s)	75.93	89.67	48.23	83.54
Total reboiler duty per unit (kJ/s)	37.97	44.84	24.12	41.77
dl-Limonene overall recovery (%)	95.00	95.00	95.00	95.00
dl-Limonene purity (wt %)	95.18	95.98	91.02	98.70
Entrainer overall recovery (%)	99.00	99.00	99.00	99.00
Entrainer purity (wt %)	99.00	99.00	99.00	99.00
CAPEX (M$)	2.45	2.4	2.11	1.68
OPEX (M$)	0.52	0.25	0.26	0.3
Total cost (M$)	2.97	2.65	2.37	1.97

Table 3.30 (cont.) Comparison of process models for different entrainers

Parameter	**Entrainer**		
	Quinoline	n-Methyl-2-pyrrolidone	n,n-Dimethyl-formamide
Number of distillation columns	2	2	4
Total reboiler duty (kJ/s)	90.21	271.51	383.91
Total reboiler duty per unit (kJ/s)	45.11	135.78	95.98
dl-Limonene overall recovery (%)	95.00	99.00	99.00
dl-Limonene purity (wt %)	98.61	95.77	95.19
Entrainer overall recovery (%)	99.00	80.56	99.00
Entrainer purity (wt %)	99.00	99.00	99.00
Water overall recovery (%)	-	99.00	99.00
Water purity (wt %)	-	99.00	99.00
CAPEX (M$)	2.33	4.72	2.24
OPEX (M$)	0.3	0.83	1.98
Total cost (M$)	2.63	5.55	4.22

Unit operations

Homogenous azeotropic distillation process using n-methyl-2-pyrrolidone, involves more unit operations compared to other processes resulting in the highest fixed capital cost. Other processes contain 2 distillation columns. However, homogenous azeotropic distillation column requires a few number of stages compared to heterogeneous azeotropic distillation and extractive distillation resulting in the lowest fixed capital cost.

Energy consumption

Extractive distillation processes require a high E/F and homogenous azeotropic distillation processes require a low E/F. Homogenous azeotropic distillation by n-methyl-2-pyrrolidone requires more unit operations, and therefore requires more reboiler energy, resulting in the highest operational cost, almost twice that incurred from other processes. Homogenous azeotropic distillation by n,n-dimethylformamide consume more energy due to high vaporisation of the entrainer resulting in . The extractive distillation process, consumes less reboiler energy compared to other processes resulting in the lowest operational cost. Heterogeneous azeotropic distillation requires high vacuum operations and more reboiler energy, although less than that of homogeneous azeotropic distillation resulting in the operational cost almost equivalent to that incurred in extractive distillation. Extractive and heterogeneous azeotropic distillation do not require vaporization of the entrainer. However, it requires energy supplied by medium pressure steam.

Separation efficiency

All process models meet the desired specification of *dl*-limonene and entrainer recovery and purity within parameter constraints, except for the process model for n,n-dimethylformamide. n,n-Dimethylformamide is not easily recovered due to the azeotrope formation between impurities and the entrainer. Separation efficiency using diethylene glycol and triethylene glycol is comparable, although entrainer diethylene glycol consumes slightly less reboiler energy. Extractive distillation yields the highest *dl*-limonene purity compared to other processes. Homogenous azeotropic distillation, however, does not yield the highest *dl*-limonene purity, requires a low E/F. This shows that n,n-dimethylformamide and n-methyl-2-pyrrolidone have a high affinity for *dl*-limonene.

Entrainer recovery

All entrainers, except for n,n-dimethylformamide and n-methyl-2-pyrrolidone, are easy to recovery using ordinary distillation with fewer number of stages. The use of water in the recovery column of n,n-dimethylformamide and n-methyl-2-pyrrolidone might place a need for waste water treatment facilities. However, in the developed process models, the required water flowrate is low and the water is easily recovered with little impurities. This reduces the load on the waste water treatment facility.

As a method of separation, heterogeneous azeotropic distillation is generally favoured compared to homogenous azeotropic distillation, as the entrainer can be separated from other components by the use of a decanter in the top section of the column (Gmehling *et al.,* 2014). However, in this work extractive distillation is favourable as it result in high *dl*-limonene purity. Homogeneous azeotropic distillation leads to an acceptable purity but entrainer recovery is difficult, making it less favourable. The *dl*-limonene separated via enhanced distillation contain the retained entrainer and other impurities among, which include aromatics and traces of sulfur compouds. These impurities result in an unpleasant odor. Therefore, the *dl*-limonene fraction obtained can be sold commercially in an untreated technical grade (Florida Chemicals Co., 1991a, b, c). An economically viable method for deodorising *dl*-limonene enriched fraction is required.

3.5. Sensitivity of *dl*-limonene concentration

Sensitivity on feed concentration is important as TDO composition depends on the type of tyre and pyrolysis conditions. As such, large variation in feed is expected for every feedstock processed. The most effective entariner is used for investigation of the minimum *dl*-limonene concentration in the feed to the enhanced distillation process to meet the desired product specifications. Quinoline is selected as it result in high purity *dl*-limonene and is readily available in TDO.

A sensitivity analysis of *dl*-limonene concentration in light naphtha cut versus purity attainable after fractionation column and enhanced distillation is investigated. The *dl*-limonene concentration will be varied between 6 wt% and 21 wt% while keeping the concentration of other compounds in same ratios. The *dl*-limonene concentration range is selected from the feed stream of of TDO for feed 1 and 2. Sensitivity analysis will conducted at constant distillation column parameters. The objective is to determine the minimum *dl*-

limonene content in light naptha cut that would result in a final *dl*-limonene purity in excess of 90 wt%. This would be useful for pyrolysis process development as it would set minimum specifications for TDO, to allow technically feasible separation of *dl*-limonene. The effect of *dl*-limonene feed concentration on purity attainable after fractionation column and extractive distillation column is shown in Figure 3.41. The effect of *dl*-limonene feed concentration on the extractive distillation total energy consumption and attainable *dl*-limonene recovery can be seen in Figure 3.42 and Figure 3.43 respectively.

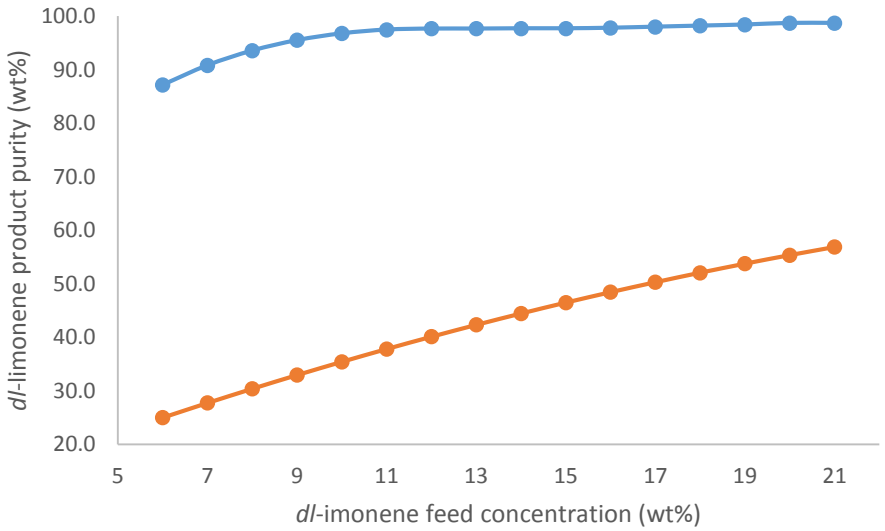

Figure 3.41 The effect of *dl*-limonene feed concentration on final purity after fractionation ● and extractive distillation operation ●

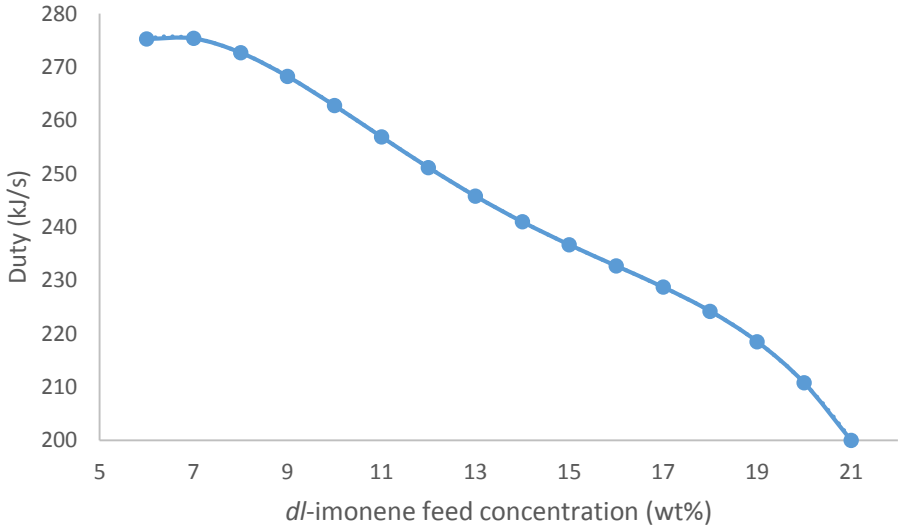

Figure 3.42 The effect of *dl*-limonene feed concentration on extractive distillation column total energy consumption

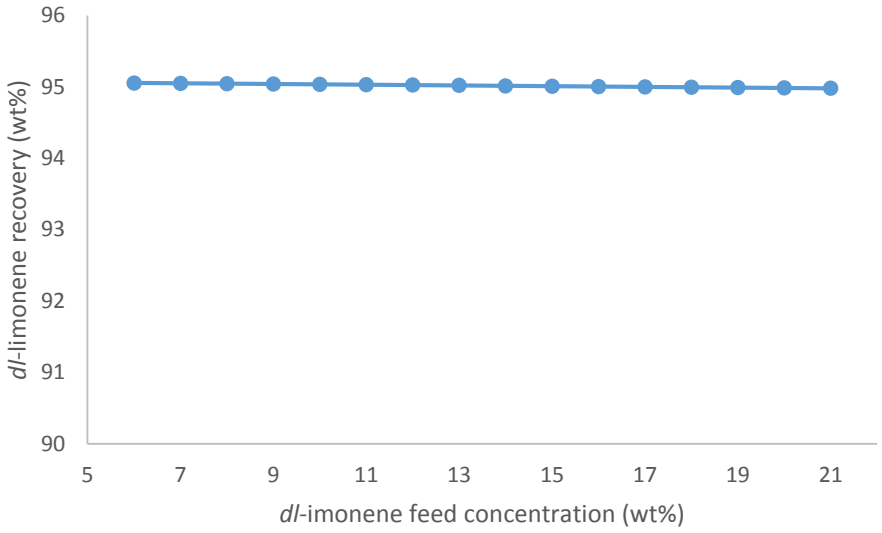

Figure 3.43 Recovery of *dl*-limonene after on extractive distillation column

From Figure 3.41, it can be seen that when using feed 1 TDO composition, the minimum *dl*-limonene concentration required in the feed is 7 wt% to achieve a *dl*-limonene purity of 27 wt% in the fractionation column resulting in a final *dl*-limonene purity of 90 wt% in the extractive distillation column.

It can be seen in Figure 3.42 that the lower the *dl*-limonene content in the feed, the higher the energy consumption in the extractive distillation column. This is due to the presence of compounds with high boiling points compared to *dl*-limonene in significant amount. Vaporisation of these high boiling compounds result in high energy consumption.

From Figure 3.43, it can be seen that the desired recovery is achieved to meet the design criteria.

3.6. Conclusion

Enhanced distillation process has shown to be an effective method for separation of *dl*-limonene from impurities in TDO. The purity and recovery of *dl*-limonene achieved from 7 optimised process models are satisfactory. The process design and the established operating conditions do not deviate from a typical industrial distillation column design as given in Chapter 2. The methodology followed in this study proved to be accurate and meet the objectives of this work. However, experimental work is necessary to validate the model developed with Aspen Plus ® V8.2 with estimated phase equilibrium parameters.

As laboratory tests are cost intensive and time consuming because of large number of parameters involved, especially in the design of new separation processes, a few entrainers are selected for model validation. An entrainer from each process type is selected to investigate to validate the results of each process option. Triethylene glycol is reasonably cheap and can be used for heterogeneous azeotropic distillation. Diethylene glycol and triethylene glycol has shown similar separation effectiveness from the models developed. Quinoline is a novel entrainer and is selected for extractive distillation to ascertain, whether it can be used as an entrainer for recovery of *dl*-limonene. n,n-Dimethylformamide and n-methyl-2-pyrrolidone are both selected for homogeneous azeotropic distillation. Although n,n-dimethylformamide and n-methyl-2-pyrrolidone are used widely, little information is available in open literature about the influence of operating conditions on the performance of homogenous azeotropic distillation processes and the recovery of these entrainers.

3.7. References

Aspen Technology. 2009. Aspen simulation user guide. Burlington, MA: Aspen Technology.

Billal, S.F., Elamin, I.H.M., Mustafa, H.M. and Gasmalseed, G.A. n.d. Separation of Azeotropes by Shifting the Azeotropic Composition.

Choi, G.G., Jung, S.H., Oh, S.J. and Kim, J.S. 2014. Total utilization of waste tire rubber through pyrolysis to obtain oils and CO2 activation of pyrolysis char. *Fuel Processing Technology,* 123: 57–64.

Gmehling, J., J. Menke, J. Krafczyk and K. Fischer. 1994. *Azeotropic Data, Part I and Part II*. New York, Weinheim: VCH-Publishers.

Goel, A., Flores, A. and Philips, A.n.d. Separations of Heptenes.

Henley, E.J., Seader, J.D. and Roper, D.K. 2011. *Separation Process Principles*. New York: Wiley.

Lee, F.M.2000.Extractive distillation. *GTC Technology Corporation.* Houston, TX, USA.

Luyben, W.L., Chien, I.L. 2011. *Design and Control of Distillation Systems for Separating Azeotropes*. New York: John Wiley & Sons.

Muñoz, R., Montón, J.B., Burguet, J. and de la Torre, J. 2006. Separation of isobutyl alcohol and isobutyl acetate by extractive distillation and pressure-swing distillation: Simulation and Optimization. Separation and Purification Technology, 50: 175-183.

Muzenda, E. and Popa, C. 2015. Waste Tyre Management in Gauteng, South Africa: Government, Industry and Community Perceptions. *International Journal of Environmental Science and Development*, 6: 311–315.

Pakdel, H., Pantea, D.M. and Roy, C. 2001. Production of *dl*-limonene by vacuum pyrolysis of used tires. *J. Anal. Appl. Pyrolysis,* 57: 91–107.

Peters, M. and Timmerhaus, K. 2003. Plant Design and Economics for Chemical Engineers. New York: McGraw-Hill.

Qu, W., Zhou, Q., Wang, Y.Z., Zhang, J., Lan, W.W., Wu, Y.H., Yang, J.W. and Wang, D.Z. 2006. Pyrolysis of waste tire on ZSM-5 zeolite with enhanced catalytic activities. *Polymer Degradation and Stability,* 91: 2389–2395.

Robbins, L.A. 1980. Liquid-Liquid Extraction: A Pretreatment Process for Wastewater. *Chem. Eng. Prog*, 76(10): 58–61.

Seider, W.D., Seader, J.D. and Lewin, D.R. 2004. *Product and process design principles: synthesis, analysis and evaluation*. New York: Wiley and Sons.

Sinnott, R.K. 2005. *Chemical engineering design*. Elsevier, Butterworth-Heinemann, Amsterdam.

Stanciulescu, M. and Ikura, M. 2006. Limonene ethers from tire pyrolysis oil. *J. Anal. Appl. Pyrolysis,* 75: 217–225.

Stanciulescu, M., Ikura, M. 2007. Limonene ethers from tire pyrolysis oil. J. *Anal. Appl. Pyrolysis,* 78: 76–84.

Turton, R., Baile, R.C., Whiting, W.B. and Shaeiwitz, J.A.2009. *Analysis, synthesis, and design of chemical processes 3rd* .Prentice Hall international series in the physical and chemical engineering sciences. Upper Sad*dl*e River, NJ: Prentice Hall.

Van Winkle, M. 1967. *Distillation*. New York: McGraw-Hill.

Young, S., 1889.The vapour-pressures of quinoline. Bristol: University College.

Zivdar, M., Zadeh, M.H., Samadi, A. and Abdoullahi, M. n.d. Simulation and Revamping of BTX Distillation Column of Bu-Ali Sina Petrochemical Complex.

Zubrick, J.W. 1997. The organic chem lab survival manual: A student's guide to techniques.

Chapter 4 Experimental validation of process modelling

4.1. Introduction

The objective of this Chapter is to validate experimentally, the model results from Aspen Plus ® V8.2, using UNIQUAC, NRTL and UNIFAC activity coefficient models. To identify the suitable thermodynamic property model and justify the best entrainer to use in azeotropic/extractive distillation, experimental verification is important.

Experimental work entails pure component vapour pressure verification for candidate entrainers, and the separation of *dl*-limonene from TDO using batch distillation. Hence, the vapour-liquid and vapour-liquid-liquid equilibrium for different entrainer and compounds in the *dl*-limonene enriched fraction can be understood.

The separation process follows two stages; fractionation of TDO to obtain a *dl*-limonene enriched naphtha fraction in a single stage batch distillation setup, and the purification of the *dl*-limonene enriched naphtha fraction using azeotropic/extractive distillation in a fractionation setup.

This chapter discusses the experimental procedure followed. The chapter is subdivided into 3 sections. Section 4.2 provides details of apparatus and experimental procedure and experimental design and planning for pure component vapour pressure verification, fractionation and purification, and a description of the analytical equipment used. Section 4.3 gives a comparison of models and experimental results, as well as error analysis. Section 4.4 reviews important findings of this chapter in terms of this investigation.

4.2. Set-up and methodology

4.2.1. Experimental set-up

This section provides details of the experimental methodology followed for the separation of TDO to produce *dl*-limonene rich fraction. Distillation separates TDO into light, medium and heavy fraction. The medium fraction enriched with *dl*-limonene contains impurities that need to be removed. This section will therefore look at separation of TDO into different fractions using single stage setup and from that, purification of the *dl*-limonene enriched fraction, using a fractionation setup.

4.2.1.1 Single stage setup

TDO is initially distilled using one stage batch distillation to recover *dl*-limonene enriched fraction. The procedure requires two consecutive distillations: separation of naphtha with a boiling point less than 155°C and from the residue, the separation of naphtha with a boiling point less than 195°C at atmospheric pressure. A single stage batch distillation is employed as this is sufficient to obtain a *dl*-limonene enriched fraction at purity of 32-37 wt% (Stanciulescu and Ikura, 2006). TDO may contain solids and tar that can plug, foul packing or trays if a fractionating setup is used. The experimental apparatus used is shown in Figure 4.1. Details of the batch distillation apparatus shown in Figure 4.1 are given in Table 4.1.

Table 4.1 Specification of batch distillation setup

Equipment	Description	Operating conditions
Three necked bottle flask (4)	Still-pot	1000 ml working volume
Heating mantle (2)	Reboiler	300 W
Condenser (3)	Condense vapours	-
Thermometer (1)	Measure operating temperature	0-300°C
Vacuum adapter (5)	Connect to vacuum line	-
Receiving flask (6)	Catch condensate	-
Vapour trap (7)	Trap uncondensed vapours	-
Pressure transducer (8)	Measure operating pressure	0-1 bar (abs)
Vacuum line	Creates vacuum in the system	Highest vacuum: 0.3 bar (abs)

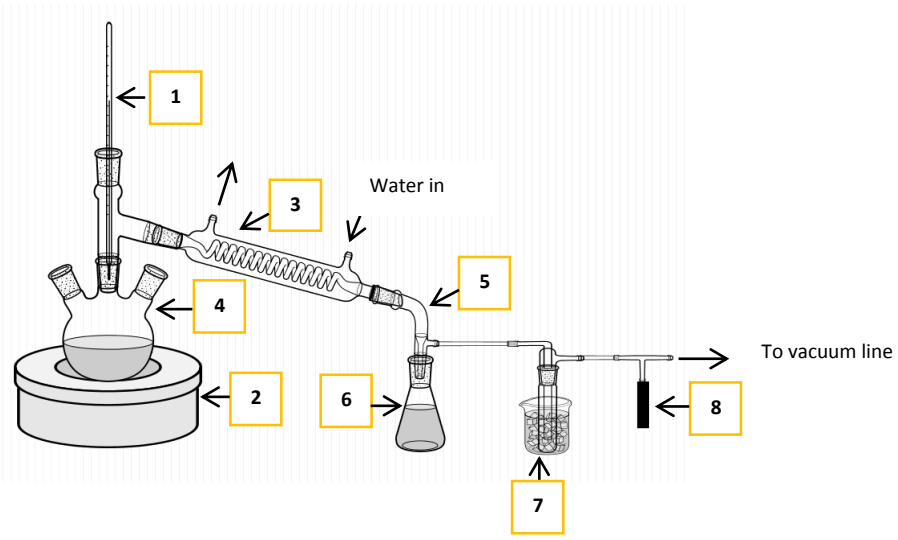

Figure 4.1 Schematic diagram of a single stage setup

TDO is charged to the still-pot (4) up to a volume of 800 ml. Cooling water is turned on in the condenser (3). The vacuum line is opened to maintain a pressure of 0.8 bar (abs). A vacuum pressure controller is used to adjust the pressure in the distillation system by comparing the pressure set value and the pressure value in the vapour trap (7), indicated by the pressure transducer (8). The pressure controller sends its signal to the solenoid valve to open or close the vacuum line. The oil is heated to 155^{o}C using the heating mantle (2). The temperature is measured using a thermometer (1). The temperature is maintained at 155^{o}C, while condensing the vapours to remove light compounds. The condensate is captured in the receiving flask (6). The uncondensed compounds are collected in the vapour trap (7), which is placed in an ice bucket. The vacuum source and the heating mantle are turned off, while the receiving flask (6) is removed and a new one is placed. The vacuum line is turned on again to maintain a pressure of 0.8bar. The heating mantle (2) is turned on and the temperature is raised to 185^{o}C to distil and condense the middle fraction, which is the *dl*-limonene enriched naphtha fraction from the still-pot (4) oil. The *dl*-limonene enriched fraction is captured in the receiving flask (6). The *dl*-limonene enriched fraction is taken for compositional analysis. The light and heavy fractions are discarded as they contain less *dl*-limonene.

4.2.1.2 Fractionation setup

The experimental setup for purification of *dl*-limonene from *dl*-limonene enriched fraction obtained is shown in Figure 4.2. Details of the batch distillation apparatus shown in Figure 4.2 are given in Table 4.2. The fraction is purified further using a packed batch distillation column. Packing is desired as it provides a large contact area between phases, allowing improved separation compared to a single stage batch distillation. Sulzer Mellapak structured packing with an estimated theoretical stages of 1-1.2 stages is used for the experiment. Structured packing is favourable as it can be used for low to moderate pressures distillation with low pressure drop (approximately 100 pa/m) (Sinnott *et al*., 2006).

Vacuum distillation overhead arrangement design is complex. It must condense the vapour from the top stage, enable reflux flow back to the column, maintain the desired operating pressure and prevent entrainment of liquid. A high cooling water flowrate will result in subcooled condensate. Vacuum distillation operations commonly intentionally sub cool reflux to reduce likelihood of product loss through the vacuum line (Buckley, 1964).

Table 4.2 Specification of *dl*-limonene fraction purification apparatus

Equipment	Description	Operating conditions
Three necked bottle flask (4)	Still pot	800 ml working volume
Heating mantle (5)	Reboiler	0-350°C
Packed column (3)	Structured packing	570 mm packed height and 27 mm diameter
Condenser (2)	Condense vapour	-
Pt100 temperature probe	Measure temperature	0-300°C
Splash head (1)	Reduce entrainment of liquid	-
Vapour trap (6)	Trap uncondensed vapour	-
Pressure transducer (7)	Measure operating pressure	0-1 bar (abs)
Solenoid valve	Control pressure	Allow flow of air
Vacuum line	Vacuum the column	Highest vacuum: 0.3 bar (abs)

The distillation feed is charged to the still-pot (4) up to a volume of 800ml. The feed contains the *dl*-limonene enriched fraction mixed with the entrainer at a specific E/F. Cooling water flow to the condenser (2) is turned on. The vacuum line is turned on to create a vacuum of 0.6bar (abs). The pressure control system and measurement used, work on the same principle as the one used in the initial experiment with a pressure transducer (7). The charge is heated by turning on the heating mantle (5) to a maximum heat duty of 300W. The temperature is measured below packing and at the top stage above packing, using PT-100 temperature probes. In this operation the column works at infinite reflux ratio to obtain the maximum purity and no product take off. The escaped condensable compounds are collected in the cold/vapour trap (6).When a constant overhead temperature has been reached at a constant pressure, a constant boil up rate is achieved and the distillation samples can be collected. For determination of the liquid and vapour phase composition, samples are taken at the bottom and top.

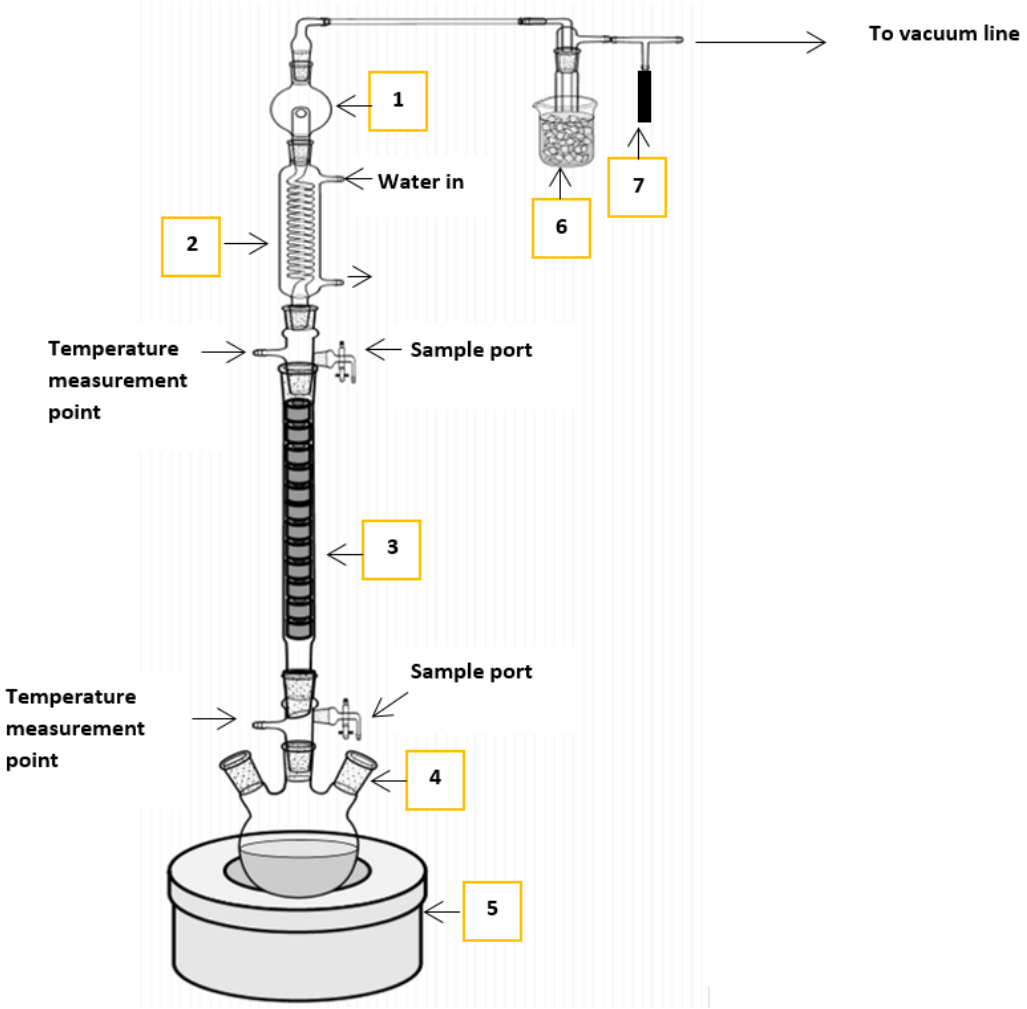

Figure 4.2 Schematic diagram of *dl*-limonene enriched fraction purification experiment using packed batch distillation column

4.2.2. Experimental design

This section describes the experimental design for vapour pressure verification, fractionation of TDO and purification of light naphtha cut. This section discusses the manipulated and response variables in the experimental work, giving their lower and upper bounds, and set points.

4.2.2.1 Vapour pressure verification

Addition of entrainer to the *dl*-limonene enriched fraction changes the phase behaviour of the mixture. In order to design effective separation processes, experimental information on the pure component phase equilibria is vital. The experimental data is required for verification

of pure component vapour pressure prediction by Aspen Plus ® V8.2, as it is used for phase equilibrium calculations. Inaccurate pure component data results in inaccurate mixture equilibrium properties and process designs.

The same fractionation setup as shown in Figure 4.2 is used. The effect of vacuum pressure on the boiling point of the pure entrainer is studied to generate vapour pressure curve. Due to equipment limitation, a minimum pressure of 0.5bar (abs) is used. Pressure is varied between 0.45 and 0.8 bar (abs) with 0.05 bar increments. The upper value of pressure is kept at 0.8 bar (abs) to avoid thermal degradation of the entrainers. The bottom and top temperatures are measured for various operating pressures. With the current setup, small errors might be introduced by partial sub-cooling of reflux and the effect of ambient temperature.

4.2.2.2 Fractionation of TDO

The aim of this experimental work is to obtain a *dl*-limonene enriched fraction after which purification is done. No process parameters are varied for this experiment. Distillation is carried at a reduced pressure. This enables the use of lower process temperatures to prevent thermally sensitive substances from degradation. A set operating pressure value of 0.8bar is sufficient. The operating temperatures range to obtain the middle fraction chosen is 15°C below and above the boiling point of *dl*-limonene, at 0.8bar (abs). A narrow temperature range is chosen as to obtain a *dl*-limonene enriched naphtha fraction with less of the light fraction and heavy fraction, while simulataenously preventing *dl*-limonene loss.

4.2.2.3 Purification of dl-limonene enriched naphtha cut

In this set of experiments, the manipulated variable is E/F, and the measured variables are temperature and concentration. The E/F is varied among three levels, i.e. E/F of 2, 4 and 6. The experiment is conducted under vacuum pressure to avoid product degradation. Pressure is fixed at 0.6 bar (abs) for all runs. A total of three experiments are conducted for one type of entrainer.

As the first step of separation imposes feed composition on the purification step, sensitivity on feed concentration is important. TDO composition depends on the type of tyre and pyrolysis conditions. As such, large variation in feed is expected for every feedstock processed.

4.2.3. Analytical method

A validated GC-MS method by Ngxangxa (2015) is used to quantify compounds of interest in the TDO sample. The TDO sample is diluted in dichloromethane, which is used as a solvent. The ratio of TDO to dichloromethane of 1:100 is used.

Analyses are performed on an HP 5890 series II GC coupled to a 5973 MS. A non-polar capillary column with dimensions: 60 m × 0.18 mm i.d × 0.10 µm d_f Rxi-5% Sil-MS is used for the separation of the analytes. Helium is used as carrier gas, with an inlet pressure of 348 kPa. The column flow of 1.2 ml/min (linear velocity of 27.9 cm/s) in constant flow mode is used.

A 1 µl volume of the diluted sample is injected with an inlet temperature of 280˚C using a split/splitless injector. Split mode is used with a split ratio of 1:20. The GC oven temperature program is used as follows: 40˚C (held for 5min), ramped at 0.7˚C/min to 104˚C and then 10˚C /min to 280˚C, and held for 5 minutes. The MS is operated in full scan mode from 35 to 350 amu at a scan rate of 4.5scans/sec and ionisation is performed at 70eV. The transfer line temperature is set at 280˚C and the MS source temperature is set at 230˚C and 150˚C for quadrupole.

The identified compounds are quantified using the internal standard method with α-pinene, deuterated toluene and deuterated naphthalene as internal standards. The calibration curves constructed for different compounds are given in Appendix A.

4.2.4. Material used

A list of chemicals, as used in the experiment, is given in Table 4.3 and Table 4.4. The chemicals are used at the purity obtained from suppliers and no further treatment was done.

Table 4.3 Summary of chemicals used in fractionation and purification of TDO experimental work

Chemical	Supplier	Purity (%)	Use
Triethylene glycol	Sigma Aldrich	≥99.0	Entrainer
n,n-Dimethylformamide	Merck	≥98.0	Entrainer
n-Methyl-2-pyrrolidone	Merck	≥98.0	Entrainer
Quinoline	Sigma Aldrich	≥97.0	Entrainer
TDO	Metsa (pty) Ltd	-	Distillation
dl-Limonene	Merck	≥99.0	Additive to TDO
p-Cymene	Sigma Aldrich	99.0	Additive to TDO
Indane	Sigma Aldrich	95.0	Additive to TDO
1,2,3-Trimethylbenzene	Sigma Aldrich	90.0	Additive to TDO

Table 4.4 Summary of chemicals used in the analytical experimental work

Chemical	Supplier	Purity (%)	Use
1,2,3-Trimethylbenzene	Sigma-Aldrich	91.7	Analytical standard
m-Cymene	Sigma-Aldrich	99.0	Analytical standard
p-Cymene	Sigma-Aldrich	99.5	Analytical standard
l-limonene	Sigma-Aldrich	99.0	Analytical standard
d-limonene	Sigma-Aldrich	99.0	Analytical standard
Indane	Sigma-Aldrich	97.5	Analytical standard
Indene	Sigma-Aldrich	96.7	Analytical standard
α-Pinene	Sigma-Aldrich	99.8	Internal standard
Deuterated toluene	Sigma-Aldrich	99.7	Internal standard
Deuterated naphthalene	Sigma-Aldrich	99.0	Internal standard
Dichloromethane	Kimix	99.0	Solvent

4.3. Results and discussion

4.3.1. Vapour pressure verification

Accurate mixture property calculations are impossible without accurate pure component properties. Pure component vapour pressure data is used in phase equilibrium calculations of compounds in enhanced distillation (Smith *et al.,* 2005). Validation of vapour pressure data in simulations is important to check for discrepancies in properties. This entails plotting vapour pressure data from Aspen Plus® V8.2 using various thermodynamic models, and comparing the results with literature data and experimental data derived in this work. Pure component vapour pressure plot for the four entrainers used are shown in Figure 4.3 to Figure 4.6.

From Figure 4.3 to Figure 4.6, it can be seen that there exists a deviation between the top temperature and bottom temperature. A possible cause for this deviation in temperature is heat loss, pressure drop across the column and partly subcooled reflux. As the inlet cooling water temperature at the condenser is significantly lower than the distillate bubble point temperature, the reflux is likely to be subcooled and result in condensation of some vapour in the top stage, which results in temperature gradient across the column (Buckley, 1964). As the column is not insulated, heat loss occurs, which result in temperature gradient. However, these effects might not be significant, as can be seen by the low temperature difference between the top and bottom stage. The effect of pressure drop is minimal when considering an estimated pressure drop of 100pa/m across a 57cm packed height. Another cause of the deviation in the boiling temperature might be a result of the use of technical grade chemicals in the experiments.

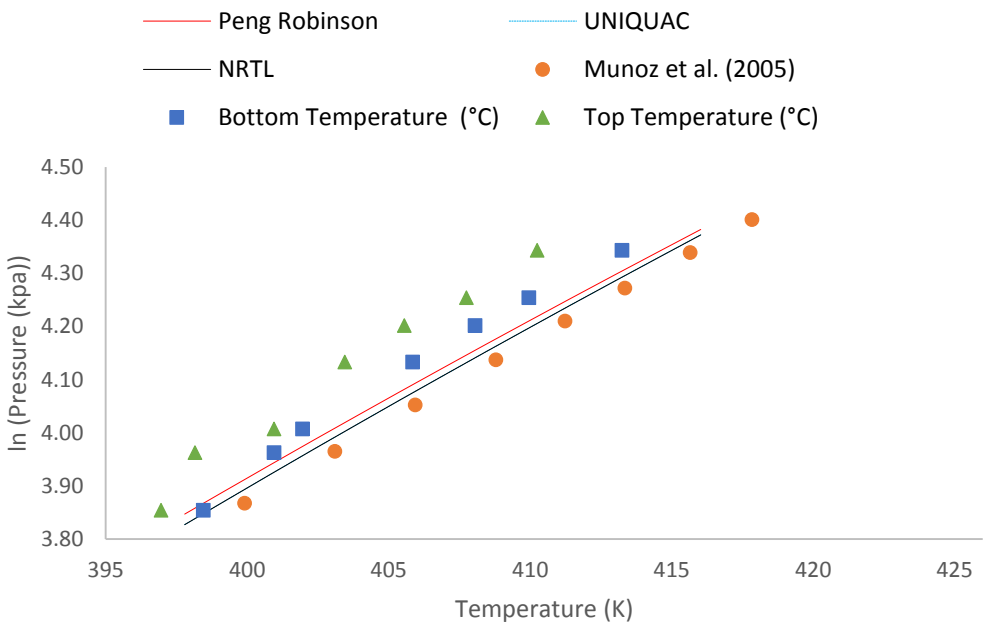

Figure 4.3 Comparison of vapour pressure data for n,n-dimethylformamide obtained in this work with literature data and Aspen Plus® V8.2 predicted data

From Figure 4.3, it can further be seen that all the property models predict the vapour pressure data in this work fairly well. The vapour pressure data generated using different property models correlate well with each other. Similar trends can be seen in Figure 4.4.

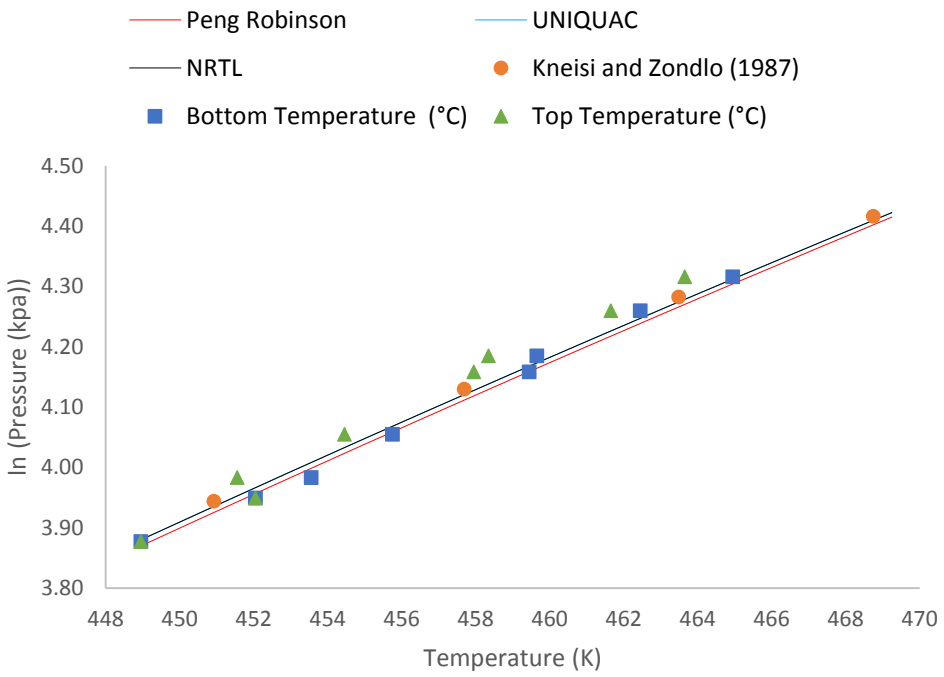

Figure 4.4 Comparison of vapour pressure data for n-methyl-2-pyrrolidone obtained in this work with literature data and Aspen Plus® V8.2 predicted data

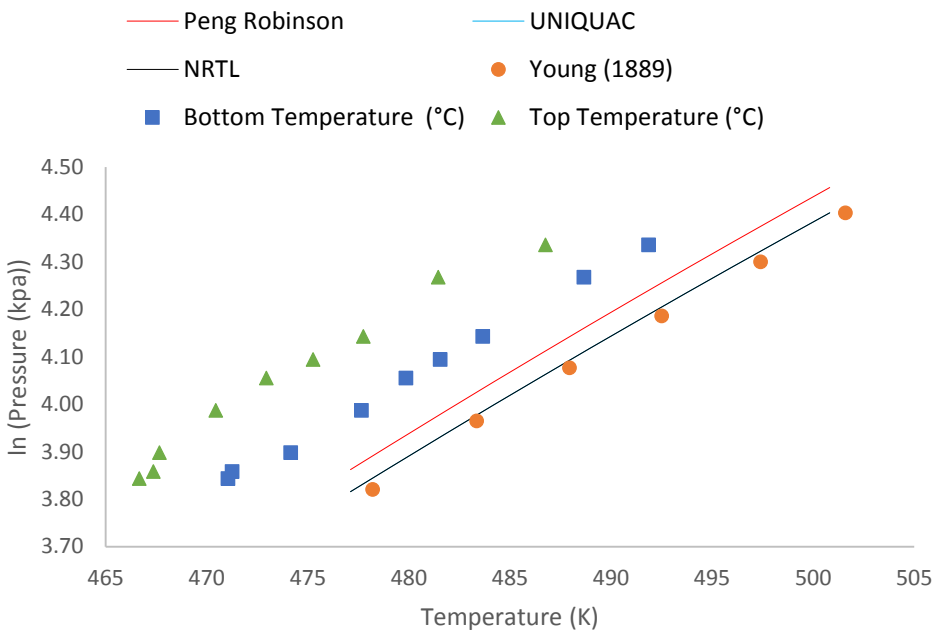

Figure 4.5 Comparison of vapour pressure data for quinoline obtained in this work with literature data and Aspen Plus® V8.2 predicted data

From Figure 4.5, it can further be seen that all the property models over predict the vapour pressure data in this work. The literature data is well predicted by activity coefficient models. The vapour pressure data generated using different property models do not correlate well with each other in comparison to the behaviour observed in Figure 4.3 and Figure 4.4.

The models prediction power and experimental data accuracy is greater when considering low boiling compounds. A possible reason for discrepancies in vapour pressure data of high boiling compounds might be the occurrence of thermal degradation. This is the limitations of using batch distillation (fractionation setup) to measure vapour pressure of high boiling compounds. The disadvantage of the fractionation setup is the long residence time in which the compounds are exposed to high temperatures. This increases the likelihood of thermal decomposition of compounds, which results in formation of side products and a change in boiling temperature. The initial decomposition temperature of triethylene glycol is 240°C, while that of quinoline compounds is reported to be around 200°C (Dow Chemical Company, 2007; Lizarraga et *al.,* 2005; Acros Organics, 2011). This is the temperature range employed in this study. Further more, a technical grade quinoline is used which might have a different boiling point from the high purity quinoline used in studies by Young (1889).

The occurrence of degradation is also concluded from slight discoloration of these compounds at high temperatures during operation. The vapour pressure data obtained from vacuum distillation should be accepted with slight inaccuracies, however, this data shows general trends and is close enough for this work's purpose. Therefore, parameters fitted to vapour pressure equations in Aspen Plus® V8.2 predict the vapour pressure reasonably well, and errors are due to limitation of experimental data accuracy. Implementation of other vapour pressure measurements could be done to for further verification of vapour pressure data for entrainers used in this work. Alternatively, the vapour pressure measurement could be conducted at low temperatures (high vacuum) and extrapolated to the high temperature range of interest to avoid thermal decomposition.

High vacuum was adopted in the separation process models developed in Chapter 3, with the maximum reboiler temperature maintained at 184°C. This bottoms temperature is well below the initial degradation temperature of the compounds in light naphtha cut. Due to equipment limitation experimental work was conducted in a batch distillation setup with a long residence time at 60 Kpa which increased the likelihood of product degradation. A continuous distillation column is recommended for industrial application with the use of packing to minimize pressure drop and working under inert atmosphere to reduce oxygen in the system.

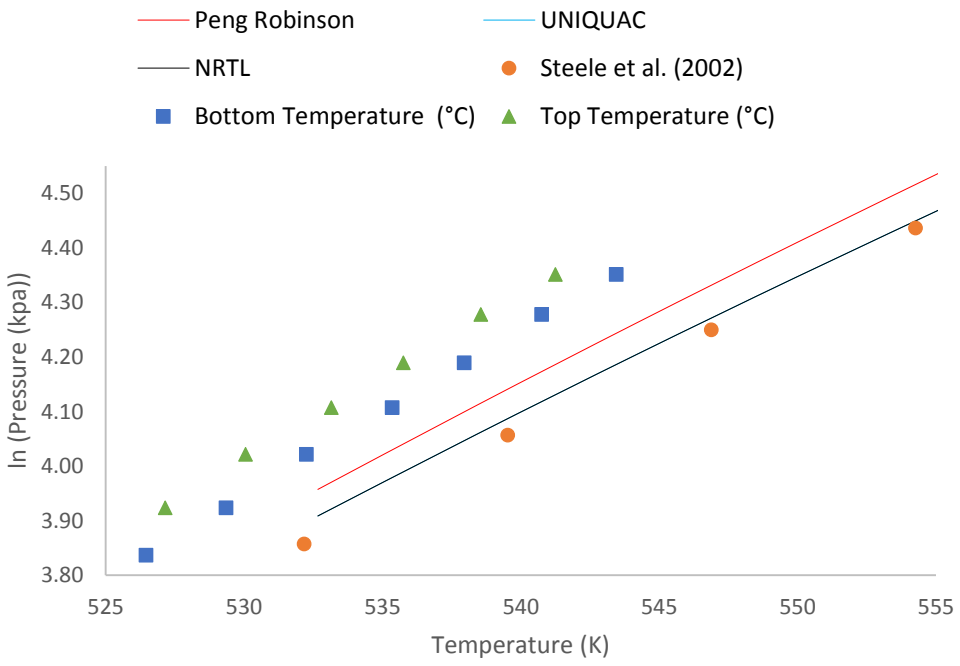

Figure 4.6 Comparison of vapour pressure data for triethylene glycol obtained in this work with literature data and Aspen Plus® V8.2 predicted data

4.3.2. Fractionation of TDO

The aim of this experimental work was to obtain a *dl*-limonene enriched fraction from TDO using a single stage batch distillation setup. Distillation of TDO was carried out at a pressure of 0.8 bar to separate the feed into light, middle (*dl*-limonene enriched fraction) and heavy fractions. The *dl*-Limonene enriched fraction obtained from batch distillation was analysed using GC-MS internal standard method. Chemical characterization of the fraction is given in Table 4.5.

Table 4.5 *dl*-Limonene enriched fraction chemical composition

Compound	Concentration (wt %)
Toluene	1.74
4-Vinycyclohexene	0.51
Ethybenzene	1.56
p-Xylene	5.65
m-Xylene	1.03
Styrene	2.80
o-Xylene	1.45
Cumene	0.26
3-Ethyltoluene	2.31
4-Ethyltoluene	3.31
1,3,5-Trimethybenzene	0.75
2-Ethyltoluene	0.85

Table 4.5 (cont.) *dl*-Limonene enriched fraction chemical composition

Compound	Concentration (wt %)
α-Methylstyrene	1.11
1,2,4-Trimethylbenzene	3.06
4-Methylstyrene	0.76
1,2,3-Trimethybenzene	3.49
m-Cymene	0.48
p-Cymene	9.52
dl-Limonene	36.96
Terpinolene	2.26
Indan	1.38
Indene	1.93
Naphthalene	1.91
Benzothiazole	12.35
Biphenyl	1.14
2,6-Dimethylnaphthalene	0.69
1,4-Dimethylnaphthalene	0.74

From Table 4.5, it can be seen that the *dl*-limonene content is low. The *dl*-limonene content of this fraction correlates with findings by Stanciulescu and Ikura (2006; 2007), who obtained 32-37 wt% *dl*-limonene using batch distillation. An improved purity of greater than 50 wt% *dl*-limonene was obtained by Pakdel *et al.* (2001). The differences lie in the fact that in this work, one stage batch distillation was used and the work done by Pakdel *et al.* (2001) entailed the use of a packed column with 25 theoretical stages. The *dl*-limonene enriched naphtha fraction contains close boiling compounds indane, 1,2,3-trimethylbenzene and cymenes obtained by Pakdel *et al*. (2001). These compounds could not be separated by ordinary distillation. The second set of experiments is conducted to remove these compounds. Only the close boiling compounds are investigated. The *dl*-limonene content of the oil is increased to above 50 wt% by adding a pure synthetic *dl*-limonene to the *dl*-limonene enriched fraction. This is a typical weight percent of *dl*-limonene that would have been obtained if a batch distillation setup with a number of theoretical stages was utilised (Pakdel *et al.*, 2001).

Synthetic *dl*-limonene is added to increase the *dl*-limonene content to 56wt%, as in the process model developed for feed 1. Therefore, the new fraction spiked with *dl*-limonene represent a typical composition that would possible have been obtained if a fractionation column was used.

4.3.3. Purification of light naphtha cut

Experimental results of the extractive/azeotropic batch distillation process are compared with Aspen Plus® V8.2 predicted data, calculated using UNIQUAC and NRTL property model. The experimental set-up is modelled in Aspen Plus ® V.8 using a Radfrac model of 4 equilibrium stages (representing the still pot, packing and condenser) operating at total reflux and similar system conditions. The top and bottom stage temperature, and their respective compositions, are compared. The results are on an entrainer free basis with only five compounds which are close boiling to *dl*-limonene and in significant concentration, included in the mass balance. Percentage error is used to determine the accuracy of the model to predict all sets of experimental data. Percentage error is defined in Equation 4.1

$$\%\, Error = \left|\frac{y_{ie} - y_{ip}}{y_{ie}}\right| . 100 \qquad (4.1)$$

where y_{ie} is the experimental data and y_{ip} is the model predicted data.

To determine the degree of separation between two components when a specific entrainer is used, separation factor is calculated. Separation factor is defined in Equation 4.2.

$$S = \frac{\left(\frac{x_{Limonene}}{x_{Other}}\right)_T}{\left(\frac{x_{Limonene}}{x_{Other}}\right)_B} \quad (4.2)$$

where x denotes mole fraction of a component, T denotes the top of the section, and B denotes the bottom of the column.

For systems forming two liquid phases, the separation factor is calculated using the average mass fraction of the two phases. A separation factor far from unity indicates that separation is feasible. The results for different entrainers at a pressure of 60kpa and E/F of 4 are shown in Table 4.6 to Table 4.17.

4.3.3.1 Triethylene glycol

Experimental and model data obtained from azeotropic distillation using triethylene glycol are given in Table 4.6.The data is compared and the percentage error calculated is given in Table 4.7. Separation factor is calculated from experimental and model data, and compared in Table 4.8.

Table 4.6 Model and experimental data for azeotropic distillation using triethylene glycol

	Experimental		**UNIQUAC**		**NRTL**	
	Top	Bottom	Top	Bottom	Top	Bottom
Number of phases	1	2	1	2	1	2
Temperature (K)	390.95	443.45	382.64	423.1	382.85	423.45
dl-Limonene (wt%)	90.12	85.95	91.42	85.585	91.94	87.585
m-Cymene (wt%)	1.19	3.68	2.18	3.105	2.05	2.725
p-Cymene (wt%)	6.66	7.69	4.64	7.475	4.37	6.555
Indan (wt%)	0.94	1.36	1.13	2	1.01	1.615
1,2,3-Trimethylbenzene (wt%)	1.1	1.32	0.63	1.845	0.64	1.52

Table 4.7 Percentage error calculation for azeotropic distillation using triethylene glycol

	UNIQUAC		**NRTL**	
	Top	Bottom	Top	Bottom
Temperature (K)	2.13	4.59	2.07	4.51
dl-Limonene (wt%)	1.45	3.68	2.02	4.39
m-Cymene (wt%)	83.64	31.93	72.82	23.24
p-Cymene (wt%)	30.25	19.32	34.38	28.53
Indan (wt%)	20.26	39.43	7.48	25.82
1,2,3-Trimethylbenzene (wt%)	43.12	14.97	42.12	22.22

Table 4.8 Separation factor for azeotropic distillation using triethylene glycol

	Experimental	UNIQUAC	NRTL
m-Cymene (wt%)	3.19	1.52	1.39
p-Cymene (wt%)	1.46	1.72	1.58
Indan (wt%)	1.91	1.89	1.68
1,2,3-Trimethylbenzene (wt%)	1.87	3.15	2.50

From Table 4.6, it can be seen that a change in *dl*-limonene purity is achieved from experimental data and model predicted data. Experimental data shows the occurrence of two liquid phases at the bottom stage of the column. The models also predict two liquid phase formation. The individual component concentration and temperatures from experimental work does not correlate well with model data.

From Table 4.7, it can be seen that the top and bottom concentrations of *dl*-limonene show the lowest error, and the top concentration of m-cymene show the highest error for both property model predictions.

The models slightly under predict the experimental temperatures, more especially the bottom temperature where liquid-liquid splitting occurs. This shows that the models cannot accurately predict liquid-liquid equilibrium temperature. The NRTL property model gives a better agreement with experimental data when compared to the UNIQUAC property model for all sets of experimental data.

Separation factor is therefore used as a guide to determine the degree of separation. From Table 4.8, it can be seen that separation factor from experimental and model data for all compounds is greater than one. The models over predict the separation of *dl*-limonene from 1,2,3-trimethylbenzene, and under predict the separation of *dl*-limonene from m-cymene. A cause for these discrepancies is a result of the poor quality of the binary interaction parameters estimated from UNIFAC model. The UNIFAC estimated binary interaction parameters result in increased uncertainty in the VLE and VLLE of multicomponent mixture when augmented with UNIQUAC and NRTL models. It is also known that ternary or higher data are not well predicted by activity coefficient models and binary interaction parameters (Smith *et al.,* 2005). Nevertheless, it can be concluded that triethylene glycol is a feasible entrainer indicated by the separation greater than unity. Triethylene glycol allows *dl*-limonene to be separated from all other compounds by heterogeneous azeotropic distillation.

4.3.3.2 n,n-dimethylformamide

Experimental and model data obtained from azeotropic distillation using n,n-dimethylformamide are given in Table 4.9. The data is compared and the percentage error calculated is given in Table 4.10. Separation factors are calculated from experimental and model data and compared in Table 4.11.

Table 4.9 Model and experimental data for azeotropic distillation using n,n-dimethylformamide

	Experimental		**UNIQUAC**		**NRTL**	
	Top	Bottom	Top	Bottom	Top	Bottom
Number of phases	1	1	2	1	1	1
Temperature (K)	397.65	401.25	397	401.88	396.52	401.82
dl-Limonene (wt%)	95.34	89.66	96.93	88.41	98.07	88.41
m-Cymene (wt%)	0.5	1.09	0.85	2.57	0.53	2.57
p-Cymene (wt%)	3.05	6.89	1.81	6.18	1.12	6.18
Indan (wt%)	0.09	0.97	0.255	1.45	0.17	1.45
1,2,3-Trimethylbenzene (wt%)	1.02	1.38	0.16	1.39	0.11	1.39

Table 4.10 Percentage error calculation for azeotropic distillation using n,n-dimethylformamide

	UNIQUAC		**NRTL**	
	Top	Bottom	Top	Bottom
Temperature (K)	0.16	0.16	0.28	0.14
dl-Limonene (wt%)	2.15	1.4	2.86	1.4
m-Cymene (wt%)	59.82	135.06	5.77	135.06
p-Cymene (wt%)	43.06	10.32	63.21	10.32
Indan (wt%)	124.61	49.18	94.23	49.18
1,2,3-Trimethylbenzene (wt%)	84.95	0.66	89.55	0.66

Table 4.11 Separation factor for azeotropic distillation using n,n-dimethylformamide

	Experimental	**UNIQUAC**	**NRTL**
m-cymene (wt%)	4.62	3.31	5.38
p-cymene (wt%)	2.30	3.75	6.10
Indan (wt%)	1.62	6.23	9.56
1,2,3 Trimethylbenzene (wt%)	1.38	9.57	14.54

From Table 4.9, it can be seen that a change in *dl*-limonene purity is achieved from experimental data and models predicted data. Only the UNIQAC model predicts two liquid phase formation at the top stage. The individual component concentration of the two liquid phases is nearly equal. It can be concluded that the UNIQUAC model does not predict the separation with great certainty.

From Table 4.10, it can be seen that the top and bottom concentration of *dl*-limonene show the lowest error and the concentration of other compounds show the highest error for both property model predictions. The greatest error is observed in the region of high purity *dl*-limonene. This indicated that a greater inaccuracy with the interaction parameters between n,n-dimethylformamide and impurities exists.

The comparison of the experimental bottom and top temperature with the model prediction shows a good correlation indicated by the low percentage error. The NRTL property model gives a better agreement with experimental data when compared to the UNIQUAC property model.

From Table 4.11, it can be seen that the separation factor from experimental and model data for all compounds is greater than one. The models over predict the separation of *dl*-limonene from 1,2,3-trimethylbenzene and indane and reasonably predict the separation of *dl*-limonene from m-cymene and p-cymene. A cause for these discrepancies is a result of the poor quality of the binary interaction parameters estimated from UNIFAC model. Nevertheless, it can be concluded that n,n-dimethylformamide is a feasible entrainer indicated by the separation greater than unity. n,n-Dimethylformamide allows *dl*-limonene to be separated from all other compounds by homogeneous azeotropic distillation.

4.3.3.3 Quinoline

Experimental and model data obtained from extractive distillation, using quinoline, are given in Table 4.12. The data is compared and the percentage error calculated is given in Table 4.13. Separation factors are calculated from experimental and model data, and compared in Table 4.14.

Table 4.12 Model and experimental data for extractive distillation using quinoline

	Experimental		**UNIQUAC**		**NRTL**	
	Top	Bottom	Top	Bottom	Top	Bottom
Number of phases	1	1	1	1	1	1
Temperature (K)	401.1	454.65	383.93	450.36	382.99	453.83
dl-Limonene (wt%)	89.42	87.226	95.19	88.41	94.59	88.41
m-Cymene (wt%)	1.067	2.6933	1.22	2.57	1.37	2.57
p-Cymene (wt%)	6.662	7.8578	2.59	6.18	2.91	6.18
Indan (wt%)	1.455	1.0447	0.55	1.45	0.61	1.45
1,2,3-Trimethylbenzene (wt%)	1.394	1.1784	0.44	1.39	0.52	1.39

Table 4.13 Percentage error calculation for extractive distillation using quinoline

	UNIQUAC		NRTL	
	Top	Bottom	Top	Bottom
Temperature (K)	4.27	0.94	4.50	0.18
dl-Limonene (wt%)	6.45	1.36	5.78	1.36
m-Cymene (wt%)	14.34	4.72	28.52	4.72
p-Cymene (wt%)	61.09	21.38	56.30	21.38
Indan (wt%)	61.93	39.17	58.03	39.17
1,2,3-Trimethylbenzene (wt%)	68.44	18.12	62.93	18.12

Table 4.14 Separation factor for extractive distillation using quinoline

	Experimental	UNIQUAC	NRTL
m-cymene (wt%)	2.59	2.27	2.00
p-cymene (wt%)	1.21	2.57	2.27
Indan (wt%)	0.74	2.83	2.55
1,2,3 Trimethylbenzene (wt%)	0.87	3.41	2.88

From Table 4.12, it can be seen that a slight change in *dl*-limonene purity is achieved from experimental data and a greater change in *dl*-limonene purity is achieved from models predicted data. No liquid phase splitting occurs. The individual component concentrations from different models are nearly equal and deviate largely from experimental data in the top stages.

From Table 4.13, it can be seen that the top and bottom concentration of *dl*-limonene show the lowest error and the concentration of other compounds show the highest error for both property model predictions. The greatest error is observed in the composition of the top stage. As such, the model over predicts the attainable purity.

The comparison of the experimental bottom and top temperature with the model prediction shows a good correlation indicated by the low percentage error. The NRTL and UNIQUAC property model reveals similar results.

From Table 4.14, it can be seen that the separation factor from experimental and model data for all compounds is far from one. The models over predict the separation of *dl*-limonene from 1,2,3-trimethylbenzene, indan and p-cymene. A cause for these discrepancies is a result of the poor quality of the binary interaction parameters estimated from the UNIFAC model. Nevertheless, it can be concluded that quinoline is a feasible entrainer indicated by the separation factor far from unity.

4.3.3.4 n-Methyl-2-pyrrolidone

Experimental and model data obtained from extractive distillation using quinoline are given in Table 4.15. The data is compared and the percentage error calculated is given in

Table 4.16. Separation factors are calculated from experimental and model data, and compared in Table 4.17.

Table 4.15 Model and experimental data for azeotropic distillation using n-methyl-2-pyrrolidone

	Experimental		**UNIQUAC**		**NRTL**	
	Top	Bottom	Top	Bottom	Top	Bottom
Number of phases	1	1	1	1	1	1
Temperature (K)	396.50	441.95	391.09	438.95	392.10	439.04
dl-Limonene (wt%)	93.07	90.14	95.86	88.41	96.06	88.41
m-Cymene (wt%)	1.20	2.35	1.09	2.57	1.05	2.57
p-Cymene (wt%)	3.86	5.12	2.31	6.18	2.24	6.18
Indan (wt%)	1.03	1.15	0.50	1.45	0.41	1.45
1,2,3-Trimethylbenzene (wt%)	0.85	1.25	0.24	1.39	0.24	1.39

Table 4.16 Percentage error calculation for azeotropic distillation using n-methyl-2-pyrrolidone

	UNIQUAC		**NRTL**	
	Top	Bottom	Top	Bottom
Temperature (K)	1.35	0.68	1.10	0.66
dl-Limonene (wt%)	3.00	1.91	3.21	1.91
m-Cymene (wt%)	9.76	9.25	12.40	9.25
p-Cymene (wt%)	40.09	20.60	41.84	20.60
Indan (wt%)	50.90	26.94	59.99	26.94
1,2,3-Trimethylbenzene (wt%)	71.56	11.59	71.86	11.60

Table 4.17 Separation factor for azeotropic distillation using n-methyl-2-pyrrolidone

	Experimental	**UNIQUAC**	**NRTL**
m-cymene (wt%)	2.02	2.57	2.65
p-cymene (wt%)	1.37	2.90	2.99
Indan (wt%)	1.15	3.13	3.85
1,2,3 Trimethylbenzene (wt%)	1.52	6.26	6.34

From Table 4.15, it can be seen that a change in *dl*-limonene purity is achieved from experimental data and models predicted data. The comparison of the experimental bottom and top temperature with the model prediction shows a good correlation indicated by the low percentage error. The NRTL and UNIQUAC property models reveal similar results.

From

Table 4.16 , it can be seen that the top and bottom concentration of *dl*-limonene and m-cymene show the lowest errors, and the concentration of other compounds show the highest error for both property model predictions. The greatest error is observed in the region of high purity *dl*-limonene. This indicated that a greater inaccuracy with the interaction parameters between n-methyl-2-pyrrolidone and impurities exists.

From Table 4.17, it can be seen that the separation factor from experimental and model data for all compounds is greater than one. The models over predict the separation of *dl*-limonene from all other compounds. Experimentally, it can be seen that it is not easy to separate *dl*-limonene from indan. Nevertheless, it can be concluded that n-methyl-2-pyrrolidone is a feasible entrainer indicated by the separation greater than unity. n-Methyl-2-pyrrolidone allows *dl*-limonene to be separated from impurities by homogeneous azeotropic distillation.

4.3.3.5 Error analysis

For error analysis, more information is gained by making multiple observations. The best entrainer investigated is n,n-dimethylformamide as it has high affinity for *dl*-limonene. In order to ensure that the sample is a true representative of the underlying phenomenon, a standard deviation is calculated to determine spread of the data. Three repeated experimental runs are used to determine the spread of the data. The average values and standard deviations are calculated for three replicates. The mean for n observation is calculated in Equation 4.4 as:

$$\bar{x} = \frac{\sum_{i=1}^{n} x_i}{n} \tag{4.4}$$

where x_i represents the i^{th} individual observation.

From this the standard deviation is calculated in Equation 4.5 as:

$$y = \sqrt{\frac{\sum_{i=1}^{n}(x_i - \bar{x})^2}{n}} \tag{4.5}$$

Numerous factors interfere with the measurement and result in variation of experimental data. Factors that interfere with measurement include experimental error and compositional analysis error. It is reported that quantification of individual compounds using 1-dimensional GC does not yield accurate results, as the compounds cannot be easily separated (Danon *et al.,* 2015). This especially occurs with close boiling compounds. Therefore, accurate

quantification of chemical compounds in the sample can be achieved by using 2-dimensional GC (Danon *et al.,* 2015). Large error arises from compounds in small concentrations. This might be because these compounds are not easily detected by GC and seldom fall outside the calibration range.

Experimental error in the laboratory arises from heat loss, entrainment of the liquid at the top stage by vacuum source and possible sub cooling of reflux. To avoid material loss at the overhead, cooling water needs to be increased, while ensuring no sub cooling of reflux, as it results in distillation column inefficiency (Buckley, 1964). While vacuum operation improves separation and prevents thermal degradation of compounds, it has operational difficulties. The standard deviation for three repeated runs of entrainer 2 at E/F of 2 is given in Table 4.18.

Table 4.18 Standard deviation of three sets experimental data

Component	Top composition (wt %)	Bottom composition (wt %)
dl-Limonene	0.25	0.66
m-Cymene	0.53	0.63
p-Cymene	0.74	0.66
Indan	0.15	0.66
1,2,3-Trimethylbenzene	0.28	0.22

From Table 4.18 it can be seen that the standard deviation is close to zero, indicating the values are close to the mean and not spread out over a wider range of values.

4.4. Conclusion

Aspen Plus ® simulation of extractive/azeotropic distillation processes, using NRTL and UNIQUAC activity coefficient models with interaction parameters, estimated with the UNIFAC model is a useful tool. This allows understanding of the vapor-liquid and vapour-liquid-liquid behaviour and the design and operation of extractive and azeotropic distillation; however, the results are not accurate enough for final design purposes for industrial operation (Turton *et al.,* 2009).

A comparison of the simulation model and experimental results was made and a better agreement with experimental results is obtained with the NRTL model. Some inconsistencies in the composition and separation factors from both models were observed when compared to experimental data.

The simulation results do not correlate well with experimental when looking at the individual concentrations. This is a result of inaccurate prediction of the thermodynamic models with

the interaction parameters from UNIFAC model. The comparison of the experimental bottom and top temperatures with model predictions, reveal that the models predict the temperatures fairly well. Consequently, the UNIFAC parameters used to predict binary phase equilibrium, predict *dl*-limonene composition well and the mixture boiling and condensation temperature.

The vapour pressure measurement in this work is not of great accuracy. This is shown by slight deviation of this work's vapour pressure data and literature data. Vapour pressure measurement of high boiling compounds is complex due to the possibility of thermal degradation during measurement. A vacuum fractionation setup is not a viable technique for vapour pressure measurement as it comes with operations difficulty. The model predicted data match correlates fairly well with published data. Therefore parameters fitted to vapour pressure equations in Aspen Plus® V8.2 predict the component vapour pressure fairly well.

As the entrainers studied have a significantly higher boiling points, increasing the E/F will increase the system temperature and would require binary interaction of *dl*-limonene and impurities, which are valid at elevated temperatures. The binary interaction between *dl*-limonene and the entrainer, as well as impurities and entrainer, also needs to be correlated well for a wide concentration range, as this determines the separation efficiency when using the entrainer.

Appropriate thermodynamic property models with reliable interaction parameters are of great importance to ensure optimum process designs. The use of UNIFAC estimated binary interaction parameters is not recommended and results in low accuracy of the models. Experimental work is necessary to obtain vapour-liquid and vapour-liquid-liquid data of entrainers and key components to derive binary interaction parameters. By using the regression tool in Aspen Plus®, the binary interaction parameters can be regressed to obtain better prediction and accurate process design.

Experimental validation of the model is strongly recommended for entrainer selection for new systems. The prediction result of the thermodynamic models led to different rankings when compared to experimental results. For example, quinoline has shown to be the best entrainer according to the process model in Chapter 3, but ranked last when examined experimentally. Although Aspen Plus ® V8.2 was not efficient in selecting best entrainer due to limiting data, it served as a guide for entrainer screening as doing so only by experimental work would be nearly impractical.

The experimental methodology utilised in this study proved to be effective in the operation and design of extractive and azeotropic distillation for close boiling mixtures. Experimental entrainer efficiency verification proved to be necessary in the situation where estimation methods are used with the property models selected. The design and optimisation of the azeotropic and extractive distillation was carried out with inaccurate sets of interaction parameters in Chapter 3. However, the design should be accepted with inaccuracies, and provide for a good base case enhanced distillation process design.

Economic evaluation of azeotropic and extractive distillation with the selected entrainers is important to determine profitability of the process. Although the thermodynamic models do not predict well the individual impurities concentration in the high purity *dl*-limonene region well, the extent of *dl*-limonene purification, and mixture boiling and condensation temperature is fairly predicted. Operational costs are mainly dependent on energy consumption and E/F. The model predicted results can be used only for a rough estimate, the proper cost of the extractive and azeotropic distillation process will largely depend on the extent of optimisation to obtain the final process design. This can be done after the VLE and VLLE data has been obtained experimentally and imported into Aspen Plus® for accurate extractive and azeotropic distillation design. The preliminary economic evaluation will also assist in determining the best entrainer among competing alternatives from the economic view point. The best entrainer from design flexibility and economic view point can be used in future work for VLE and VLLE data determination.

4.5. References

Acros Organics. 2012. Safety Data Sheet. [Online]. https://www.fishersci.ca/shop/msdsproxy?productName=AC277340250&productDescription=quinoline-yellow-water-soluble-95-acros-organics-2. [2015, Septermber 10]

Buckley, P.S. 1964. *Techniques of process control*. New York: Wiley.

Danon, B., van der Gryp, P., Schwarz, C.E. and Görgens, J.F. 2015. A review of dipentene (*dl*-limonene) production from waste tire pyrolysis. *Journal of Analytical and Applied Pyrolysis*, 112: 1–13.

Das, A., Frenkel, M., Gadalla, N.A.M., Kudachadker, S., Marsh, K.N., Rodgers , A.S. and Wilhoit, R.C. 1993. Thermodynamic and thermophysical properties of organic nitrogen compounds. *J.Phys. Chem. Ref. Data*, 22: 3

Henley, E.J., Seader, J.D. and Roper, D.K. 2011. *Separation Process Principles*. New York: Wiley.

Kneisl, P., Zon*dl*o. and J.W. 1987. Vapor pressure, liquid density, and the latent heat of vaporization as functions of temperature for four dipolar aprotic solvents. *Journal Of Chemical And Engineering Data,* 32: 11–13.

Muñoz, R., Montón, J.B., Burguet, M.C. and de la Torre, J. 2005. Phase equilibria in the systems isobutyl alcohol+N,N-dimethylformamide, isobutyl acetate+N,N-dimethylformamide and isobutyl alcohol+isobutyl acetate+N,N-dimethylformamide at 101.3kPa. *Fluid Phase Equilibria*, 232: 62–69.

Ngxangxa, S. 2016. Development of high resolution gas chromatography-mass spectrometry methods for analysis of tyre derived oils. Master's thesis. University of Stellenbosch.

Pakdel, H., Pantea, D.M. and Roy, C. 2001. Production of *dl*-limonene by vacuum pyrolysis of used tires*. J. Anal. Appl. Pyrolysis,* 57: 91–107.

Pakdel, H., Roy, C., Aubin, H. and Jean, G., Coulombe, S. 1991. Formation of *dl*-limonene in used tire vacuum pyrolysis oils. *Environmental Science & Technology*, 25: 1646–1649.

Smith, J.M., Ness, H.V. and Abbott, M.M. 2005. *Introduction to Chemical Engineering Thermodynamics*. McGraw-Hill Education.

Sinnott, R.K. 2005. *Chemical engineering design*. Elsevier, Butterworth-Heinemann, Amsterdam.

Stanciulescu, M. and Ikura, M. 2006. Limonene ethers from tire pyrolysis oil. *J. Anal. Appl. Pyrolysis,* 75: 217–225.

Stanciulescu, M. and Ikura, M. 2007. Limonene ethers from tire pyrolysis oil. *J. Anal. Appl. Pyrolysis,* 78: 76–84.

Steele, W.V., Chirico, R.D., Knipmeyer, S.E. and Nguyen, A. 2002. Measurements of Vapor Pressure, Heat Capacity, and Density along the Saturation Line for ε-Caprolactam, Pyrazine, 1,2-Propanediol, Triethylene Glycol, Phenyl Acetylene, and Diphenyl Acetylene. *Journal of Chemical & Engineering Data,* 47: 689–699.

The Dow Chemical Company. 2007. Triethylene glycol.

Lizarraga, E., Zabaleta, C. and Juan, A.P. 2005. Thermal decomposition and stability of quinoline compounds using thermogravimetry and differential scanning calorimetry. *Thermochimica Acta*, 427: 171–174.

Young, S. 1889. The vapour-pressures of quinoline. Bristol: University College.

Chapter 5 Economic Analysis

5.1. Introduction

The success of a tyre pyrolysis processing technology depends on the environmental performance and process economics (Wotjowicz and Serio, 1996). Waste tyre pyrolysis project profitability depends on: scale, production rate, operation cost, capital investment and tipping fees (Williams, 2005). The selling price of tyre pyrolysis products yields low revenues because of their low market value and low quality (Wotjowicz and Serio, 1996). Process models based on the recovery of the value added product, *dl*-limonene at high purity from TDO were developed with the intention of achieving an improvement in the process economics.

To ensure continuity of the developed process, the economic viability is assessed using economic modelling techniques. The key economic indicators used to measure economic performance, i.e. profitability, are: the discounted cash flow rate of return (DCFROR), net present value (NPV) and payback period (PBP) (Turton *et al.*, 2009).

The purpose of this chapter is to conduct an economic feasibility assessment to determine the economic benefits of the proposed separation process for recovery of *dl*-limonene from TDO simulated in Aspen Plus® V8.2 in Chapter 3. The chapter allows the comparison of the different process models on profitability. The chapter is divided into 5 sections. Section 5.2 gives the methodology and assumptions used for the economic analysis. Section 5.3 discusses the various components that make up the capital cost of the separation process and the operating cost. Section 5.4 investigates profitability and comparison of the developed process options, using the key economic indicators. Section 5.5 gives sensitivity analysis to investigate the effect of economic parameters on profitability. Section 5.6 reviews important findings of this chapter in terms of this investigation.

5.2. Assumptions and framework

The economic cost method used, was the study estimate obtained from Turton *et al.* (2009). Figure 5.1 show the methodological framework followed in this study to achieve the project objectives.

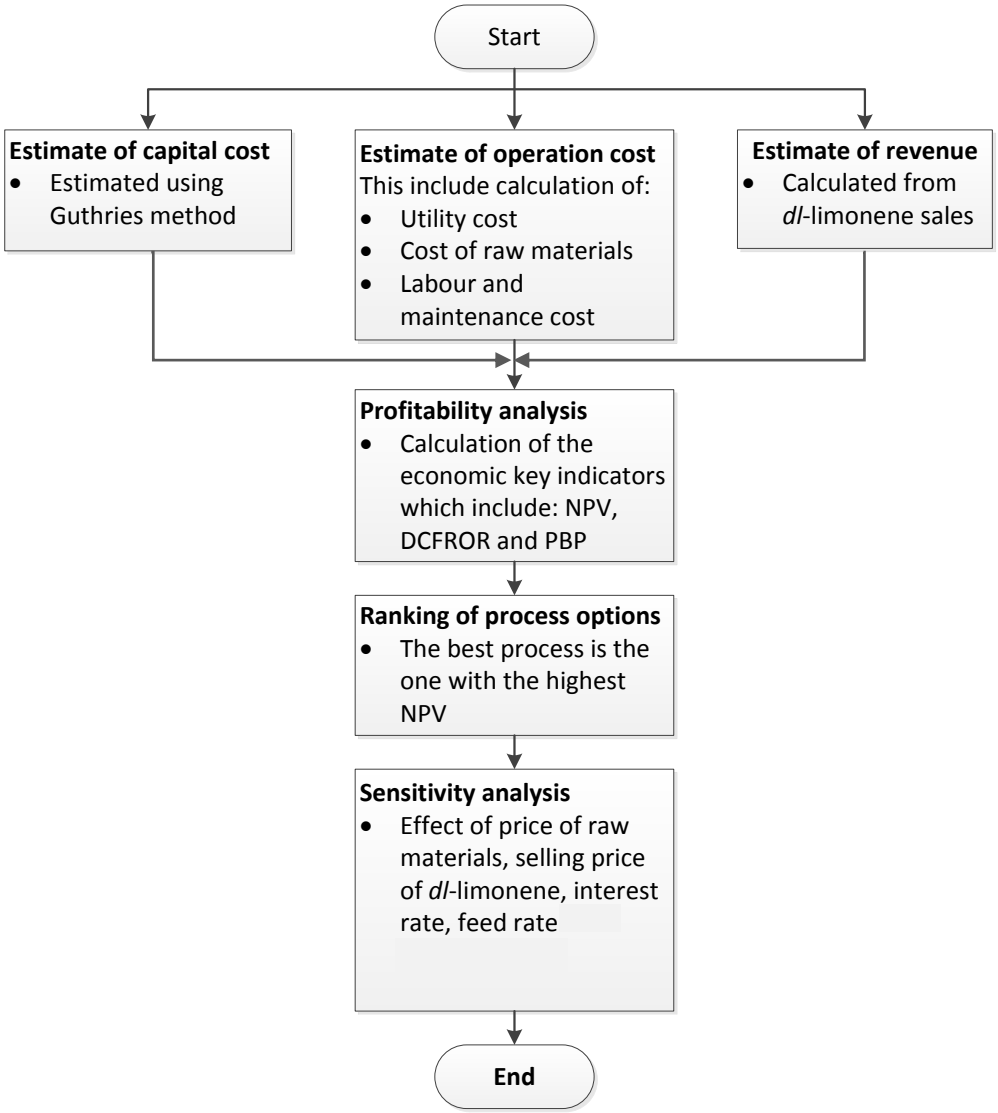

Figure 5.1 Step followed in the economic analysis

The first step required for the development of the *dl*-limonene recovery process model, is to develop a process flow diagram (PFD). In this study, a conventional flowsheet was generated according to literature. The process flowsheet for different process options was simulated in Aspen Plus ® V8.2 in Chapter 3 and the necessary mass and energy balance was generated.

The cost of major equipment in the process flowsheet, which includes all pumps, vessels, columns and heat exchangers sized in Aspen Plus® V8.2, was determined and then factored to give the estimated capital cost. The cost technique was adjusted for any difference in elapsed time since the cost data was generated. The cost data used in this study was reported in 2006. To account for time value of money, several cost indices can be used. These cost indices have proved to show similar inflationary trends (Turton *et al.*, 2009). The Chemical engineering plant cost index and Marshall and Swift equipment cost index are the most

generally accepted indices (Turton *et al.*, 2009). The chemical engineering plant cost index (CEPCI) was used for estimation of the purchasing cost of the equipment in 2015 in this study. The items indluded in CEPCI are: equipment, buildings, construction labour and supervision. The CEPCI for base case in the year 2006 is 500 and the CEPCI for 2015 is 576 (Turton *et al.*, 2009; Economic indicators: CEPCI, 2015).

The capital cost was estimated first, based on total installed cost of equipment. The operating cost was estimated next and lastly the estimate of revenue. These were used in a cash flow analysis to assess profitability.The economic performance of the project was judged on several criterions. These criteria enable the comparison of the economic performance of the process options derived. The criteria used to judge their economic performances were: the pay-back period (PBP), the discounted cash flow rate on return (DCFROR) and the net present value (NPV), (Turton *et al.,* 2009).

PBP: The time required after the start of the project to pay off initial investment from income generated. The PBP is an indicator as to when the break-even point is reached (Turton *et al.,* 2009). This does not necessarily measure profitability. A PBP of longer than four years is usually not acceptable when evaluating profitability of chemical plants (Seider *et al.,* 2004).

NPV: Money earned in the initial years of the project is more valuable than that earned in later years. This time value of the money can be incorporated for by calculating the NPV. The net cash flow for a specific year of the project is brought to its present value by discounting it at some chosen compound interest rate. The interest rate reveals the earning power of the money (Turton *et al.,* 2009). An NPV of greater than zero indicates profitability, while an NPV of less than zero indicates that profitability is not achieved. An NPV of zero indicates that the project breaks even.

DCFROR: An interest rate at which the cumulative net present value at the end of the project is zero. DCFROR is a measure of the maximum interest rate that the project could pay at the end of the project life and still break even. Discounted cash flow analysis used to calculate time value of the money is sensitive to the assumed interest rate. DCFROR of greater than the assumed interest rate yield positive returns with an NPV greater than zero. It is therefore important to calculate the NPV for various interest rates to see when the project will break even. The higher the DCFROR the project can afford to pay, the more profitable the project is (Turton *et al.,* 2009).

The effects of changes in major economic input parameters were also studied through sensitivity analysis. The following section describes, in detail, the procedure and the assumptions used in developing the economic models, after which results are presented in Section 5.3 to 5.5.

5.2.1. Estimate of capital cost

The bare module equipment costing technique is used to estimate the cost of the separation process plant. The cost factors incorporated into the bare module factor include the direct cost items and indirect cost incurred in the construction of the plant. The module costing technique introduced by Guthrie is used in this study and accepted as the best for making preliminary cost estimates (Turton *et al.,* 2009).

The working capital is the additional investment needed to start up the plant and operate it to the point where income is earned. Working capital varies from 5% of the fixed capital for single product projects, to as high as 30% for multi commodity projects (Sinnott, 2005). Most of the working capital is recovered at the end of project life.

5.2.2. Operating cost estimation

Operating costs are the expenses related to the operation of the plant equipment and the cost of resources used to maintain its existence (Turton *et al.,* 2009). Factors affecting the operating cost in this study include: the cost of raw materials, utilities, maintenance, and operating labour.

The raw material costs include the price of TDO and entrainers. The prices of entrainers are derived from Alibaba Group ® (Alibaba Group ®, 2015). The price of TDO is obtained from studies by Muzenda and Popa (2015). TDO is taken as a raw material and purchased at the price of heavy fuel oil. Utility costs include: the cost of cooling tower water, steam from the boilers and electrical substation.

Utility costs are derived from Turton *et al.* (2009). The price data is given in Table 5.1. As the operating cost is dependent on the capacity of the plant at any given time period, the production rate for the process is chosen. Muzenda and Popa (2015) found that waste tyre pyrolysis projects would become profitable if the TDO production is 104 000.00 litres per month. For this study, a TDO feed rate of 312000 litres per month was used to ensure a high *dl*-limonene production volume. The effect of feed rate on profitability will form part of the sensitivity analysis.

Table 5.1 Cost of raw materials and utilities

Raw materials	Unit	$/unit	Reference
Entrainers			
n,n-Dimethylformamide	kg	0.865	(Alibaba Group ®,1999)
N-Methylpyrrolidone	Kg	2.544	(Alibaba Group ®,1999)
N-Formylmorpholine	Kg	5.500	(Alibaba Group ®,1999)
Quinoline	Kg	3.750	(Alibaba Group ®,1999)
Diethylene glycol	Kg	1.195	(Alibaba Group ®,1999)
Triethylene glycol	Kg	1.396	(Alibaba Group ®,1999)
Tetraethylene glycol dimethyl ether	Kg	1.615	(Alibaba Group ®,1999)
TDO	L	0.040	(Muzenda and Popa, 2015)
Utilities			
Cooling water	m^3	0.015	(Turton *et al.,* 2009)
Low pressure steam	ton	29.290	(Turton *et al.,* 2009)
Mild pressure steam	ton	29.59	(Turton *et al.,* 2009)
Electricity	kwh	0.060	(Turton *et al.,* 2009)

5.2.3. Estimation of revenue

Revenue of the project is derived from *dl*-limonene sales. Revenue is calculated from *dl*-limonene sales linked to the basic *dl*-limonene price derived from citrus oils, as the price of *dl*-limonene from TDO is unavailable in literature. The sale price of *dl*-limonene at different grades is derived from GreenTerpenes ™ (2014) and is shown in Table 5.2.

Table 5.2 *dl*-Limonene price for different grades as obtained from GreenTerpenes ™ (2014)

Material	Unit	Price per unit ($)
dl-Limonene (98.5 wt%)	Kg	24.532
dl-Limonene (95 wt%)	Kg	15.138
dl-Limonene (90 wt%)	Kg	8.251

5.2.4. Economic modelling assumptions

A summary of some additional assumptions and economic investiment parameters are given in Table 5.3. The cash flow considers taxes on profits and depreciation of the total investment over a certain number of years. The depreciation method commonly used in the production of biofuels in South Africa is used in this study. The capital investment is depreciated over 3 years at 50%, 30% and 20% in the first, second and third year respectively (Deloitte, 2011). Depreciating an investment as early as possible is advantageous as it reduces taxes paid (Turton *et al.,* 2009). This is because money now has more value than in later years. Therefore, it is better to pay less tax in the early stages of the project than later.

A project life of more than 15 years, which is common for chemical processes, is used in this study. Inflation is ignored due to uncertainty of changes in economic conditions. This can be accepted on the assumption that inflation on revenue and expenses cancel out (Seider *et al.,* 2004). As the separation process is a small plant, it is assumed that the plant is constructed and commissioned in one year.

It is assumed that only operators are required, and the hourly wage is approximately $26.48 (Turton *et al.,* 2009). The number of operators required is related to the number of equipment installed on the process, and is estimated using Equation 5.3 (Turton *et al.,* 2009). The operating hours are taken as 8300 assuming an onstream percentage of 95% (Douglas, 1988).

$$Number\ of\ operators = (6.29 + 0.23 \sum Number\ of\ process\ equipments)^{0.5} \qquad 5.3$$

The tax rate is set at 28%, which is the highest rate at which industries in South Africa are taxed for positive cash flow (South African Revenue Service, 2009).

The interest rate is roughly equivalent to the current interest rate that the money would earn if invested. A nominal interest rate of 10% is used in this study. Inflation is ignored due to uncertainty of changes in economic conditions. It is assumed that inflation on revenue and expenses cancel out (Short *et al.,* 2005). The annual inflation rate in South Africa is approximately 5% (Triami Media BV, 2016). The minimum hurdle rate used for comparison to the DCFROR in this study is 15%. A rate of return of 25% is targeted to ensure the project is attractive to investors (Richardson *et al.,* 2007). Investors look for a minimum rate of return of 25% due to the risk and limited liquidity options in mid-market companies. If there is a large difference between the rate of return and the hurdle rate, the project is rendered worthy (Richardson *et al.,* 2007).

As the capital is not recovered at the end of the project life, the salvage value which is recovered at the end of the project life is determined. The salvage value falls within the range of 5-15% (Peter and Timmerhaus, 2003). The selected economic investment parameters used are given in Table 5.3.

Table 5.3 Economic analysis parameters

Parameter	Value	Reference
General investment parameters		
Project life	15	(Turton *et al.,* 2009)
Depreciation method	3 years depreciation	(Deloitte, 2011)
Tax rate	28%	(South African Revenue Service, 2009).
Interest rate	10%	(Short *et al.,* 1995)
Salvage value	5% of capital cost	(Peter and Timmerhaus, 2003)
Exchange rate	R16/$	
Project capital parameters		
Working capital	5% of capital cost	(Sinnott and Towler 2009)
Maintenance	5% of capital cost	(Seider *et al.,* 2004)
Facility Operating Parameters		
Continous operating mode	24 hours	
Operating hours per year	8300	(Sinnott and Towler 2009)
Labour		
Labour cost	$26.48	(Turton *et al.,* 2009)

5.3. Results: Cost estimations

For each process option, the economic results, which include: capital cost investment, operating costs and products sales revenues, are discussed in the following sections.

5.3.1. Capital cost investment

A summary of individual bare module equipment cost and the total bare module equipment cost for the separation process using different entrainers is shown in Figure 5.2.

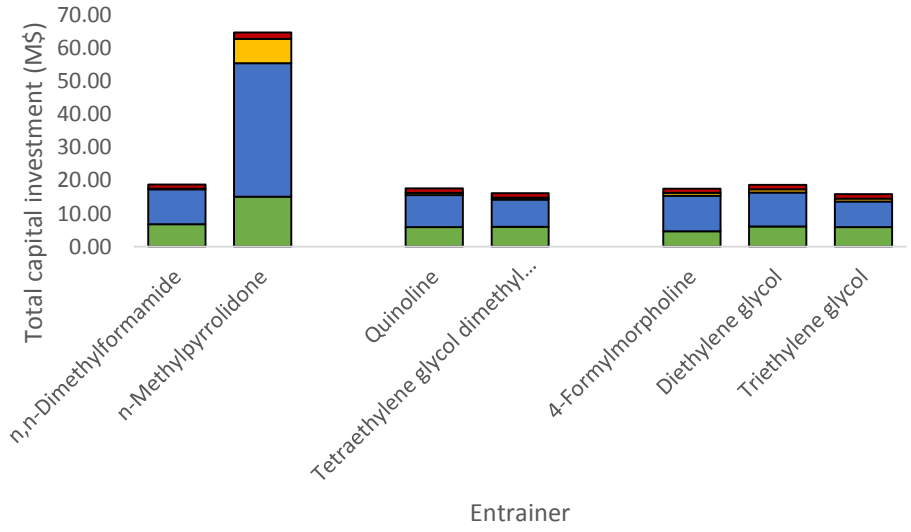

Figure 5.2 Cost contribution of individual equipment, distillation columns ■, heat exchangers ■, pumps ■ and vessels ■ to the total investment for separation processes developed using different entrainers

From Figure 5.2, it can be seen that homogenous azeotropic distillation, using n-methyl pyrrolidone, requires the highest total investment. This is a result of the large number of equipment required. Azeotropic and extractive distillation using other entrainers, need the lowest total investment. The reason for this, is the fewer units of equipment required. Therefore, the total investment cost from process options using other entrainers is quite comparable. From Figure 5.2, it can be concluded that the purchase cost of the distillation columns and heat exchangers are the decisive factor for the amount of the total investment.

5.3.2. Operating costs estimation

Operating costs, which are the expenses related to the operation of the plant equipment and cost of resources used to maintain it for different process options, is given in Figure 5.3.

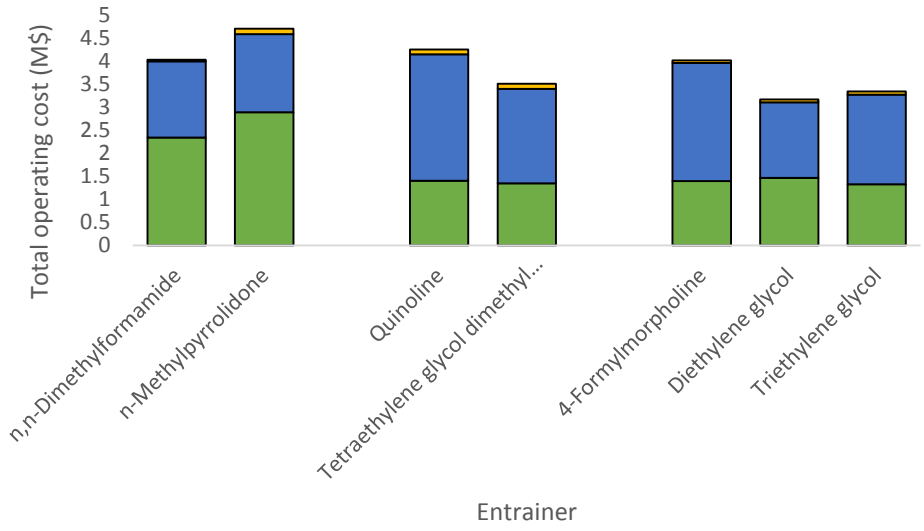

Figure 5.3 Total operating cost from summation of costs of raw materials ■, utilities ■ and operating labour and maintenance ■ for separation processes developed using different entrainers

From Figure 5.3 it can be seen that heterogeneous azeotropic distillation using 4-formylmorpholine, homogeneous azeotropic distillation using n-methyl-2-pyrrolidone and extractive distillation using quinoline, requires the highest operating cost. The high operating cost of heterogeneous azeotropic distillation using 4-formylmorpholine and extractive distillation using quinoline is a result of the required high E/F and the high cost of entrainer. The cost of utilities is reasonably low. This is because of the adoption of vacuum operation which lowers the amount of steam required, which is the most expensive utility. The high operating cost of n-methylpyrrolidone is a result of the large number of equipment needed which requires more maintenance and operators. Operating labour and maintenance costs

are relatively similar for all other process options, as the number of equipment required is not significantly different for all processes except homogeneous azeotropic distillation. Heterogenous azeotropic distillation by diethylene glycol and triethylene glycol are the process options that need the lowest operating cost. The reason for this is the relatively low cost of the entrainer. From Figure 5.3, it can be concluded that the purchasing price of the entrainer is the decisive factor for the amount of total operating cost.

5.3.3. Estimation of revenue

The revenue of the project is derived from the total product sales for different process options, and is given in Figure 5.4.

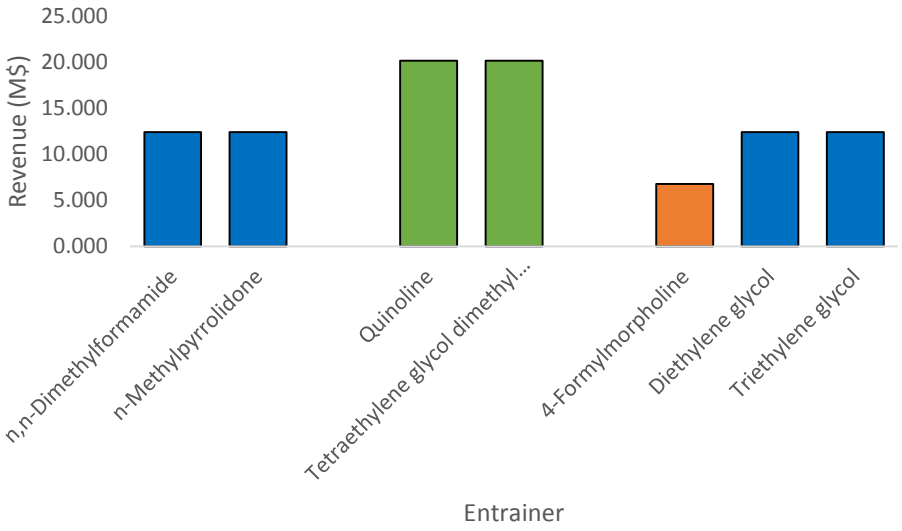

Figure 5.4 Revenue estimation for the separation process developed using different entrainers to yield *dl*-limonene at purity of 91 wt%, 95 wt% and 99 wt%.

From Figure 5.4, it can be seen that extractive distillation with quinoline and tetraethylene glycol dimethyl ether results in the highest annual income due to the high purity *dl*-limonene recovered, which can be sold at a high market price. Azeotropic distillation by 4-formylmorpholine has the lowest revenue as a result of the low purity *dl*-limonene recovered. It can be deduced further from Figure 5.4 that extractive distillation processes yield high returns.

5.4. Results: Profitability analysis

After calculation of the key economic indicators, the process options are compared and the best process is selected. The selection of the best process is based on the algorithm recommend by Turton *et al.* (2009). The minimum acceptable rate of return on investment is

set. The NPV is calculated and the process option with a negative NPV is eliminated. From the remaining process options with a positive NPV, the process with the highest NPV is selected. The minimum acceptable DCFROR is 15%. The effect of economic parameters of the selected process option on profitability is further assessed to account for uncertainties and risks involved in the project (Turton *et al.,* 2009). Profitability for different process options is given in Table 5.4.

Table 5.4 Profitability analysis using the key economic indicators

Entrainer	PBP (Years)	DCFROR (%)	NPV (M$)
n-Methylpyrrolidone	>15.00	7.72	-6.61
4-Formylmorpholine	13.93	9.89	-0.10
n,n-Dimethylformamide	8.84	14.34	10.12
Diethylene glycol	2.59	40.06	35.14
Triethylene glycol	2.10	48.87	37.96
Quinoline	1.39	73.50	73.81
Tetraethylene glycol dimethyl ether	1.23	83.21	79.00

From Table 5.4, it can be seen that all process options except azeotropic distillation using 4-formylmorpholine and n-methylpyrrolidone are profitable based on the DCFROR, which is greater than 15% and an NPV of greater than zero. The process option which does not meet the requirements of a PBP less than four years and DCFROR greater than the hurdle rate of 15% to attract investors, is azeotropic distillation with 4-formylmorpholine, n-methyl-2-pyrrolidone and n,n-dimethylformamide.

The best process in terms of economic performance is extractive distillation using tetraethylene glycol dimethyl ether. This is because extractive distillation with tetraethylene glycol dimethyl ether is capable of achieving *dl*-limonene at purity as high as 99wt%, and can therefore be sold at the highest price. This option has the highest NPV value, low PBP and high DCFROR above 25% to attract investors. The worst process option is azeotropic distillation using 4-formylmorpholine due to the low NPV and DCFROR, and high PBP which is not attractive.

5.5. Results: Sensitivity analysis

The effect of a change in a given parameter on profitability criterion of interest is investigated. Any key economic indicator can be used to measure profitability (Turton *et al.,* 2009). The DCFROR and NPV are used for sensitivity analysis in this study. The three different process options, which include: extractive distillation using quinoline, heterogeneous azeotropic

distillation using triethylene glycol and homogeneous azeotropic distillation using n-methylpyrrolidone are used for sensitivity analysis. These process options are chosen as the entrainers were evaluated experimentally and also cover the extreme case and best case in terms of economic performance. Sensitivity analysis is done on entrainer and *dl*-limonene price, interest rate and feed rate.

5.5.1. Effect of raw material price

The price of entrainers is estimated from literature with uncertainties. It is of great importance to investigate fluctuations in selling prices. To investigate the influence of small changes in the price of raw materials, the calculations are made by taking a price change of ±50 %. The effect of prices of n-methylpyrrolidone, triethylene glycol and quinoline on NPV and DCFROR is shown in Figure 5.5 and Figure 5.6 respectively. The effect on NPV is expressed as a percentage deviation from the design base case NPV. The minimum acceptable DCFROR to attract investors is shown on the plot.

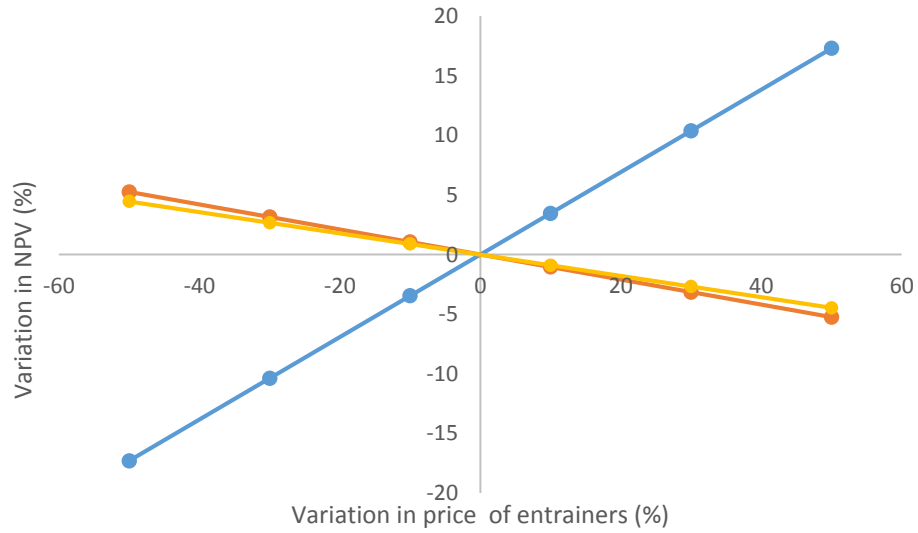

Figure 5.5 Effect of variation in price of entrainer on NPV using n-methyl-2-pyrrolidone●, triethylene glycol ●and quinoline●

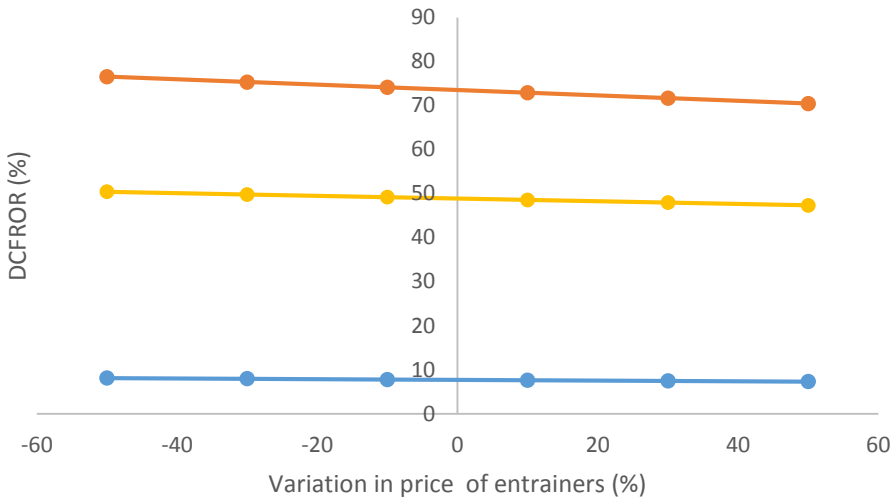

Figure 5.6 Effect of variation in price of entrainer on DCFROR using n-methyl-2-pyrrolidone ●, triethylene glycol ● and quinoline ●

As can be seen from Figure 5.5 and Figure 5.6, a change in the price of entrainers has a small impact on the NPV and DCFROR. This is because most of the entrainers are recovered at a high purity in the entrainer recovery column after the extractive/azeotropic distillation process. The operation cost mainly come from the purchasing of the initial entrainer during start-up and entrainer make-up which is only a portion of the required entrainer. It is assumed that the entrainer is regenerated with no loss of entrainer activity. The variation in NPV for n-methyl-2-pyrrolidone shows a different trend due to the negative NPV value.

5.5.2. Effect of *dl*-limonene price

Due to uncertainties in the price of *dl*-limonene from TDO, it is of great importance to investigate fluctuations in the selling price. To investigate the influence of small changes in the price of *dl*-limonene, the calculations are made by taking a price change of -50 to 50 %. This allows calculation of the minimum selling price to yield a DCFROR of greater than 15% to prevent loss of investment, and DCFROR of greater than 25% to ensure attractiveness of the project. The effect of price of *dl*-limonene on the NPV and DCFROR is shown in Figure 5.7 and Figure 5.8, respectively.

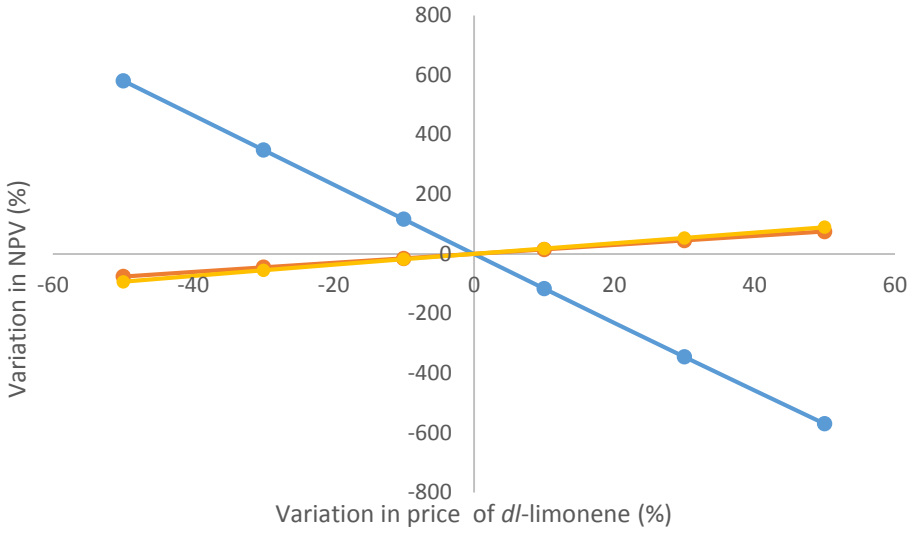

Figure 5.7 Effect of variation in price of *dl*-limonene on NPV using n-methyl-2-pyrrolidone ●, triethylene glycol ● and quinoline ●

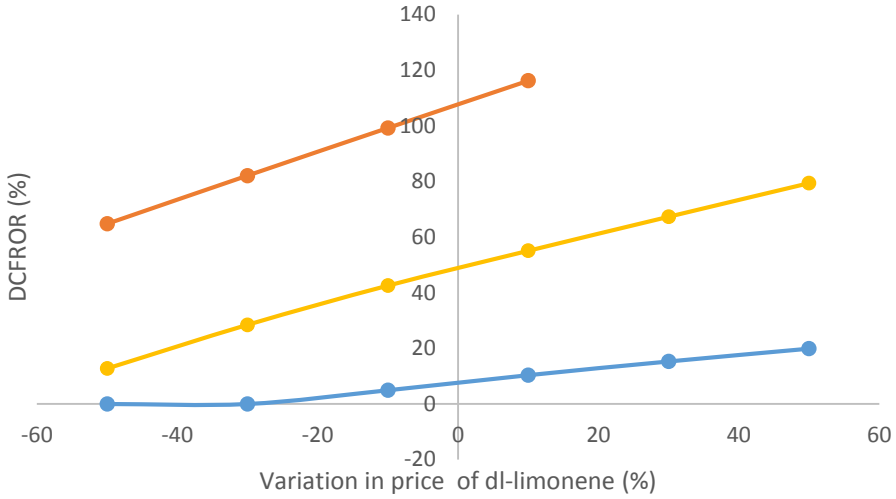

Figure 5.8 Effect of variation in price of *dl*-limonene on DCFROR using n-methylpyrrolidone ●, triethylene glycol ● and quinoline ●

As can be seen in Figure 5.7 and Figure 5.8, a change in the price of *dl*-limonene has a significant influence on the NPV and DCFROR. The developed processes are extremely sensitive to fluctuations in the price of *dl*-limonene, as can be seen by the large variation in NPV and DCFROR. The variation in NPV for n-methyl-2-pyrrolidone shows a different trend due to the negative NPV value.

The minimum selling price of *dl*-limonene to yield a positive return is below -50% and above 10% in price change for extractive distillation with quinoline and homogenous azeotropic distillation, with n-methylpyrrolidone respectively. The minimum selling price of *dl*-limonene

to yield a positive return is below -50% in price change for heterogeneous azeotropic distillation with triethylene glycol.

The minimum selling price of *dl*-limonene to yield an attractive positive return is below -50% for extractive distillation with quinoline, above -30% in price change for heterogeneous azeotropic distillation with triethylene glycol and above 50% for homogenous azeotropic distillation with n-methylpyrrolidone. These values are valid under the restriction that the prime interest rates is not higher than the assumed value of 10%.

5.5.3. Effect of interest rate

Additionally, sensitivity in interest rate is calculated as it is not easy to predict future economic conditions. To investigate the influence of small changes in interest rate on NPV, the calculations are made by taking interest change in the range of 5-30%. The NPV is calculated and shown in Figure 5.9.

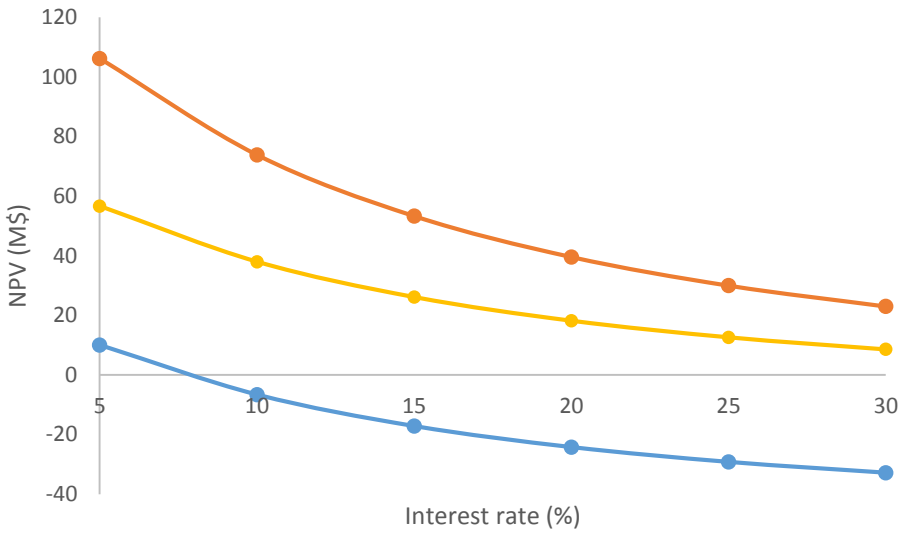

Figure 5.9 Effect of interest rate on NPV using n-methyl-2-pyrrolidone ●, triethylene glycol and ● quinoline ●

As can be seen in Figure 5.9, a change in the interest rate has a significant influence on the NPV. When prime interest rate increase, the NPV decrease rapidly. If the interest rate goes as high as 30%, profit can still be made from other processes as indicated by the positive NPV. This is different for homogenous azeotropic distillation using n-methylpyrroldione which yield negative return at interest rate above 5%, as indicated by the negative NPV.

5.5.4. Effect of feed rate

The effect of feed rate is important to determine the plant capacity, which will ensure economic feasibility for recovery of *dl*-limonene from TDO. Based on findings by Muzenda and Popa (2015), a successful waste tyre pyrolysis project would yield oil at a rate of 104 000 litres per month. To investigate the influence of changes in feed rate on the separation process, the NPV and DCROR calculations are done by taking the feed rate change in the range of 1 to 6 times the capacity of tyre pyrolysis throughput found by Muzenda and Popa (2015). This is because the TDO production rate imposes feed on the separation process in this study. The NPV and DCROR are calculated and shown in Figure 5.10 and Figure 5.11, respectively for different ratios of the tyre pyrolysis project TDO yield to the TDO feed rate on the separation process.

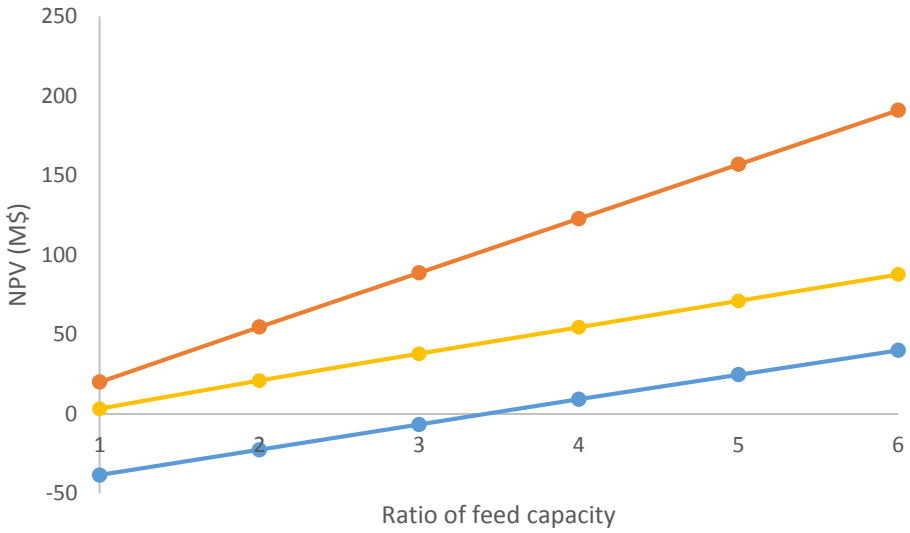

Figure 5.10 The effect of feed capacity on NPV using n-methyl-2-pyrrolidone●, triethylene glycol● and quinoline●

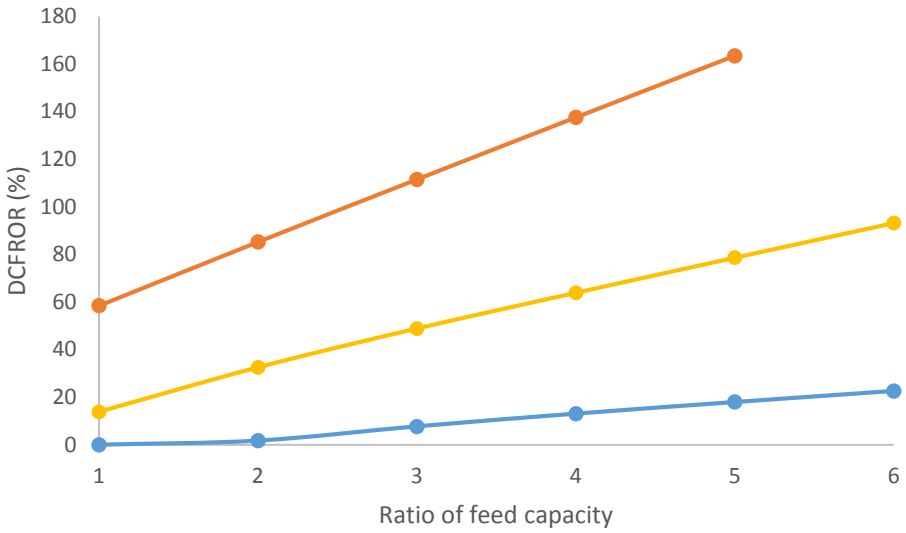

Figure 5.11 The effect of feed capacity on DCFROR using n-methyl-2-pyrrolidone ●, triethylene glycol ● and quinoline ●

From Figure 5.10 and Figure 5.11, it can be seen that an increase in feed capacity result in an increase in DCFROR and NPV. From Figure 5.10 and Figure 5.11, it can be deduced that the minimum feed rate to ensure high NPV and DCFROR greater than 15% is above 4 times the TDO yield from pyrolysis of tyre by Muzenda and Popa (2015) when considering homogenous azeotropic distillation using n-methylpyrrolidone. When considering extractive distillation with quinoline, the minimum feed rate to ensure high NPV and DCFROR greater than 15% is approximately 1 and heterogeneous azeotropic distillation with diethylene glycol is 1.5 times the TDO yield from pyrolysis of tyre by Muzenda and Popa (2015). The selected feed rate of 3 times the TDO yield from pyrolysis of tyre by Muzenda and Popa (2015) is acceptable to ensure improvement in economic performance of the separation process for majority of entrainers investigated. A higher throuput would require large equipment, high operations cost and high maintenance cost which might result in operational difficulty.

5.6. Concluding remarks

An economic analysis on a study estimate level was conducted to evaluate the processes models developed for separation of *dl*-limonene. Comparison based on capital cost investment showed that homogenous azeotropic distillation, using n-methylpyrrolidone, is the most expensive process. The difference in capital investment between other process options was not highly significant, as they have more or less similar equipment configurations. The total operating cost for homogeneous azeotropic distillation, using n-methylpyrrolidone

was found to be higher than other process options. The process using n-methyl-2-pyrrolidone requires large capital and operating costs, therefore a high selling price of *dl*-limonene, low entrainer and utility cost is needed to ensure positive returns.

The process with the highest revenue was found to be extractive distillation with quinolone and tetraethylene glycol, and the lowest was found to be heterogeneous azeotropic distillation with 4-formylmorpholine.

From profitability analysis, extractive distillation with tetraethylene glycol dimethyl ether proved to be the most economically feasible option with an NPV as high as $79.00 million, a PBP of 1.23 years, and a DCFROR of 83.21%, high enough for the project to be attractive. The least profitable process option was found to be homogeneous azeotropic distillation using n-methyl-2-pyrrolidone with a negative NPV, a payback period greater than 15 years and a DCFROR of 17.72%.

Sensitivity analysis on raw material has shown that enhanced distillation techniques using liquid entrainers are not sensitive to price of entrainers as the entrainer can be recycled in the process throughout.

Sensitivity analysis on *dl*-limonene price has shown that *dl*-limonene price has a significant impact on profitability.

Sensitivity analysis on interest rate has shown that interest rate affect the NPV, but the selected processes have shown to be sustainable, with an NPV value greater than zero for interest rate in the range of 5-15%.

Sensitivity analysis on feed rate has shown that separation of *dl*-limonene yield positive returns for a feed rate greater than the TDO production rate by Muzenda and Popa (2015).

From the economic analysis, it can be concluded that azeotropic and/or extractive distillation is viable technology for recovery of *dl*-limonene from TDO. The study estimate economic analysis proved to be sufficient to provide information upon which decisions can be based.

Heterogeneous azeotropic distillation processes using diethylene glycol and triethylene glycol and extractive distillation processes using entrainers investigated are robust to changes in prices of raw materials. Homogeneous azeotropic distillation processes requires high fixed capital cost and therefore yield negative returns for all changes in price of raw materials. Heterogeneous azeotropic distillation processes using diethylene glycol and triethylene glycol and extractive distillation processes using entrainers investigated are robust to changes in prices of raw materials due to low fixedcapital cost and operatinal cost. Heterogeneous

azeotropic distillation processes using diethylene glycol and triethylene glycol and extractive distillation processes using entrainers investigated are robust to changes in interest rate and have shown to be sustainable, with an NPV value greater than zero for interest rate above 15%. Heterogeneous azeotropic distillation and extractive distillation yield positive returns even at low feed rates. Homogeneous azeotropic distillation requires high capital cost and operating cost therefore yield negative returns at low feed rates. The revenue generated from *dl*-limonene sales is not enough to overcome the total costs incurred during homogeneous azeotropic distillation operation.

Heterogeneous azeotropic distillation processes using diethylene glycol and triethylene glycol and extractive distillation processes using entrainers investigated have shown to be robust in economic performance, even when multiple economic inputs change simultaneously

5.7. References

Alibaba Group ®.1999. [Online]. http://www.alibaba.com/. [2015, September 1].

Aspen Technology.2009. Aspen simulation user guide. Burlington, MA: Aspen Technology.

Deloitte: South Africa Taxation and Investment Guide. 2011. [Online]. www.deloitte.com/.../dttl_tax_guide_2011_South%20Africa.pdf. [2014, June 20].

Douglas, J.M. 1988. *Conceptual design of chemical processes*. McGraw-Hill.

Green Terpene ™.2014. [Online]. Available: www.greenterpene.com [2014, June 20].

South African Revenue Service: Budget 2009/10 – Tax Pocket Guide .2009. [Online]. http//www.treasury.gov.za/documents/national%20budget/2009/guides/Budget%20Pocket gui d%202009.pdf. [2014, June 20].

Henley, E.J., Seader, J.D. and Roper, D.K. 2011. *Separation Process Principles*. New York: Wiley.

Pakdel, H., Pantea, D.M. and Roy, C. 2001. Production of *dl*-limonene by vacuum pyrolysis of used tires. *J. Anal. Appl. Pyrolysis*, 57: 91–107.

Peters, M. and Timmerhaus, K. 2003. *Plant Design and Economics for Chemical Engineers*. New York: McGraw-Hill.

Richardson, J.W., Lemmer, W.J. and Outlaw, J.L. 2007. Bioethanol production from wheat in the winter rainfall region of South Africa: A qualitative risk analysis. *International Food and Agribusiness Management Review*, 10: 181-204.

Seider, W.D., Seader, J.D. and Lewin, D.R. 2004. *Product and process design principles: synthesis, analysis and evaluation.* New York: Wiley and Sons.

Short, W., Packey, D.J. and Holt, T. 1995. A manual for the economic evaluation of energy efficiency and renewable energy technologies. National Renewable Energy Laboratory Technical Report.

Sinnott, R.K. 2005. *Chemical engineering design*. Elsevier, Butterworth-Heinemann, Amsterdam.

Stanciulescu, M. and Ikura, M. 2007. Limonene ethers from tire pyrolysis oil. *J. Anal. Appl. Pyrolysis,* 78: 76–84.

Stanciulescu, M. and Ikura, M. 2006. Limonene ethers from tire pyrolysis oil. *J. Anal. Appl. Pyrolysis,* 75: 217–225.

Triami Media BV. 2016. [Online]. Available: http://www.info@inflation.eu. [2016, November 01].

Turton, R., Baile, R.C., Whiting, W.B. and Shaeiwitz, J.A.2009. *Analysis, synthesis, and design of chemical processes 3rd* .Prentice Hall international series in the physical and chemical engineering sciences. Upper Sad*dl*e River, NJ: Prentice Hall.

Chapter 6 Conclusions and recommendations

6.1. Conclusions

The objective of this project was to design a separation process to separate and purify *dl*-limonene from TDO. This entailed:

1. Identifying candidate entrainers
2. Conducting process modelling
3. Testing process models experimentally
4. Conducting economic analysis
5. Providing outcome as to possible separation

Identifying candidate entrainers

Azeotropic and extractive distillation techniques were chosen out of a wide range of separation process options found in literature. Various entrainers from different chemical groups were used for modelling of azeotropic and extractive distillation to separate dl-limonene from impurities. The entrainers investigated were: diethylene glycol, triethylene glycol, n,n-dimethylformamide, n-methyl-2-pyrrolidone, quinoline, 4-formylmorpholine and tetratethylene glycol dimethyl ether.

Conducting process modelling

Various process models were developed with the aid of Aspen Plus ® V8.2 and compared. The simulation results showed that all entrainers investigated alter the relative volatility of the mixture, and thus allow for *dl*-limonene purities to above 90 wt% at recoveries greater than 95%. The highest purity of *dl*-limonene (> 98 wt%) was obtained by using extractive distillation with quinoline and tetraethylene glycol dimethyl ether as an entrainer. The lowest purity (~ 91 wt%) was obtained by using 4-formylmorpholine in heterogeneous azeotropic distillation. Other entrainers gave purity within the range of 91-99% using homogenous or heterogeneous azeotropic distillation. All the entrainers, except n,n-dimethylformamide, were recovered at high purity (above 99wt %). While other entrainers could be recovered by ordinary distillation, n,n-dimethylformamide and n-methylpyrrolidone required extra steps to recover.

The best process options were found to be extractive distillation using tetraethylene glycol dimethyl ether and quinolone as entrainers, and heterogeneous azeotropic distillation using diethylene glycol and triethylene glycol as entrainers. These processes:

- Resulted in high recovery and purity *dl*-limonene

- Resulted in high recovery and purity entrainer
- Required less equipment and consumed less energy

Homogenous azeotropic distillation with n,n-dimethylformamide and n-methylpyrrolidone were the worst process options as they:

- Required more equipment and consume more energy
- Resulted in difficulty in entrainer recovery

Testing process models experimentally

Experimental work using a lab scale batch distillation unit was conducted at 60 kpa and various entrainer to feed ratios to determine model adequacy.

Comparison of extractive and azeotropic distillation experimental data with model data revealed that that the model NRTL and UNIQUAC satisfactorily predict the top and bottom temperatures of the batch distillation processes. The models further proved to predict the occurrence of liquid-liquid de-mixing. Although no consistency in chemical composition of the distillation products was noticeable, both the models and experimental data have shown separation factors of greater than one, indicating feasible separation. This was also evident by the improved purity of *dl*-limonene achieved. The NRTL property model gave a better agreement with experimental data when compared to the UNIQUAC property model for all sets of experimental data. The use of UNIFAC estimated binary interaction parameters thus yield less accurate results. Nevertheless, the use of UNIFAC model provide for a good base case and allow screening of the entrainer and understanding of azeotropic and extractive distillation processes when detailed VLE and VLLE data are unavailable.

Conducting economic analysis

An economic analysis was done on the separation processes. Economic analysis showed that four out of the seven process options developed using different entrainers were profitable. The non-profitable process options were azeotropic distillation using n,n-dimethylformamide, n-methylpyrrolidone and 4-formylmorpholine. The process that resulted in the greatest gross income was extractive distillation by tetraethylene glycol dimethyl ether while the least gross income came from homogeneous azeotropic distillation using n-methyl-2-pyrrolidone.

The best process in terms of economic performance was found to be extractive distillation using tetraethylene glycol dimethyl ether with a payback period of 1.23 years and a DCFROR

of 83.21%. The worst process option was found to be azeotropic distillation using n-methyl-2-pyrrolidone with a payback period of greater than 15 years and a DCFROR of 7.72%.

Providing outcome as to possible separation

Comparison of the two processes were made on the number of key unit operations, energy requirements, *dl*-limonene purities and recoveries, entrainer purities and recoveries, model validation and process economics. Out of the seven entrainers investigated, triethylene glycol, diethylene glycol, quinoline and triethylene glycol proved to be viable entrainers for extraction of *dl*-limonene from TDO light naphtha cut under the proviso that the thermodynamics prediction is valid.

6.2. Recommendations

All the candidate entrainers investigated have shown to be effective entrainers for recovery of *dl*-limonene from TDO light naphtha cut using enhanced distillation. Future work could consider generating experimental binary and ternary vapour-liquid and vapour-liquid-liquid data. By using the regression tool in Aspen Plus®, the interaction parameters can be regressed to propose modifications to UNIQUAC and NRTL parameters and obtain a better correlation between predicted and experimental data resulting in accurate process design. Measurement of equilibrium data should be conducted in an equilibrium still, that is able to handle low pressure operation and result in short residence times. An inert atmosphere should be maintained in the still to ensure the setup is nearly oxygen free. The following systems given in Table 6.1 are proposed. Impuritie in this investigation include compounds with close boiling point to *dl*-limonene. This include: cymene, indane and 1,2,3-trimethylbenzene.

Table 6.1 Pure component, binary and ternary systems for phase equilibrium measurment

Pure component Pressure: 5-50kpa	**Binary systems Pressure: 5-50kpa**	**Ternary systems Pressure: 5-50kpa E/F: 1-6**
n,n-Dimethylformamide n-Methyl-2-pyrrolidone 4-Formylmorpholine Diethylene glycol Triethylene glycol Quinoline Tetratethylene glycol dimethyl ether	Limonene/cymene Limonene/indane Limonene/1,2,3-trimethylbenzene	Limonene/impurity/n,n-dimethylformamide Limonene/impurity/n-methyl-2-pyrrolidone Limonene/impurity/4-formylmorpholine Limonene/impurity/diethylene glycol Limonene/impurity/triethylene glycol Limonene/impurity/quinoline Limonene/impurity/tetratethylene glycol dimethyl ether

The operating condition of equilibrium data measurement should closely match what is typically used in industry. Additionally, the models developed with the new parameters can be compared with experimental work in this study for verification.

In the measurement of equilibrium data, high vacuum pressure operation (below pressure measurements used in this work) should be adopted to prevent degradation of compounds and to investigate the effect of pressure on separation. The system temperature should not exceed 184°C as this is the maximum temperature of mild steam in industrial distillation columns. High pressure steam is costly and result in operational difficulties (Turton *et al.,* 2009). The E/F should be varied to obtain the optimum E/F that result in better separation. This will allow evaluation of the trade off between pressure variation and E/F variation. TDO is composed of a wide range of chemicals with broad functionality. Further work could consider extracting some chemical compounds that could be used as potential entrainers instead of purchasing external entrainers. Quinoline has shown to be a good entrainer and it could be extracted from TDO. Extracting quinoline is feasible as it is soluble in water.

n,n-Dimethylformamide has shown to be a potential entrainer but due to difficulty in its recovery, there's a need for development of better entrainer recovery methods to overcome azeotrope limitations.

Batch extractive distillation processes should be done at pressure below 60 kpa prevent to degradation of the distillation content when considering high boiling entrainers.

Appendix AGC Calibration curves

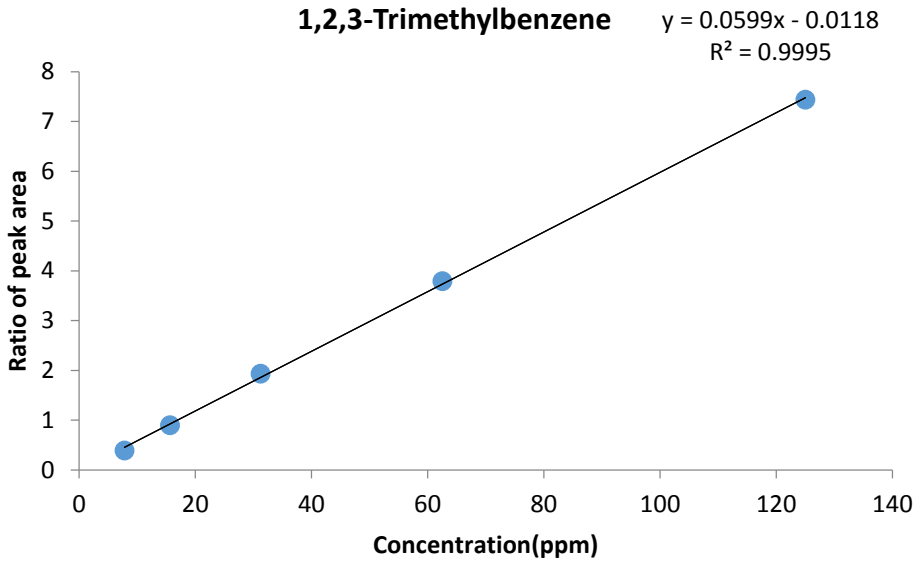

Figure A.1 GC Calibration curve for 1,2,3-trimethylbezene

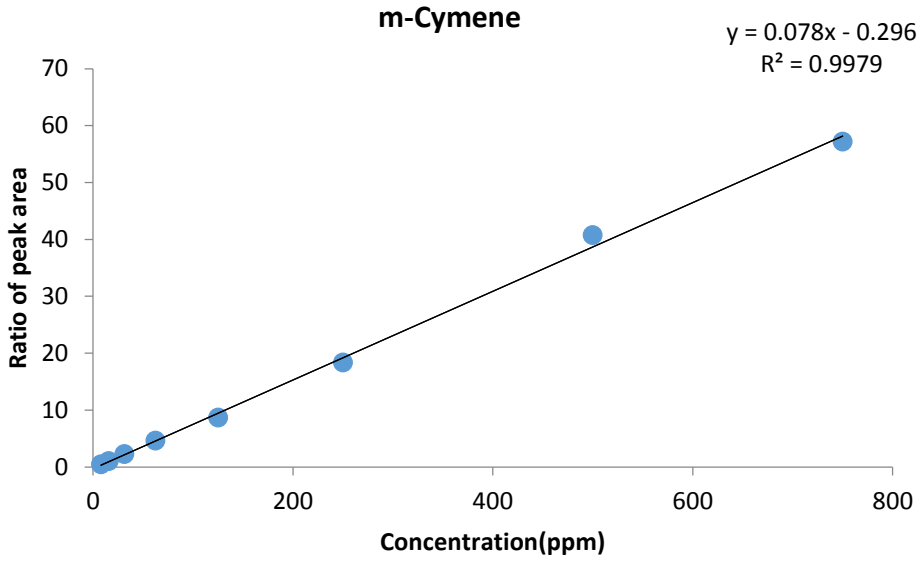

Figure A.2 GC Calibration curve for m-cymene

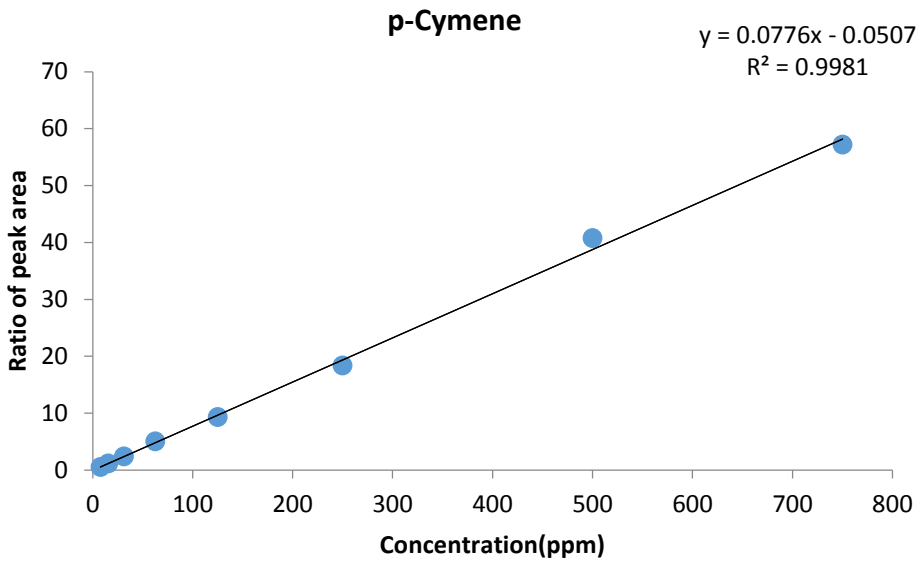

Figure A.3 GC Calibration curve for p-cymene

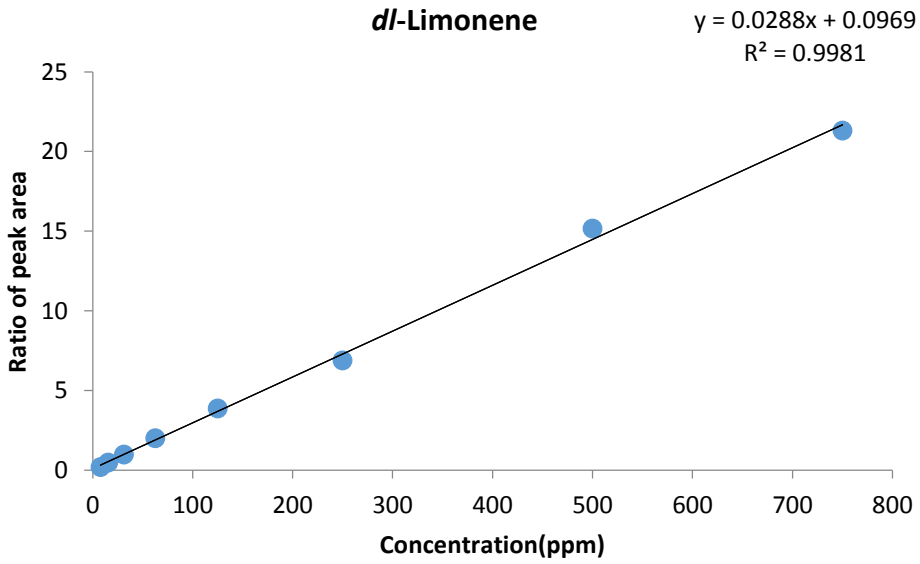

Figure A.4 GC Calibration curve for *dl*-limonene

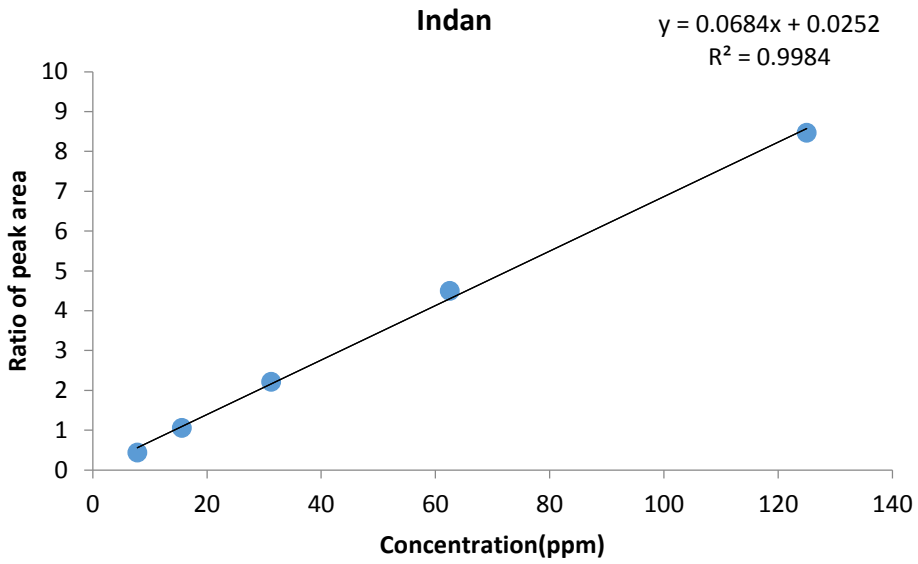

Figure A.5 GC Calibration curve for indane

Appendix BVapour pressure data

Table B.1 Vapour pressure data for n,n-dimethylformamide

Top Temperature (°C)	Bottom Temperature (°C)	Pressure (kpa)
125.3	126.8	47.2
126.5	129.3	52.6
129.3	130.3	55.0
131.8	134.2	62.4
133.9	136.4	66.8
136.1	138.3	70.4
138.6	141.6	77.0
125.3	126.8	47.2

Table B.2 Vapour pressure data for n-methyl-2-pyrrolidone

Top Temperature (°C)	Bottom Temperature (°C)	Pressure (kpa)
175.8	177.3	48.3
178.9	180.4	51.9
178.4	181.9	53.7
181.3	184.1	57.7
184.8	187.8	64.0
185.2	188	65.7
188.5	190.8	70.8
190.5	193.3	74.9

Table B.3 Vapour pressure data for quinoline

Top Temperature (°C)	Bottom Temperature (°C)	Pressure (kpa)
197.0	199.9	46.7
197.7	200.1	47.4
198.0	203.0	49.3
200.8	206.5	53.9
203.3	208.7	57.7
205.6	210.4	60.0
208.1	212.5	63.0
211.8	217.5	71.4
217.1	220.7	76.4

Table B.4 Vapour pressure data for triethylene glycol

Top Temperature (°C)	Bottom Temperature (°C)	Pressure (kpa)
252.6	254.8	46.9
255.5	257.7	51.1
258.4	260.6	56.3
261.5	263.7	61.3
264.1	266.3	66.5
266.9	269.1	72.6
269.6	271.8	78.1

Table B.5 Vapour pressure data for *dl*-limonene enriched fraction with various entrainers

Entrainer	E/F	Top Temperature (°C)	Bottom Temperature (°C)	Pressure (Kpa)
Dimethylformamide	2	122.2	128.8	60
Triethylene glycol	2	100.7	167.7	60
Quinoline	2	97.6	172.1	60
Methyl-pyrrolidone	2	107.1	166.7	60
Dimethylformamide	4	124.5	128.1	60
Triethylene glycol	4	117.8	170.3	60
Quinoline	4	127.9	181.5	60
Methyl-pyrrolidone	4	123.3	168.8	60
Dimethylformamide	6	124.1	129.9	60
Triethylene glycol	6	120.0	178.7	60
Quinoline	6	122.5	190.2	60
Methyl-pyrrolidone	6	131.1	172.7	60

Appendix CPurification of light naphtha

C.1.1. Feed

Table C.1 *dl*-Limonene enriched fraction composition for experimental batch enhanced distillation

Component	Feed composition (wt %)
dl-Limonene	88.41
m-Cymene	2.57
p-Cymene	6.18
Indan	1.45
1,2,3-Trimethylbenzene	1.40

Table C.2 Synthetic feed solution composition for experimental batch enhanced distillation

Component	Feed composition (wt %)
dl-Limonene	50.29
m-Cymene	0.00
p-Cymene	18.30
Indan	11.91
1,2,3-Trimethylbenzene	19.51

C.1.2. Azeotropic distillation using n,n-dimethylformamide

Table C.3 Experimental data for azeotropic distillation using n,n-dimethylformamide at E/F of 2

Component	Top composition (wt %)		Bottom composition (wt %)	
	1st Liquid	2nd Liquid	1st Liquid	2nd Liquid
dl-Limonene	95.22	0.00	89.51	0.00
m-Cymene	0.97	0.00	1.35	0.00
p-Cymene	2.62	0.00	6.92	0.00
Indan	0.97	0.00	0.79	0.00
1,2,3-Trimethylbenzene	0.22	0.00	1.43	0.00

Table C.4 Second experimental data for azeotropic distillation using n,n-dimethylformamide at E/F of 2

Component	Top composition (wt %)		Bottom composition (wt %)	
	1st Liquid	2nd Liquid	1st Liquid	2nd Liquid
dl-Limonene	95.77	0.00	88.97	0.00
m-Cymene	1.25	0.00	1.34	0.00
p-Cymene	1.37	0.00	7.31	0.00
Indan	0.73	0.00	1.47	0.00
1,2,3-Trimethylbenzene	0.89	0.00	0.92	0.00

Table C.5 Third experimental data for azeotropic distillation using n,n-dimethylformamide at E/F of 2

Component	Top composition (wt %)		Bottom composition (wt %)	
	1st Liquid	2nd Liquid	1st Liquid	2nd Liquid
dl-Limonene	95.23	0.00	90.56	0.00
m-Cymene	0.00	0.00	0.00	0.00
p-Cymene	3.12	0.00	5.74	0.00
Indan	1.08	0.00	2.40	0.00
1,2,3-Trimethylbenzene	0.57	0.00	1.30	0.00

Table C.6 Experimental data for azeotropic distillation using n,n-dimethylformamide at E/F of 6

Component	Top composition (wt %)		Bottom composition (wt %)	
	1st Liquid	2nd Liquid	1st Liquid	2nd Liquid
dl-Limonene	95.22	94.15	92.94	0.00
m-Cymene	0.97	0.00	0.00	0.00
p-Cymene	2.62	3.17	4.74	0.00
Indan	0.97	1.33	1.27	0.00
1,2,3-Trimethylbenzene	0.22	1.35	1.05	0.00

C.1.3. Azeotropic distillation using n-methyl-2-pyrrolidone

Table C.7 Experimental data for azeotropic distillation using n-methyl-2-pyrrolidone at E/F of 2

Component	Top composition (wt %)		Bottom composition (wt %)	
	1st Liquid	2nd Liquid	1st Liquid	2nd Liquid
dl-Limonene	92.27	0.00	90.32	0.00
m-Cymene	1.44	0.00	3.98	0.00
p-Cymene	4.12	0.00	3.56	0.00
Indan	1.33	0.00	1.11	0.00
1,2,3-Trimethylbenzene	0.84	0.00	1.04	0.00

Table C.8 Experimental data for azeotropic distillation using n-methyl-2-pyrrolidone at E/F of 6

Component	Top composition (wt %)		Bottom composition (wt %)	
	1st Liquid	2nd Liquid	1st Liquid	2nd Liquid
dl-Limonene	92.93	0.00	91.49	0.00
m-Cymene	1.77	0.00	1.80	0.00
p-Cymene	3.37	0.00	4.62	0.00
Indan	1.24	0.00	1.31	0.00
1,2,3-Trimethylbenzene	0.69	0.00	0.79	0.00

C.1.1. Extractive distillation using quinoline

Table C.9 Experimental data for extractive distillation using quinoline at E/F of 2

Component	Top composition (wt %)		Bottom composition (wt %)	
	1st Liquid	2nd Liquid	1st Liquid	2nd Liquid
dl-Limonene	89.42	0.00	87.23	0.00
m-Cymene	1.07	0.00	2.69	0.00
p-Cymene	6.66	0.00	7.86	0.00
Indan	1.46	0.00	1.05	0.00
1,2,3-Trimethylbenzene	1.39	0.00	1.18	0.00

Table C.10 Experimental data for extractive distillation using quinoline at E/F of 6

Component	Top composition (wt %)		Bottom composition (wt %)	
	1st Liquid	2nd Liquid	1st Liquid	2nd Liquid
dl-Limonene	91.29	0.00	89.08	0.00
m-Cymene	0.00	0.00	1.02	0.00
p-Cymene	6.87	0.00	7.22	0.00
Indan	0.00	0.00	1.23	0.00
1,2,3-Trimethylbenzene	1.85	0.00	1.45	0.00

C.1.2. Azeotropic distillation using triethylene glycol

Table C.11 Experimental data for azeotropic distillation using triethylene glycol at E/F of 2

Component	Top composition (wt %)		Bottom composition (wt %)	
	1st Liquid	2nd Liquid	1st Liquid	2nd Liquid
dl-Limonene	88.27	0.00	85.76	81.96
m-Cymene	1.05	0.00	1.45	1.60
p-Cymene	8.28	0.00	9.22	12.01
Indan	1.34	0.00	1.49	1.96
1,2,3-Trimethylbenzene	1.09	0.00	2.09	2.48

Table C.12 Experimental data for azeotropic distillation using triethylene glycol at E/F of 6

Component	Top composition (wt %)		Bottom composition (wt %)	
	1st Liquid	2nd Liquid	1st Liquid	2nd Liquid
dl-Limonene	89.63	0.00	88.59	81.59
m-Cymene	0.86	0.00	0.00	3.23
p-Cymene	7.00	0.00	8.88	10.39
Indan	1.41	0.00	0.91	1.82
1,2,3-Trimethylbenzene	1.11	0.00	1.62	2.97

C.1.1. Sythetic solution azeotropic distillation

Table C.13 Experimental data for azeotropic distillation using n,n-dimethylformamide at E/F of 2

Component	**Top composition (wt %)**		**Bottom composition (wt %)**	
	1st Liquid	2nd Liquid	1st Liquid	2nd Liquid
dl-Limonene	88.86	0.00	66.81	52.89
m-Cymene	0.00	0.00	0.00	0.00
p-Cymene	3.83	0.00	11.67	17.10
Indan	3.51	0.00	8.00	7.49
1,2,3-Trimethylbenzene	3.81	0.00	13.51	22.52

Table C.14 Experimental data for azeotropic distillation using n,n-dimethylformamide at E/F of 4

Component	**Top composition (wt %)**		**Bottom composition (wt %)**	
	1st Liquid	2nd Liquid	1st Liquid	2nd Liquid
dl-Limonene	89.07	0.00	70.23	52.26
m-Cymene	0.00	0.00	0.00	0.00
p-Cymene	3.33	0.00	11.17	15.96
Indan	3.52	0.00	7.43	10.81
1,2,3-Trimethylbenzene	4.08	0.00	11.17	20.97

Appendix D Property model selection

The selection of thermodynamic model as by Aspen Plus® guide, Eric Carlson and Bob Seader's recommendation is shown in Figure D.1 to Figure D.4 (Seider *et al.,* 2004)**.** A pathway in selecting the right model for the fractionation of raw TDO is highlighted in the flow diagrams.

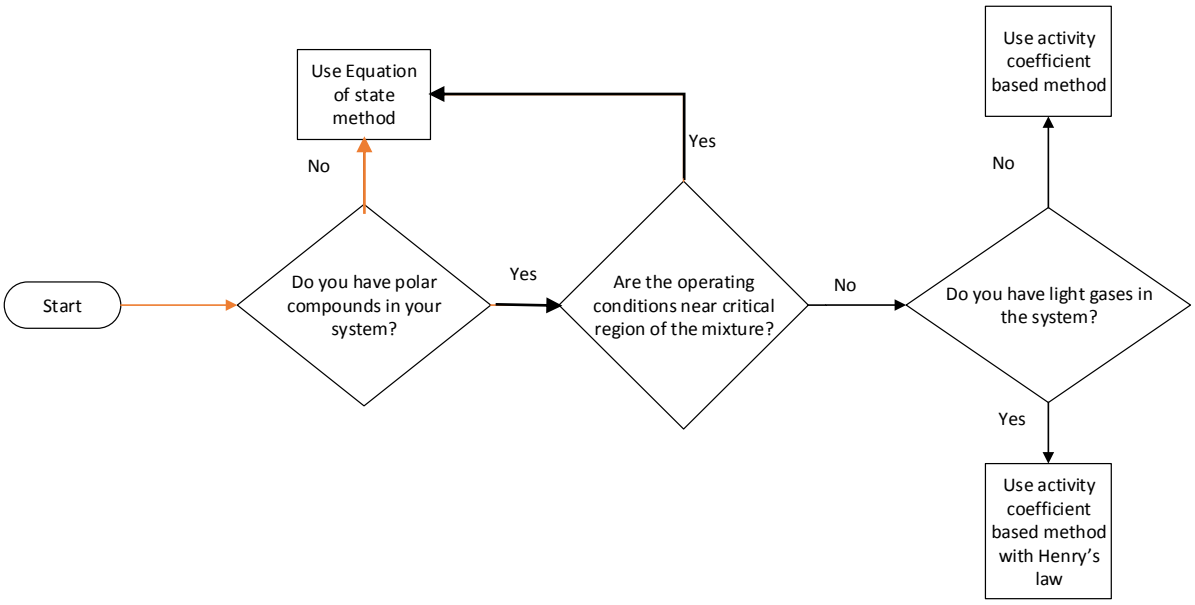

Figure D.1 Aspen method guide (Aspen Technology, 2009)

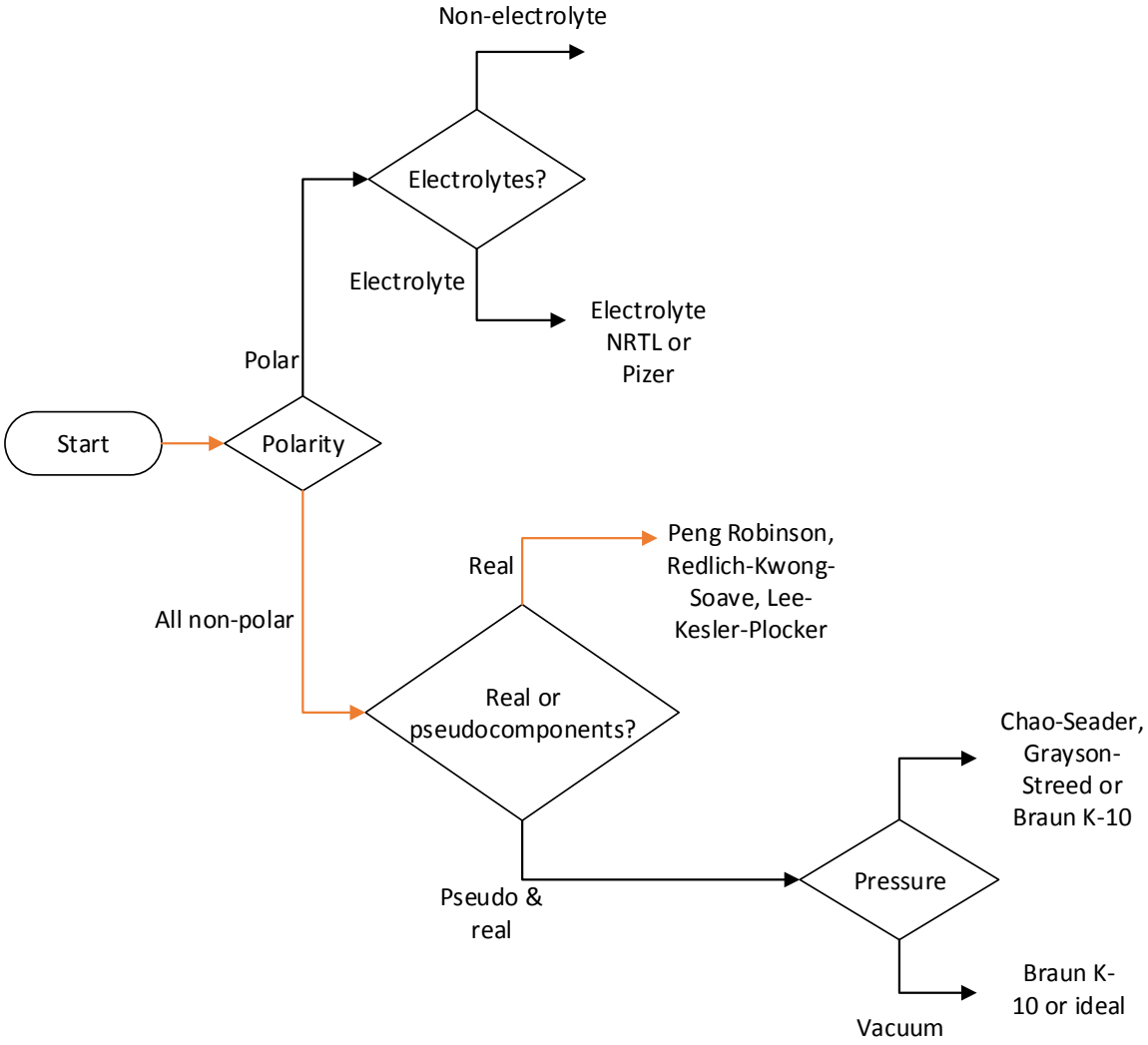

Figure D.2 Eric Carlson method guide (*Seider et al.*, 2004)

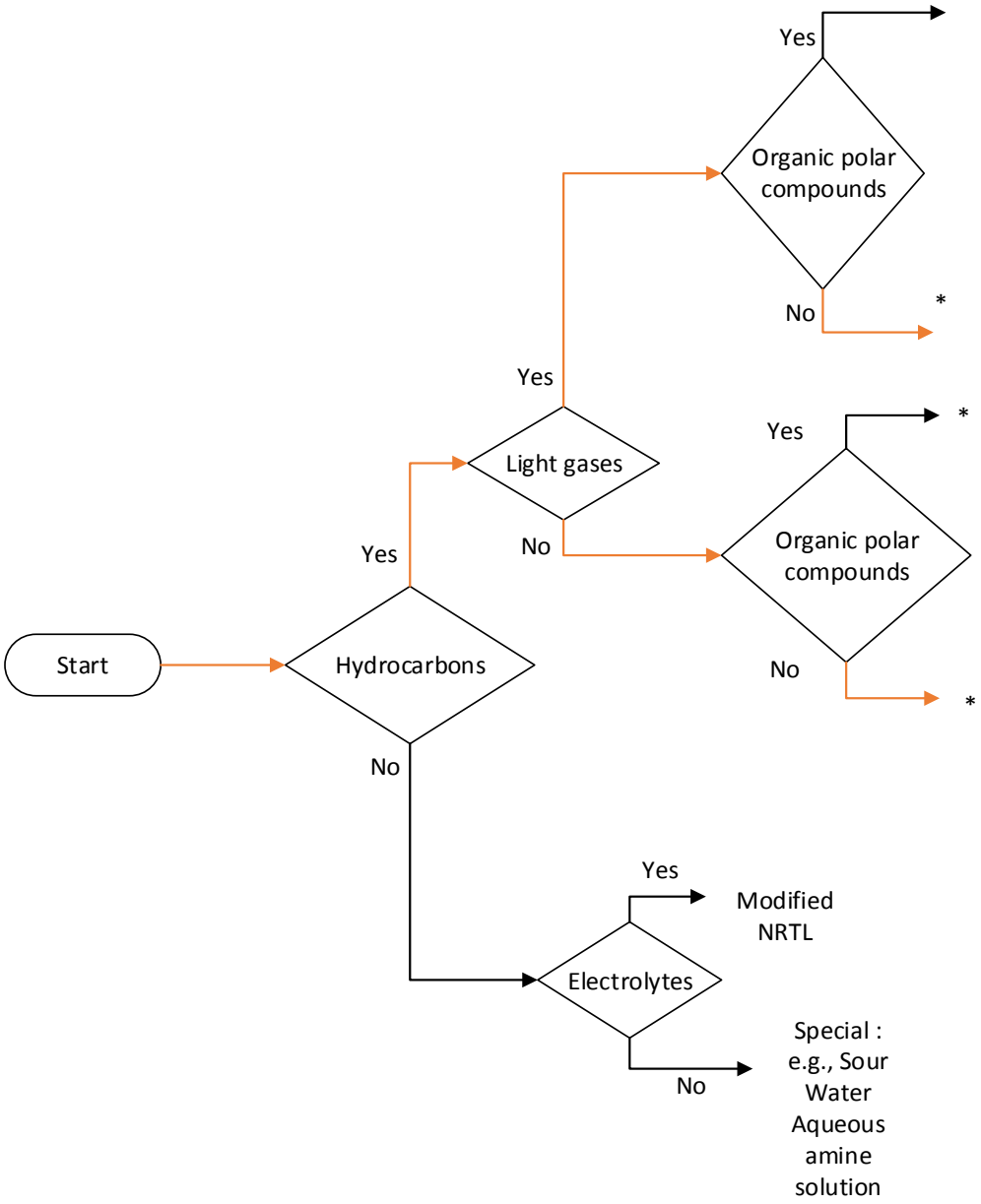

Figure D.3 Bob Seader method guide (Seider *et al.,* 2004)

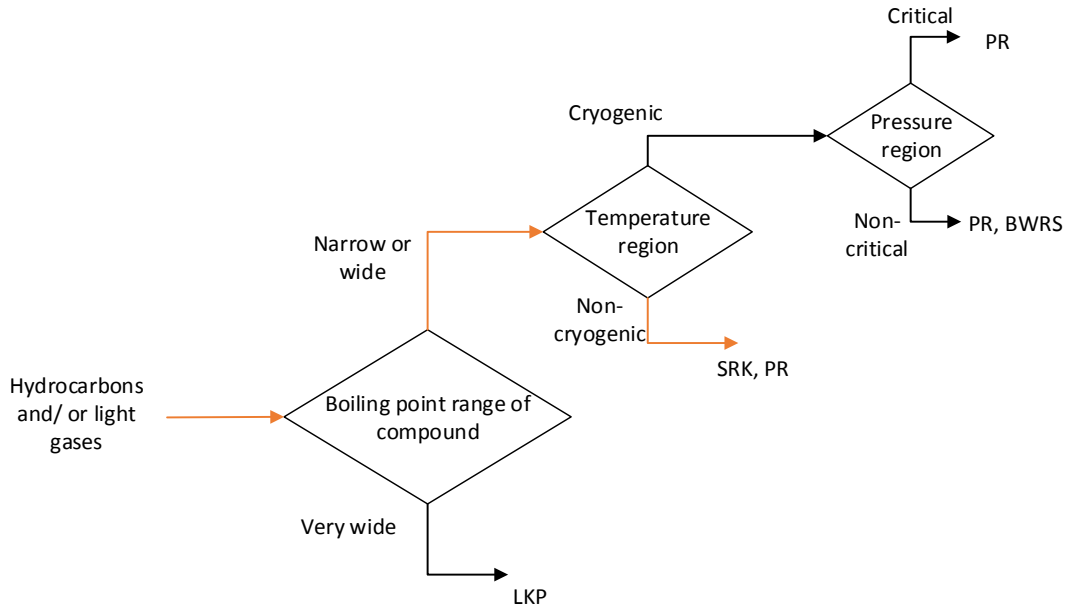

Figure D.4 Bob Seader method guide continue (Seider *et al.,* 2004)

A pathway in selecting the right model for enhanced distillation process is highlighted in the flow diagrams given in Figure D.5 to Figure D.10.

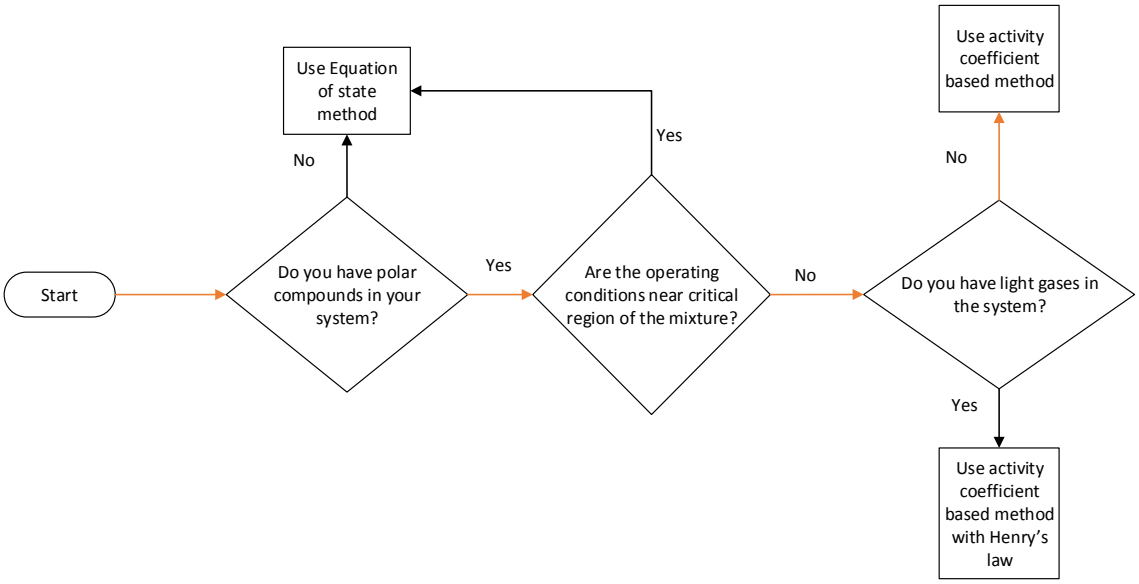

Figure D.5 Aspen method guide for polar compounds (Aspen Technology, 2009)

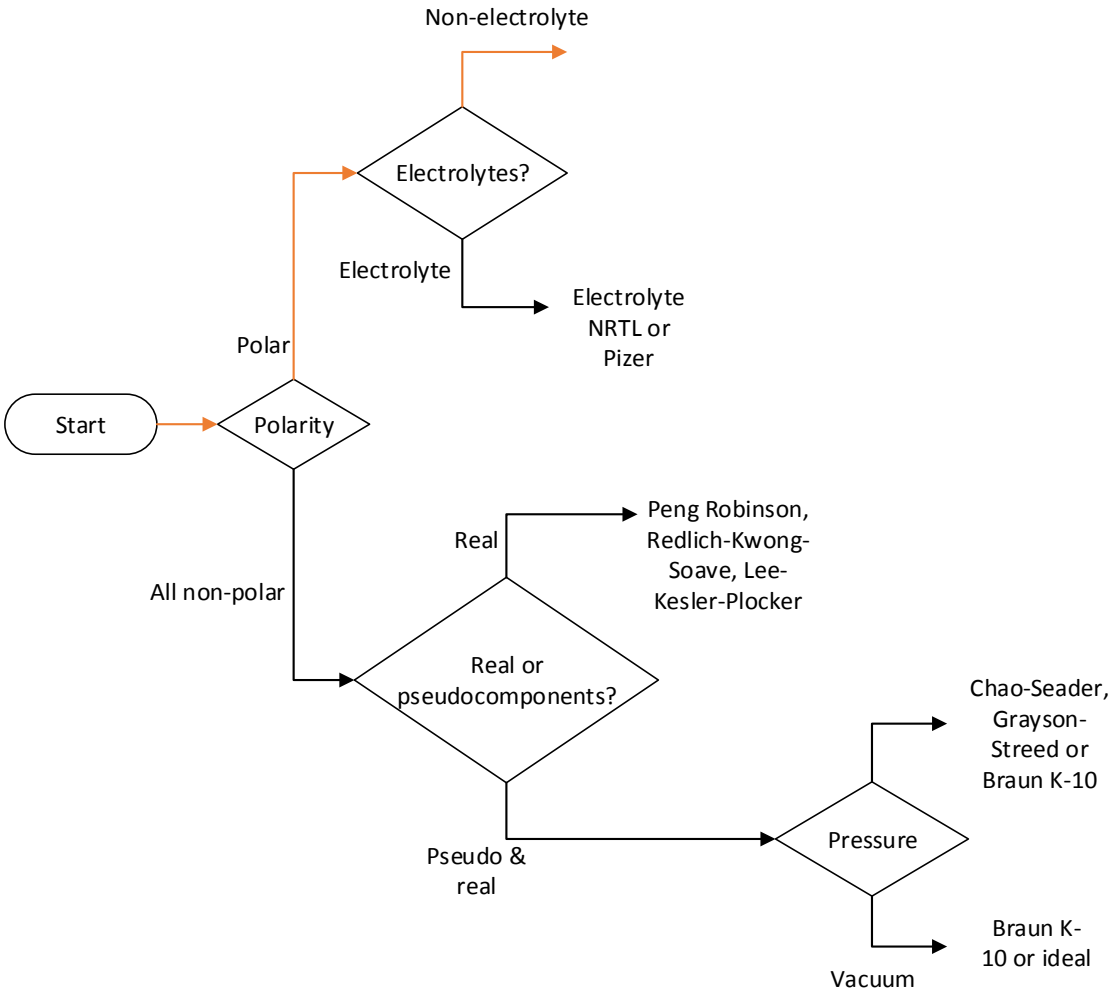

Figure D.6 Eric Carlson method guide for polar compounds (*Seider et al.*, 2004)

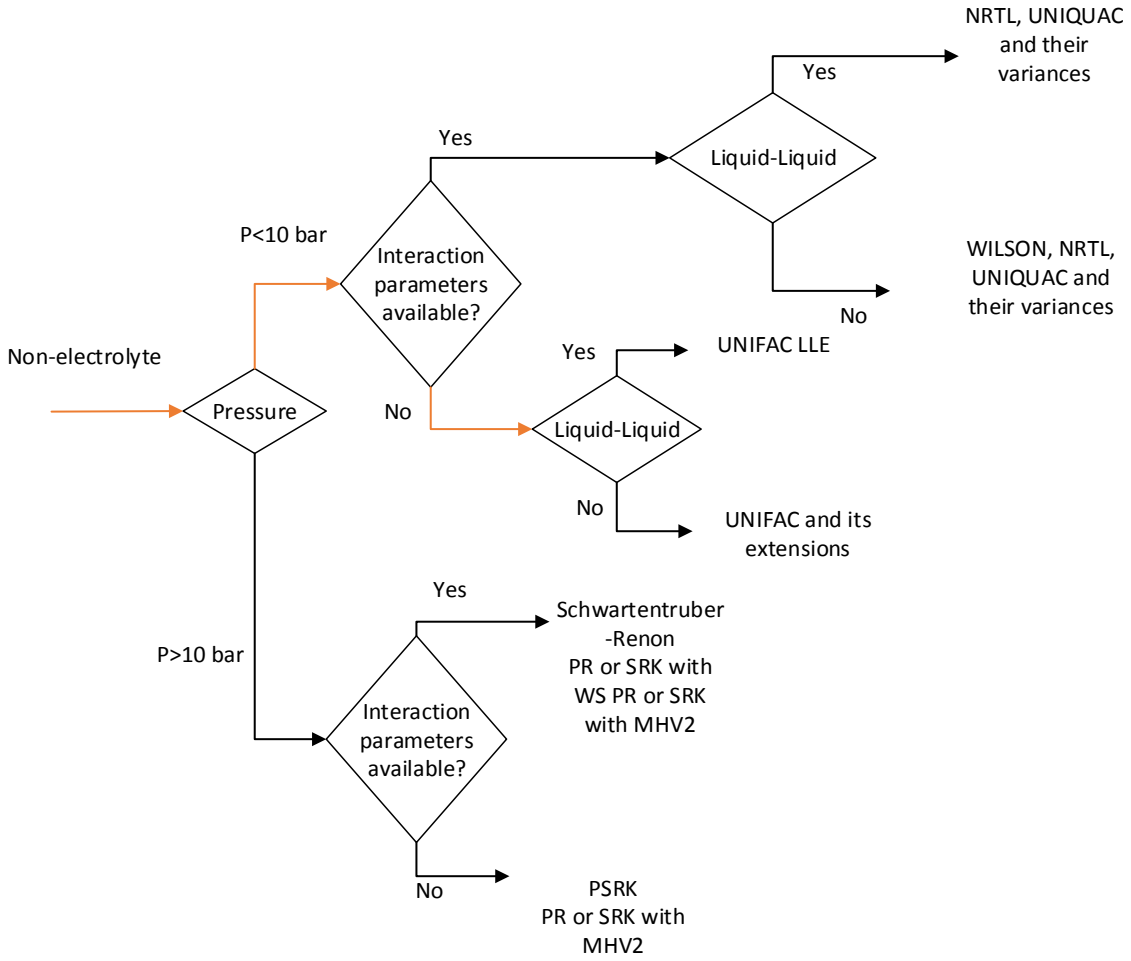

Figure D.7 Eric Carlson method guide for polar compounds continue (*Seider et al.*, 2004)

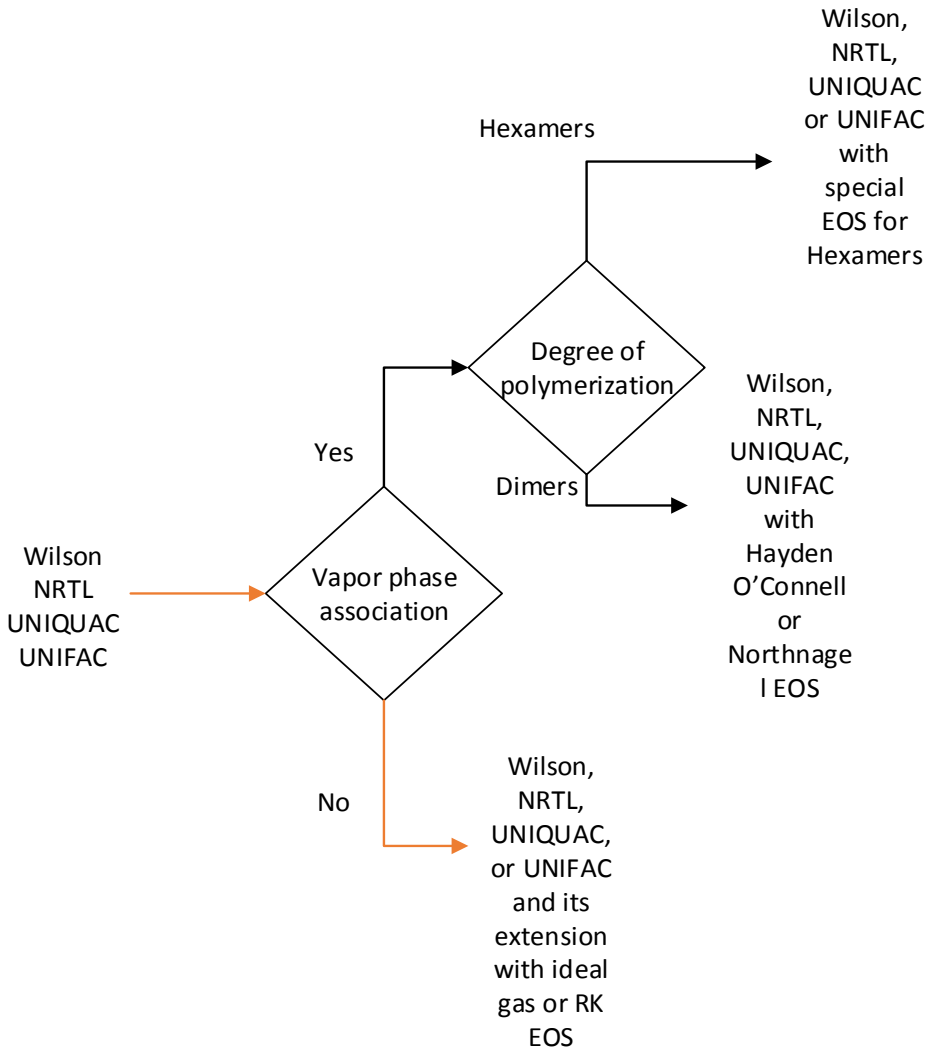

Figure D.8 Eric Carlson method guide for polar compounds continue (*Seider et al.*, 2004)

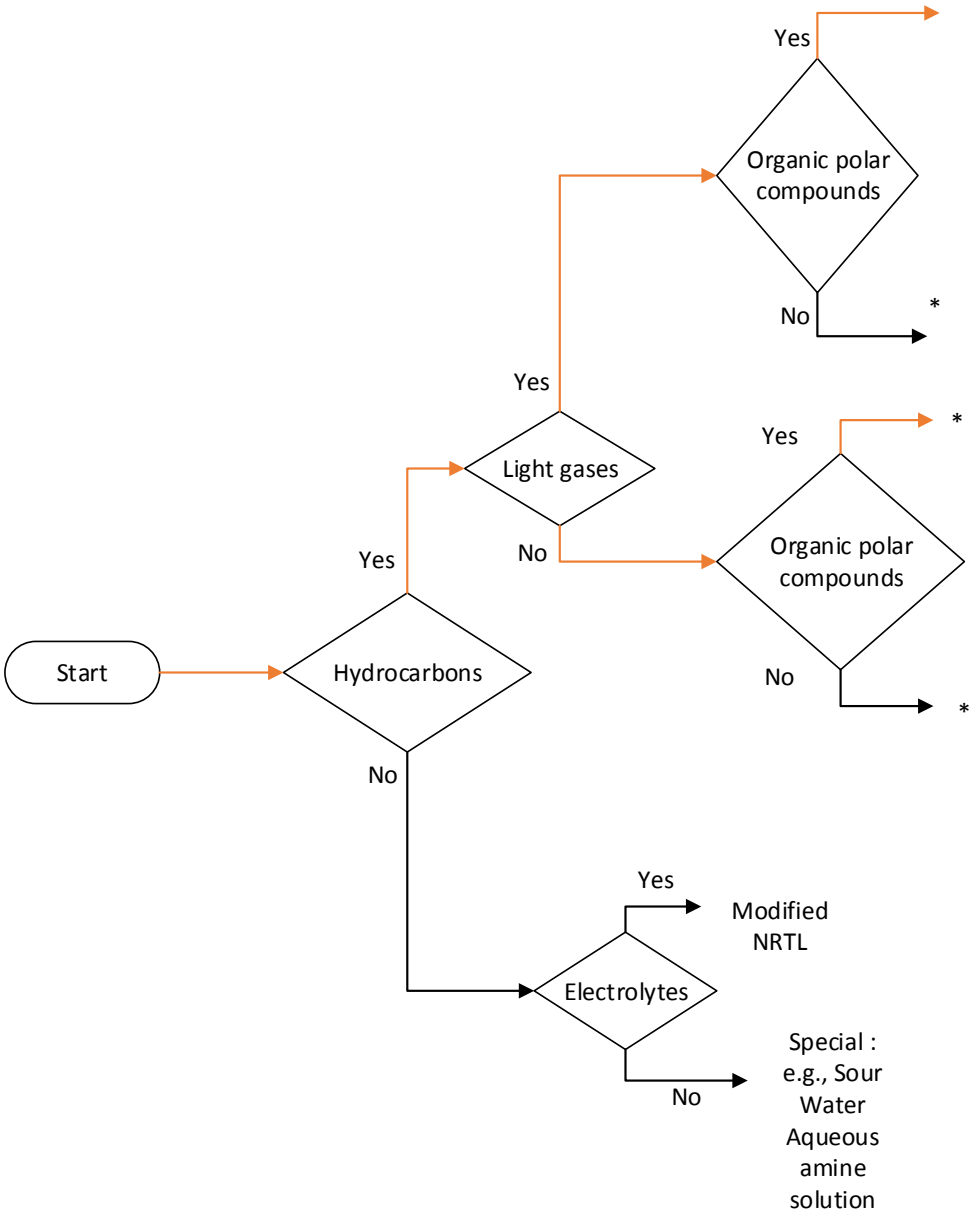

Figure D.9 Bob Seader method guide for polar compounds (*Seider et al.*, 2004)

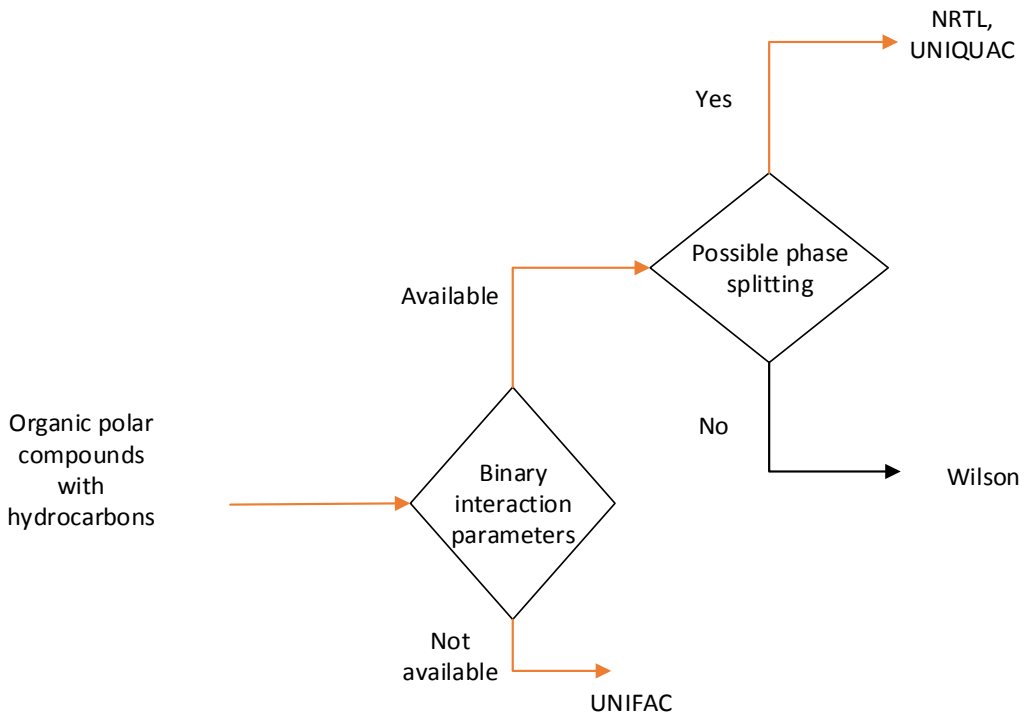

Figure D.10 Bob Seader method guide for polar compounds continue (*Seider et al.*, 2004)

Appendix E Sensitivity analysis

E.1. Process model for feed 2 (Fractionation)

E.1.1. Distillation column (T101)

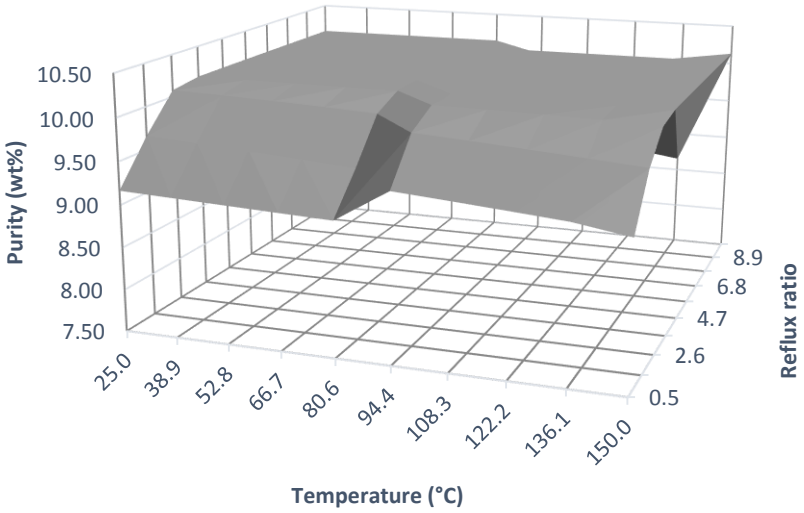

Figure E.1 Effect of feed temperature on the distillate purity of *dl*-limonene for different molar reflux ratios

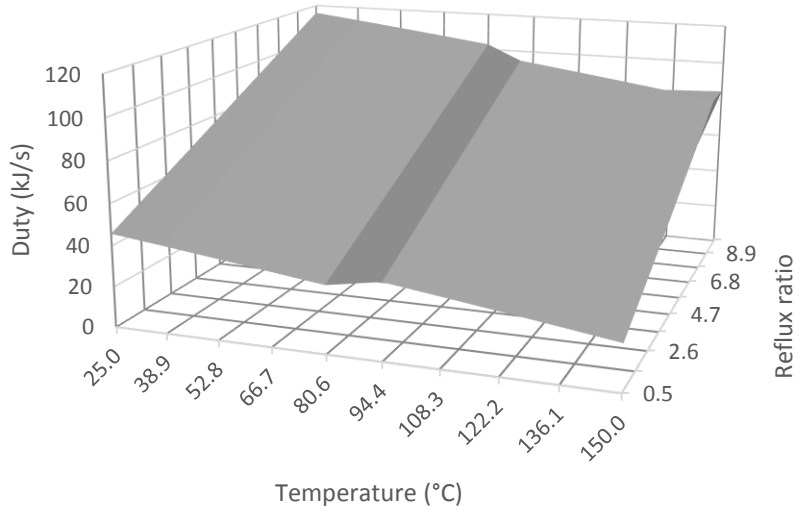

Figure E.2 Effect of feed temperature on the distillation column reboiler duty for different molar reflux ratios

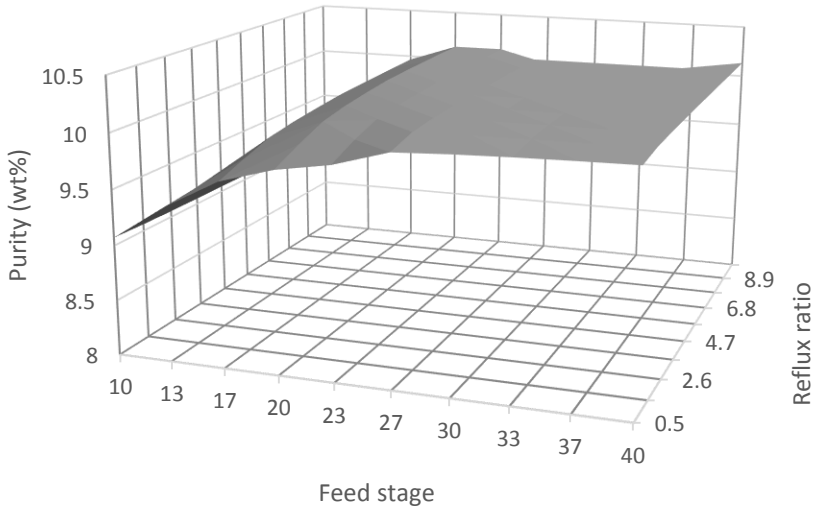

Figure E.3 Effect of feed stage on *dl*-limonene purity for different molar reflux ratios

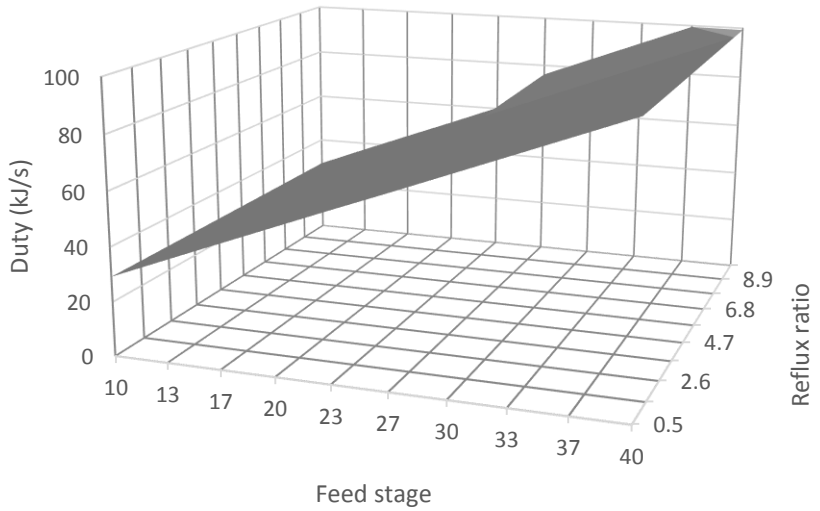

Figure E.4 Effect of feed stage on the distillation column reboiler duty for different molar reflux ratios

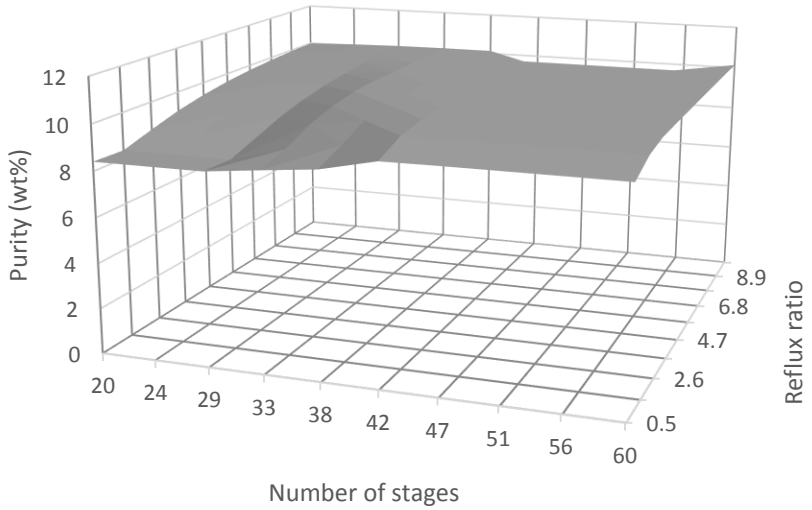

Figure E.5 Effect of number of stages on the distillate purity of *dl*-limonene for different molar reflux ratios

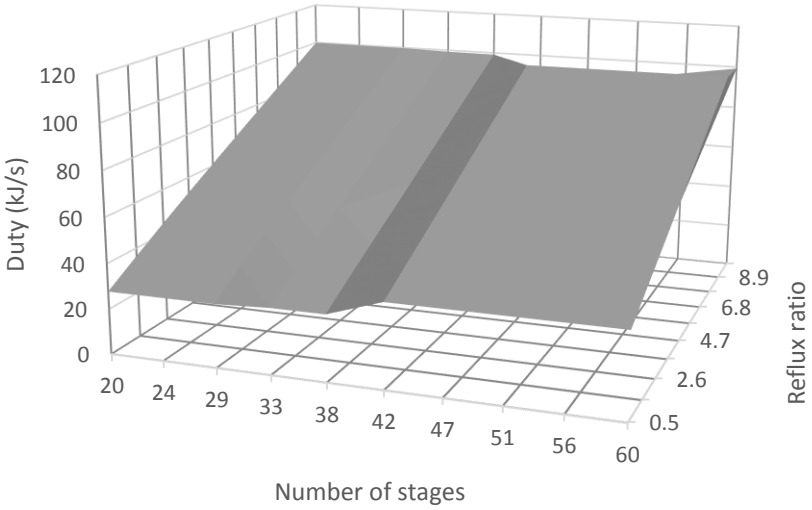

Figure E.6 Effect of number of stages on the distillation column reboiler duty for different molar reflux ratios

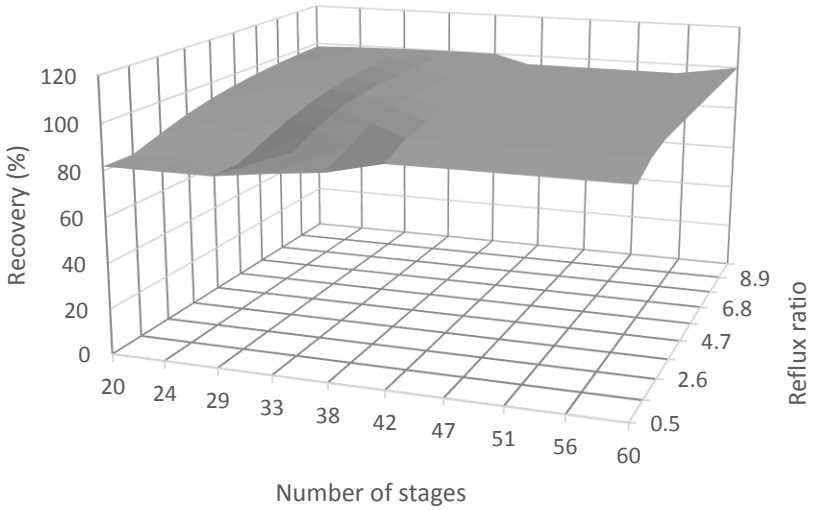

Figure E.7 Effect of number of stages on *dl*-limonene recovery for different molar reflux ratios

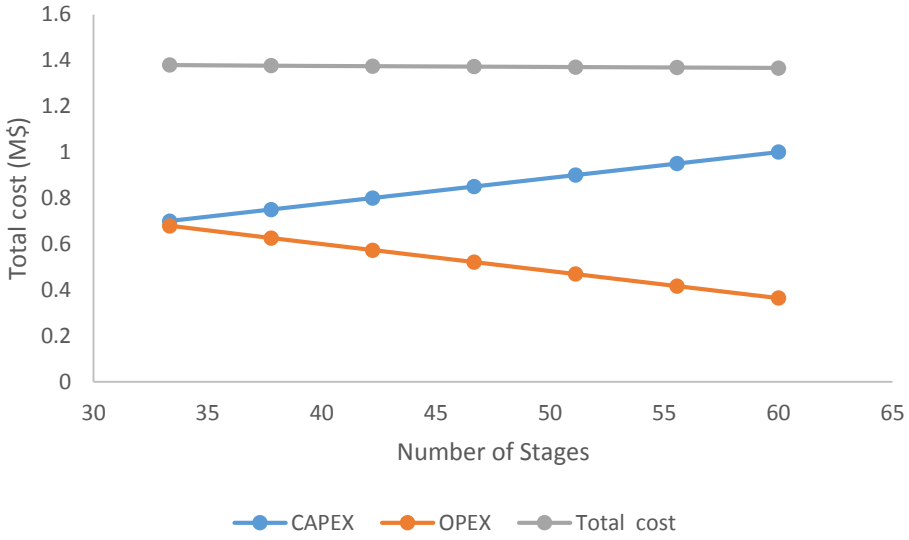

Figure E.8 Optimal number of stages for distillation column T101 operation

E.1.2. Distillation column (T102)

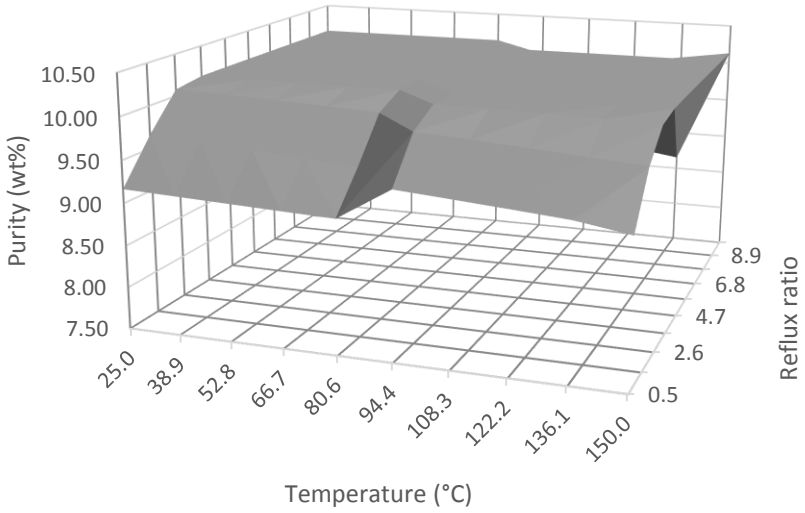

Figure E.9 Effect of feed temperature on the distillate purity of *dl*-limonene for different molar reflux ratios

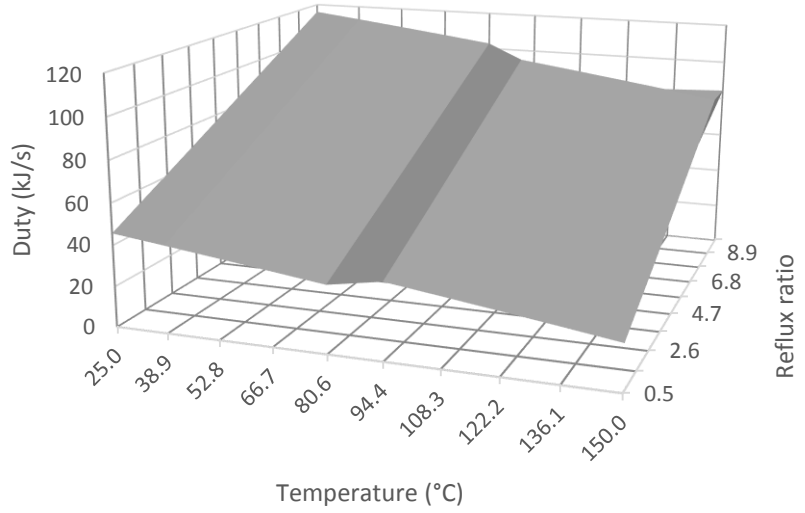

Figure E.10 Effect of feed temperature on the distillation column reboiler duty for different molar reflux ratios

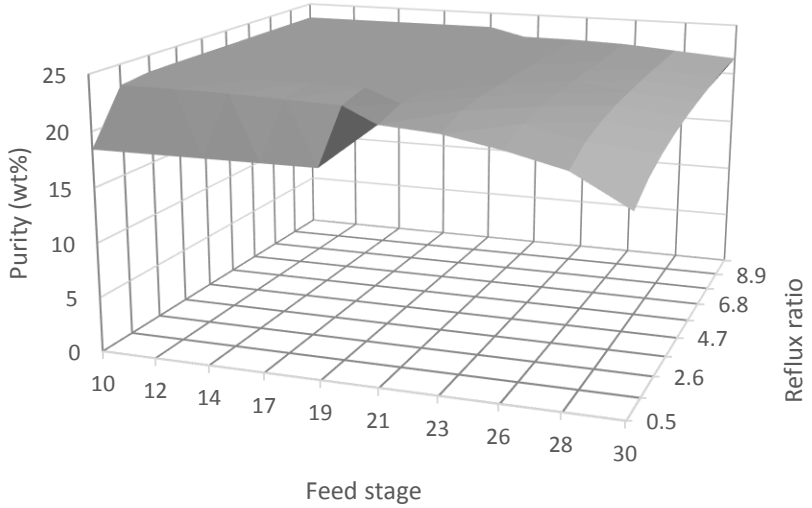

Figure E.11 Effect of feed stage on *dl*-limonene purity for different molar reflux ratios

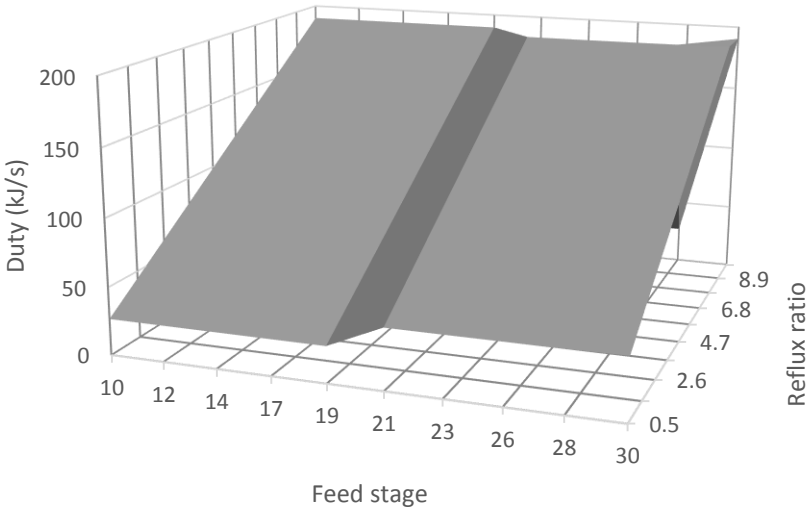

Figure E.12 Effect of feed stage on the distillation column reboiler duty for different molar reflux ratios

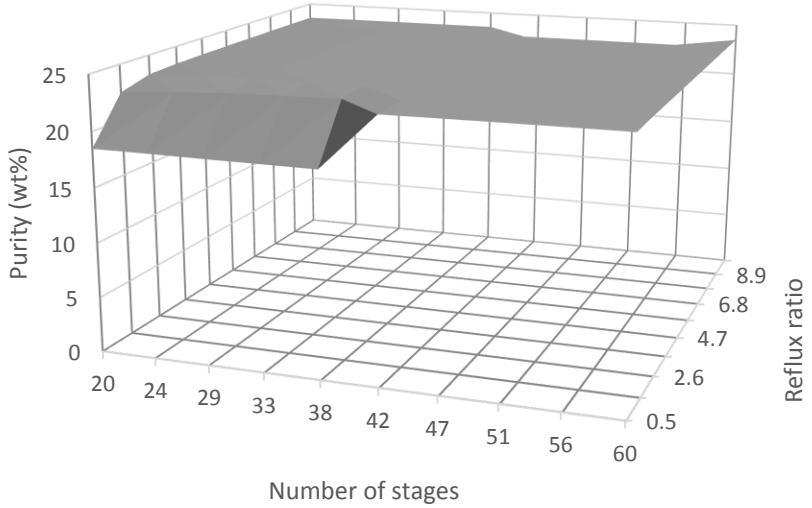

Figure E.13 Effect of number of stages on the distillate purity of *dl*-limonene for different molar reflux ratios

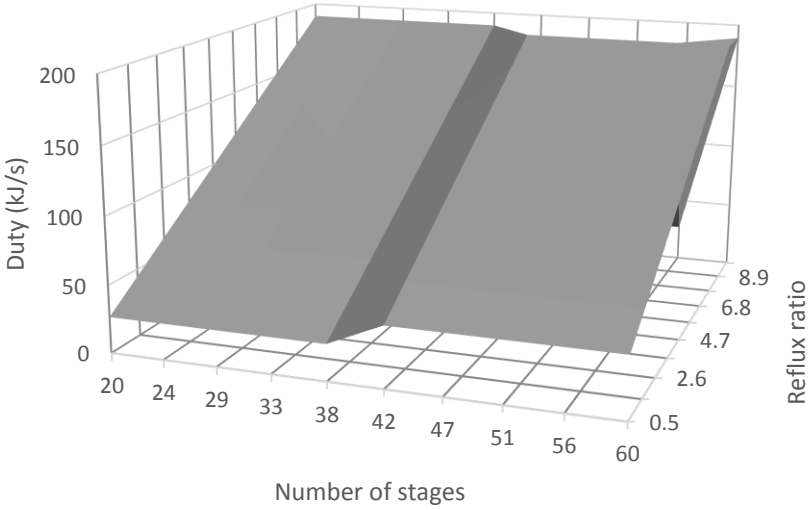

Figure E.14 Effect of number of stages on the distillation column reboiler duty for different molar reflux ratios

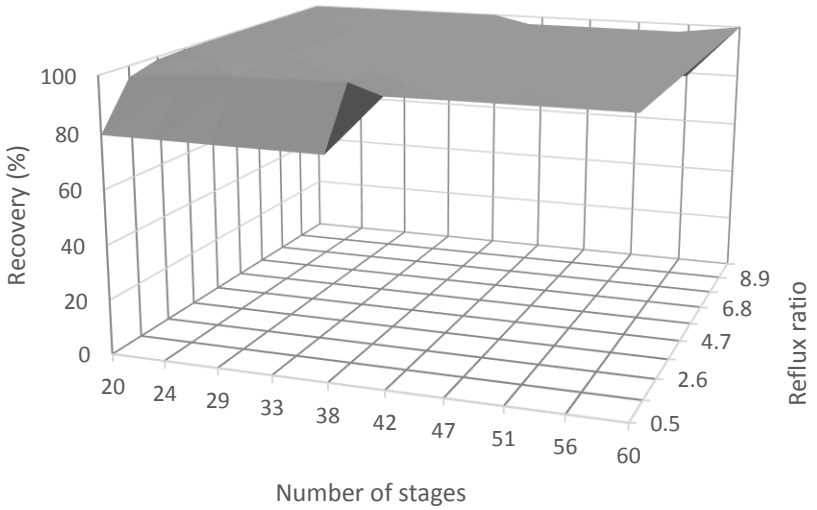

Figure E.15 Effect of number of stages on *dl*-limonene recovery for different molar reflux ratios

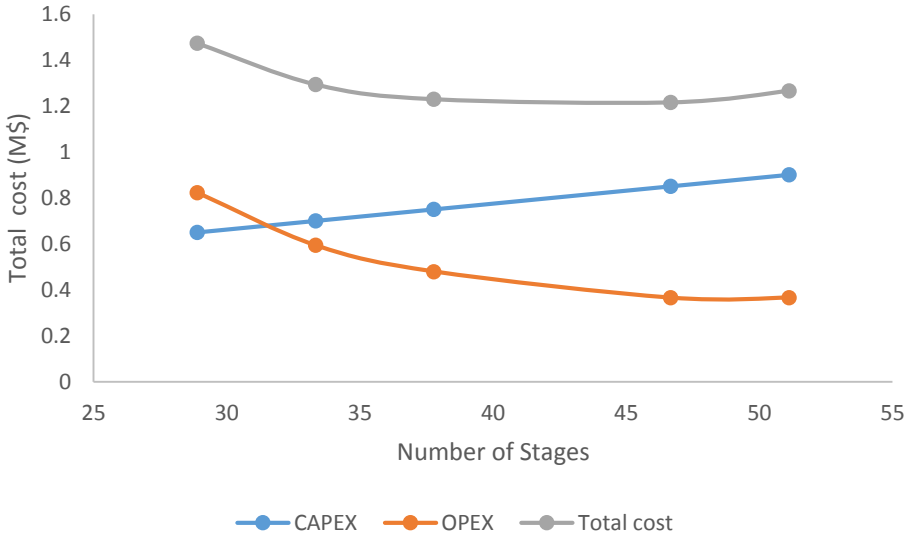

Figure E.16 Optimal number of stages for distillation column T102 operation

E.2. Triethylene glycol

E.2.1. Azeotropic distillation column

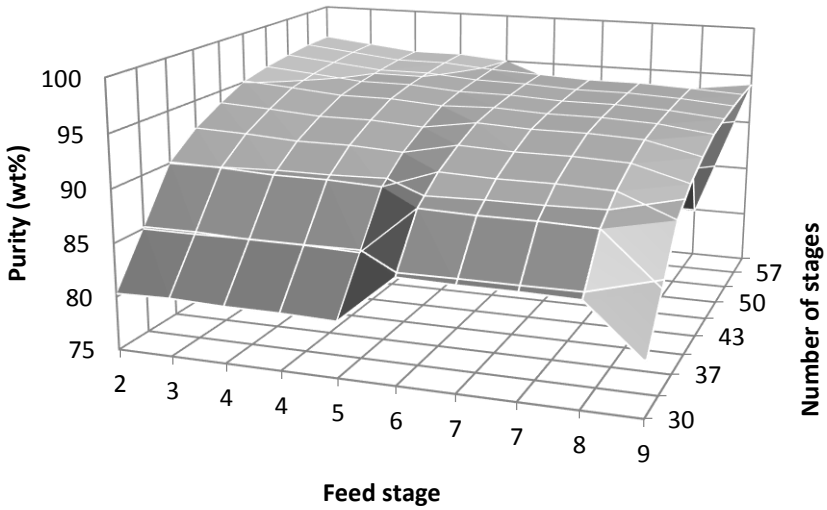

Figure E.17 Effect of entrainer feed stage on purity of *dl*-limonene for different number of theoretical stages

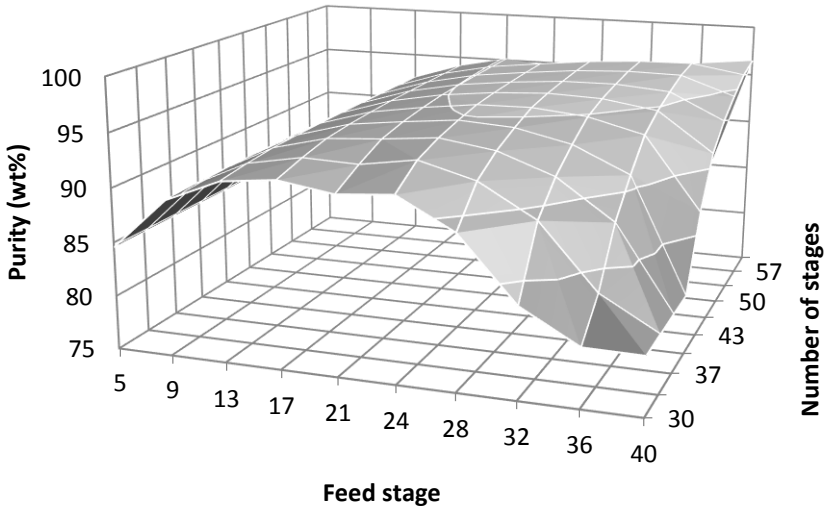

Figure E.18 Effect of *dl*-limonene fraction feed stage on purity of *dl*-limonene for different number of theoretical stages

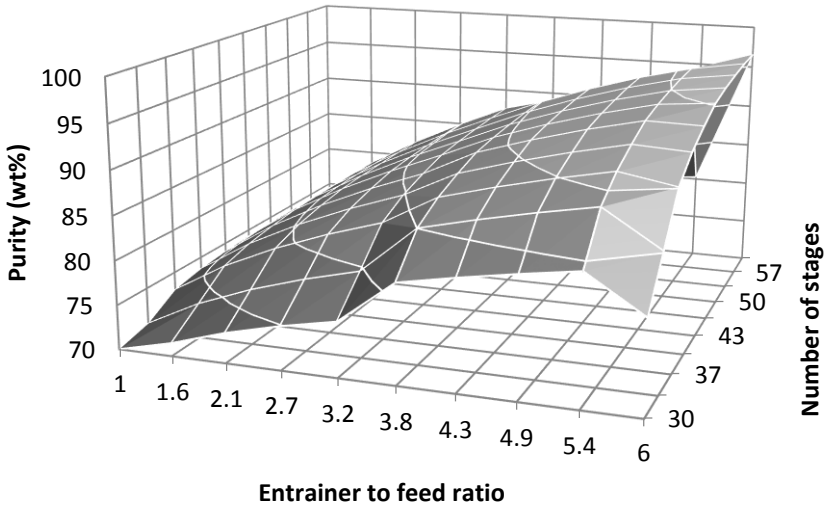

Figure E.19 Effect of E/F on purity of *dl*-limonene for different number of theoretical stages

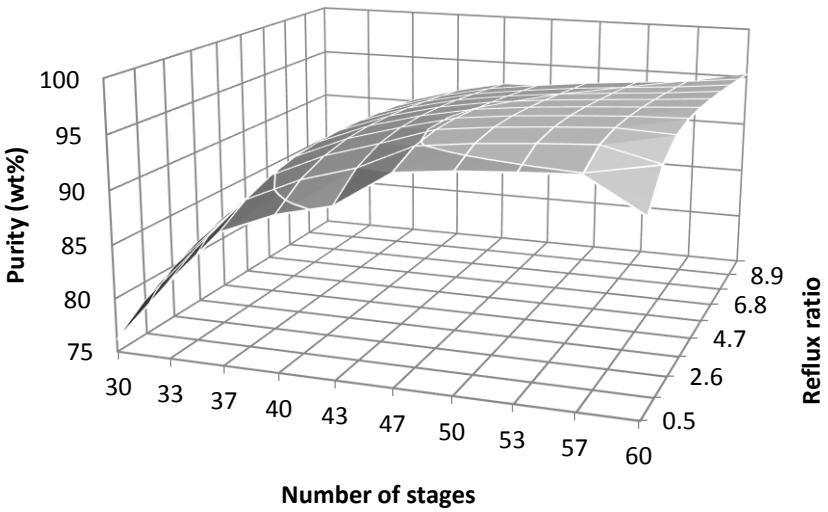

Figure E.20 The effect of number of stages on purity of *dl*-limonene for different reflux ratios

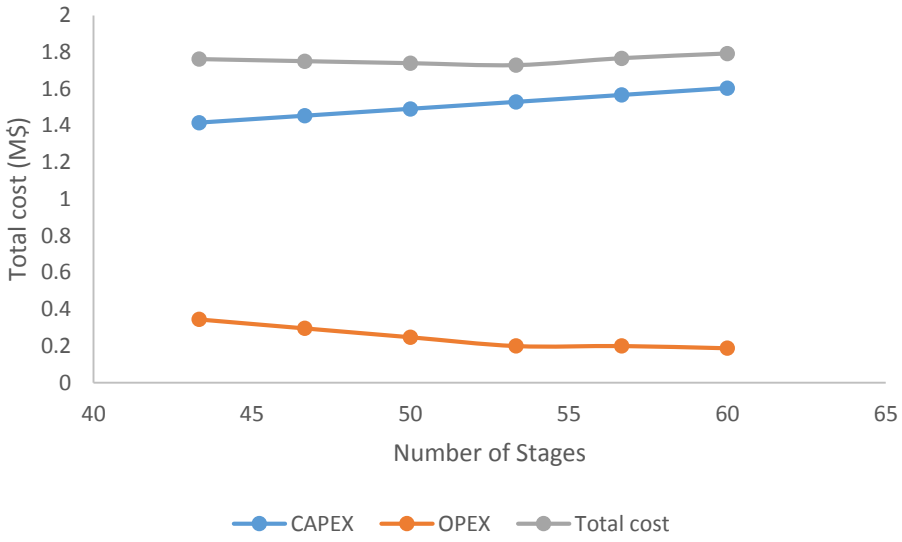

Figure E.21 Optimal number of stages for distillation column T102 operation

E.2.2. Entrainer recovery column

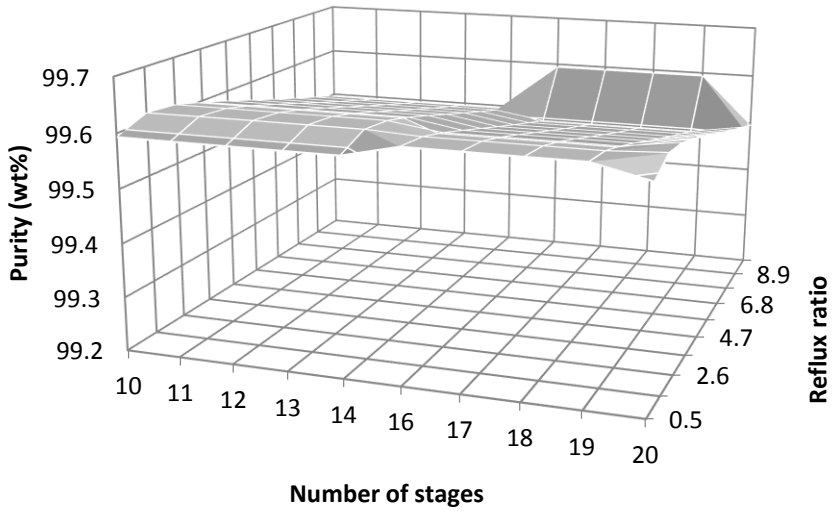

Figure E.22 The effect of number of stages on purity of the entrainer for different reflux ratios

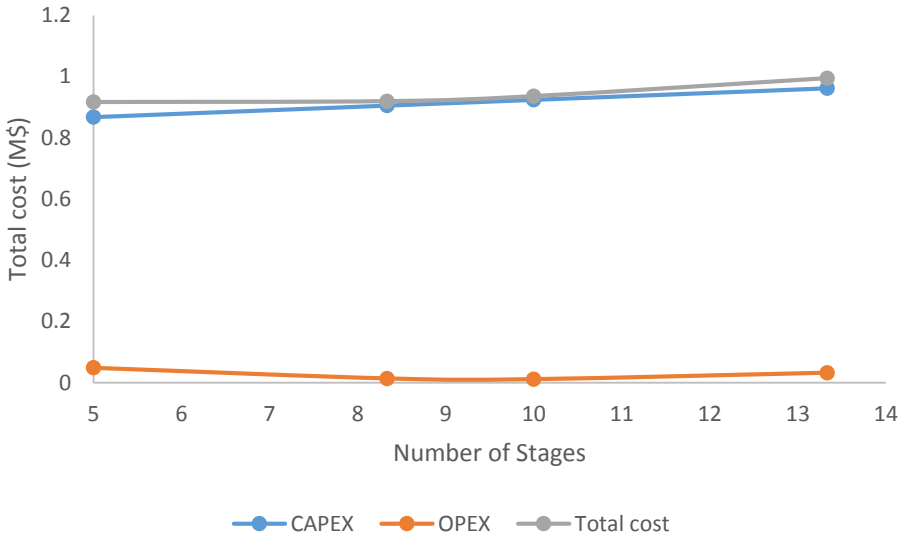

Figure E.23 Optimal number of stages for distillation column T103 operation

E.3. 4-Formylmorpholine

E.3.1. Azeotropic distillation column

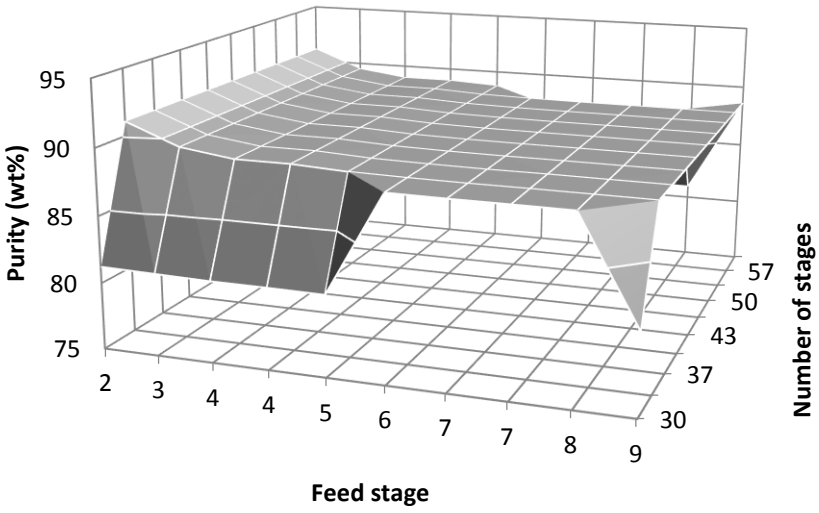

Figure E.24 Effect of entrainer feed stage on purity of *dl*-limonene for different number of theoretical stages

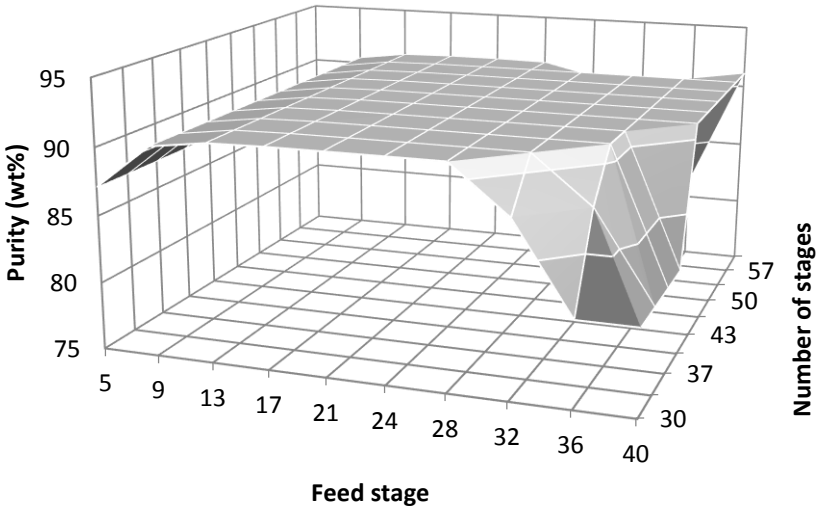

Figure E.25 Effect of *dl*-limonene fraction feed stage on purity of *dl*-limonene for different number of theoretical stages

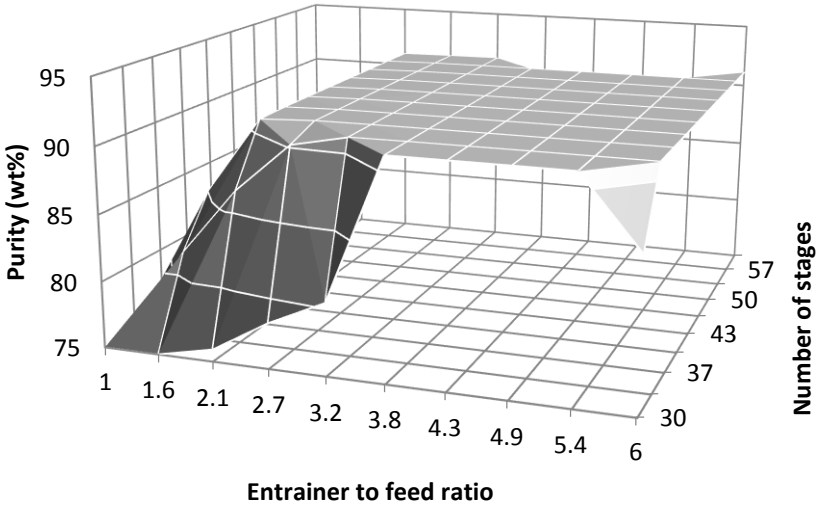

Figure E.26 Effect of E/F on purity of *dl*-limonene for different number of theoretical stages

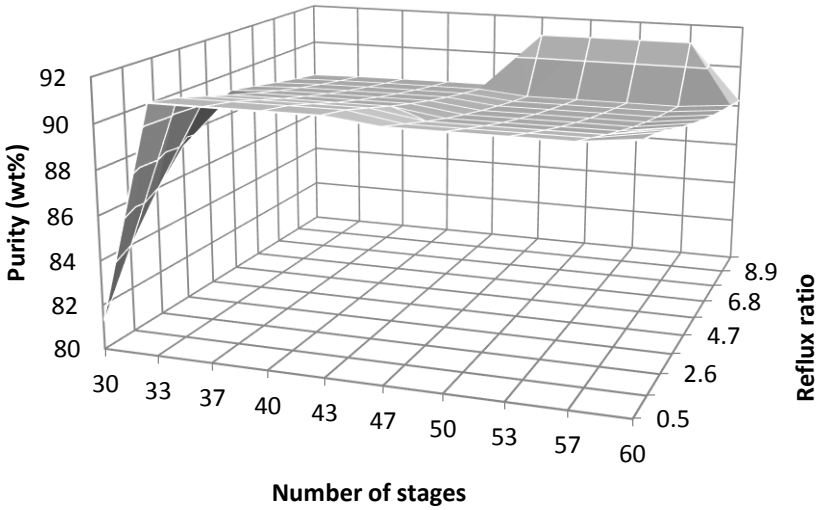

Figure E.27 The effect of number of stages on purity of *dl*-limonene for different reflux ratios

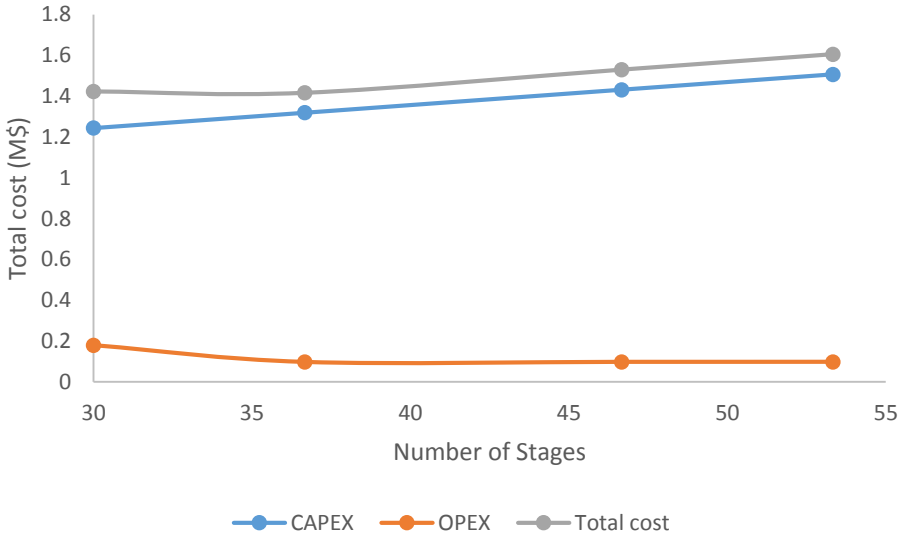

Figure E.28 Optimal number of stages for distillation column T102 operation

E.3.2. Entrainer recovery column

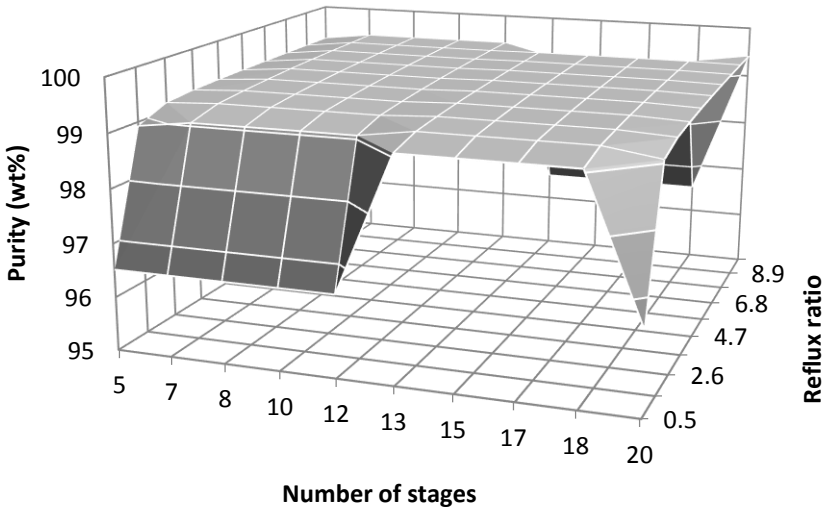

Figure E.29 The effect of number of stages on purity of the entrainer for different reflux ratios

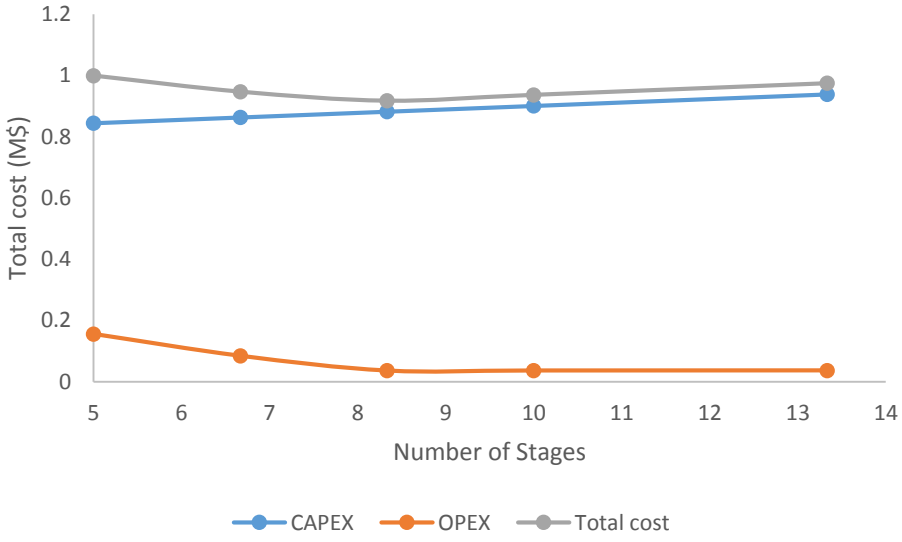

Figure E.30 Optimal number of stages for distillation column T103 operation

E.4. Quinoline

E.4.1. Extractive distillation

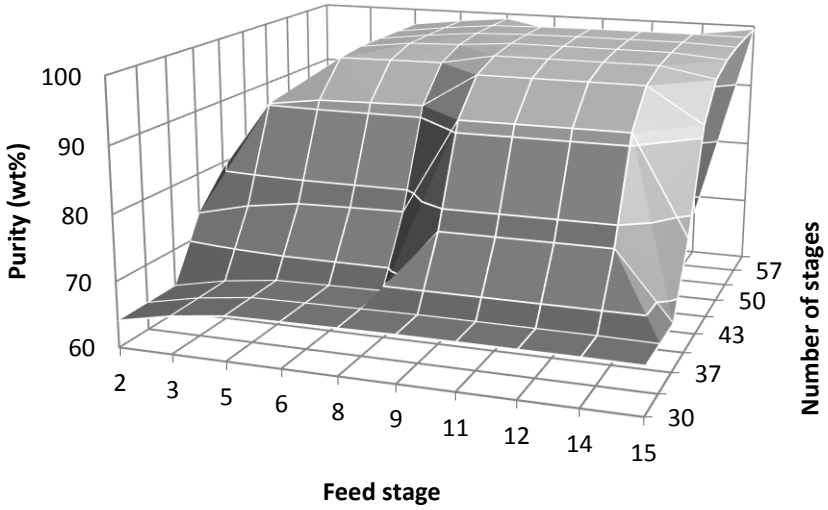

Figure E.31 Effect of entrainer feed stage on purity of *dl*-limonene for different number of theoretical stages

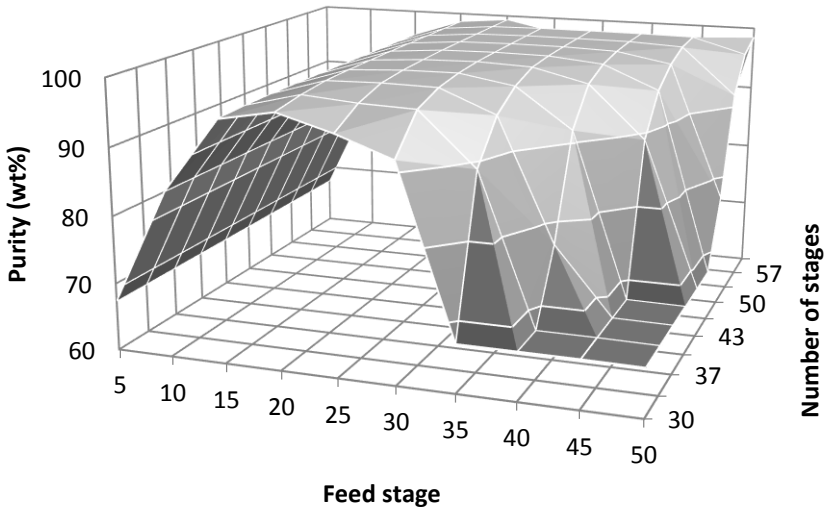

Figure E.32 Effect of *dl*-limonene fraction feed stage on purity of *dl*-limonene for different number of theoretical stages

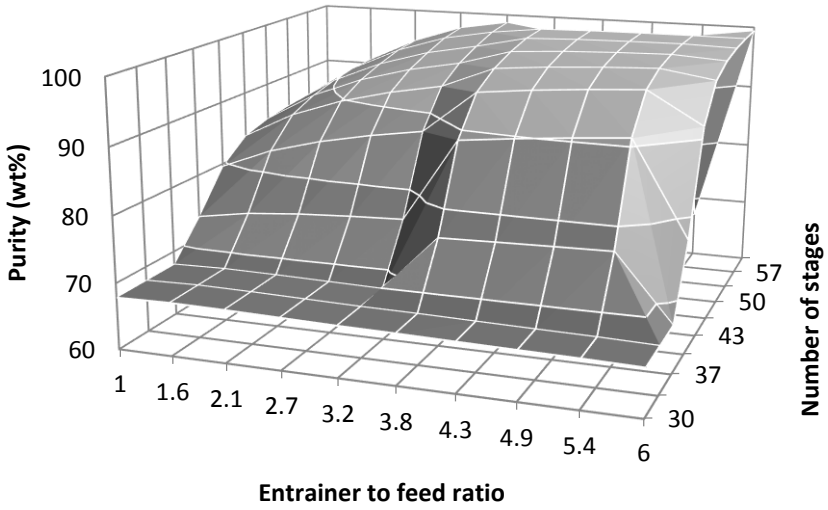

Figure E.33 Effect of E/F on purity of *dl*-limonene for different number of theoretical stages

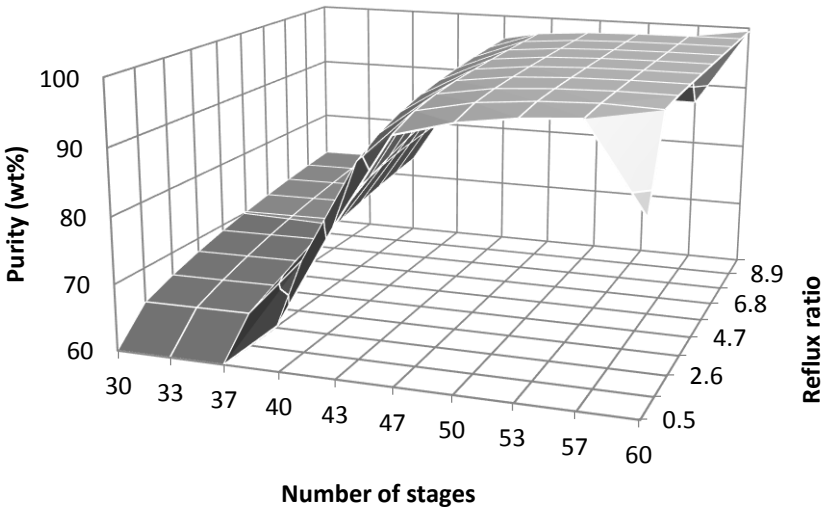

Figure E.34 The effect of number of stages on purity of *dl*-limonene for different reflux ratios

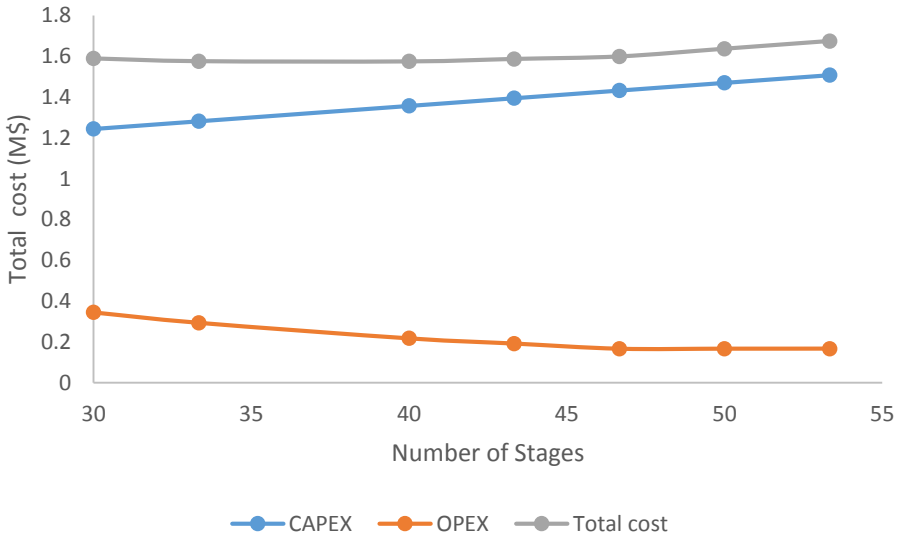

Figure E.35 Optimal number of stages for distillation column T103 operation

E.4.2. Entrainer recovery column

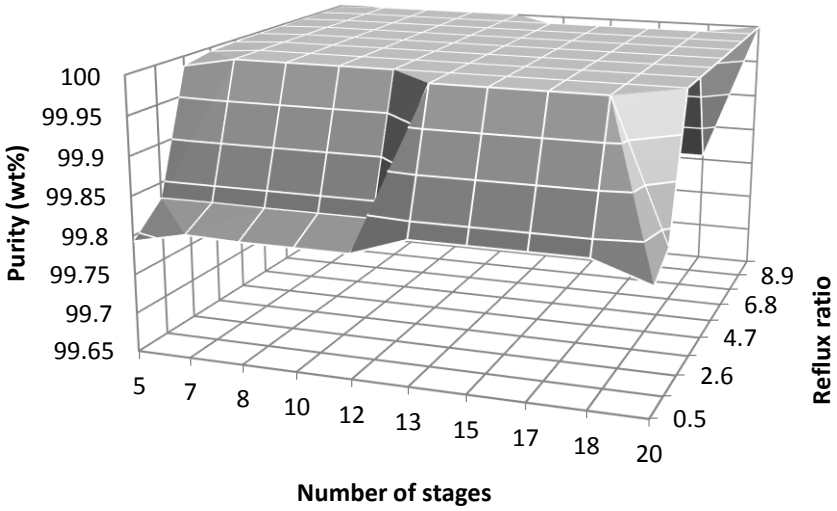

Figure E.36 The effect of number of stages on purity of the entrainer for different reflux ratios

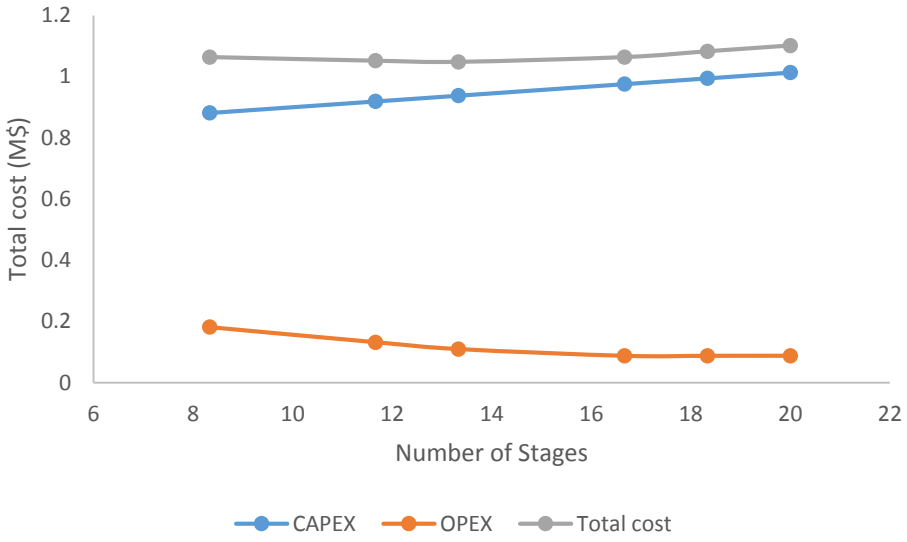

Figure E.37 Optimal number of stages for distillation column T103 operation

E.5. Triethylene glycol dimethyl ether

E.5.1. Extractive distillation

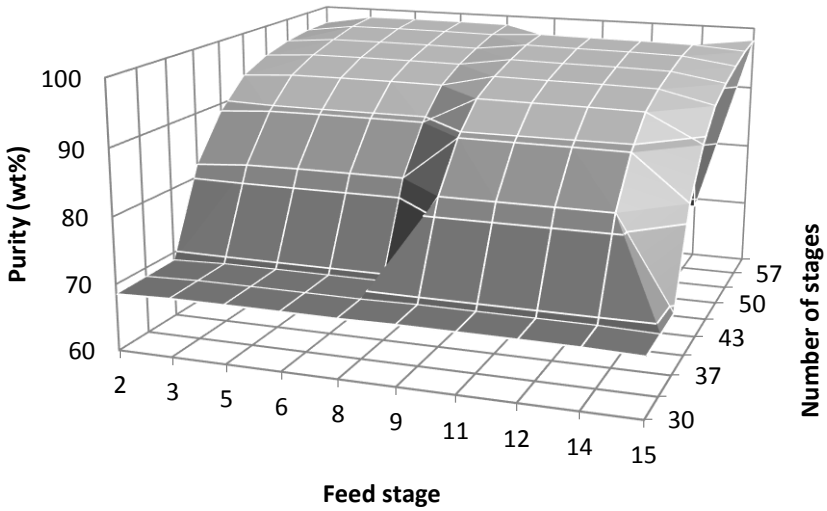

Figure E.38 Effect of entrainer feed stage on purity of *dl*-limonene for different number of theoretical stages

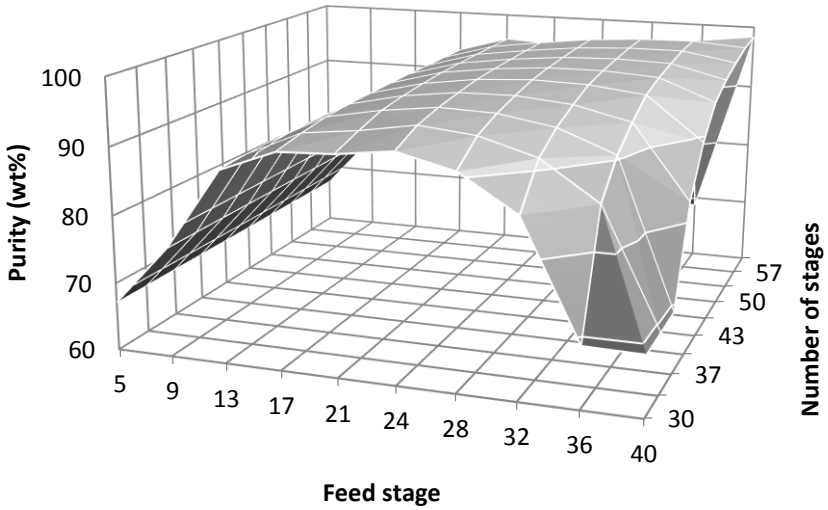

Figure E.39 Effect of *dl*-limonene fraction feed stage on purity of *dl*-limonene for different number of theoretical stages

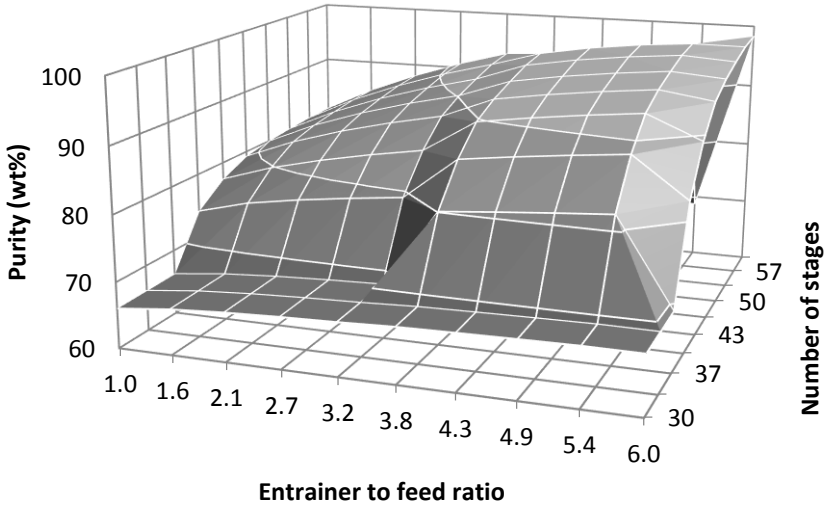

Figure E.40 Effect of E/F on purity of *dl*-limonene for different number of theoretical stages

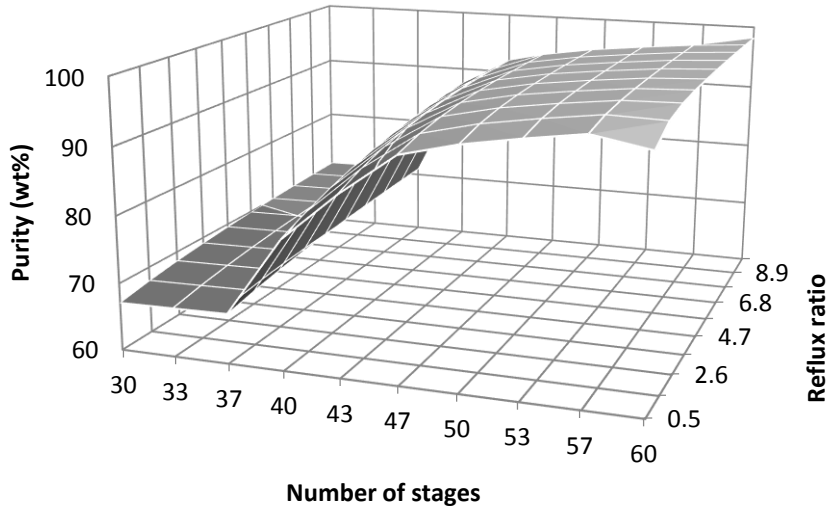

Figure E.41 The effect of number of stages on purity of *dl*-limonene for different reflux ratios

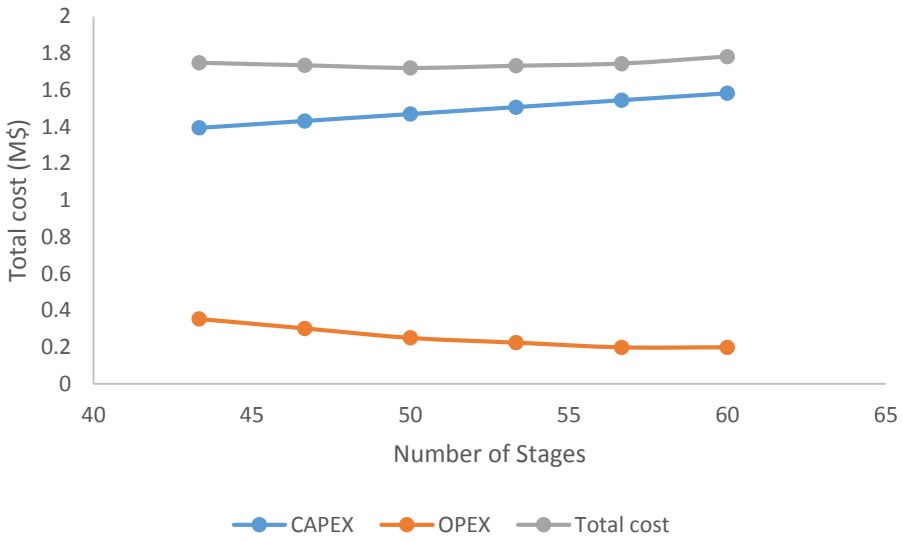

Figure E.42 Optimal number of stages for distillation column T102 operation

E.5.2. Entrainer recovery column

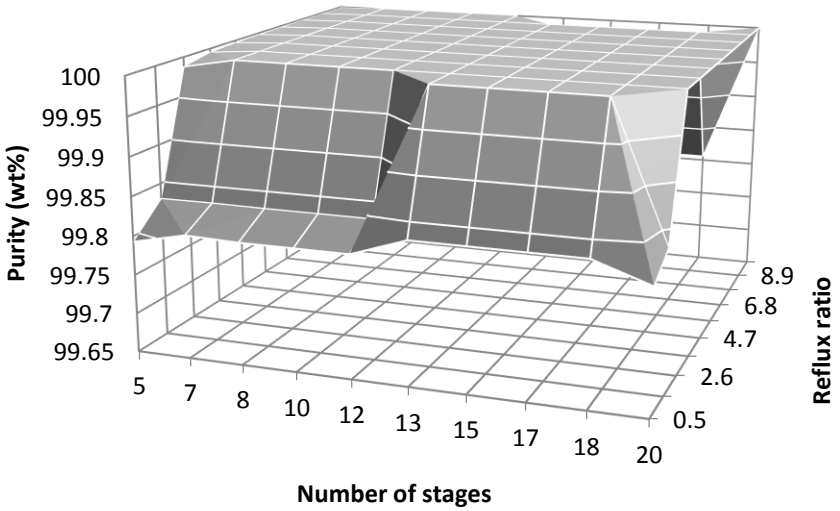

Figure E.43 The effect of number of stages on purity of entrainer for different reflux ratios

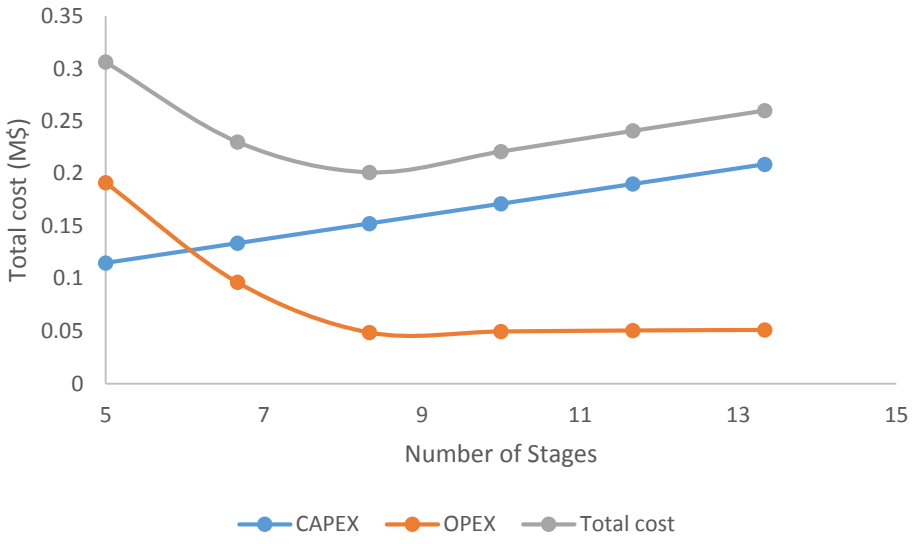

Figure E.44 Optimal number of stages for distillation column T103 operation

E.6. n-Methyl-2-pyrrolidone

E.6.1. Azeotropic distillation

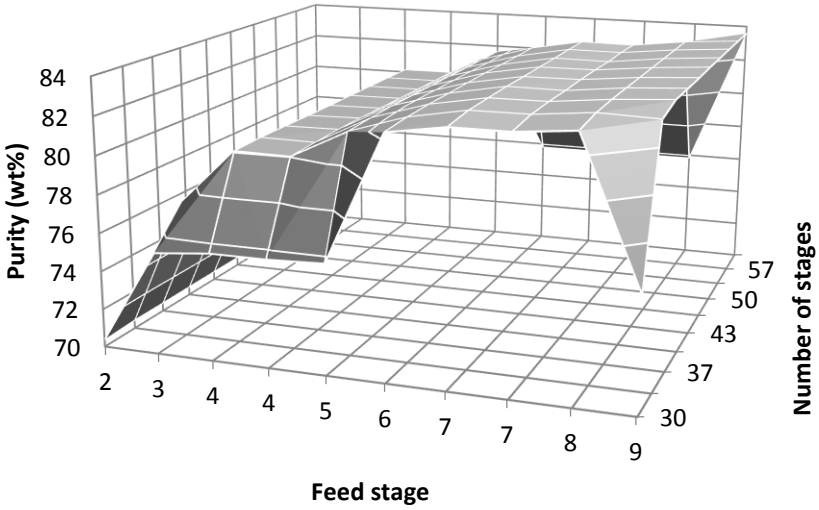

Figure E.45 Effect of entrainer feed stage on purity of *dl*-limonene for different number of theoretical stages

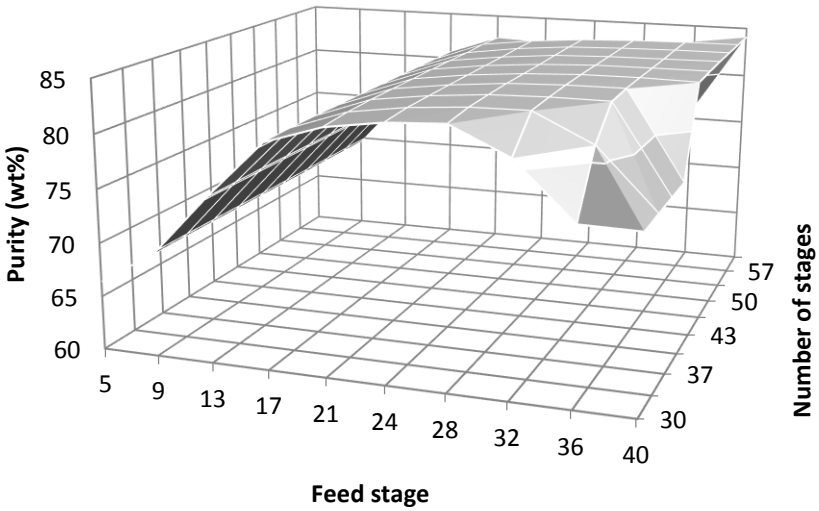

Figure E.46 Effect of *dl*-limonene fraction feed stage on purity of *dl*-limonene for different number of theoretical stages

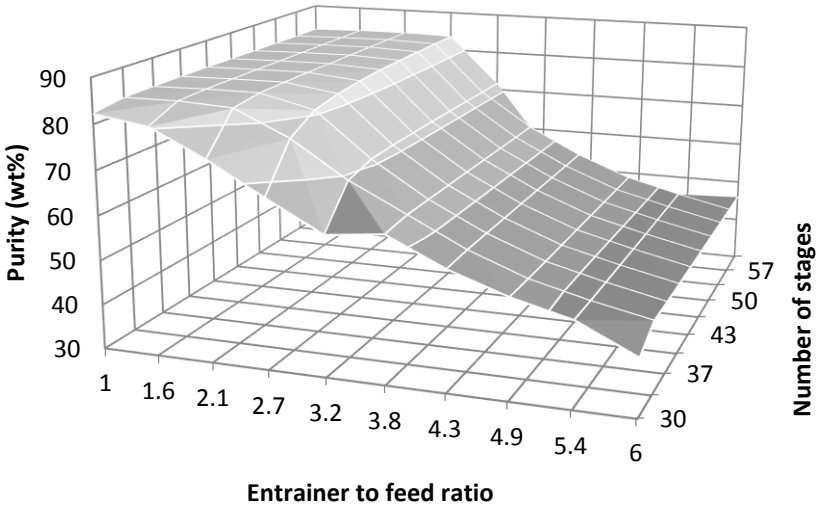

Figure E.47 Effect of E/F on purity of *dl*-limonene for different number of theoretical stages

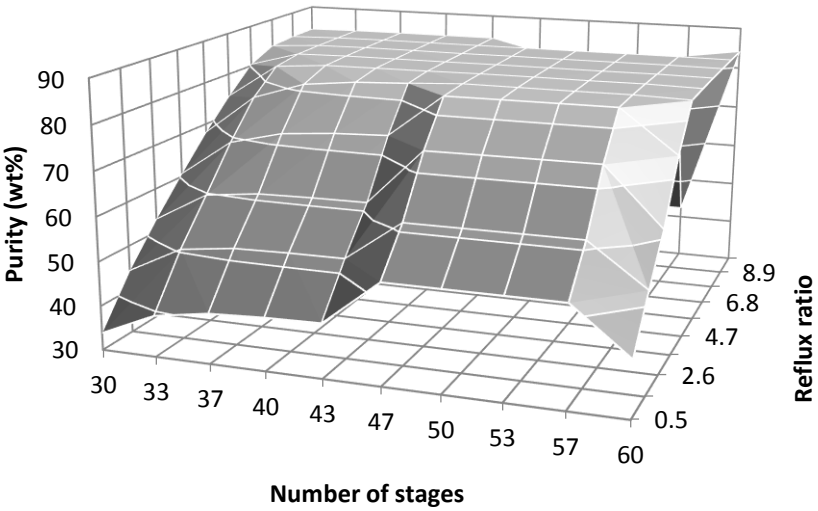

Figure E.48 The effect of number of stages on purity of *dl*-limonene for different reflux ratios

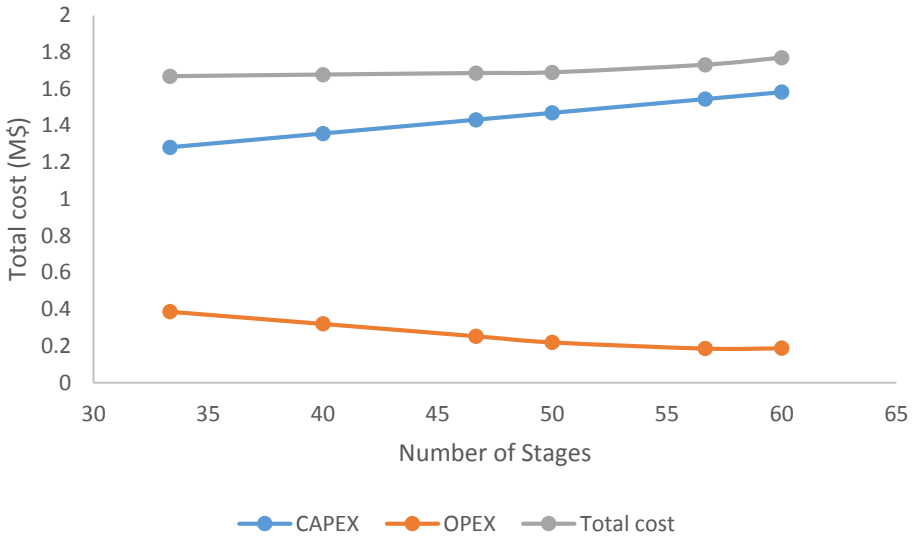

Figure E.49 Optimal number of stages for distillation column T102 operation

E.6.2. Water addition

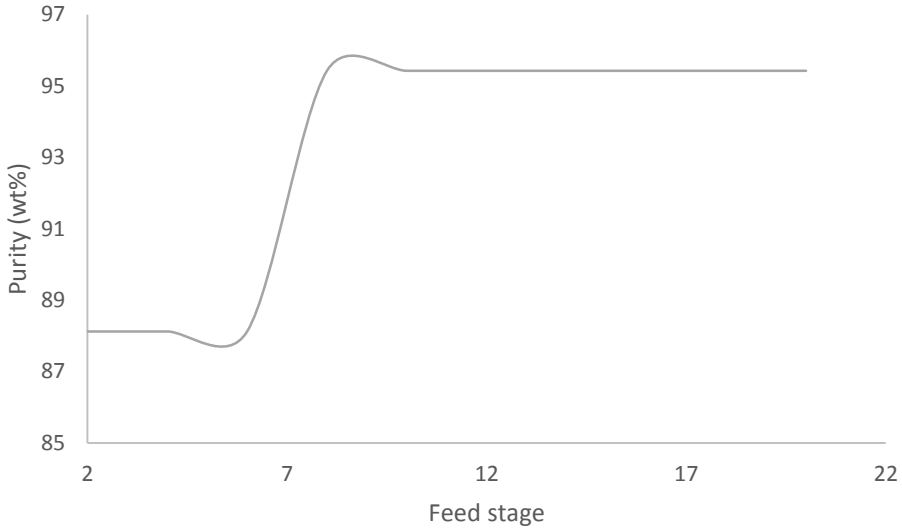

Figure E.50 Effect of water feed stage on purity of *dl*-limonene for 60 theoretical stages

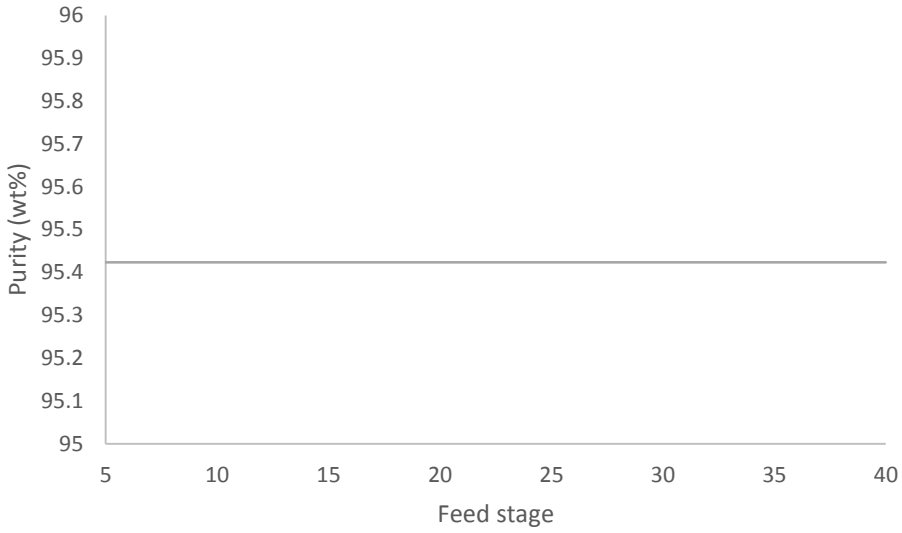

Figure E.51 Effect of *dl*-limonene fraction feed stage on purity of *dl*-limonene for 60 theoretical stages

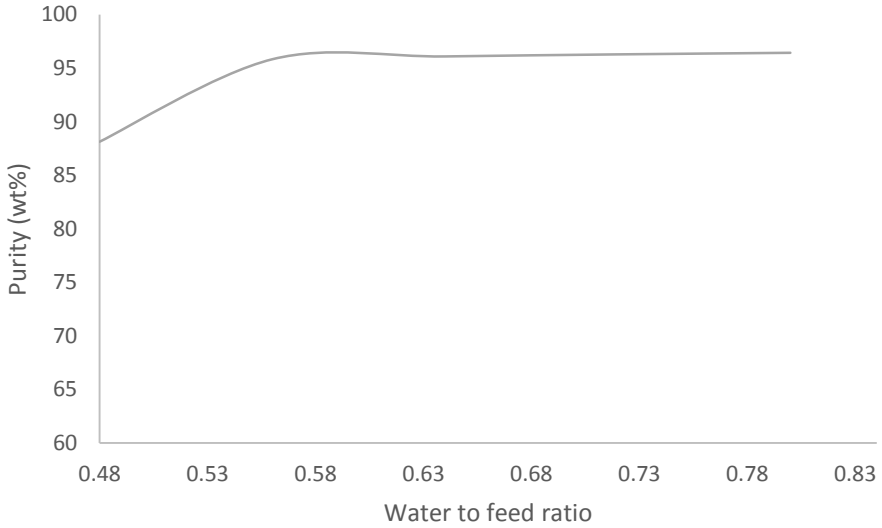

Figure E.52 Effect of water to feed ratio on purity of *dl*-limonene for 60 theoretical stages

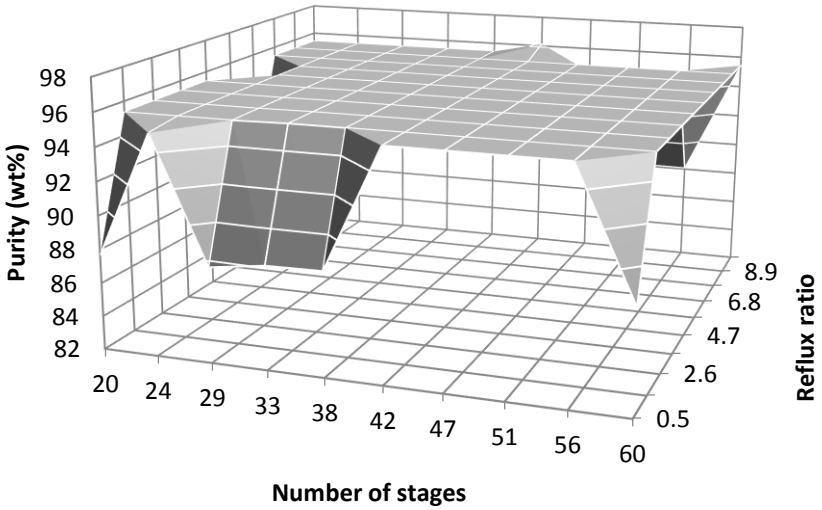

Figure E.53 The effect of number of stages on purity of *dl*-limonene for different reflux ratios

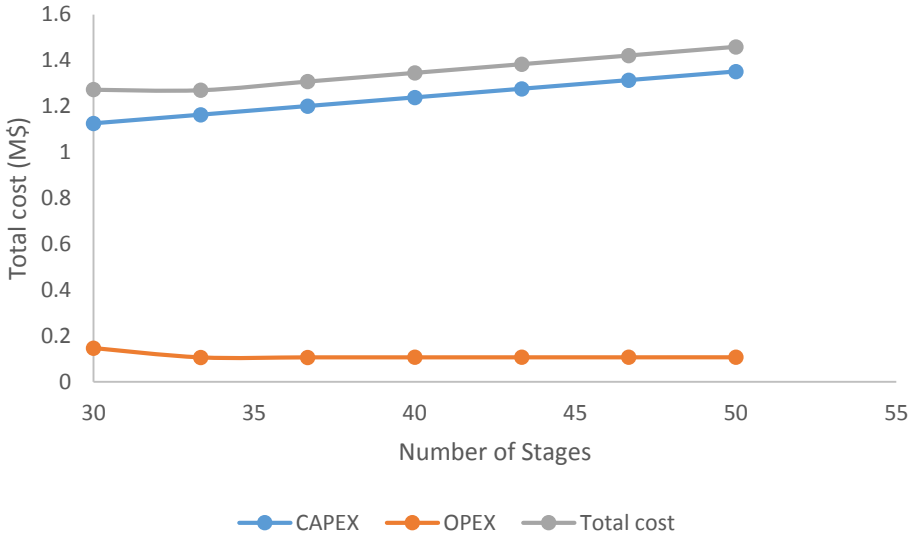

Figure E.54 Optimal number of stages for distillation column T103 operation

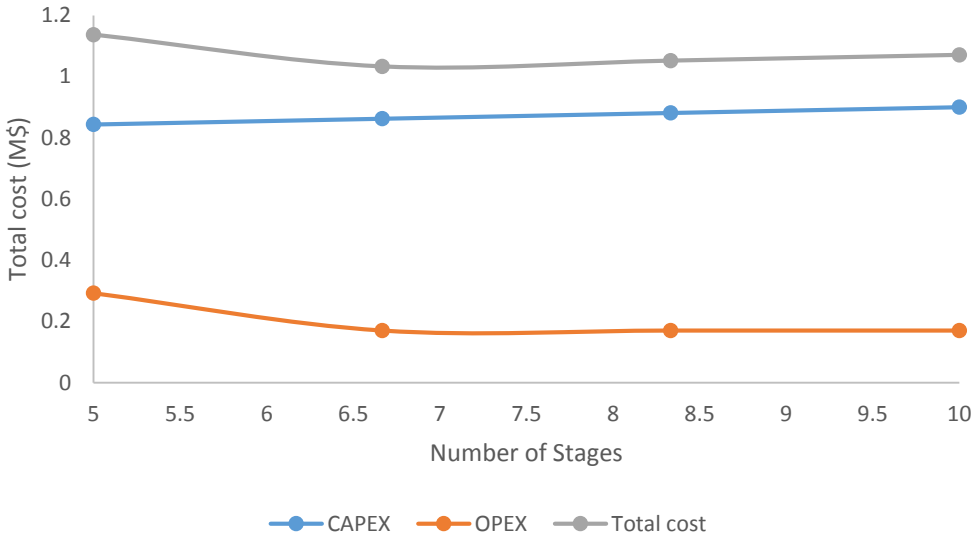

Figure E.55 Optimal number of stages for distillation column T104 operation

E.6.3. Entrainer recovery

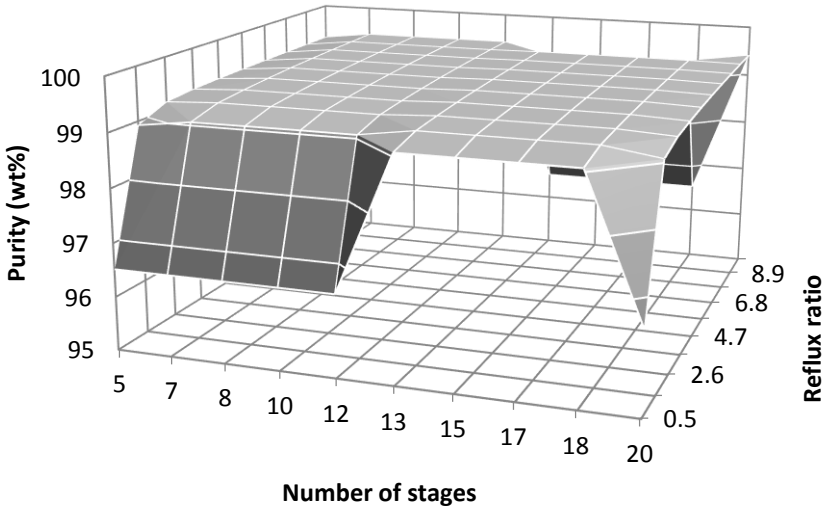

Figure E.56 The effect of number of stages on purity of entrainer for different reflux ratios

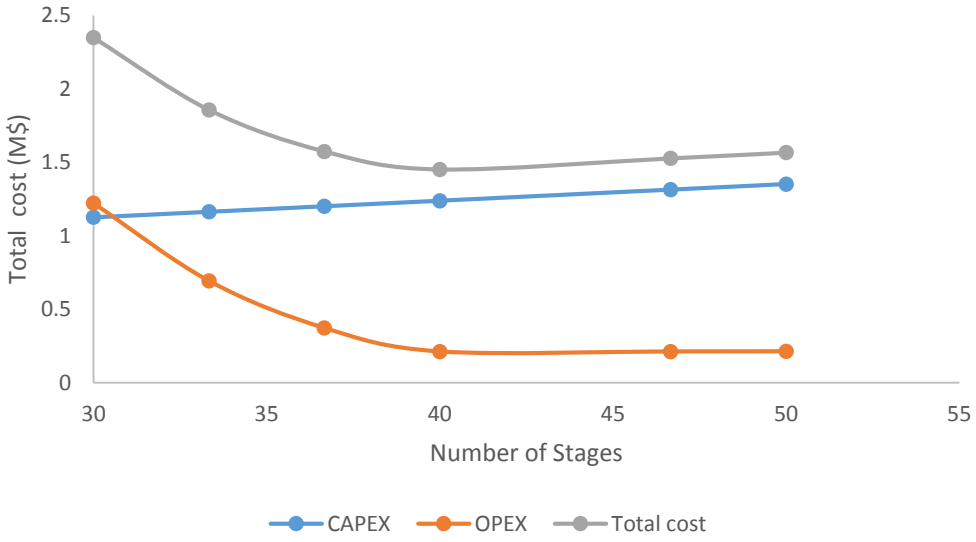

Figure E.57 Optimal number of stages for distillation column T105 operation

E.7. n,n-Dimethylformamide

E.7.1. Azeotropic distillation

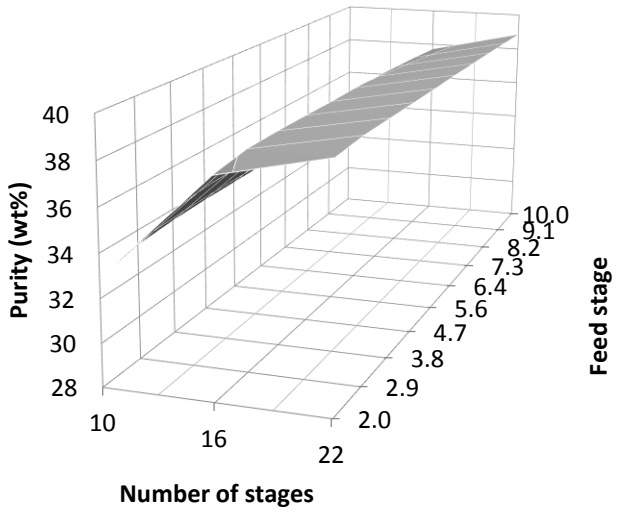

Figure E.58 Effect of entrainer feed stage on purity of *dl*-limonene for different number of theoretical stages

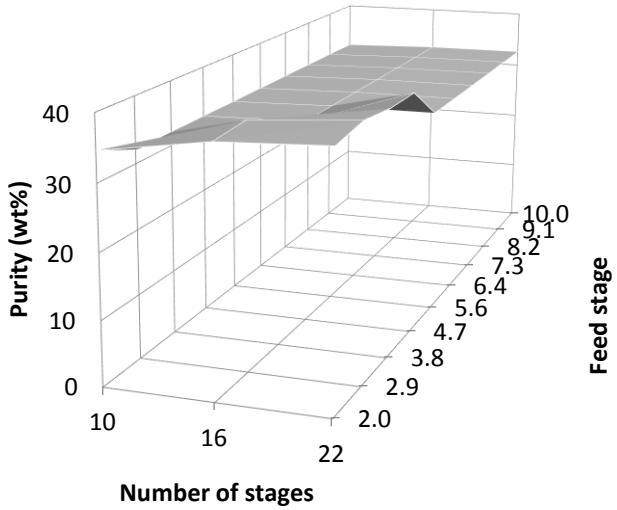

Figure E.59 Effect of *dl*-limonene fraction feed stage on purity of *dl*-limonene for different number of theoretical stages

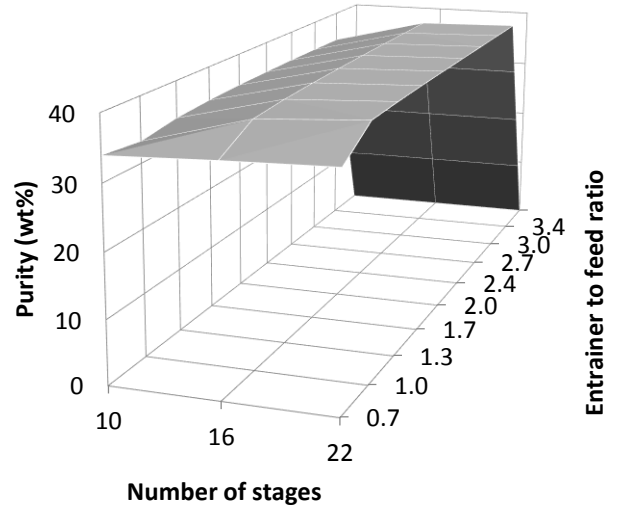

Figure E.60 Effect of E/F on purity of *dl*-limonene for different number of theoretical stages

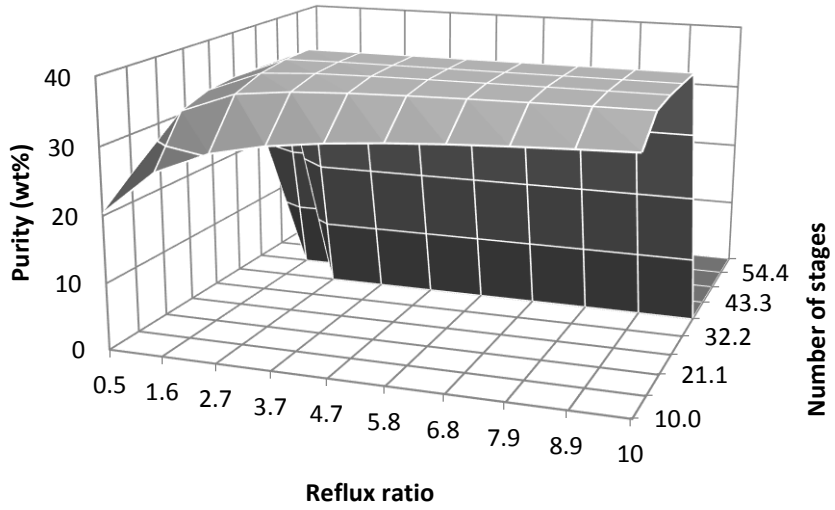

Figure E.61 The effect of number of stages on purity of *dl*-limonene for different reflux ratios

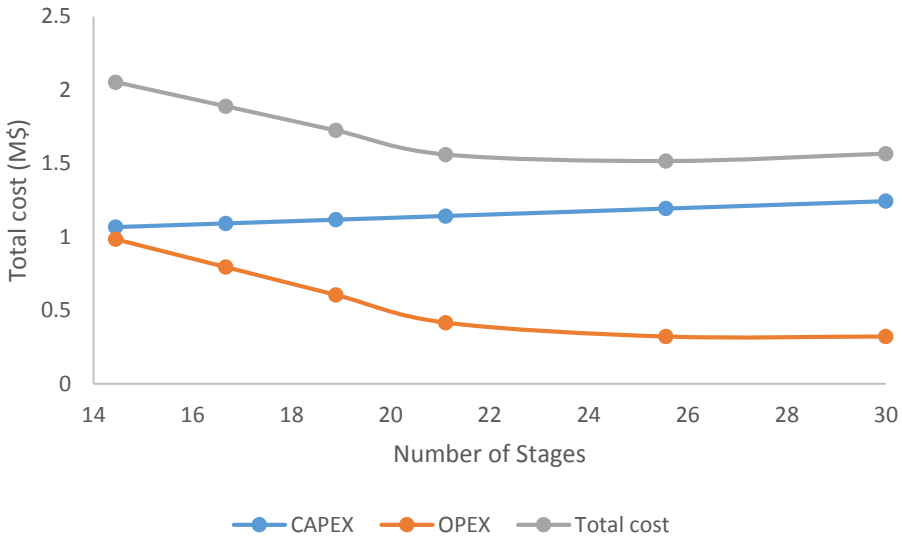

Figure E.62 Optimal number of stages for distillation column T102 operation

E.7.2. Water addition

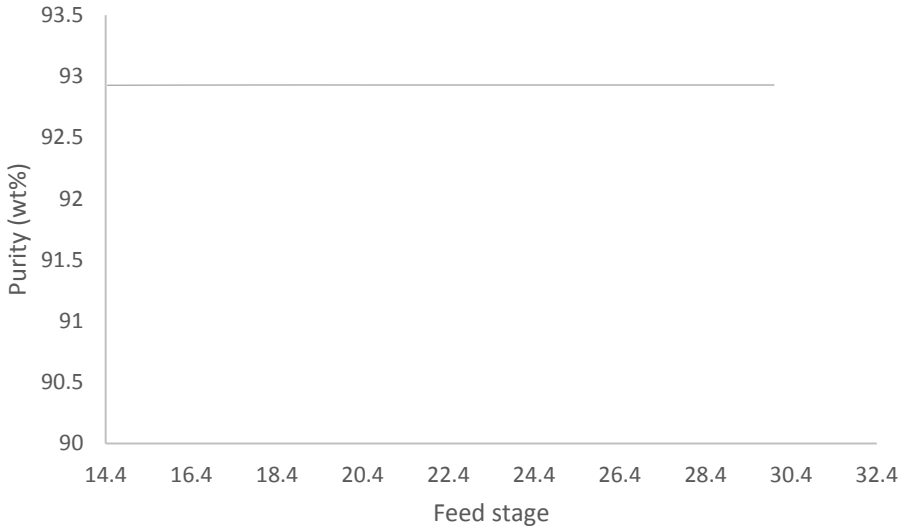

Figure E.63 Effect of water feed stage on purity of *dl*-limonene for 60 theoretical stages

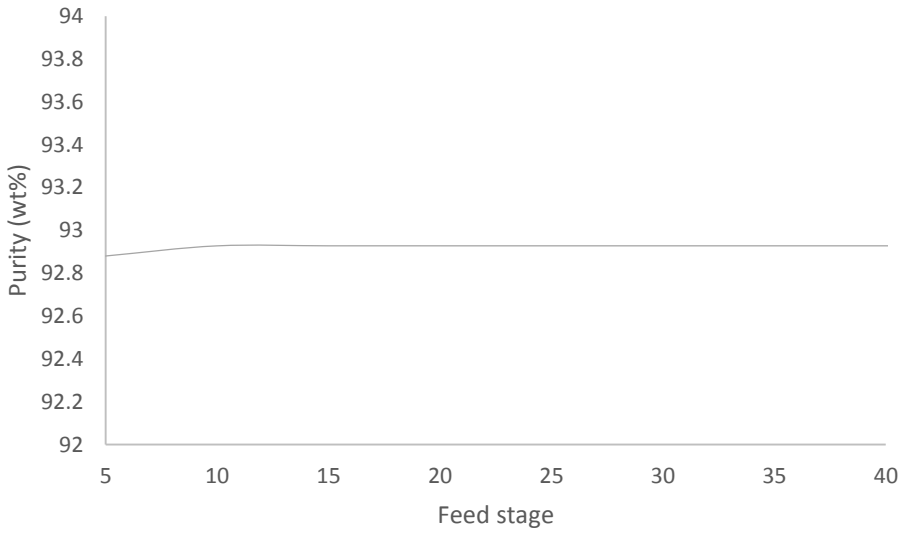

Figure E.64 Effect of *dl*-limonene fraction feed stage on purity of *dl*-limonene for 60 theoretical stages

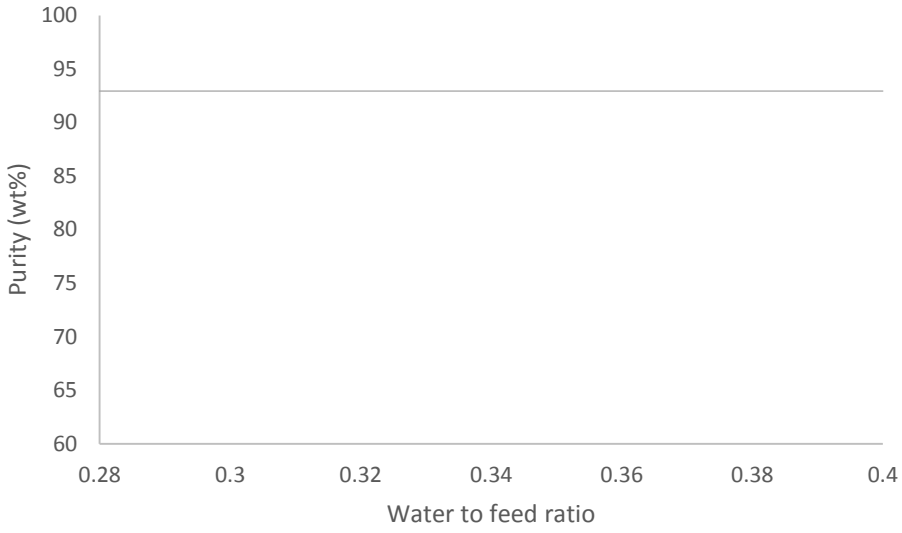

Figure E.65 Effect of water to feed ratio on purity of *dl*-limonene for 60 theoretical stages

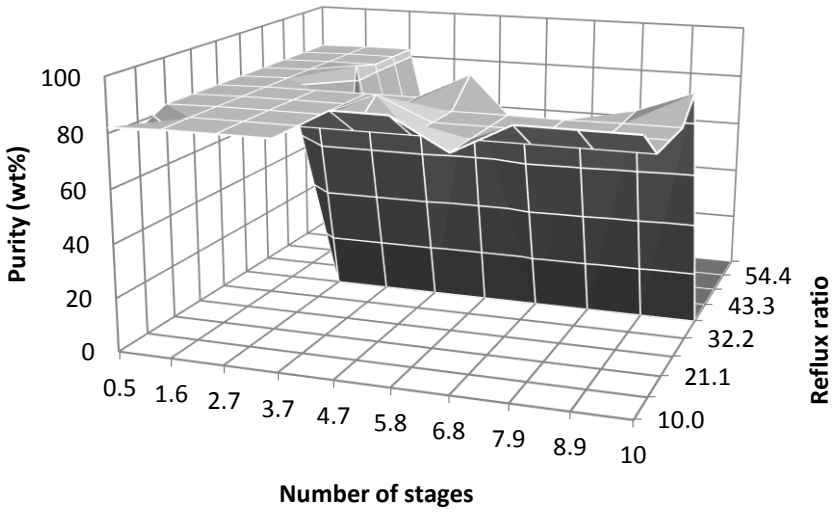

Figure E.66 The effect of number of stages on purity of *dl*-limonene for different reflux ratios

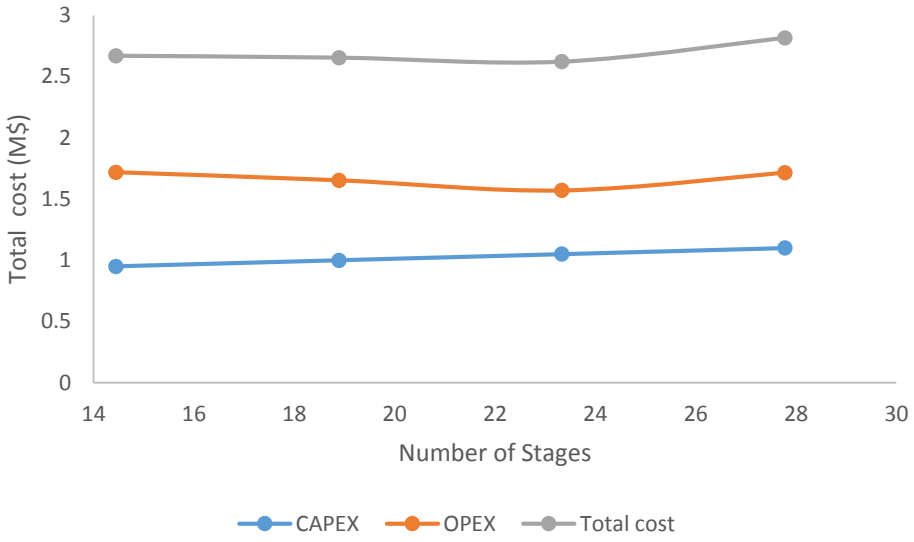

Figure E.67 Optimal number of stages for distillation column T103 operation

Appendix F Equipment sizing

Table F.1 Equipment specification for heterogeneous azeotropic distillation developed using different entrainers

	Diethylene glycol	**Triethylene glycol**	**4-Formylmorpholine**
Equipment	**Equipment specification**	**Equipment specification**	**Equipment specification**
T101	Stages: 55 Diameter: 0.46 m Condenser Area: 3.56 m^2 Reboiler Area: 23.21 m^2 Reflux drum: 19.38 m^3		
T102	Stages: 76 Diameter: 0.46 m Condenser Area: 0.34 m^2 Reboiler Area: 4.21 m^2 Decanter: 19.38 m^3	Stages: 76 Diameter: 0.46 m Condenser Area: 0.94 m^2 Reboiler Area: 8.61 m^2 Decanter: 19.38 m^3	Stages: 40 Diameter: 0.46 m Condenser Area: 0.33 m^2 Reboiler Area: 3.2 m^2 Decanter: 19.38 m^3
T103	Stages 12 Diameter 0.46 m Condenser Area: 0.34 m^2 Reboiler Area: 1.58 m^2 Reflux drum: 19.38 m^3	Stages: 5 Diameter: 0.46 m Condenser Area: 0.94 m^2 Reboiler Area: 8.61 m^2 Reflux drum: 19.38 m^3	Actual number of stages: 8 Diameter: 0.46 m Condenser Area: 0.92 m^2 Reboiler Area: 8.61 m^2 Reflux drum: 19.38 m^3
E101	Area: 0.21 m^2		
E102	Area: 3.57 m^2		
E103	Area: 0.5 m^2	Area: 0.51 m^2	Area: 0.34 m^2
E104	Area: 0.65 m^2	Area: 0.61 m^2	Area: 0.93 m^2
P101	1.92 kW		
P102	0.0004 kW	0.0004 kW	0.0004 kW
P103	10.50 kW	10.50 kW	2.81 kW
T101 reflux pump	0.67 kW		
T102 reflux pump	0.94 kW	0.94 kW	0.49 kW
T103 reflux pump	0.12 kW	0.05 kW	0.08 kW

Table F.2 Equipment specification for extractive distillation developed using different entrainers

	Quinoline	**Triethylene glycol dimethyl ether**
Equipment	**Equipment specification**	**Equipment specification**
T102	Stages: 62 Diameter: 0.46 m Condenser Area: 0.41 m^2 Reboiler Area: 9.49 m^2 Reflux drum: 19.38 m^3	Stages: 76 Diameter: 0.46 m Condenser Area: 0.47m^2 Reboiler Area: 4.22 m^2 Reflux drum: 19.38 m^3
T103	Stages: 19 Diameter: 0.46 m Condenser Area: 0.38 m^2 Reboiler Area: 3.56 m^2 Reflux drum: 19.38 m^3	Stages: 8 Diameter: 0.46 m Condenser Area: 0.54 m^2 Reboiler Area: 2.26 m^2 Reflux drum: 19.38 m^3
E103 **E104**	Area 0.48 m^2 Area 0.60 m^2	Area 0.81 m^2 Area 0.84 m^2
P102 **P103**	0.0007 kW 7.41 kW	0.0004 kW 10.50 kW
T102 reflux pump **T103 reflux pump**	0.76 kW 0.18 kW	0.94 kW 0.05 kW

Table F.3 Equipment specification for homogeneous azeotropic distillation developed using different entrainers

	n,n-Dimethylformamide	**n-Methyl-pyrrolidone**
Equipment	**Equipment specification**	**Equipment specification**
T102	Stages: 40 Diameter: 0.46 m Condenser Area: 1.94 m^2 Reboiler Area: 7.54 m^2 Reflux drum: 19.38 m^3	Stages: 69 Diameter: 0.46 m Condenser Area: 0.56 m^2 Reboiler Area: 9.95 m^2 Reflux drum: 19.38 m^3
T103	Stages: 8 Diameter: 0.46m Condenser Area: 0.36m^2 Reboiler Area: 1.19m^2 Reflux drum: 19.38 m^3	Stages: 40 Diameter: 0.46 m Condenser Area: 0.36 m^2 Reboiler Area: 1.19 m^2 Reflux drum: 19.38 m^3
T104		Stages: 48 Diameter: 0.91 m Condenser Area: 4.14 m^2 Reboiler Area: 25.62 m^2 Reflux drum: 19.38 m^3
T105		Stages: 3 Diameter: 0.61 m Condenser Area: 2.18 m^2 Reboiler Area: 2.38 m^2 Reflux drum: 19.38 m^3
E103 **E104** **E105**	Area: 0.16 m^2 Area: 0.84 m^2 Area: 0.05 m^2	Area: 0.16 m^2 Area: 0.84 m^2 Area: 0.05 m^2
P102 **P103** **P104** **P105**	0.0004 kW 0.59 kW 0.78 kW	1.92 kW 0.68 kW 0.00004 kW 0.0002 kW
T102 reflux pump **T103 reflux pump** **T104 reflux pump** **T105 reflux pump**	0.84 kW 0.31 kW	0.85 kW 0.36 kW 0.59 kW 0.02 kW

Appendix G Cash flow analysis

Table G.1 Cash flow for azeotropic distillation process using diethylene glycol (all values are in million dollars)

Year	Fixed capital	Working capital	Production costs	Revenue	Depreciation	Tax	Net income	Cash flow	Cumulative cash flow	Discounted cash flow	Cumulative Discounted cash flow
0	-18.29	-0.91	0.00	0.00	0.00	0.00	0.00	-19.20	-19.20	-19.20	-19.20
1	0.00	0.00	-3.36	12.44	9.14	0.00	9.08	9.08	-10.12	8.26	-10.94
2	0.00	0.00	-3.36	12.44	5.49	1.01	8.08	8.08	-2.04	6.68	-4.27
3	0.00	0.00	-3.36	12.44	3.66	1.52	7.57	7.57	5.53	5.68	1.42
4	0.00	0.00	-3.36	12.44	0.00	2.54	6.54	6.54	12.07	4.47	5.88
5	0.00	0.00	-3.36	12.44	0.00	2.54	6.54	6.54	18.61	4.06	9.95
6	0.00	0.00	-3.36	12.44	0.00	2.54	6.54	6.54	25.15	3.69	13.64
7	0.00	0.00	-3.36	12.44	0.00	2.54	6.54	6.54	31.69	3.36	16.99
8	0.00	0.00	-3.36	12.44	0.00	2.54	6.54	6.54	38.23	3.05	20.05
9	0.00	0.00	-3.36	12.44	0.00	2.54	6.54	6.54	44.77	2.77	22.82
10	0.00	0.00	-3.36	12.44	0.00	2.54	6.54	6.54	51.31	2.52	25.34
11	0.00	0.00	-3.36	12.44	0.00	2.54	6.54	6.54	57.85	2.29	27.63
12	0.00	0.00	-3.36	12.44	0.00	2.54	6.54	6.54	64.40	2.08	29.72
13	0.00	0.00	-3.36	12.44	0.00	2.54	6.54	6.54	70.94	1.89	31.61
14	0.00	0.00	-3.36	12.44	0.00	2.54	6.54	6.54	77.48	1.72	33.34
15	0.09	0.91	-3.36	12.44	0.00	2.54	6.54	7.54	85.02	1.81	35.14

Table G.2 Cash flow for azeotropic distillation process using triethylene glycol (all values are in million dollars)

Year	Fixed capital	Working capital	Production costs	Revenue	Depreciation	Tax	Net income	Cash flow	Cumulative cash flow	Discounted cash flow	Cumulative Discounted cash flow
0	-15.34	-0.77	0.00	0.00	0.00	0.00	0.00	-16.11	-16.11	-16.11	-16.11
1	0.00	0.00	-3.51	20.18	7.67	2.52	14.15	14.15	-1.97	12.86	-3.25
2	0.00	0.00	-3.51	20.18	4.60	3.38	13.29	13.29	11.32	10.98	7.73
3	0.00	0.00	-3.51	20.18	3.07	3.81	12.86	12.86	24.18	9.66	17.39
4	0.00	0.00	-3.51	20.18	0.00	4.67	12.00	12.00	36.17	8.19	25.58
5	0.00	0.00	-3.51	20.18	0.00	4.67	12.00	12.00	48.17	7.45	33.03
6	0.00	0.00	-3.51	20.18	0.00	4.67	12.00	12.00	60.17	6.77	39.80
7	0.00	0.00	-3.51	20.18	0.00	4.67	12.00	12.00	72.16	6.16	45.96
8	0.00	0.00	-3.51	20.18	0.00	4.67	12.00	12.00	84.16	5.60	51.56
9	0.00	0.00	-3.51	20.18	0.00	4.67	12.00	12.00	96.16	5.09	56.64
10	0.00	0.00	-3.51	20.18	0.00	4.67	12.00	12.00	108.16	4.63	61.27
11	0.00	0.00	-3.51	20.18	0.00	4.67	12.00	12.00	120.15	4.20	65.47
12	0.00	0.00	-3.51	20.18	0.00	4.67	12.00	12.00	132.15	3.82	69.30
13	0.00	0.00	-3.51	20.18	0.00	4.67	12.00	12.00	144.15	3.48	72.77
14	0.00	0.00	-3.51	20.18	0.00	4.67	12.00	12.00	156.14	3.16	75.93
15	0.07	0.77	-3.51	20.18	0.00	4.67	12.00	12.84	168.98	3.07	79.00

Table G.3 Cash flow for azeotropic distillation process using 4-formylmorpholine (all values are in million dollars)

Year	Fixed capital	Working capital	Production costs	Revenue	Depreciation	Tax	Net income	Cash flow	Cumulative cash flow	Discounted cash flow	Cumulative Discounted cash flow
0	-16.54	-0.83	0.00	0.00	0.00	0.00	0.00	-17.37	-17.37	-17.37	-17.37
1	0.00	0.00	-4.02	6.78	8.27	0.00	2.76	2.76	-14.61	2.51	-14.86
2	0.00	0.00	-4.02	6.78	4.96	0.00	2.76	2.76	-11.85	2.28	-12.58
3	0.00	0.00	-4.02	6.78	3.31	0.00	2.76	2.76	-9.08	2.08	-10.50
4	0.00	0.00	-4.02	6.78	0.00	0.77	1.99	1.99	-7.09	1.36	-9.14
5	0.00	0.00	-4.02	6.78	0.00	0.77	1.99	1.99	-5.10	1.24	-7.91
6	0.00	0.00	-4.02	6.78	0.00	0.77	1.99	1.99	-3.11	1.12	-6.78
7	0.00	0.00	-4.02	6.78	0.00	0.77	1.99	1.99	-1.12	1.02	-5.76
8	0.00	0.00	-4.02	6.78	0.00	0.77	1.99	1.99	0.87	0.93	-4.83
9	0.00	0.00	-4.02	6.78	0.00	0.77	1.99	1.99	2.86	0.84	-3.99
10	0.00	0.00	-4.02	6.78	0.00	0.77	1.99	1.99	4.85	0.77	-3.22
11	0.00	0.00	-4.02	6.78	0.00	0.77	1.99	1.99	6.83	0.70	-2.53
12	0.00	0.00	-4.02	6.78	0.00	0.77	1.99	1.99	8.82	0.63	-1.89
13	0.00	0.00	-4.02	6.78	0.00	0.77	1.99	1.99	10.81	0.58	-1.32
14	0.00	0.00	-4.02	6.78	0.00	0.77	1.99	1.99	12.80	0.52	-0.79
15	0.08	0.83	-4.02	6.78	0.00	0.77	1.99	2.90	15.70	0.69	-0.10

Table G.4 Cash flow for extractive distillation process using quinoline (all values are in million dollars)

Year	Fixed capital	Working capital	Production costs	Revenue	Depreciation	Tax	Net income	Cash flow	Cumulative cash flow	Discounted cash flow	Cumulative Discounted cash flow
0	-16.75	-0.84	0.00	0.00	0.00	0.00	0.00	-17.59	-17.59	-17.59	-17.59
1	0.00	0.00	-4.26	20.18	8.38	2.11	13.81	13.81	-3.78	12.55	-5.04
2	0.00	0.00	-4.26	20.18	5.03	3.05	12.87	12.87	9.09	10.64	5.60
3	0.00	0.00	-4.26	20.18	3.35	3.52	12.40	12.40	21.49	9.32	14.92
4	0.00	0.00	-4.26	20.18	0.00	4.46	11.46	11.46	32.95	7.83	22.74
5	0.00	0.00	-4.26	20.18	0.00	4.46	11.46	11.46	44.41	7.12	29.86
6	0.00	0.00	-4.26	20.18	0.00	4.46	11.46	11.46	55.87	6.47	36.33
7	0.00	0.00	-4.26	20.18	0.00	4.46	11.46	11.46	67.34	5.88	42.21
8	0.00	0.00	-4.26	20.18	0.00	4.46	11.46	11.46	78.80	5.35	47.56
9	0.00	0.00	-4.26	20.18	0.00	4.46	11.46	11.46	90.26	4.86	52.42
10	0.00	0.00	-4.26	20.18	0.00	4.46	11.46	11.46	101.72	4.42	56.84
11	0.00	0.00	-4.26	20.18	0.00	4.46	11.46	11.46	113.19	4.02	60.86
12	0.00	0.00	-4.26	20.18	0.00	4.46	11.46	11.46	124.65	3.65	64.51
13	0.00	0.00	-4.26	20.18	0.00	4.46	11.46	11.46	136.11	3.32	67.83
14	0.00	0.00	-4.26	20.18	0.00	4.46	11.46	11.46	147.57	3.02	70.85
15	0.08	0.84	-4.26	20.18	0.00	4.46	11.46	12.38	159.95	2.96	73.81

Table G.5 Cash flow for extractive distillation process using tetraethylene glycol dimethyl ether (all values are in million dollars)

Year	Fixed capital	Working capital	Production costs	Revenue	Depreciation	Tax	Net income	Cash flow	Cumulative cash flow	Discounted cash flow	Cumulative Discounted cash flow
0	-15.34	-0.77	0.00	0.00	0.00	0.00	0.00	-16.11	-16.11	-16.11	-16.11
1	0.00	0.00	-3.51	20.18	7.67	2.52	14.15	14.15	-1.97	12.86	-3.25
2	0.00	0.00	-3.51	20.18	4.60	3.38	13.29	13.29	11.32	10.98	7.73
3	0.00	0.00	-3.51	20.18	3.07	3.81	12.86	12.86	24.18	9.66	17.39
4	0.00	0.00	-3.51	20.18	0.00	4.67	12.00	12.00	36.17	8.19	25.58
5	0.00	0.00	-3.51	20.18	0.00	4.67	12.00	12.00	48.17	7.45	33.03
6	0.00	0.00	-3.51	20.18	0.00	4.67	12.00	12.00	60.17	6.77	39.80
7	0.00	0.00	-3.51	20.18	0.00	4.67	12.00	12.00	72.16	6.16	45.96
8	0.00	0.00	-3.51	20.18	0.00	4.67	12.00	12.00	84.16	5.60	51.56
9	0.00	0.00	-3.51	20.18	0.00	4.67	12.00	12.00	96.16	5.09	56.64
10	0.00	0.00	-3.51	20.18	0.00	4.67	12.00	12.00	108.16	4.63	61.27
11	0.00	0.00	-3.51	20.18	0.00	4.67	12.00	12.00	120.15	4.20	65.47
12	0.00	0.00	-3.51	20.18	0.00	4.67	12.00	12.00	132.15	3.82	69.30
13	0.00	0.00	-3.51	20.18	0.00	4.67	12.00	12.00	144.15	3.48	72.77
14	0.00	0.00	-3.51	20.18	0.00	4.67	12.00	12.00	156.14	3.16	75.93
15	0.07	0.77	-3.51	20.18	0.00	4.67	12.00	12.84	168.98	3.07	79.00

Table G.6 Cash flow for azeotropic distillation process using n,n-dimethylformamide (all values are in million dollars)

Year	Fixed capital	Working capital	Production costs	Revenue	Depreciation	Tax	Net income	Cash flow	Cumulative cash flow	Discounted cash flow	Cumulative Discounted cash flow
0	-40.23	-2.01	0.00	0.00	0.00	0.00	0.00	-42.24	-42.24	-42.24	-42.24
1	0.00	0.00	-4.03	12.44	20.11	0.00	8.41	8.41	-33.83	7.65	-34.60
2	0.00	0.00	-4.03	12.44	12.07	0.00	8.41	8.41	-25.42	6.95	-27.64
3	0.00	0.00	-4.03	12.44	8.05	0.10	8.31	8.31	-17.11	6.24	-21.40
4	0.00	0.00	-4.03	12.44	0.00	2.35	6.06	6.06	-11.06	4.14	-17.27
5	0.00	0.00	-4.03	12.44	0.00	2.35	6.06	6.06	-5.00	3.76	-13.51
6	0.00	0.00	-4.03	12.44	0.00	2.35	6.06	6.06	1.05	3.42	-10.09
7	0.00	0.00	-4.03	12.44	0.00	2.35	6.06	6.06	7.11	3.11	-6.98
8	0.00	0.00	-4.03	12.44	0.00	2.35	6.06	6.06	13.16	2.82	-4.16
9	0.00	0.00	-4.03	12.44	0.00	2.35	6.06	6.06	19.22	2.57	-1.59
10	0.00	0.00	-4.03	12.44	0.00	2.35	6.06	6.06	25.27	2.33	0.75
11	0.00	0.00	-4.03	12.44	0.00	2.35	6.06	6.06	31.33	2.12	2.87
12	0.00	0.00	-4.03	12.44	0.00	2.35	6.06	6.06	37.38	1.93	4.80
13	0.00	0.00	-4.03	12.44	0.00	2.35	6.06	6.06	43.44	1.75	6.55
14	0.00	0.00	-4.03	12.44	0.00	2.35	6.06	6.06	49.49	1.59	8.15
15	0.19	2.01	-4.03	12.44	0.00	2.35	6.06	8.26	57.75	1.98	10.12

Table G.7 Cash flow for azeotropic distillation process using n-methylpyrrolidone (all values are in million dollars)

Year	Fixed capital	Working capital	Production costs	Revenue	Depreciation	Tax	Net income	Cash flow	Cumulative cash flow	Discounted cash flow	Cumulative Discounted cash flow
0	-52.40	-2.62	0.00	0.00	0.00	0.00	0.00	-55.02	-55.02	-55.02	-55.02
1	0.00	0.00	-4.71	12.44	26.20	0.00	7.73	7.73	-47.29	7.03	-47.99
2	0.00	0.00	-4.71	12.44	15.72	0.00	7.73	7.73	-39.56	6.39	-41.60
3	0.00	0.00	-4.71	12.44	10.48	0.00	7.73	7.73	-31.83	5.81	-35.80
4	0.00	0.00	-4.71	12.44	0.00	2.17	5.57	5.57	-26.26	3.80	-31.99
5	0.00	0.00	-4.71	12.44	0.00	2.17	5.57	5.57	-20.69	3.46	-28.54
6	0.00	0.00	-4.71	12.44	0.00	2.17	5.57	5.57	-15.13	3.14	-25.39
7	0.00	0.00	-4.71	12.44	0.00	2.17	5.57	5.57	-9.56	2.86	-22.54
8	0.00	0.00	-4.71	12.44	0.00	2.17	5.57	5.57	-3.99	2.60	-19.94
9	0.00	0.00	-4.71	12.44	0.00	2.17	5.57	5.57	1.58	2.36	-17.58
10	0.00	0.00	-4.71	12.44	0.00	2.17	5.57	5.57	7.14	2.15	-15.43
11	0.00	0.00	-4.71	12.44	0.00	2.17	5.57	5.57	12.71	1.95	-13.48
12	0.00	0.00	-4.71	12.44	0.00	2.17	5.57	5.57	18.28	1.77	-11.71
13	0.00	0.00	-4.71	12.44	0.00	2.17	5.57	5.57	23.84	1.61	-10.09
14	0.00	0.00	-4.71	12.44	0.00	2.17	5.57	5.57	29.41	1.47	-8.63
15	0.25	2.62	-4.71	12.44	0.00	2.17	5.57	8.44	37.85	2.02	-6.61